CONTRACT NO. 95-330
FINAL REPORT
MARCH 1999

# Impact of Reformulated Fuels on Particle and Gas-Phase Emissions from Motor Vehicles

CALIFORNIA ENVIRONMENTAL PROTECTION AGENCY

AIR RESOURCES BOARD
Research Division

# IMPACT OF REFORMULATED FUELS ON PARTICLE AND GAS-PHASE EMISSIONS FROM MOTOR VEHICLES

Final Report
Contract No. 95-330

Prepared for:

California Air Resources Board
Research Division
2020 L Street
Sacramento, California 95814

Prepared by:

Thomas W. Kirchstetter
and
Robert A. Harley
Principal Investigator

Department of Civil and Environmental Engineering
University of California
Berkeley, California 94720-1710

March 1999

For more information about the ARB's Research Division,
its research and activities, please visit our Web site:

http://www.arb.ca.gov/rd/rd.htm

## Disclaimer

The statements and conclusions in this Report are those of the contractor and not necessarily those of the California Air Resources Board. The mention of commercial products, their source, or their use in connection with material reported herein is not to be construed as actual or implied endorsement of such products.

# Acknowledgments

The research presented here parallels Thomas Kirchstetter's doctoral research at UC Berkeley. The other main researchers involved in this project include: Brett Singer, Linsey Marr, and Katharine Hammond of UC Berkeley; Gary Kendall, Michael Traverse, James Hesson, and Rudy Zerrudo of the Bay Area Air Quality Management District; Susanne Hering, Nathan Kreisberg, and Mark Stolzenburg of Aerosol Dynamics Inc.; and Antonio Miguel, currently at UC Riverside.

Technical assistance was provided by Doug Black, David Dreher, Rex Ganding, Greg Noblet, and Charles Perrino of UC Berkeley; Waymond Chan, Chris Gee, Graham Scovell, and the staff of the Technical Services Division of the Bay Area Air Quality Management District; Kent Hoekman, David Kohler, Andrea Tiedemann, and coworkers at Chevron Research and Technology Co.; Kochy Fung of Atmospheric Assessment Associates; Jim McGetrick of ARCO; Pablo Cicero-Fernandez, Jim Pederson, and colleagues at the California Air Resources Board; and Caltrans staff at the Caldecott tunnel.

In addition to support received from ARB, assistance was provided through major in-kind contributions to this research by the Bay Area Air Quality Management District. The University of California Transportation Center supported measurements at the tunnel during summer 1994 and 1995. Speciated liquid gasoline and tunnel aldehyde analyses were provided by Chevron.

This Report was submitted in fulfillment of ARB contract 95-330, Impact of Reformulated Fuels on Particle and Gas-Phase Emissions from Motor Vehicles by the University of California at Berkeley under the sponsorship of the California Air Resources Board. Work was completed as of March 31, 1999.

# Table of Contents

# List of Tables

# List of Figures

# Abstract

A major air pollution control strategy in California in the 1990s has been the reformulation of gasoline and diesel fuel to reduce vehicle emissions. A multi-year field study was conducted in northern California at the Caldecott tunnel to assess the impact of reformulated fuels on vehicle emissions, and to provide an updated characterization of gas and particle-phase emissions from on-road vehicles.

The introduction of reformulated gasoline (RFG) in California led to large changes in gasoline composition. The combined effects of RFG and fleet turnover between summers 1994 and 1997 were large decreases in exhaust emissions of carbon monoxide (CO), non-methane organic compounds (NMOC), and nitrogen oxides ($NO_x$). Although it was difficult to separate the fleet turnover and RFG contributions to these changes, it was clear that the effect of RFG was greater for NMOC than for $NO_x$. The effects of RFG on emissions of toxic organics such as benzene and formaldehyde, and on the mass and reactivity of evaporative VOC emissions were significant.

Per unit mass of fuel burned, heavy-duty diesel trucks emit about 5 times the $NO_x$, 25 times more fine particle ($PM_{2.5}$) mass and 15-20 times the number of fine particles compared to light-duty vehicles. Results of this study suggest that diesel vehicles in California are responsible for nearly half of $NO_x$ emissions and greater than three quarters of exhaust fine particle emissions from on-road motor vehicles. Diesel trucks were found to be the major source of lower molecular weight polycyclic aromatic hydrocarbons (PAH), but light-duty gasoline vehicles were found to be an important source of some higher molecular weight PAH. Size-resolved measurements were made to determine the distribution of particulate PAH across the ultrafine and accumulation size modes.

# Executive Summary

Motor vehicles are a major source of air pollution in California. Statewide emission estimates for 1995 (ARB, 1997) indicate that on-road motor vehicles were responsible for 44% of reactive organic gas emissions, 60% of nitrogen oxide ($NO_x$) emissions, and 68% of carbon monoxide (CO) emissions. In urban areas, motor vehicle emissions can account for even larger fractions of total anthropogenic emissions. For example, in the San Francisco Bay Area in 1995, motor vehicles were estimated to contribute 53% of reactive organic gas emissions, 60% of $NO_x$ emissions, and 78% of CO emissions (ARB, 1997).

Many motor vehicle emission control strategies emphasize technological changes to vehicles such as use of catalytic converters and exhaust gas recirculation. Another approach to reducing vehicle emissions involves reformulation of fuels. Major reformulations of both gasoline and diesel fuel occurred in California during the 1990s.

### Reformulated Gasoline

California's reformulated gasoline (RFG) program was implemented in two phases; the first phase took effect in 1992 and required a reduction in Reid vapor pressure to 7.8 psi during the summer (high-ozone) season. Addition of detergent additives to gasoline and the elimination of lead-based anti-knock compounds were also required in Phase 1 of California's RFG program. Phase 2 of California's RFG program, which took effect during the first half of 1996, required further modifications to fuel properties including: reduction in Reid vapor pressure to meet a 7.0 psi limit; addition of oxygenated compounds such as ethers or alcohols; reduction in benzene, aromatic, olefin, and sulfur content in gasoline; and lower $T_{50}$ and $T_{90}$ distillation temperatures.

### Heavy-Duty Vehicles and Reformulated Diesel Fuel

Although heavy-duty diesel trucks represent only about 1% of all on-road vehicles in California (ARB, 1996a), they contribute significantly to air pollution. California's motor vehicle emission inventory model (MVEI 7G) indicates that in 1995, heavy-duty diesel trucks were responsible for 21% of all $NO_x$ emissions and 75% of exhaust particulate matter emissions from on-road vehicles statewide (ARB, 1996a). To reduce emissions

from diesel trucks, the following changes to diesel fuel composition were required starting in 1993: sulfur content was limited to 0.05% by weight, and aromatic content was limited to 10% by volume (ARB, 1988). Refiners in California developed alternative formulations of diesel fuel with higher aromatic content that were less costly to produce while still providing equivalent emissions reductions (Nikanjam, 1993).

**Research Objectives**

The objectives of this research were to: (1) assess changes in CO, $NO_x$, speciated volatile organic compound, and gas-phase toxic organic emissions due to Phase 2 RFG; (2) assess changes in the chemical speciation and reactivity of liquid gasoline and gasoline headspace vapors due to Phase 2 RFG; (3) characterize fine particle emissions from light- and heavy-duty vehicles; and (4) characterize the emissions rates and size distribution of particle-phase polycyclic aromatic hydrocarbons (PAH). Emissions from a large sample of in-use vehicles were measured in a roadway tunnel to complement previous assessments that have relied on laboratory dynamometer testing of individual vehicles.

**Impact of California Phase 2 RFG**

Light-duty vehicle emission rates were measured in the Caldecott tunnel located on state highway 24 between Alameda and Contra Costa Counties in summers 1994-1997. Large reductions in pollutant emissions were measured in the tunnel over the course of this study, due to a combination of RFG and fleet turnover effects. Between summers 1994 and 1997, emissions of carbon monoxide decreased by 31±5%, non-methane organic compounds (NMOC) decreased by 43±8%, and nitrogen oxides ($NO_x$) decreased by 18±4%. It was difficult to separate clearly the fleet turnover and RFG contributions to these changes. Nevertheless, it was clear that the effect of RFG was greater for NMOC than for $NO_x$. The RFG effect on vehicle emissions of benzene was estimated to be a 30-40% reduction. Use of RFG increased formaldehyde emissions by about 10%, while acetaldehyde emissions did not change significantly. RFG effects on evaporative emissions are also important. The combined effect of Phases 1 and 2 of California's RFG program was a 20% reduction in gasoline vapor pressure, about one fifth of which occurred following the introduction of Phase 2 RFG.

The introduction of Phase 2 RFG affected the composition and reactivity of motor vehicle exhaust and evaporative emissions. Addition of methyl tert-butyl ether (MTBE) and reduction of alkenes and aromatics in gasoline between summers 1995 and 1996 led to corresponding changes in the composition of gasoline headspace vapors. Normalized reactivity of liquid gasoline and headspace vapors decreased by 23 and 19%, respectively.

The reactivity of on-road vehicle emissions measured in the tunnel decreased by only ~5% because of increased weight fractions of highly-reactive isobutene and formaldehyde in vehicle exhaust.

**Fine Particles**

A new assessment of fine particle emissions from light- and heavy-duty vehicles was obtained by making separate measurements of emissions from uphill traffic in two bores of the Caldecott tunnel: one bore carried both light-duty vehicles and heavy-duty diesel trucks, and the second bore was reserved for light-duty vehicles, nearly all of which were gasoline-powered. Heavy-duty diesel trucks were found to emit 24, 38, and 21 times more fine particle, black carbon, and sulfate mass per unit mass of fuel burned than light-duty vehicles. In addition, heavy-duty diesel trucks emitted 15-20 times the number of particles per unit mass of fuel burned compared to light-duty vehicles. Fine particle emissions from both vehicle classes were composed mostly of carbon; diesel-derived particulate matter contained more black carbon (51±11% of $PM_{2.5}$ mass) than did light-duty fine particle emissions (33±4%). Sulfate comprised only 2% of total fine particle emissions for both vehicle classes. Sulfate emissions measured in this study for heavy-duty diesel vehicles are significantly lower than values reported in earlier studies conducted before the introduction of low-sulfur diesel fuel. Combining statewide on-road fuel consumption data with emission factors measured in this study suggests that diesel vehicles in California are responsible for nearly half (~45%) of oxides of nitrogen emissions and greater than three quarters of exhaust fine particle emissions from on-road motor vehicles.

**Polycyclic Aromatic Hydrocarbons**

A similar tunnel sampling approach was used to assess on-road emissions of polycyclic aromatic hydrocarbons (PAH). Diesel trucks were the major source of lighter PAH, whereas light-duty gasoline vehicles were a significant source of higher molecular weight PAH. Size-resolved measurements of particulate PAH showed significant fractions of diesel-derived PAH to be present in both the ultrafine size mode (< 0.12 μm) and the accumulation mode (0.12–2 μm). The ultrafine mode was more prominent for gasoline engine-derived PAH emissions. PAH concentrations were also quantified in gasoline and diesel fuel samples. Light-duty vehicle emission factors for particle-phase PAH were correlated with PAH concentrations in gasoline.

**Recommendations**

- Continued on-road surveillance of vehicle emissions at the Caldecott tunnel would be useful for tracking long-term trends in light- and heavy-duty vehicle emissions. Permanent installation of continuous CO, $CO_2$, $NO_x$, and hydrocarbon analyzers in climate-controlled rooms at both ends of the tunnel is recommended.

- The air quality impacts of changes in motor vehicle emissions that resulted from use of reformulated gasoline in the San Francisco Bay Area should be investigated using Eulerian photochemical air quality models.

- Analyses of the impact of reformulated gasoline should always consider evaporative emissions. Reductions in gasoline vapor pressure and changes to fuel composition are expected to reduce both VOC mass emission rates and reactivity of evaporative emissions significantly.

- Greater attention to the role of heavy-duty diesel engine emissions in California's air pollution problems is needed. Measured emission rates at the Caldecott tunnel suggest that diesel engines are the dominant source of on-road exhaust fine particle emissions. Furthermore, the contribution of heavy-duty engines to on-road $NO_x$ emissions is ~45% of the total in California, which is higher than previous estimates would suggest. Emissions from off-road diesel engines also contribute to air pollution problems.

- Further consideration is needed of the relative importance of light-duty (gasoline) versus heavy-duty diesel engines as sources of PAH emissions.

- Fuel reformulation may help to reduce PAH emissions. Relationships between PAH emissions and fuel composition should be studied further for both gasoline and diesel-powered vehicles.

# 1 Introduction

## 1.1 Motivation

Many of the air quality problems faced by the United States and other countries worldwide are due in large part to motor vehicle use. Motor vehicles emit primary pollutants including carbon monoxide (CO), benzene, and soot which are of direct concern to human health. In addition, atmospheric photochemical reactions involving vehicular emissions of volatile organic compounds (VOC) and oxides of nitrogen ($NO_x$) contribute to the formation of secondary pollutants such as ozone and particulate matter. Statewide estimates for California in 1995 (ARB, 1997) indicate that on-road motor vehicles accounted for 44, 60, and 68% of total anthropogenic emissions of reactive organic gases, $NO_x$, and CO, respectively. In urban areas, motor vehicle emissions typically account for even larger fractions of total anthropogenic air pollutant emissions. For example, in the San Francisco Bay Area in 1995, on-road vehicles were estimated to contribute 53% of reactive organic gas emissions, 60% of $NO_x$ emissions, and 78% of CO emissions (ARB, 1997).

These air quality problems persist today despite substantial efforts to reduce vehicle emissions. Efforts to control emissions from light-duty passenger cars and trucks have been ongoing since the 1960s. Increasingly stringent emission standards for gasoline-powered vehicles have led to the development and use of control technologies such as positive crankcase ventilation to reduce VOC emissions; exhaust gas recirculation for $NO_x$ control; and the 3-way catalytic converter for simultaneous control of VOC, $NO_x$, and CO emissions (Black, 1991). In-use exhaust emissions of VOC and CO from today's new cars are about one-tenth of the levels emitted by cars sold prior to 1975. In-use $NO_x$ and evaporative VOC emissions also have been reduced. Unfortunately, increased vehicle travel, degradation and malfunction of emission control systems, and poor vehicle maintenance have offset some of the expected air quality benefits of the motor vehicle emission control program (Calvert et al., 1993).

Although heavy-duty diesel trucks represent only about 1% of all on-road vehicles (ARB, 1996a), they contribute significantly to air pollution. The importance of heavy-duty vehicle emissions has increased as the degree of control of light-duty vehicle emissions has

improved. California's motor vehicle emission inventory model (MVEI 7G) indicates that in 1995, heavy-duty diesel trucks were responsible for 21% of all $NO_x$ emissions and 75% of exhaust particulate matter (PM) emissions from on-road vehicles statewide (ARB, 1996a). Diesel-derived particles, which are composed largely of carbonaceous material, contribute significantly to fine carbon particle concentrations in urban atmospheres (Cass and Gray, 1995). Heavy-duty vehicle emission standards have lagged behind those for light-duty vehicles, both in time of introduction and in stringency (Sawyer and Johnson, 1995). Diesel engine manufacturers have met increasingly stringent $NO_x$ and PM emission standards in the 1990s through advances in engine and control technology (Sawyer et al., 1998).

A major air pollution control strategy in California has been the reformulation of motor vehicle fuels to reduce emissions. California's reformulated gasoline (RFG) program was implemented in two phases. The first phase took effect in 1992 and required a reduction in Reid vapor pressure to 7.8 psi during the summer (high-ozone) season, use of engine deposit control additives, and the elimination of lead-based anti-knock compounds. Phase 2 of California's RFG program, which took effect during the first half of 1996, required further modifications to fuel properties including: reduction in Reid vapor pressure to meet a 7.0 psi limit during the summertime; addition of oxygenated compounds such as ethers or alcohols; reduction in benzene, aromatic, olefin, and sulfur content in gasoline; and lower $T_{50}$ and $T_{90}$ distillation temperatures. Refiners may choose to meet California RFG program requirements either by following a set recipe that specifies flat and average limits for each regulated fuel property, or by using a predictive model to develop alternate gasoline formulations with equivalent emissions reduction benefits.

Federal requirements that apply to areas in California with severe ozone air pollution problems (currently the South Coast, San Diego, and Sacramento Valley air basins) remove some of the flexibility provided by California's RFG program because addition of oxygenated compounds to gasoline in these areas is mandatory. The required oxygen content in gasoline is 2% by weight, which is equivalent to 11% by volume of the most widely used oxygenate methyl *tert*-butyl ether (MTBE). Other oxygenates that may be used include *tert*-amyl methyl ether (TAME), methanol, and ethanol. In contrast to the South Coast Air Basin, the San Francisco Bay Area was not subject to Federal RFG requirements in 1995, and therefore experienced a sharper transition to California Phase 2 RFG over a single year (i.e., between summer 1995 and 1996).

To reduce emissions from diesel trucks in California, changes to diesel fuel composition were required starting in 1993. Sulfur content was limited to 0.05% by weight and aromatic content was limited to 10% by volume (ARB, 1988). Refiners in

California developed alternative formulations of diesel fuel with higher aromatic content that were less costly to produce while still providing equivalent emissions reductions (Nikanjam, 1993).

Most studies to determine the effects of fuel composition on vehicle emissions have been conducted in the laboratory where emissions from individual vehicles are measured one at a time on a dynamometer (e.g., Burns et al., 1991). Since the laboratory test procedures are time consuming and expensive, only small numbers of vehicles can be tested. On-road infrared remote sensing studies of light-duty vehicle emissions (Zhang et al., 1995) consistently show that the distribution of pollutant emission rates across the vehicle fleet is highly skewed. In the United States, it is common for 10% of the vehicles to be responsible for 50% of the emissions of CO, VOC, and $NO_x$, although it is not necessarily the same high-emitting vehicles that are responsible for 50% of the emissions of all three pollutants (Stedman et al., 1994; Zhang et al., 1996). Laboratory studies of vehicle emissions are often unable to recruit a sufficiently large random sample to represent the contribution from high-emitting vehicles accurately (Howard et al., 1997). Furthermore, even when high-emitting vehicles are included in dynamometer tests, their emissions vary erratically, and this variability can mask the fuel effects under study (Knepper et al., 1993).

## 1.2 Research Objectives

The principal objectives of this research were to assess the impact of reformulated fuels on vehicle emissions, and to provide an updated characterization of gas and particle-phase emissions from on-road vehicles. Specific objectives were to: (1) assess changes in CO, $NO_x$, speciated VOC, and gas-phase toxic organic emissions due to Phase 2 RFG; (2) assess changes in the chemical speciation and reactivity of liquid gasoline and gasoline headspace vapors due to Phase 2 RFG; (3) characterize fine particle emissions from light- and heavy-duty vehicles; and (4) characterize the emission rates and size distribution of particle-phase polycyclic aromatic hydrocarbons.

## 1.3 Approach

To complement previous assessments of reformulated fuels that have relied on laboratory dynamometer testing of individual vehicles, in this study vehicle emissions were measured in a roadway tunnel. In addition to measuring pollutant concentrations, vehicle characteristics and driving conditions in the tunnel were characterized. Fuel samples were collected and analyzed to relate measured emissions to fuel properties.

Throughout this research, vehicle emissions are normalized to total carbon (mainly $CO_2$) concentrations measured in the tunnel. By carbon balance, emission factors are expressed per unit mass of fuel burned, rather than per unit distance of vehicle travel. Normalization of emissions to fuel consumption eliminates the need to measure the tunnel ventilation rate, and therefore eliminates a significant source of measurement uncertainty (Rogak et al., 1998a). Additionally, emission factors normalized to fuel consumption rather than distance traveled fluctuate less as a function of driving condition because fuel consumption is approximately proportional to engine load and emissions over a wide range of driving conditions. Finally, fuel-based emission factors can be combined with fuel sales data to develop motor vehicle emission inventories (Singer and Harley, 1996; Black et al., 1997; Dreher and Harley, 1998).

## 1.4 Field Site

Vehicle emissions were measured in the Caldecott tunnel. Located east of San Francisco Bay on state highway 24, the Caldecott tunnel runs in the east-west direction connecting cities in Contra Costa County with Oakland, Berkeley, and San Francisco. The tunnel comprises three two-lane traffic bores, is 1100 m long, and has a roadway grade of 4.2%, uphill in the eastbound direction. Forced transverse ventilation along the length of the tunnel is provided by adjustable pitch fans that are located in portal buildings above the entrance and exit of the tunnel. Additional longitudinal ventilation is induced by the flow of vehicles and by prevailing westerly winds. A schematic of the tunnel is presented in Figure 1.1.

Traffic direction is always westbound in the northernmost bore and always eastbound in the southernmost bore. To accommodate large traffic volumes during weekday rush hour periods, the center bore of the tunnel carries westbound traffic toward San Francisco in the morning, and eastbound traffic in the afternoon. Field sampling was conducted in the southernmost bore (bore 1) and in the center bore (bore 2) during the afternoon when vehicles traveled in the eastbound (uphill) direction toward Contra Costa County. The vehicle fleet traveling through bore 2 was composed almost entirely of light-duty vehicles whereas the fleet traveling in bore 1 contained a mix of light- and heavy-duty vehicles.

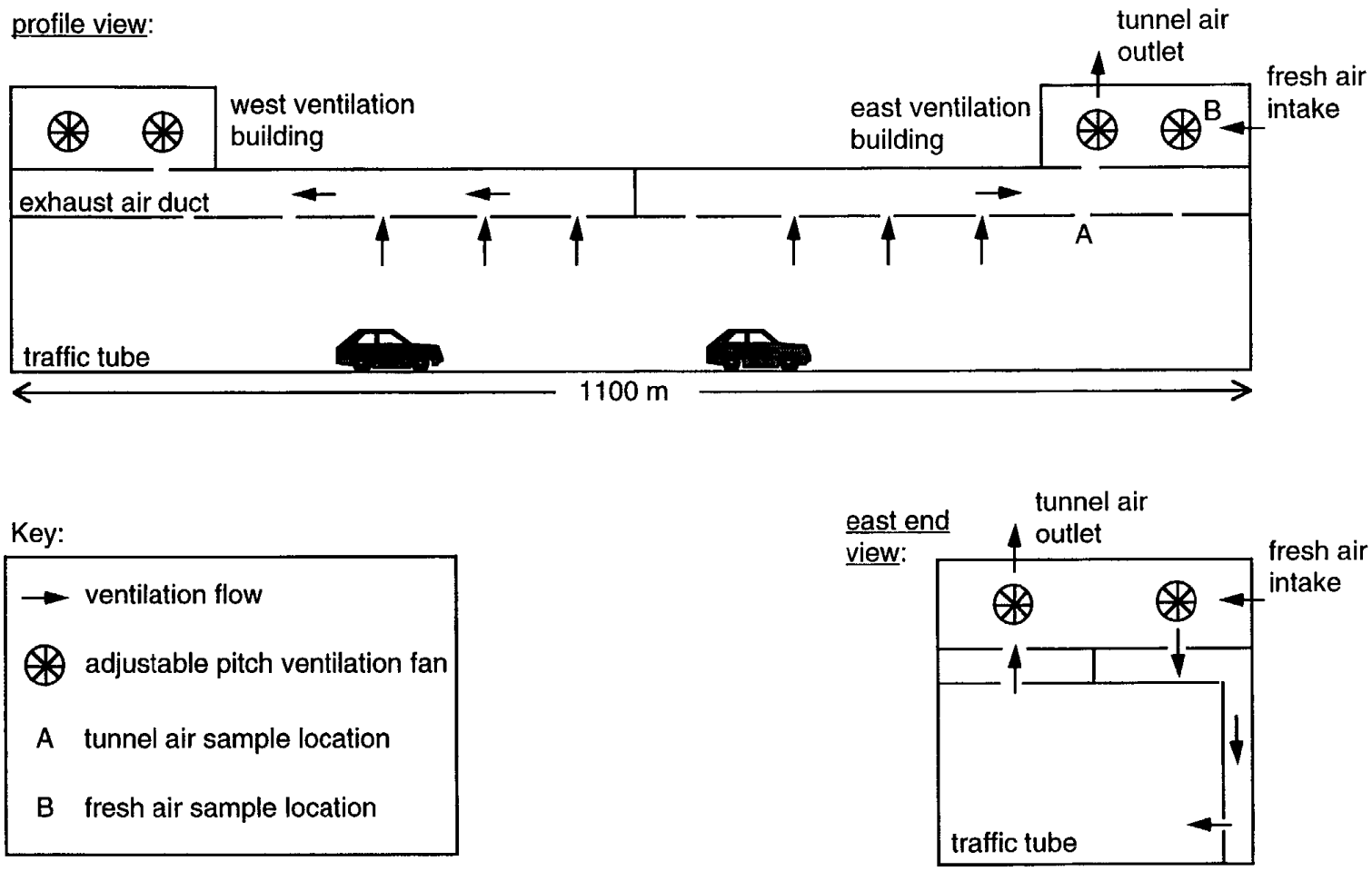


**Figure 1.1.** Schematic of the Caldecott tunnel showing ventilation air flows and air sampling locations (figure not drawn to scale).

## 1.5 Overview

Vehicle emissions were measured at the Caldecott during four field monitoring campaigns. Chapters 2 and 3 report on the impacts of California reformulated gasoline. Gasoline properties and vehicle emission rates measured in the tunnel during the summers of 1994, 1995, 1996, and 1997 are considered in the evaluation. Changes to gasoline composition included an increase in oxygen content, and decreases in alkene, aromatic, benzene, and sulfur contents between summers 1995 and 1996 when reformulated gasoline was required for use statewide. A model is developed to relate the composition of headspace vapors to that of liquid gasoline. The effects of reformulated gasoline on both tailpipe exhaust and evaporative emissions are assessed. In addition, the effects of changes to gasoline composition on the speciation and reactivity of VOC emissions are examined.

Chapters 4 and 5 present an updated assessment of exhaust fine particle emissions from light- and heavy-duty motor vehicles. Sampling was conducted during the summers of 1996 and 1997 to characterize the chemical composition of $PM_{2.5}$ emissions and to assess the relative contributions of light- and heavy-duty vehicles to fine particle and $NO_x$ emissions. Chapter 4 considers $PM_{2.5}$, black carbon, organic carbon, and $NO_x$ emission rates; emissions of polycyclic aromatic hydrocarbons are the focus of Chapter 5.

In Chapters 6 and 7, the major findings of this research are summarized, and areas for future research are recommended. Appendices follow with detailed chemical speciation profiles for whole liquid gasoline, gasoline headspace vapors, and motor vehicle VOC emissions measured in the Caldecott tunnel. Time series plots of pollutant concentrations measured inside the tunnel are presented in a final appendix.

# 2 Impact of RFG on Mass Emission Rates

## 2.1 Introduction

Use of reformulated gasoline (RFG) was mandated in the 1990 Clean Air Act Amendments in areas of the country with severe ozone air pollution problems. While Federal RFG is required in only some areas in California (currently South Coast, San Diego, and Sacramento Valley air basins), a statewide reformulated gasoline program has been implemented by the California Air Resources Board.

In Phase 1 of the California program, effective 1992, the maximum allowed Reid vapor pressure (RVP) of gasoline sold during summer months was reduced from 9.0 to 7.8 psi, the use of lead in gasoline was eliminated, and the use of detergent additives to control engine deposits was required (ARB, 1990). Phase 2 of the California program took effect in the first half of 1996, and required more extensive changes to gasoline properties (ARB, 1991; ARB, 1994). These changes included: further reduction of summertime RVP to 7.0 psi maximum; reduction of benzene, total aromatic, olefin, and sulfur contents in gasoline; addition of oxygenates; and reductions in distillation temperatures, $T_{50}$ and $T_{90}$. Refiners can choose to produce gasoline with the prescribed formulation shown in Table 2.1, or they may use a predictive model to establish alternative gasoline formulations that result in equivalent or greater emissions reductions (ARB, 1994). Estimates of the effect of Phase 2 RFG on vehicle emissions, including cold-start, running exhaust, and evaporative emissions, are reductions of reactive organic gases by 17%, oxides of nitrogen ($NO_x$) and carbon monoxide (CO) by 11%, and toxic air contaminants by 30% in its first year of use (ARB, 1994).

The Auto/Oil Air Quality Improvement Research Program (Auto/Oil, 1992; Auto/Oil, 1993; Auto/Oil, 1995) demonstrated through laboratory testing that vehicle emissions can be reduced by modifying fuel properties. Tests were conducted using a stop-and-go urban dynamometer driving cycle, and gasoline composition was carefully controlled in each test. Individual and combined effects of changes in gasoline properties on exhaust emissions were examined. However, fuel effects were determined for only a small number of well-maintained, low-emitting vehicles, whereas on-road emissions are

dominated by small numbers of gross-polluting vehicles (Zhang et al., 1995). Since the effects of fuel changes on emissions from gross-polluting vehicles could not be characterized definitively (Knepper et al., 1993), the Auto/Oil results may not be indicative of RFG effects for the in-use vehicle fleet (Howard et al., 1997).

To complement the results of dynamometer studies, the effects of changes in fuel composition on vehicle emissions can be determined in on-road settings. For example, remote sensing (Bishop and Stedman, 1990; Lyons and Fox, 1993) and tunnel (Kirchstetter et al., 1996; Gertler et al., 1997) studies have investigated the impact of modifying fuel properties on exhaust emissions from thousands of in-use vehicles, including gross-polluters, driven under real-world conditions. Tunnel studies, in particular, are well-suited for measuring the effects of reformulated gasoline because many pollutants can be measured, including CO, VOC, $NO_X$, and individual toxic compounds.

This chapter reports on the emission impact of California Phase 2 RFG. Vehicle emissions were measured in the Caldecott tunnel during the summers prior to and after the introduction of RFG. Each summer, the composition of gasoline sold in the Bay Area was determined. The impact of RFG on mass emission rates is considered here. The effect of RFG on the speciation and reactivity of exhaust and evaporative organic gas emissions is addressed in Chapter 3.

## 2.2 Experimental

### 2.2.1 Gasoline Sampling and Analysis

Gasoline sold in the San Francisco Bay Area was collected and analyzed by Southwest Research Institute. Measured gasoline properties included: RVP; density; aromatic, alkene, alkane, oxygenate, sulfur, and benzene contents; and distillation temperatures including $T_{50}$ and $T_{90}$. For the purpose of this study, fuel survey data were obtained for regular, mid-, and premium grade gasoline samples collected during summers 1994-1997 (McGetrick, 1997). Each year, about 35 gasoline samples of major gasoline brands were collected at service stations in Concord and San Francisco in July and August, respectively.

Composite properties were computed for each brand of gasoline according to the market share of each gasoline grade: 58% regular, 20% mid, and 22% premium (Gilson, 1995). Average gasoline properties were computed by averaging together all brand composites with equal weighting.

### 2.2.2 Field Site

Vehicle emissions were measured at the Caldecott tunnel. The important features of the tunnel have already been discussed and illustrated in Chapter 1. Field measurements were conducted on 10 or more days during each summer from 1994 through 1997.

Emissions were measured in the center bore (bore 2) during the afternoon commute period from 1600-1800 h when vehicles traveled in the eastbound (uphill) direction. On selected days in summers 1996 and 1997, additional measurements were made earlier in the afternoon, starting at 1300 h, before the afternoon peak traffic period.

Vehicles observed in this study were operating in a warmed-up mode. There are two nearby on-ramps that serve highway 24, at distances of 0.3 and 1.0 km from the western end of the tunnel. The nearer on-ramp is close enough to allow some vehicles to enter the tunnel while operating in cold start mode, but this on-ramp directs traffic into the southernmost bore (bore 1) of the tunnel, not the center bore (bore 2) where measurements for this study were made. Vehicles merging onto highway 24 via the further on-ramp are exiting another highway, and are therefore already operating in hot stabilized mode. Moreover, the overwhelming majority of vehicles that drove through the tunnel (both bores) during the afternoon commute had traveled longer distances from Berkeley, Oakland, or San Francisco prior to entering the tunnel.

### 2.2.3 Traffic Monitoring

The vehicle fleet traveling through the center bore of the Caldecott tunnel was monitored on all days when emissions were measured. Visual counts were used to determine traffic volumes and composition. Vehicles were assigned to one of three categories: cars; light-duty trucks including pickups, sport utility vehicles, and small vans; and heavy-duty vehicles. License plate surveys were conducted to determine the age distribution and the fuel type of the vehicles being monitored. License plates were recorded using a Hi-8 format video camera and were later matched with vehicle registration data. Driving conditions inside the tunnel were monitored by following traffic with a chase car. Average vehicle speed was determined using the tunnel length and measured transit time for each "drivethrough". Two hundred fifty drivethroughs were conducted during summers 1995-1997. In addition, an instrumented vehicle that logged speed at one second intervals was used in summer 1996 to measure the speed profile inside the tunnel. Finally, a video camera was used each summer to record a wide view of all traffic exiting the tunnel.

### 2.2.4 Pollutant Measurements

Pollutant concentrations were measured in the traffic tube ~50 m before the tunnel exit (position A in Figure 1.1) and in the clean background air which was injected into the tunnel by the ventilation fans (position B in Figure 1.1). Concentrations of $CO_2$, CO, and $NO_x$ were measured continuously. $CO_2$ and CO concentrations were quantified using infrared gas filter correlation spectrometers, and $NO_x$ concentrations were measured by chemiluminescence. Continuous air monitoring data were recorded as five-minute average

concentrations. Using traceable gas standards, zero and span checks were performed several times a week on each analyzer.

Two-hour integrated air samples were collected in 6-liter stainless steel canisters for subsequent analysis to quantify methyl *tert*-butyl ether (MTBE) and hydrocarbon concentrations. Similarly, two-hour integrated samples were collected using DNPH-impregnated silica cartridges for subsequent analysis to quantify carbonyl concentrations. A coiled copper tube, coated on the inside with potassium iodide, was placed upstream of the silica cartridge for the ventilation intake air samples. This was done to remove ozone from the sample air stream since ozone interferes with the quantification of carbonyl concentrations (Arnts and Tejada, 1989). An ozone scrubber was not needed for the tunnel samples because any ozone drawn into the tunnel is rapidly removed by reaction with nitric oxide. All hydrocarbon and carbonyl samples were collected concurrently with measurements of CO, $CO_2$, and $NO_x$ concentrations. Hydrocarbon and carbonyl samples were collected only during the 1600-1800 h sampling periods.

Total and individual non-methane hydrocarbon (NMHC), methane, and MTBE concentrations were determined by gas chromatography (GC) at the Bay Area Air Quality Management District's laboratory in San Francisco. Hydrocarbon samples were preconcentrated using a Nutech model 8548 cryogenic concentrator, and injected into a Perkin Elmer model 8500 gas chromatograph (GC) equipped with a flame ionization detector (FID). The DB-1 column used in the GC was 30 m long, with an inner diameter of 0.32 mm and a 5 μm film thickness. Following sample injection, the column temperature was held at -51°C for five minutes, then increased at 5°C per minute to 100°C, at 3°C per minute to 160°C, at 5°C per minute to 200°C, and held at that temperature for seven minutes. This method was used to quantify speciated hydrocarbons in the $C_5$ to $C_{10}$ range. A GS-alumina column, 50 m long by 0.53 mm inner diameter, was used to speciate and quantify the $C_2$ to $C_4$ hydrocarbons. For quantification of NMHC concentrations during summer 1997 analyses only, a Nutech model 3550A cryogenic concentrator was used to preconcentrate samples, and a DB-1 column was used to quantify all $C_2$ to $C_{10}$ hydrocarbons. Total non-methane hydrocarbon (NMHC) concentrations were quantified with the same GC at an oven temperature of 105 °C. An analytical column was not used. Total NMHC in the sample was determined by comparison of peak area to that of an NIST certified propane standard.

Methane was quantified separately by direct injection of samples into a Perkin Elmer model 8500 GC equipped with FID and a 3.7 m long by 3.2 mm inner diameter stainless steel column packed with Chromosorb 102, 100 to 120 mesh. MTBE concentrations were determined using a Varian Model 3400 GC equipped with PID/ECD in

series. Samples were preconcentrated using a Tekmar 5010 Automatic Desorber and a Tenax trap. The column used in the GC was packed with 1% SP1000/Carbopack B, 60/80 mesh; was 4 m long; and had an inner diameter of 0.32 cm. Following sample injection, the oven temperature was increased at 2 °C per minute from 85 to 125 °C, and held at that temperature for 15 minutes. MTBE concentrations were not quantified for samples collected in summer 1994.

During the 1994 field campaign, it was found that 1,3-butadiene was unstable in the tunnel hydrocarbon samples during several weeks of sample storage prior to analysis (Kirchstetter et al., 1996). Therefore, no measurements of butadiene concentrations are reported for 1994. In summers 1995-1997, canisters were usually analyzed in the laboratory within 24 hours of sample collection to minimize loss of 1,3-butadiene.

After each two-hour sampling period, DNPH-cartridges were eluted with 5 mL of acetonitrile and the extracted samples were stored in tightly capped glass vials in a refrigerator. All elutions were completed within a few hours of sample collection. At the end of each year's sampling program, the extracted samples were analyzed by high-performance liquid chromatography using a procedure nearly identical to that developed for the Auto/Oil Air Quality Improvement Research Program (Siegl et al., 1993). Carbonyl samples were analyzed by Hoekman and coworkers at Chevron Research and Technology Co. from 1994 to 1996, and by Fung at Atmospheric Assessment Associates Inc. in 1997.

### 2.2.5 Quality Assurance

Each summer, the Quality Assurance Section of the California Air Resources Board (ARB) conducted performance audits of the CO and $NO_x$ analyzers used at the Caldecott tunnel. In all cases, the analyzers were found to operate well within ARB's ±15% control limits. Tunnel CO and $NO_x$ analyzers were always accurate within ±2 and ±5%, respectively.

Measured total NMHC concentrations were compared with independent analyses of tunnel air samples collected in parallel. Independent analyses were performed by the Monitoring and Laboratory Division of the ARB, Desert Research Institute, and Rasmussen. Six comparisons were made in summers 1995-1997. Total NMHC concentrations reported for samples collected in this study were between 1 and 9% higher than the values reported by the other investigators.

## 2.3 Results

### 2.3.1 Gasoline Properties

Average San Francisco Bay Area gasoline properties derived from fuel survey data for summers 1994-1997 are shown in Table 2.1. Also shown are the flat limits for California's Phase 2 RFG program, which took effect in the first half of 1996. As

**Table 2.1.** Average (± 1 standard deviation) properties of gasoline sold in the San Francisco Bay Area during summers 1994-1997 compared with California Phase 2 RFG specifications.

| gasoline property | 1994 | 1995 | 1996 | 1997 | Phase 2 RFG[a] |
|---|---|---|---|---|---|
| RVP (psi) | 7.4 ± 0.1 | 7.4 ± 0.1 | 7.0 ± 0.1 | 7.1 ± 0.1 | 7.0[b] |
| sulfur (ppmw) | 131 ± 41 | 81 ± 36 | 16 ± 9 | 12 ± 11 | 40 |
| oxygen (wt %) | 0.5 ± 0.3 | 0.2 ± 0.2 | 2.0 ± 0.3 | 1.6 ± 0.6 | 1.8 - 2.2 |
| MTBE (vol %) | 2.7 ± 1.7 | 1.0 ± 0.9 | 10.7 ± 1.7 | 8.2 ± 3.7 | |
| alkane (vol %) | 57.4 ± 4.8 | 56.6 ± 5.1 | 62.6 ± 2.5 | 65.4 ± 3.7 | |
| alkene (vol %) | 7.9 ± 4.4 | 8.8 ± 3.5 | 3.3 ± 0.9 | 3.4 ± 1.2 | 6.0 |
| aromatic (vol %) | 31.9 ± 2.1 | 33.7 ± 3.3 | 23.5 ± 1.4 | 22.7 ± 1.4 | 25 |
| benzene (vol %) | 1.6 ± 0.4 | 1.5 ± 0.4 | 0.4 ± 0.1 | 0.4 ± 0.1 | 1.0 |
| $T_{50}$ (°F) | 214 ± 8 | 218 ± 4 | 199 ± 4 | 200 ± 3 | 210 |
| $T_{90}$ (°F) | 334 ± 8 | 341 ± 8 | 300 ± 4 | 299 ± 6 | 300 |
| density (g $L^{-1}$) | 761 ± 8 | 760 ± 4 | 743 ± 2 | 741 ± 5 | |

[a] The phase 2 RFG specifications shown here are flat limits; refiners may also comply with average limits. Gasoline sold in California should not exceed flat limits unless refiners use the California predictive model to establish alternative RFG specifications that provide equivalent or greater emissions reductions (ARB, 1994).

[b] The limit on fuel volatility applies only during summer months, defined as April 1 through October 31 for the Bay Area.

expected, significant changes to gasoline occurred between summers 1995 and 1996. Large changes included decreases in benzene, olefin, and aromatic contents; and an increase in oxygen content to 2.0 ± 0.3 wt%. Distillation temperatures, $T_{50}$ and $T_{90}$, and gasoline density also decreased between 1995 and 1996. Gasoline properties shown in Table 2.1 did not change between summers 1994 and 1995, or between summers 1996 and 1997, with the exception of changes to sulfur and oxygen content discussed below.

A trend toward lower sulfur content in gasoline was already evident in summer 1995. The magnitude of the reduction in sulfur content was comparable between 1994-1995 and 1995-1996. In the earlier two years, there was large brand-to-brand variability in gasoline sulfur levels, whereas by 1996 all gasoline samples had low sulfur content (< 40 ppmw).

Oxygen content in gasoline was low in summers 1994 and 1995, and then rose dramatically in 1996, as indicated in Table 2.1. Compared to 1996 levels, average oxygen content decreased to 1.6 ± 0.6 wt% in 1997, and showed greater variability across gasoline brands and grades, with some gasoline samples having very low oxygen content. Presumably, Bay Area refiners used California's predictive model (ARB, 1994) to determine modifications to other fuel properties to compensate for reduced use of oxygenate in summer 1997.

The predominant oxygenate found in gasoline was MTBE. Small amounts of tert-amyl methyl ether (TAME) and methanol, typically < 0.1% by volume, were detected in some 1996 gasoline samples. In 1997, some gasoline samples contained greater amounts of TAME, which contributed about 5% of the oxygen content found in gasoline on average. The remaining 95% of the fuel oxygen content continued to be supplied in the form of MTBE.

### 2.3.2 Fuel Economy

The energy content of MTBE (26 MJ $L^{-1}$), as measured by its lower heating value (LHV), is less than that of conventional gasoline (33 MJ $L^{-1}$). Since the volumetric energy content of gasoline is a good predictor of fuel economy (Hochhauser et al., 1993), reformulation may decrease fuel economy. To estimate the effect of switching to Phase 2 RFG on fuel economy, heating values were computed using the detailed chemical composition of regular and premium grade gasolines collected at high-volume service stations in Berkeley (discussed in Chapter 3). Heating values were calculated using the following equation:

$$LHV = -\left[\sum_{i=1}^{n}\left(\Delta h_{c,i} \cdot w_i\right)\right] \cdot \rho_f \qquad (2.1)$$

where LHV is the lower heating value (J $L^{-1}$), $\rho_f$ is the density of gasoline (g $L^{-1}$), $w_i$ is the weight fraction of compound i in gasoline, and $\Delta h_{c,i}$ is the enthalpy of combustion of compound i (J $g^{-1}$). Enthalpies of combustion for each compound in gasoline were calculated from tabulated enthalpies of formation (Reid et al., 1987) assuming complete combustion to carbon dioxide and water vapor, and are reported in Appendix A.

Overall, the LHV of gasoline decreased from 32.8 MJ $L^{-1}$ in 1995 to 31.7 MJ $L^{-1}$ in 1996, mainly due to a decrease in gasoline density and addition of MTBE. This decrease in the volumetric energy content of gasoline corresponds to a ~3% decrease in fuel economy for most vehicles (Hochhauser et al., 1993).

### 2.3.3 Traffic Characteristics

Attributes of the traffic that traveled through the Caldecott tunnel from 1600-1800 h are presented in Table 2.2. The number of vehicles traveling through the tunnel, ~8400 during each two-hour sampling period, was consistent on all sampling days across all four summers. Traffic consisted of light-duty vehicles almost exclusively because heavy-duty vehicles were required to use other tunnel bores. Heavy-duty trucks comprised < 0.3% of the vehicles in the center bore in each year. About two-thirds of the vehicles were cars and the remainder were pickups, sport utility vehicles, and small vans. A gradual increase was seen between 1994 and 1997 in the fraction of light-duty trucks, as indicated in Table 2.2.

**Table 2.2.** Attributes of vehicles using the center bore of the Caldecott tunnel between 1600-1800 h in summers 1994-1997.

| attribute | 1994 | 1995 | 1996 | 1997 |
|---|---|---|---|---|
| volume (# $h^{-1}$) | 4260 ± 240 | 4220 ± 260 | 4220 ± 220 | 4220 ± 170 |
| cars (%) | 69 | 67 | 66 | 65 |
| light-duty trucks[a] (%) | 31 | 33 | 34 | 35 |
| heavy-duty vehicles[b] (%) | 0.2 | 0.2 | 0.3 | 0.2 |
| mean model year | n/a[c] | 1989.3 | 1990.1 | 1990.9 |
| light-duty diesel[d] (%) | n/a | 1.0 | 1.5 | 1.8 |

[a] Light-duty trucks included pickups, sport utility vehicles, and small vans.

[b] Heavy-duty vehicles included large delivery trucks (i.e., UPS delivery vans and larger vehicles).

[c] Not available.

[d] The fraction of cars and light-duty trucks that were diesel-fueled, as determined from vehicle registration information.

Each successive summer, the average vehicle model year was about one year newer. The average vehicle age was ~7 years in all cases. Pre-1980 model year vehicles comprised about 4% of the fleet; pre-1975 non-catalyst vehicles comprised 2% or less of the fleet each summer. The light-duty fleet was almost entirely gasoline-powered; the fraction of vehicles identified as diesel-fueled ranged from 1 to 2%. Therefore, > 95% of the vehicles in the tunnel were originally equipped with catalytic converters.

The distributions of average vehicle speeds measured during 200 tunnel drivethroughs that took place between 1600-1800 h are shown in Figure 2.1. Average vehicle speeds of 60 km $h^{-1}$ were typical, and no major changes in driving conditions were observed from one year to the next. Eighty-six percent or more of the drivethroughs in each summer had average speeds between 50 and 80 km $h^{-1}$. Slower speeds resulted from an occasional disruption in traffic flow, such as a vehicle stall inside the tunnel or heavy congestion downstream of the tunnel. Stalled vehicles were cleared rapidly from the tunnel by Caltrans personnel.

Instrumented vehicle measurements conducted in 1996 provided additional information about driving conditions. Figure 2.2 shows the average speed profile of the instrumented vehicle measured during 26 trips through the tunnel from 1600-1800 h. Average speed was 52 km $h^{-1}$ at the entrance, and 69 km $h^{-1}$ at the exit of the tunnel. Speeds were slower at the entrance because heavy congestion during the afternoon peak traffic period resulted in a queue of vehicles ahead of the tunnel entrance. Vehicle speeds beyond the middle of the tunnel were more uniform than in the first half of the tunnel. The driving pattern depicted in Figure 2.2 was very repeatable. Heavy accelerations and stop-and-go driving were seldom observed.

Figure 2.3 shows the instantaneous speeds and accelerations of the instrumented vehicle while driving through the tunnel. To account for the increase in engine load when driving on the 4.2% uphill grade inside the tunnel, an acceleration of $g \cdot \sin\theta = 0.41$ m $s^{-2}$, where $\sin\theta \approx \tan\theta = 0.042$, has been added to the measured vehicle acceleration. The outer boundary of the speed/acceleration domain of the LA-4 city driving cycle used in the Federal Test Procedure (FTP) is shown in Figure 2.3 for comparison with the driving conditions in the tunnel. Most of the driving in the tunnel occurred within a small range of speeds and accelerations, which were largely within the FTP domain. Nearly all points that were outside of this domain were due to higher accelerations. For some vehicles, this may have led to enrichment of the air/fuel mixture.

Driving conditions earlier in the afternoon differed from those observed from 1600-1800 h. Traffic volume from 1300-1500 h averaged 2740 ± 660 and 2620 ± 520 vehicles per hour in 1996 and 1997, respectively, which was about 60% of the 1600-1800 h

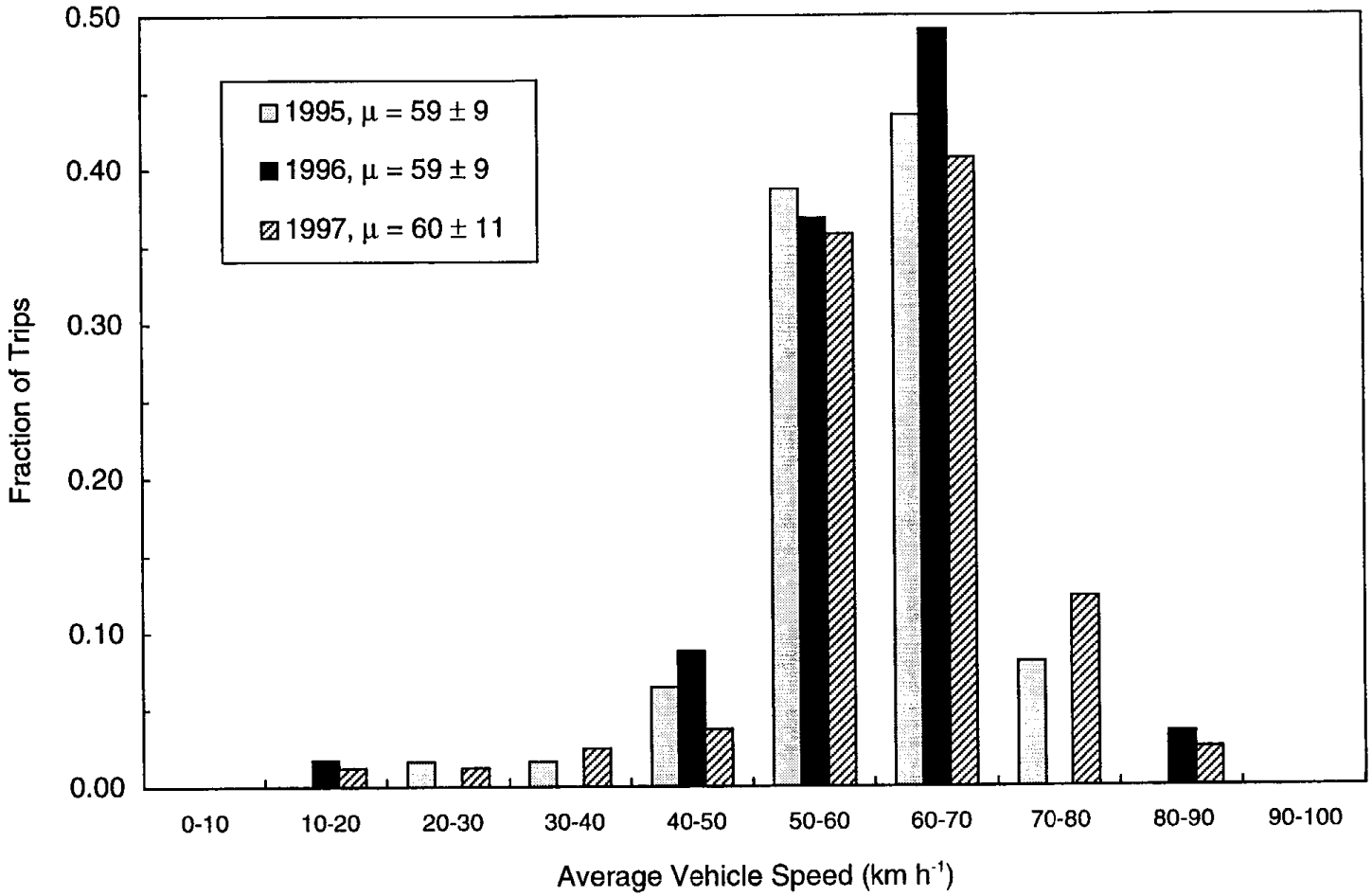


**Figure 2.1.** Histogram of average vehicle speeds measured during 200 drivethroughs in the Caldecott tunnel from 1600-1800 h.

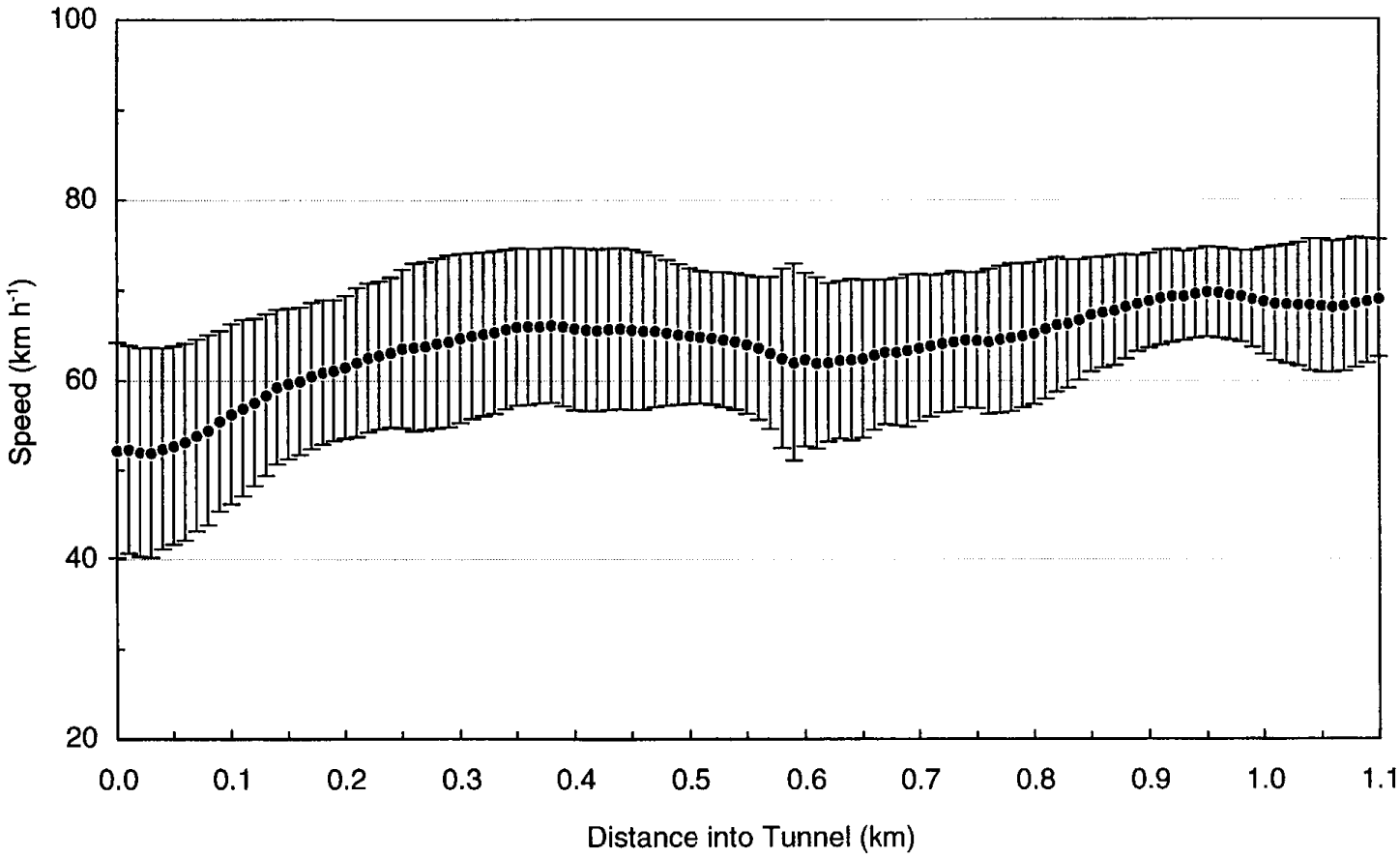


**Figure 2.2.** Average (± 1 standard deviation) speed profile in the Caldecott tunnel measured during 26 trips with an instrumented vehicle from 1600-1800 h in summer 1996.

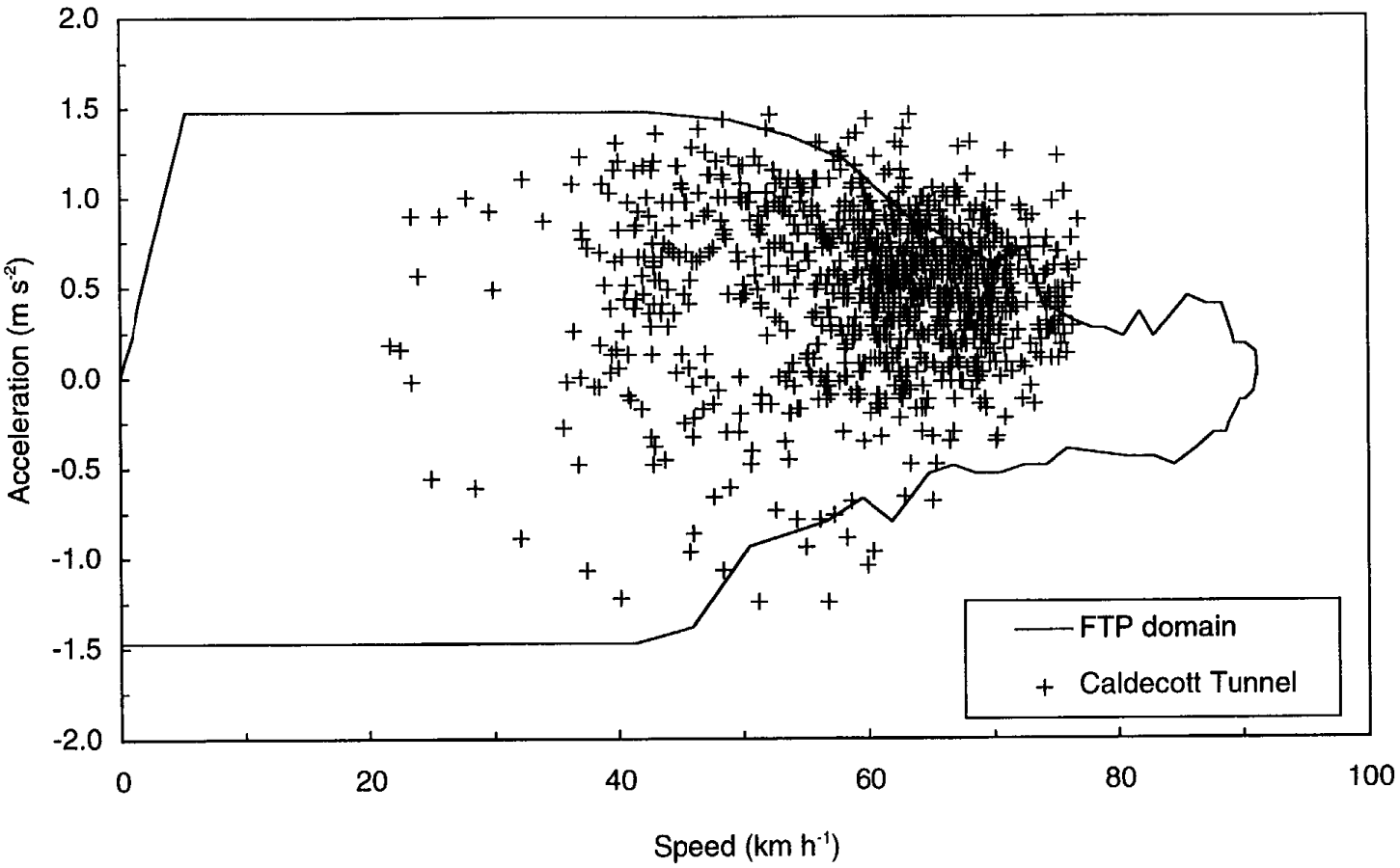


**Figure 2.3.** Second-by-second acceleration vs. speed plot for driving inside the Caldecott tunnel during summer 1996 (1600-1800 h).

volume. Since traffic was lighter, there was no queue of vehicles waiting to enter the tunnel. Vehicles typically entered, traveled through, and exited the tunnel at about the same speed. Vehicle speeds measured from 1300-1500 h during 50 additional drivethroughs were 79 ± 7 and 81 ± 7 km $h^{-1}$ in summers 1996 and 1997. These were ~20 km $h^{-1}$ faster than typical vehicle speeds observed from 1600-1800 h.

Traffic volume was lower, and vehicle speeds were higher, during the 1600-1800 h sampling period on August 6, 1996, relative to conditions observed on other sampling days due to a closure of multiple lanes on the San Francisco-Oakland Bay bridge, which is located to the west of the tunnel. Average traffic volume during this sample period was 3910 ± 210 vehicles per hour; the average speed was 71 ± 11 km $h^{-1}$, about 10 km $h^{-1}$ faster than usual. Therefore, measurements of vehicle emissions on August 6 were excluded from the calculation of summer 1996 emission factors.

### 2.3.4 Pollutant Concentrations

Background-subtracted pollutant concentrations measured during summers 1994-1997 at the Caldecott tunnel are presented in Table 2.3. Pollutant concentrations measured inside the tunnel were much higher than in background air. Concentrations of CO, $NO_x$, and NMHC were typically 25, 30, and 10 times higher in the tunnel air compared to background air. In all years, background concentrations of CO and $NO_x$ were very low and indicated that there was little or no recirculation of tunnel exhaust air back to the ventilation intake. For example, background CO concentrations were typically less than 2 ppm, whereas CO concentrations inside the tunnel were 20-30 ppm. Measured background $CO_2$ concentrations in summers 1996 and 1997 were 383 ± 36 and 380 ± 13 ppm, respectively. In 1994 and 1995, background $CO_2$ concentrations were not monitored continuously, so a typical concentration of 380 ppm was used to compute background-subtracted values of $CO_2$ shown in Table 2.3 for these summers.

### 2.3.5 Emission Factors

Vehicle emission factors were calculated from the measured pollutant concentrations shown in Table 2.3. Emission factors were computed as mass of pollutant emitted per unit volume of gasoline burned using the following equation:

$$E_P = \left(\frac{\Delta[P]}{\Delta[CO_2]+\Delta[CO]+\Delta[VOC]}\right)\left(\frac{MW_P}{MW_c}\right)w_c\rho_f \qquad (2.2)$$

where $E_P$ is the emission factor for pollutant P (g $L^{-1}$), $\Delta[P]$ is the increase in the concentration of pollutant P above background levels (ppm), $MW_P$ is the molecular weight of pollutant P (g $mol^{-1}$), $MW_c$ = 12 g $mol^{-1}$ is the molecular weight of carbon, $w_c$ is the

**Table 2.3.** Background-subtracted pollutant concentrations[a] measured from 1600-1800 h in the center bore of the tunnel.

| date | CO (ppm) | $CO_2$ (ppm) | $NO_x$ (ppm) | NMHC (ppmC) | benzene (ppbC) | formaldehyde (ppbC) | acetaldehyde (ppbC) | 1,3-butadiene (ppbC) | MTBE (ppbC) |
|---|---|---|---|---|---|---|---|---|---|
| **summer 1994** | | | | | | | | | |
| Aug 22 | n/a[b] | 573 | n/a | 2.86 | 202.3 | 24.0 | 7.1 | n/a | n/a |
| Aug 23 | 33.0 | 568 | n/a | 3.22 | 153.7 | 23.5 | 6.6 | n/a | n/a |
| Aug 24 | 32.8 | 640 | 2.08 | 3.08 | 189.7 | 26.4 | 8.6 | n/a | n/a |
| Aug 25 | 34.9 | 618 | 2.12 | 3.33 | 232.8 | 25.6 | 7.9 | n/a | n/a |
| Aug 26 | 33.1 | 558 | 1.85 | 3.03 | 240.7 | 23.7 | 7.4 | n/a | n/a |
| Aug 29 | 36.7 | 676 | 2.20 | 3.34 | 233.4 | 27.2 | 8.6 | n/a | n/a |
| Aug 30 | 29.1 | 459 | 1.70 | 2.58 | 175.8 | 17.4 | 5.7 | n/a | n/a |
| Aug 31 | 30.1 | 537 | 1.79 | 2.91 | 211.2 | 21.3 | 7.9 | n/a | n/a |
| Sep 01 | 27.9 | 468 | 1.57 | 2.73 | 209.4 | 18.2 | 5.8 | n/a | n/a |
| Sep 02 | 27.8 | 432 | 1.61 | 2.87 | 200.4 | 18.3 | 6.0 | n/a | n/a |

[a] Pollutant concentrations were measured in the tunnel air and in the background air injected into the tunnel by the ventilation fans. Shown here are background-subtracted values.

[b] Not available.

**Table 2.3.** continued.

| date | CO (ppm) | $CO_2$ (ppm) | $NO_x$ (ppm) | NMHC (ppmC) | benzene (ppbC) | formaldehyde (ppbC) | acetaldehyde (ppbC) | 1,3-butadiene (ppbC) | MTBE (ppbC) |
|---|---|---|---|---|---|---|---|---|---|
| **summer 1995** | | | | | | | | | |
| Jul 31 | 30.2 | 631 | 1.99 | n/a | n/a | 23.1 | 6.8 | n/a | n/a |
| Aug 01 | 33.8 | 696 | 2.02 | n/a | n/a | 25.3 | 7.1 | n/a | n/a |
| Aug 02 | 33.7 | 720 | 2.16 | n/a | n/a | 28.0 | 8.4 | n/a | n/a |
| Aug 03 | 32.6 | 681 | 2.04 | 3.84 | 193 | 25.8 | 7.9 | 27.7 | 14.5 |
| Aug 07 | 34.0 | 700 | 1.97 | 4.03 | 222 | 25.5 | 7.9 | 19.5 | 27.0 |
| Aug 08 | 34.4 | 711 | 2.32 | 3.23 | 198 | 24.5 | 7.1 | 24.2 | 17.5 |
| Aug 09 | 33.5 | 702 | 2.24 | 3.38 | 199 | 26.8 | 8.2 | 18.3 | 15.5 |
| Aug 10 | 31.6 | 676 | 2.08 | 3.49 | 191 | 26.3 | 7.8 | 26.6 | 21.1 |
| Aug 11 | 32.2 | 656 | 1.92 | 3.17 | 198 | 29.1 | 7.4 | 18.4 | 19.0 |
| Aug 14 | 32.6 | 688 | 2.08 | 3.10 | 186 | 22.6 | 6.4 | 16.5 | 14.5 |
| Aug 15 | 28.4 | 623 | 1.86 | 2.80 | 168 | 21.2 | 5.3 | 27.2 | 20.0 |
| Aug 16 | 28.9 | 618 | 1.91 | 2.66 | 170 | 23.0 | 5.4 | 22.9 | 18.5 |
| Aug 17 | 35.8 | 773 | 2.35 | 3.94 | 257 | 30.0 | 8.5 | 18.5 | 22.5 |

**Table 2.3.** continued.

| date | CO (ppm) | $CO_2$ (ppm) | $NO_x$ (ppm) | NMHC (ppmC) | benzene (ppbC) | formaldehyde (ppbC) | acetaldehyde (ppbC) | 1,3-butadiene (ppbC) | MTBE (ppbC) |
|---|---|---|---|---|---|---|---|---|---|
| **summer 1996** | | | | | | | | | |
| Jul 29 | 24.3 | 637 | 1.78 | 2.19 | 84.9 | 21.4 | 5.1 | 12.0 | 93.0 |
| Jul 30 | 26.8 | 664 | 1.77 | 2.38 | 91.9 | 25.5 | 4.8 | 11.2 | 99.0 |
| Jul 31 | 26.5 | 677 | 1.89 | 2.76 | 101.6 | 24.9 | 7.4 | 12.5 | 123.7 |
| Aug 01 | 25.0 | 658 | 1.91 | 2.70 | 91.7 | 28.9 | 6.0 | 11.7 | 136.0 |
| Aug 05 | 22.0 | 603 | 1.68 | 2.13 | 77.9 | 27.2 | 5.7 | 17.0 | 79.0 |
| Aug 06[c] | 23.2 | 504 | 1.52 | 1.59 | 74.8 | 23.3 | 4.4 | 9.0 | 68.5 |
| Aug 07 | 26.4 | 669 | 1.98 | 2.45 | 96.5 | 28.6 | 5.8 | 12.2 | 104.0 |
| Aug 08 | 27.0 | 627 | 1.86 | 2.66 | 95.7 | 27.4 | 5.7 | 11.9 | 125.5 |
| Aug 12 | 27.7 | 699 | 2.05 | 2.65 | 97.0 | 24.1 | 5.8 | 18.3 | 155.0 |
| Aug 13 | 25.2 | 626 | 1.74 | 2.42 | 85.2 | 22.5 | 6.4 | 10.0 | 119.5 |
| Aug 14 | 25.1 | 633 | 1.82 | 2.22 | 84.9 | 24.5 | 5.6 | 9.6 | 91.7 |
| Aug 15 | 26.4 | 686 | 2.18 | 2.67 | 94.6 | 25.0 | 5.8 | 18.2 | 131.0 |

[c] Traffic speeds were unusually high on August 6, 1996 during the 1600-1800 h sampling period, so pollutant concentrations measured on this day were excluded from the calculation of emission factors.

**Table 2.3.** continued.

| date | CO (ppm) | $CO_2$ (ppm) | $NO_x$ (ppm) | NMHC (ppmC) | benzene (ppbC) | formaldehyde (ppbC) | acetaldehyde (ppbC) | 1,3-butadiene (ppbC) | MTBE (ppbC) |
|---|---|---|---|---|---|---|---|---|---|
| **summer 1997** | | | | | | | | | |
| Jul 31 | 26.4 | 633 | 1.83 | 1.99 | 83.0 | 11.8 | 3.9 | 15.0 | 72.5 |
| Aug 01 | 24.8 | 605 | 1.76 | 1.97 | 78.3 | 14.2 | 4.0 | 14.8 | 65.0 |
| Aug 04 | 25.6 | 678 | 1.90 | 1.59 | 67.0 | 13.6 | 3.7 | 12.4 | 63.5 |
| Aug 05 | 27.6 | 723 | 2.02 | 2.02 | 80.7 | 15.4 | 4.5 | 14.4 | 92.5 |
| Aug 06 | 26.3 | 676 | 1.87 | 2.26 | 89.3 | 14.1 | 3.0 | 18.0 | 102.5 |
| Aug 07 | 28.2 | 701 | 1.89 | 2.37 | 94.4 | 15.7 | 5.7 | 17.2 | 96.9 |
| Aug 11 | 24.7 | 597 | 1.70 | 1.60 | 65.6 | 10.1 | 4.0 | 12.8 | 50.0 |
| Aug 12 | 25.5 | 621 | 1.73 | 1.78 | 79.7 | 15.8 | 4.8 | 18.0 | 68.3 |
| Aug 13 | 28.4 | 710 | 2.05 | 2.69 | 104.7 | 21.4 | 6.3 | 20.8 | 98.5 |
| Aug 14 | 27.4 | 718 | 1.98 | 2.47 | 92.0 | 21.6 | 6.3 | 18.4 | 97.1 |

weight fraction of carbon in gasoline, and $\rho_f$ is the density of gasoline (g $L^{-1}$). $NO_x$ emission factors are reported as nitrogen dioxide (i.e., a molecular weight of 46 g $mol^{-1}$ was used in eq 2.2 for $NO_x$ calculations), even though NO constituted 99% of the $NO_x$ measured in the tunnel. Since the FID is known to give a partial response to MTBE, equal to 86% of propane's response on a per carbon basis (Hoekman, 1992), NMHC concentrations reported in Table 2.3 include a small contribution from MTBE. True NMHC concentrations were calculated by subtracting 86% of the directly-measured MTBE concentrations (ppbC) from reported total NMHC concentrations measured by FID. NMHC emission factors were then computed assuming a molecular weight of 14 g per mole of C. Non-methane organic carbon (NMOC) emission factors were calculated as the sum of NMHC, MTBE, and formaldehyde emission factors. Additional contributions to total NMOC mass from other aldehydes and ketones were negligible. Gasoline densities used in eq 2.2 were obtained from fuel survey data shown in Table 2.1. Carbon weight fractions for summers 1994-1995 and summers 1996-1997 were 0.87 and 0.85, respectively. The lower carbon weight fraction for the more recent summers is a result of having ~2% oxygen by weight in gasoline.

### 2.3.6 Emission Trends

Average emission factors of regulated and toxic air pollutants measured each summer are shown in Figures 2.4 and 2.5. Note that for plotting purposes, emission factors for CO, benzene, and formaldehyde (HCHO) shown in these figures have been divided by a factor of ten. Within each year, emission factors were consistent from one day to the next, as reflected by the confidence intervals shown on the figures. This day-to-day consistency was expected because driving conditions were similar, and many of the same commuter vehicles traveled through the tunnel each day. Emission factors for 1,3-butadiene, which was found to be unstable in stainless steel canisters during tunnel sampling in 1994 (Kirchstetter et al., 1996), showed larger day-to-day variability.

Year-to-year and overall changes in emission factors from 1994 to 1997 are reported in Table 2.4. Whereas vehicle emissions shown in Figures 2.4 and 2.5 are expressed per unit volume of fuel burned and have not been adjusted to account for the 3% decrease in fuel economy due to RFG use, changes in vehicle emission rates reported in Table 2.4 do account for changes in fuel economy. Measured emission factors for 1996 and 1997 were multiplied by 1.03 to account for the 3% decrease in fuel economy relative to 1994 and 1995. Thus, values shown in Table 2.4 are representative of changes in emissions per km of vehicle travel.

As indicated in Figures 2.4 and 2.5, and in Table 2.4, vehicle emissions were significantly lower in 1997 than in 1994. Over the course of this study, emissions (per km

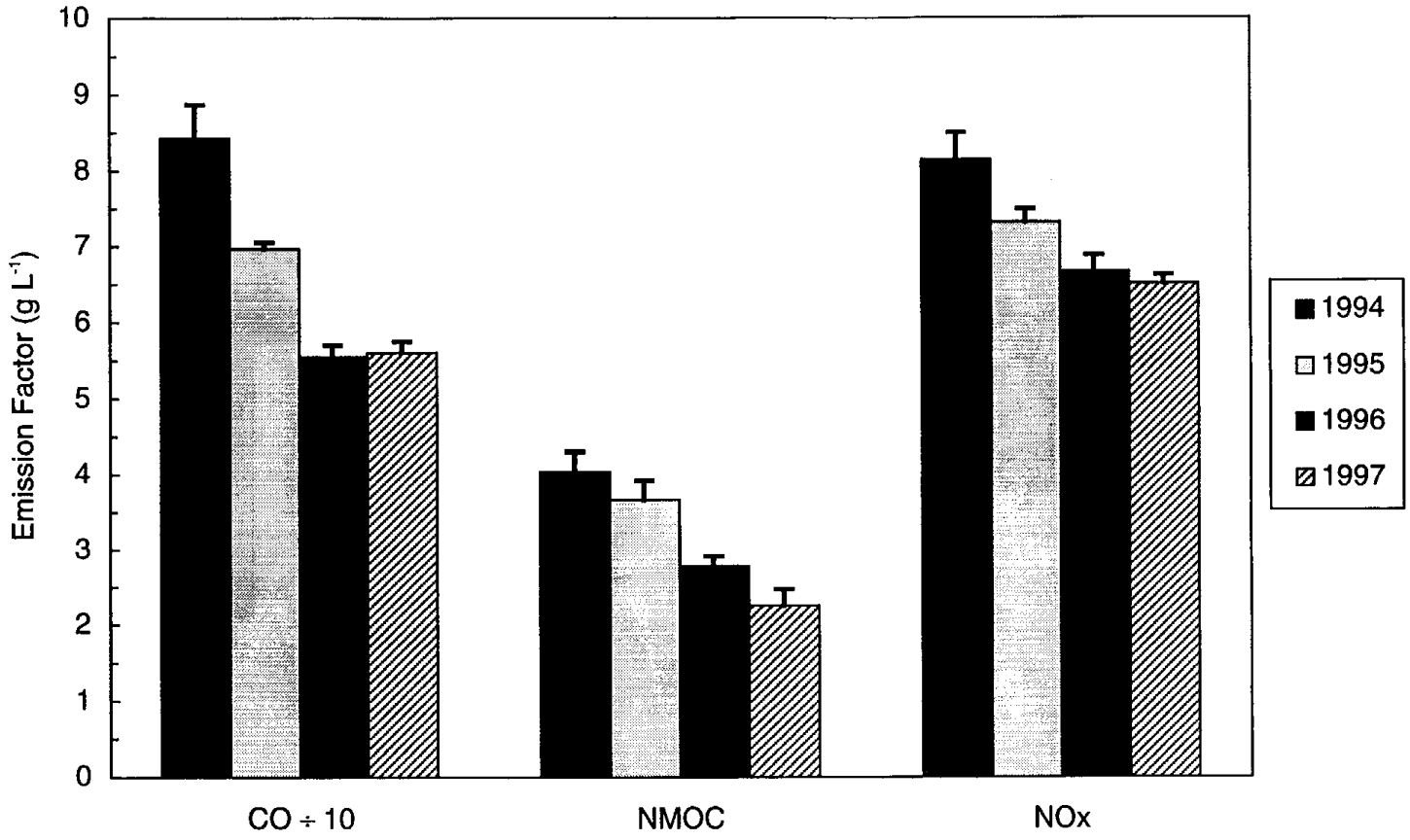


**Figure 2.4.** Average (+ 95% C.I.) light-duty vehicle emission factors for regulated pollutants measured in the Caldecott tunnel during summers 1994-1997.

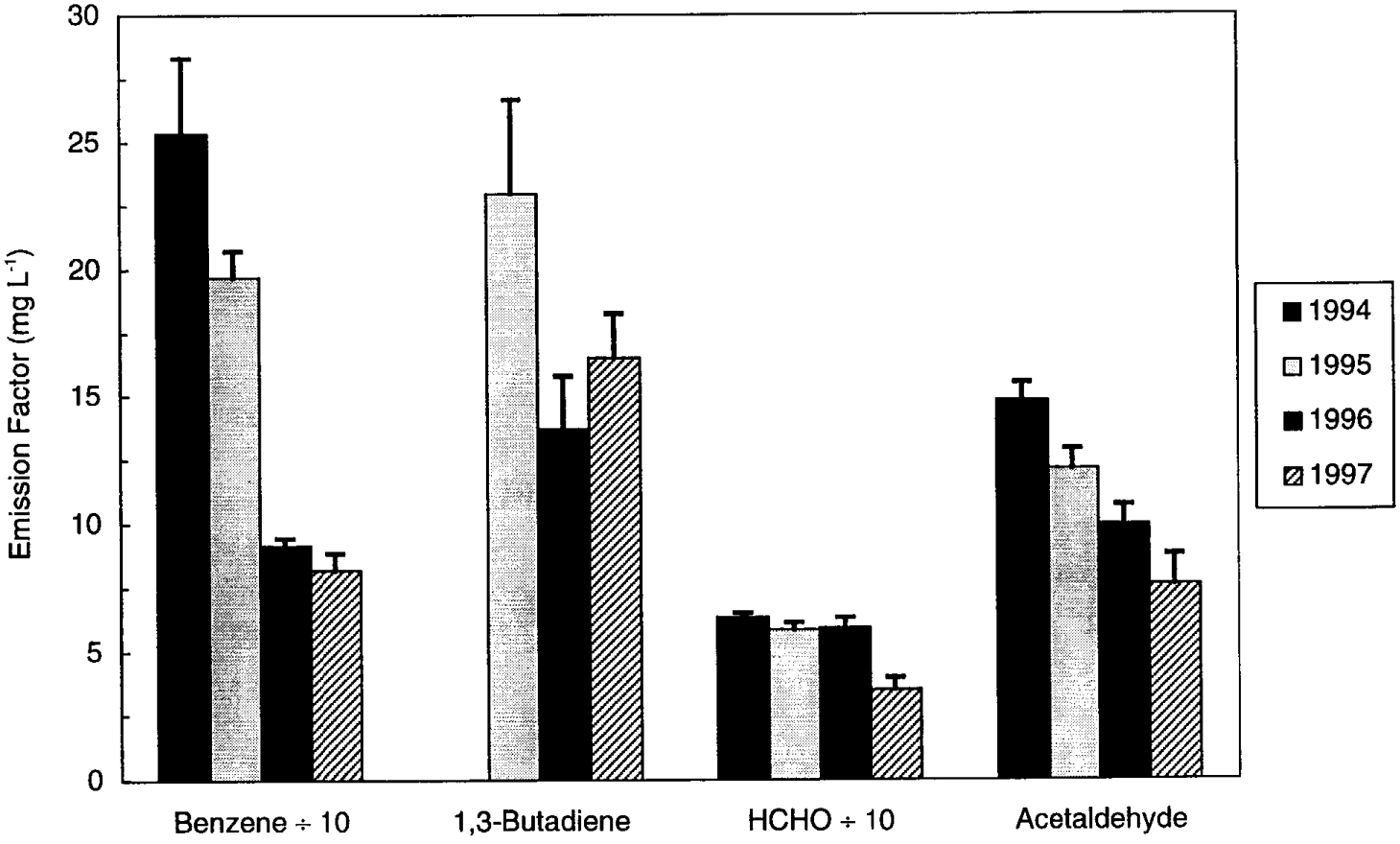


**Figure 2.5.** Average (+ 95% C.I.) light-duty vehicle emission factors for toxic pollutants measured in the Caldecott tunnel during summers 1994-1997.

**Table 2.4.** Percent changes between summers in vehicle emissions (g $km^{-1}$) measured during the 1600-1800 h sampling period.

| | % change in vehicle emissions[a] | | | |
|---|---|---|---|---|
| pollutant | 1994-1995 | 1995-1996 | 1996-1997 | overall 1994-1997 |
| CO | –17 ± 4 | –18 ± 2 | +1 ± 4 | –31 ± 5 |
| NMOC | –9 ± 8 | –22 ± 7 | –19 ± 8 | –43 ± 8 |
| $NO_x$ | –10 ± 4 | –6 ± 4 | –2 ± 3 | –18 ± 4 |
| benzene | –22 ± 11 | –52 ± 5 | –10 ± 7 | –67 ± 11 |
| 1,3-butadiene | n/a[b] | –39 ± 17 | +21 ± 10 | –26 ± 17[c] |
| formaldehyde | –8 ± 5 | +4 ± 8 | –41 ± 10 | –44 ± 8 |
| acetaldehyde | –18 ± 7 | –15 ± 9 | –23 ± 13 | –47 ± 8 |

[a] 95% confidence intervals for changes in vehicle emission factors calculated using eq 2.2. Emission factors shown in Figures 2.4 and 2.5 for 1996 and 1997 have been multiplied by 1.03 to account for the 3% decrease in fuel economy that occurred between 1995 and 1996. Thus, values reported here are representative of emission changes per km of vehicle travel.

[b] Not available.

[c] The overall change in 1,3-butadiene reported here is the change between 1995 and 1997, discounted for the decrease in fuel economy between 1995 and 1996.

of vehicle travel) decreased by 18% for $NO_x$; 31% for CO; ~45% for NMOC, HCHO, and acetaldehyde; and 67% for benzene. Butadiene was not measured in 1994; however, the emission factor for butadiene in 1997 was 26% lower than in 1995. For all pollutants except formaldehyde, a significant portion of the overall decrease in emissions occurred between 1995 and 1996, which is when most of the changes to gasoline composition occurred. Emission factors also changed between 1994-1995 and 1996-1997, when most gasoline properties were comparatively stable. Decreases in CO and $NO_x$ emissions between 1994-1995 were comparable to decreases between 1995-1996.

### 2.3.7 Temperature Effect

Ambient air temperature may influence vehicle emissions. For instance, greater use of air conditioning on hotter days increases engine load. Average 1600-1800 h temperatures in Berkeley, near the Caldecott tunnel, were 18, 20, 20, and 19°C during sampling periods in summers 1994-1997, respectively (Thorson, 1997). The differences from year to year

were negligible. In fact, afternoon temperatures varied much more from day to day within each summer than they did from one summer to the next. For example, the maximum and minimum afternoon temperatures during sampling in summer 1995 were 27 and 15°C, but there was no correlation between air temperature and emission factors (normalized to fuel consumption) measured at the tunnel. It is unlikely that air temperature had any effect on year-to-year changes in emissions measured in this study.

### 2.3.8 Emissions vs. Driving Condition

Emission factors for CO and $NO_x$ are plotted as a function of time of day in Figures 2.6 and 2.7. For both pollutants, emission factors decreased steadily during the course of the afternoon. Average CO and $NO_x$ emission factors measured from 1300-1500 h were about 40 and 20% higher, respectively, than from 1600-1800 h. This trend is attributed to the decrease in vehicle speeds, and hence in engine loads, during the course of the afternoon. As noted above, vehicle speeds were ~20 km $h^{-1}$ faster from 1300-1500 h compared to the later 1600-1800 h sampling period.

As noted above, vehicle speeds during the 1600-1800 h sample period on August 6, 1996 were about 10 km $h^{-1}$ higher than usual. Measured CO and $NO_x$ emission factors for this period were 15 and 4% higher, respectively, than the average 1600-1800 h emission factors measured on all other days in 1996. These changes are consistent with emissions trends during the period from 1300 to 1800 h described above. NMOC emissions on August 6 were 15% lower than the average for the other sampling days in summer 1996.

The CO emission factor exhibited a more pronounced trend than did the $NO_x$ emission factor, indicating that the CO emission factor was more sensitive to changes in engine load and air/fuel ratio. Fuel enrichment was probably more common from 1300-1500 h and during the high speed event of August 6, 1996 than during the typical 1600-1800 h period when most of the driving occurred within the domain of the FTP city driving cycle (see Figure 2.3). The same decreasing trend in CO and $NO_x$ emissions factors was observed over the course of the afternoon in both 1996 and 1997, and was expected since the same pattern of increasing traffic volume and decreasing average speeds from 1300-1800 h was observed in both years.

## 2.4 Discussion

Vehicle emissions were measured during four consecutive summers, 1994-1997, in order to quantify emission changes between summers 1995-1996 which spanned the transition to Phase 2 RFG use, and to measure the impact of fleet turnover on vehicle emissions between summers 1994-1995 and 1996-1997 when gasoline composition was expected to

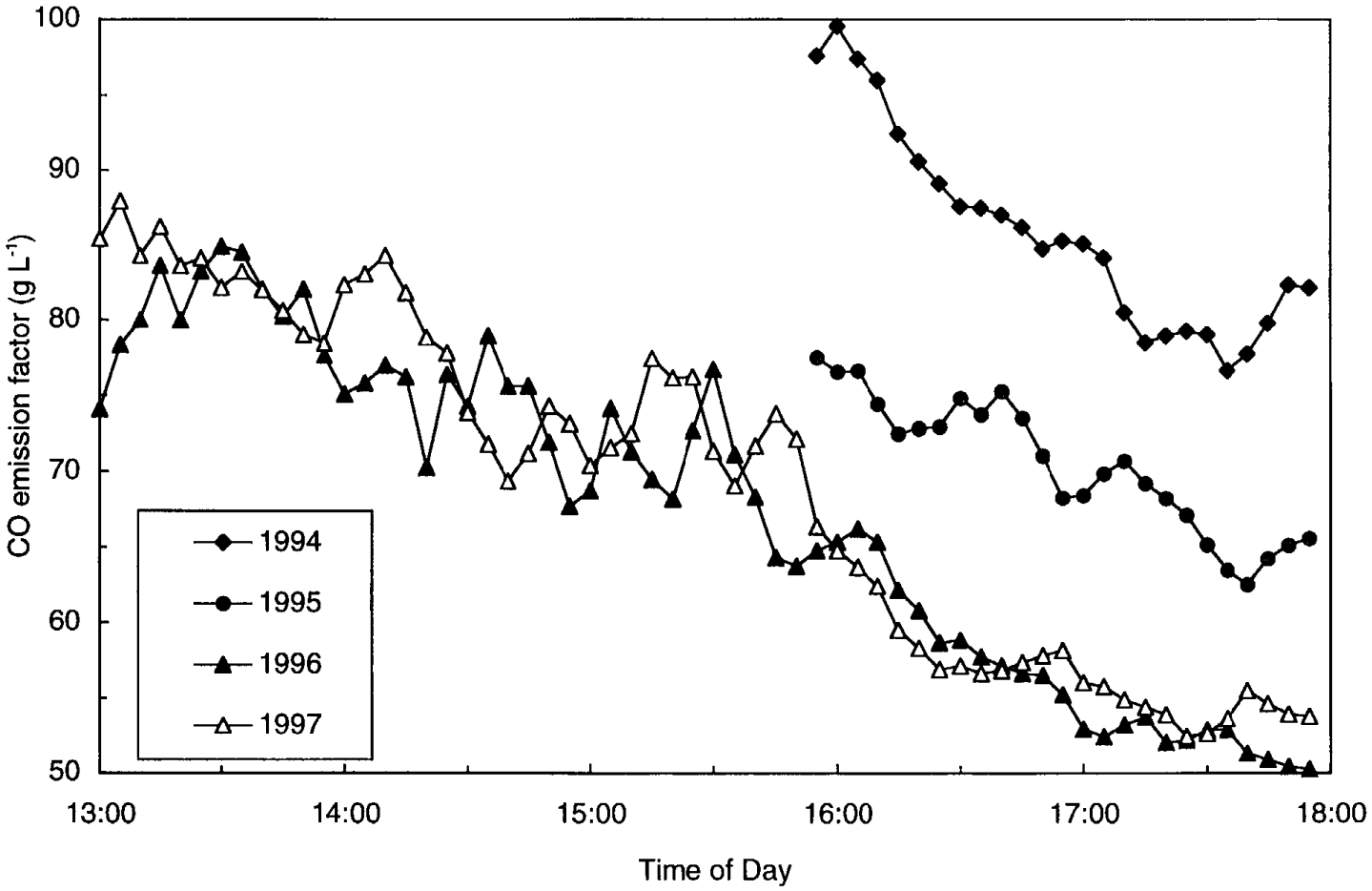


**Figure 2.6.** Fifteen-minute running average light-duty CO emission factors measured in the Caldecott tunnel.

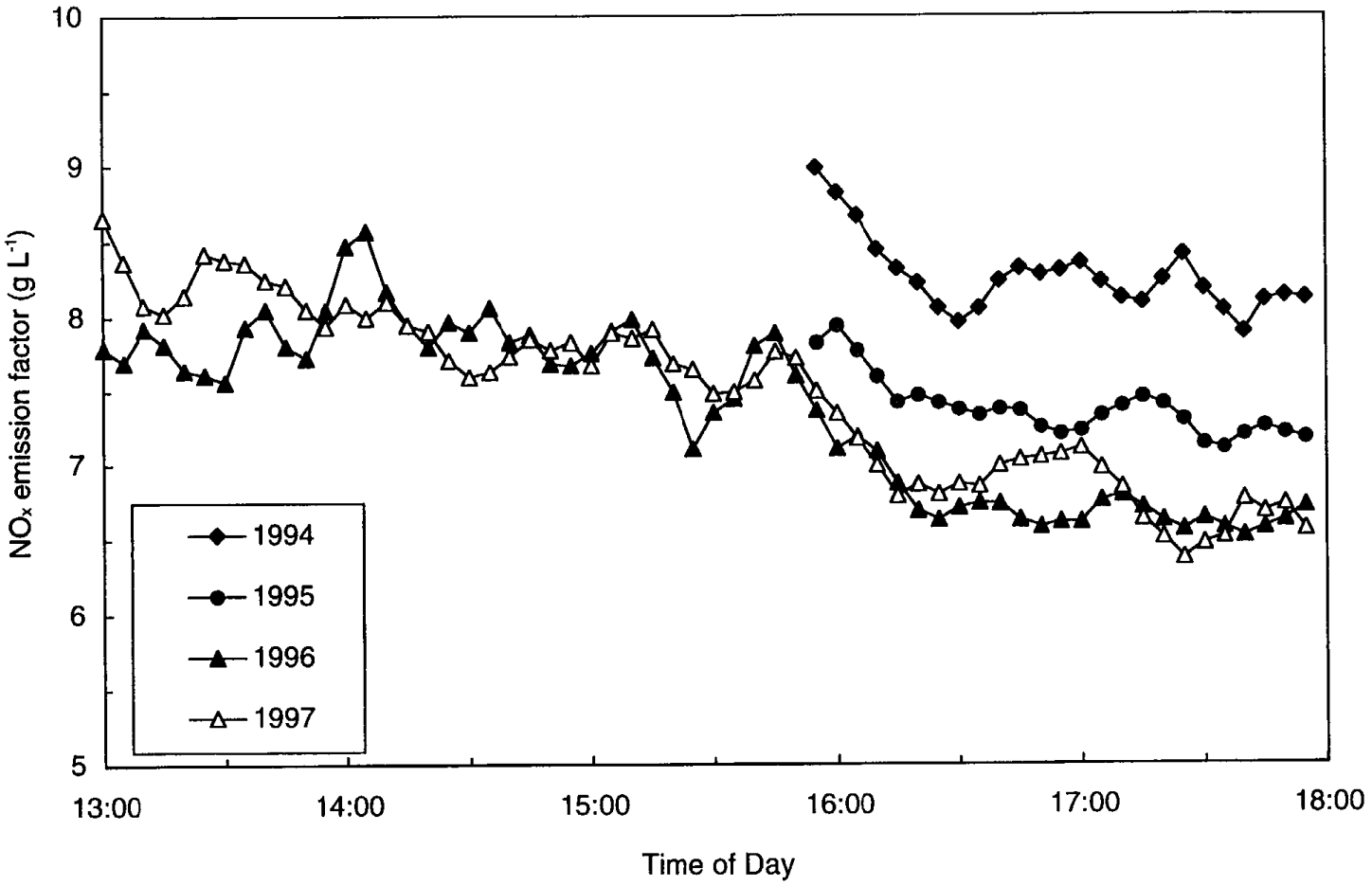


**Figure 2.7.** Fifteen-minute running average light-duty NOx emission factors measured in the Caldecott tunnel.

be relatively stable. It was anticipated that changes in emissions between summers 1995-1996 would express the combined effects of RFG use and fleet turnover, and that the RFG effect could be separated using measurements of the effect of fleet turnover alone.

Replacement of older vehicles with newer ones that have more robust emission controls and meet increasingly stringent emissions standards reduces fleet-average emissions. This is supported by a study of long-term vehicle emission trends in highway tunnels prior to the introduction of reformulated gasoline, which indicates that fleet turnover is the primary cause for reductions in on-road light-duty vehicle emissions (Pierson, 1995). Light-duty on-road vehicle emissions of CO decreased an average of 8.5% per year over the period from 1981 to 1992 (Pierson, 1995). The vehicle fleet traveling in the Caldecott tunnel was newer during each successive summer that measurements were conducted (see Table 2.2). Thus, it is reasonable to expect that fleet turnover contributed to the measured changes in emission factors.

Although it was expected in this study that changes in emission factors between 1994-1995 and 1996-1997 would be the result of fleet turnover alone, it appears that changes in fuel composition also may have been important. Assuming, for example, the 17% decrease in CO emissions measured at the Caldecott tunnel between 1994-1995 was due entirely to fleet turnover would be inconsistent with long-term trends in vehicle emissions measured in other tunnels (Pierson, 1995). Additionally, California's motor vehicle emission factor model, EMFAC version 7F, predicts only a 5-7% reduction in running exhaust emissions of CO, total organic gases, and $NO_x$ due to fleet turnover between 1993 and 1994 when fuel properties were stable.

Gasoline sulfur content decreased by about 50 ppm between 1994-1995 (Table 2.1). Experiments conducted during the Auto/Oil program indicate that reductions in gasoline sulfur content alone can have a significant impact on emissions, even when sulfur content is already low (Koehl et al., 1993). Average hot stabilized NMHC, CO, and benzene emissions from ten 1989 model year vehicles decreased by 32, 29, and 57% when gasoline sulfur content was reduced from 138 to 44 ppm. Average stabilized formaldehyde and acetaldehyde emissions also decreased significantly in the same test, and $NO_x$ emissions remained about the same. Therefore, changes in gasoline sulfur content may have affected emissions measured in the tunnel between 1994 and 1995, although the magnitude of the sulfur effect on the in-use fleet is uncertain.

Between summers 1996 and 1997, gasoline oxygen content decreased from $2.0 \pm 0.3$ to $1.6 \pm 0.6$ wt%; MTBE content decreased by about 2.8 vol% whereas alkane content in gasoline increased by about the same amount. Previous on-road studies indicate that addition of oxygenates to gasoline, in combination with other changes to fuel

properties such as a decrease in aromatics content, led to reduced CO and NMOC emissions (Bishop and Stedman, 1990; Lyons and Fox, 1993; Kirchstetter et al., 1996). In the Caldecott tunnel, Kirchstetter at al. (1996) measured decreases in CO and NMOC emissions of about 12 and 11%, respectively, per wt% increase in gasoline oxygen content. $NO_x$ emissions were not affected. The decrease in Bay Area gasoline oxygenate content between 1996-1997 may have affected emissions, but since other fuel properties such as sulfur and aromatics content did not change much during this period, the impact was likely less than a 4-5% increase in CO and NMOC emissions, offsetting some of the potential reductions due to fleet turnover. This may explain why CO emissions did not change between these years. It is unclear, however, why measured NMOC emissions decreased over the same period.

In conclusion, emission changes between summers 1994-1995 and 1996-1997 may be the result of both fleet turnover and changes to gasoline composition. Thus, it would be inappropriate to use these periods to estimate the pure effect of fleet turnover. Use of emissions changes between 1994-1995 as an estimate of the fleet turnover effect could negatively bias an estimate of the RFG effect if reduced gasoline sulfur content between 1994-1995 decreased emissions in the Caldecott tunnel. Any decrease in emissions between 1994-1995 due to reduced sulfur content should be included in, not subtracted from, estimates of the RFG effect. Similarly, use of emissions changes between 1996-1997 as an estimate of the fleet turnover effect may lead to an overestimation of the RFG effect. More precise estimates of the impacts of RFG would be possible if the fleet turnover effect was better understood.

### 2.4.1 Impact of Phase 2 RFG

Despite the uncertainties mentioned above, it was possible to reach several conclusions about the effects of RFG on vehicle emissions. Most notably, the impact of RFG was larger for NMOC than for $NO_x$. NMOC and $NO_x$ showed similar decreases between 1994-1995, whereas NMOC decreased nearly four times more than $NO_x$ between 1995-1996. A clear benefit of RFG use is reduced benzene emissions. Given the emissions changes reported in Table 2.4, the estimated impact of RFG on benzene emissions was a 30-40% reduction. The large reduction in butadiene emissions between 1995-1996 also suggests a significant RFG impact. It is not clear why butadiene emissions increased between 1996-1997. The overall reduction in butadiene from 1995-1997 (26±17%) is likely a lower bound estimate of the RFG benefit. Acetaldehyde emissions decreased about the same amount between each summer, indicating that there was no significant effect of RFG on acetaldehyde. An increase in acetaldehyde emissions would be expected if ethanol or ethyl tert-butyl ether (ETBE) were used instead of MTBE (Reuter et al., 1992).

Formaldehyde emissions increased between 1995-1996 despite the overall decrease in NMOC emissions, consistent with the increase in gasoline MTBE content (Gorse et al., 1991). Using the change in formaldehyde emissions between 1994-1995 as an estimate of the fleet turnover effect, the estimated RFG effect was a 12% increase. As shown in Table 2.4, formaldehyde emissions decreased substantially between 1996 and 1997. This decrease was due in part to the reduction in NMOC emissions, and to lower MTBE levels in 1997 gasoline as well (see Table 2.1). In addition, use of different DNPH-impregnated cartridges in 1997 led to less stable sample air flow rates which may have biased 1997 carbonyl measurements. The decrease in formaldehyde emissions between 1996 and 1997 was larger than expected given the fuel changes that occurred; the formaldehyde emission factor reported for 1997 appears to have been significantly affected by the change in DNPH cartridges that were used in field sampling.

Vehicle emissions of MTBE increased due to the introduction of reformulated gasoline. Emission factors calculated using eq 2.2 and MTBE concentrations shown in Table 2.3 increased from $26 \pm 4$ mg $L^{-1}$ in 1995 to $160 \pm 20$ mg $L^{-1}$ in 1996, and then decreased to $110 \pm 10$ mg $L^{-1}$ in 1997. The decrease in 1997 was the result of lower MTBE content in gasoline. Given that MTBE contributed 11 and 8% of gasoline mass in 1996 and 1997, respectively, and that gasoline density was ~740 g $L^{-1}$, then it follows that only 0.2% of MTBE in gasoline escaped combustion during tunnel driving.

RFG effects reported here do not apply to the entire California vehicle fleet. In this study, emissions were measured from on-road vehicles operating in a warmed-up mode, under loaded conditions, traveling at moderate steady speeds. The effects of RFG on emissions under cold-start or stop-and-go city driving conditions, and on other vehicle fleets may differ from those reported here and thus should be studied to assess more completely the impacts of RFG. For example, Gertler et al. (1997) measured vehicle emissions in the Sepulveda tunnel in southern California in 1995 and 1996. The vehicle fleet in that tunnel was about 3 years older, on average, than vehicles observed traveling through the Caldecott tunnel in the present study. As shown in Figure 2.8, the age distribution of vehicles traveling through the Caldecott tunnel in summers 1995-1997 was similar to the age distribution specified by California's motor vehicle emission inventory (MVEI) models for the Bay Area. Compared to the age distribution used in MVEI, there were more current model year vehicles, and fewer of the very oldest vehicles (15 or more years old) observed in the tunnel. The MVEI age distribution shown in Figure 2.8 already accounts for the fact that newer vehicles tend to be driven more than older ones.

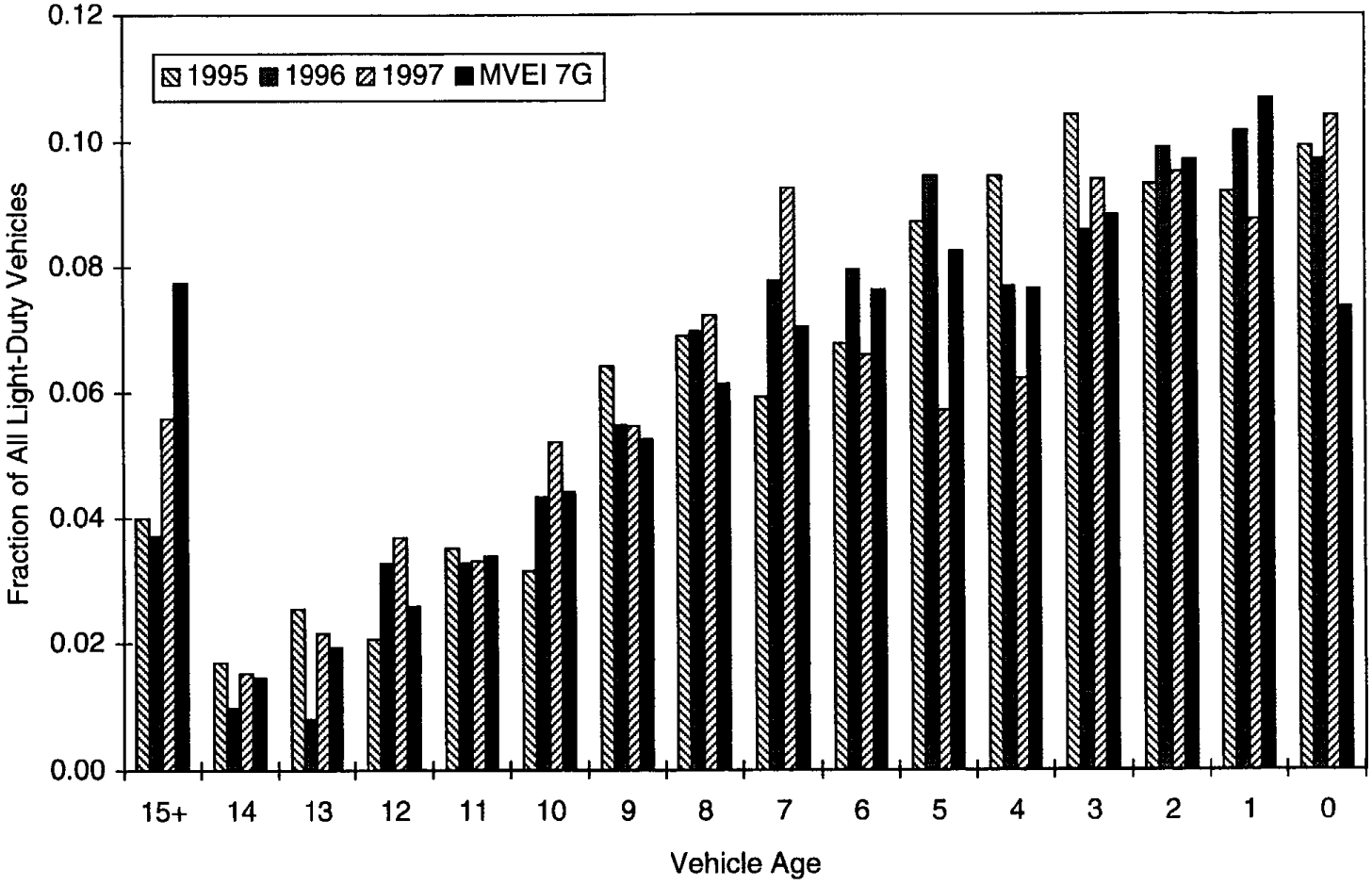


**Figure 2.8.** Observed age distributions of vehicles traveling through the center bore of the Caldecott tunnel. Also shown is the distribution of vehicle travel by model year as specified in MVEI 7G for the Bay Area.

### 2.4.2 Evaporative Emissions

The combined effect of Phases 1 and 2 of California's RFG program is a reduction of gasoline vapor pressure of ~20%. About one fifth of the overall reduction occurred between 1995 and 1996; most of the reduction occurred in 1992 in accordance with Phase 1 RFG specifications. Refueling and diurnal evaporative VOC emissions are expected to be reduced due to reductions in gasoline vapor pressure.

While use of RFG is expected to reduce evaporative emissions, it should be noted that, with the exception of running losses, evaporative emissions are not captured or reflected in the results from tunnel sampling reported in this study.

### 2.4.3 Implications for Air Pollution Control

A major objective of California's RFG program is to reduce toxic compound and ozone precursor emissions from motor vehicles. Motor vehicles contribute about 90% of all benzene emissions in the San Francisco Bay Area (BAAQMD, 1998). Use of RFG led to much lower benzene exhaust emissions. Consistent with the large benzene reductions measured in the Caldecott tunnel, average benzene concentrations in Bay Area ambient air decreased 56% between summers 1995 and 1996 (BAAQMD, 1998).

Despite difficulties in separating the effect of RFG from fleet turnover, this study indicated that RFG is more effective in reducing VOC emissions than it is in reducing $NO_x$ emissions. As discussed in the Chapter 3, additional benefits of RFG were found when the reactivity of evaporative VOC emissions was considered. When coupled with the fact that diesel engines contribute half or more of mobile source $NO_x$ emissions (ARB, 1995; EPA, 1996; Sawyer et al., 1998), it appears that California's RFG program is most attractive as an ozone control strategy in situations where ozone formation is VOC-limited. The RFG program is effective in reducing benzene emissions regardless of whether ozone formation is VOC or $NO_x$-limited.

# 3 Impact of RFG on Organic Gas Speciation and Reactivity

## 3.1 Introduction

Use of California reformulated gasoline (RFG) is intended to reduce summertime ozone air pollution by reducing emissions of ozone precursors: volatile organic compounds (VOC) and oxides of nitrogen ($NO_x$). RFG is also intended to reduce emissions of carbon monoxide and toxic organic compounds. In addition to expected reductions in mass emission rates, changes to gasoline composition can affect the speciation and reactivity of VOC emissions. The replacement of high-reactivity compounds such as alkenes with low-reactivity compounds such as methyl *tert*-butyl ether (MTBE) in gasoline is expected to result in corresponding changes in the composition of VOC emissions. Hoekman (1992) reported significant changes in the speciation of exhaust VOC emissions when vehicles were fueled with a reformulated gasoline.

While tailpipe exhaust emissions of VOC are important, significant additional emissions of VOC are associated with gasoline evaporation (Burns et al., 1992; Reuter et al., 1994; Brooks et al., 1995). Evaporative emissions occur, for example, due to vehicle fuel system leaks, during refueling, during the "hot soak" period immediately following vehicle operation, and over the course of a diurnal temperature cycle, which causes pressure changes in the vapor space above liquid fuel in gasoline tanks. Depending on the mechanism by which evaporative VOC are emitted, the chemical composition may resemble either whole liquid gasoline or gasoline headspace vapors. The composition of whole fuel provides a good description of liquid leak emissions, and headspace vapors describe certain refueling emissions. The compositions of diurnal, hot-soak, and running loss emissions lie somewhere between these extremes.

The goal of this study was to determine the impacts of California Phase 2 RFG on pollutant emissions. To this end, motor vehicle emissions were measured in the Caldecott tunnel, and gasoline samples were collected from service stations, prior to and after the introduction of RFG. Changes in the speciation and reactivity of exhaust and evaporative organic gas emissions that resulted from the switch to RFG are reported in this chapter.

## 3.2 Methods

### 3.2.1 Gasoline Sampling and Analysis

Regular and premium grade gasoline samples were collected from high-volume service stations located in Berkeley in August 1995 and 1996. The service stations represented the top five gasoline brands in northern California. Composite liquid samples for each gasoline grade were prepared by mixing measured amounts of individual samples in a low-temperature bath. The resulting regular and premium grade composites were sales-weighted mixtures of the individual brand samples (Gilson, 1995). Analytical results for these two composite gasoline samples were combined in proportions of 68% by volume regular and 32% premium to estimate the composition of the overall gasoline pool (Gilson, 1995).

Detailed liquid gasoline speciation was determined for the composite gasoline samples by gas chromatography (GC) (Kohler, 1997). Analyses were run on a Hewlett-Packard model 5890 II GC equipped with dual flame ionization detectors (FID) and electric flow control. Primary analysis was performed using a 60 m DB-1 capillary column of 0.25 mm ID and 0.25 μm stationary phase thickness. Secondary analysis was performed in parallel using a 60 m DB-5 capillary column of 0.25 mm ID and 0.25 μm stationary phase thickness. Where the primary DB-1 analysis suffered from co-elutions, the secondary DB-5 analysis was used to resolve the co-eluting peaks. Each run was temperature programmed from sub-ambient to approximately 250 °C. Peak identifications were based on spiking of authentic samples or corroborated by GC-MS identifications. Individual hydrocarbon mass response factors in the FID were calculated based on methane = 1.000. Oxygenate response factors were based on direct calibration with weighed standards.

### 3.2.2 Headspace Vapors

The composition of gasoline headspace vapors was predicted using the measured composition of liquid gasoline. Equilibrium headspace partial pressure for each compound identified in gasoline was predicted as:

$$P_i = \gamma_i x_i P_i^o \qquad (3.1)$$

where $P_i$ denotes the equilibrium partial pressure of species i in headspace vapor [atm], $\gamma_i$ is the activity coefficient of species i in liquid gasoline, $x_i$ denotes the measured mole fraction of species i in liquid gasoline, and $P_i^o$ is the vapor pressure of pure species i. Ideal solution behavior ($\gamma_i = 1$) was assumed in the application of eq 3.1. This assumption is

reasonable for hydrocarbon and MTBE mixtures, but is not valid for ethanol-gasoline mixtures (Bennett et al., 1993).

Individual compound vapor pressures, $P_i^o$, were determined with the Wagner equation:

$$\ln P_r^o = \frac{a\tau + b\tau^{1.5} + c\tau^3 + d\tau^6}{T_r} \qquad (3.2)$$

where $P_r^o = P_i^o/P_c$ is reduced vapor pressure, $T_r = T/T_c$ is reduced temperature, $P_c$ and $T_c$ are critical point pressure [atm] and temperature [K], $\tau = 1 - T_r$, and constants a, b, c, and d are tabulated for numerous organic compounds by Reid et al. (1987). Organic compound vapor pressures were predicted for T = 311 K (38 °C), the standard temperature for Reid vapor pressure determination. Parameters used in eq 3.2 to predict individual compound vapor pressures are given in Appendix D.

It has been noted (Reid et al., 1987) that extrapolation of the more widely-used Antoine equation to temperatures outside the range for which Antoine coefficients were determined may lead to serious errors in calculated vapor pressures. The Wagner equation is more robust and gives the correct shape of a vapor pressure curve over a wider range of temperatures, from $T_r = 0.5$ to $T_r = 1.0$ (Reid et al., 1987). Only the heaviest constituents of gasoline have critical point temperatures above 600 K, so the Wagner equation provides accurate vapor pressure estimates for all of the lighter compounds that are important contributors to gasoline headspace vapor composition and reactivity.

### 3.2.3 Field Sampling Site

As discussed in Chapter 2, vehicle emissions were measured in the center bore of the Caldecott tunnel during summers 1994-1997. Sampling was conducted during the afternoon commute period from 1600-1800 h when traffic direction through the tunnel was eastbound (uphill). The vehicles under study were operating in a warmed-up mode.

### 3.2.4 Vehicle Attributes

Chapter 2 reports in detail the driving conditions and the composition of the traffic in the tunnel. The main findings are summarized here. The number of vehicles traveling through the tunnel was consistently about 8400 during each two-hour sampling period. Traffic flow was generally smooth and vehicles drove through the tunnel at an average speed of about 60 km $h^{-1}$. Traffic consisted almost exclusively of light-duty vehicles, about two-thirds of which were cars and one-third were a combination of pickups, sport utility vehicles, and small vans. Heavy-duty trucks comprised < 0.3% of the vehicles in the center bore in each year. The average vehicle age was about 7 years in all four summers,

and the average vehicle model year was about one year newer each summer. Only 1 to 2% of the light-duty fleet was diesel-fueled and pre-1975 model year vehicles always comprised 2% or less of the fleet. Therefore, > 95% of the vehicles traveling in the tunnel were originally equipped with catalytic converters.

### 3.2.5 Organic Gas Measurements

Pollutant concentrations were measured in the traffic tube ~50 m before the tunnel exit, and in the clean background air which was injected into the tunnel by ventilation fans. Background concentrations were subtracted from pollutant concentrations measured inside the tunnel to determine vehicle emissions. Two-hour integrated air samples were collected in 6-liter stainless steel canisters for subsequent analysis to quantify hydrocarbon and MTBE concentrations. Similarly, two-hour integrated samples were collected using DNPH-impregnated silica cartridges for subsequent analysis to quantify carbonyl concentrations. Laboratory analytical procedures are discussed in Chapter 2.

### 3.2.6 Reactivity

The maximum incremental reactivity (MIR) scale developed by Carter (1994) was used to calculate the reactivity of whole liquid gasoline, gasoline headspace vapors, and on-road non-methane organic carbon (NMOC) emissions. The MIR scale is defined under conditions where VOC control is most effective in reducing ozone. Published MIR values (ARB, 1993a) were combined with detailed chemical composition profiles developed in this study. Reactivity was expressed per unit mass of NMOC emissions using the following equation:

$$R = \sum_{i=1}^{n} (MIR)_i \, w_i \qquad (3.3)$$

where R is the normalized reactivity [g of $O_3$ formed per g of NMOC emitted], $(MIR)_i$ is the maximum incremental reactivity for species i [g of $O_3$ formed per g of species i emitted], and $w_i$ is the weight fraction of species i in total NMOC emissions. MIR values used here are included in Appendix A, B, and C.

### 3.2.7 Quality Assurance

Measured NMOC concentrations were compared with independent analyses of tunnel air samples collected in parallel in summers 1995-1997. Independent analyses were performed by the California Air Resources Board, Desert Research Institute, and Rasmussen.

Measured concentrations of most individual hydrocarbons were in good agreement with independent analyses. In almost all cases, measured values agreed to within ±30%

for species concentrations above 20 ppbC (total NMOC concentrations in the tunnel were typically 2 to 4 ppmC). Measured MTBE concentrations were in good agreement with measurements by Rasmussen, but were 30% higher than values reported by Desert Research Institute. MTBE was not quantified in tunnel samples analyzed by the Air Resources Board.

Normalized reactivity was computed for each paired hydrocarbon sample using the speciation profile reported by each laboratory and eq 3.3. Computed normalized reactivity (R) for each co-located sample pair agreed within ±5%.

## 3.3 Results

### 3.3.1 Liquid Gasoline

As shown in summary form in Figure 3.1, the composition of the gasoline pool in 1996 differed markedly from that measured in 1995. Aromatic hydrocarbons constituted 44% of gasoline mass in 1995, and decreased to 29 wt% in 1996. Benzene content (included with aromatics in Figure 3.1) decreased from 2.0 to 0.6 wt%. Alkene content decreased from 5.7 to 2.6 wt%, mainly due to a reduction of $C_5$ and $C_6$ compounds, which comprised about two-thirds of gasoline alkene mass. These decreases were offset by increases in gasoline oxygenate and isoalkane content. The increase in oxygenate content from 1 to 11 wt% was due almost entirely to addition of MTBE to gasoline. Small amounts of tert-amyl methyl ether (TAME), typically less than 0.1 wt%, were present in some gasoline samples in both summers. Isoalkane content increased from 32 to 40 wt% between 1995 and 1996. Notable contributors to the increase in isoalkane content were highly branched, high-octane alkanes such as 2,2,4-trimethylpentane and 2,3,4-trimethylpentane which increased from 0.92 and 0.43 wt% in 1995 to 3.6 and 1.7 wt% of gasoline in 1996, respectively. Full liquid gasoline speciation profiles are included in Appendix A.

Figure 3.2 shows the contributions of NMOC groups to the total normalized reactivity of liquid gasoline. As indicated, aromatic hydrocarbons dominate the reactivity of unburned gasoline. Comparison of Figures 3.1 and 3.2 illustrates that aromatics and alkenes contribute more to gasoline reactivity than to gasoline mass, whereas alkanes and MTBE contribute much less to gasoline reactivity than to gasoline mass. Compared to unburned liquid gasoline in 1995, the reactivity of RFG was lower by 23%. The decrease in gasoline reactivity was due primarily to the decrease in gasoline aromatic content. The replacement of aromatic compounds in gasoline with MTBE was partly responsible for the decrease in gasoline reactivity because MTBE has low reactivity compared to most high-octane gasoline hydrocarbons. The reduction in alkene content also contributed to the reduction in gasoline reactivity.

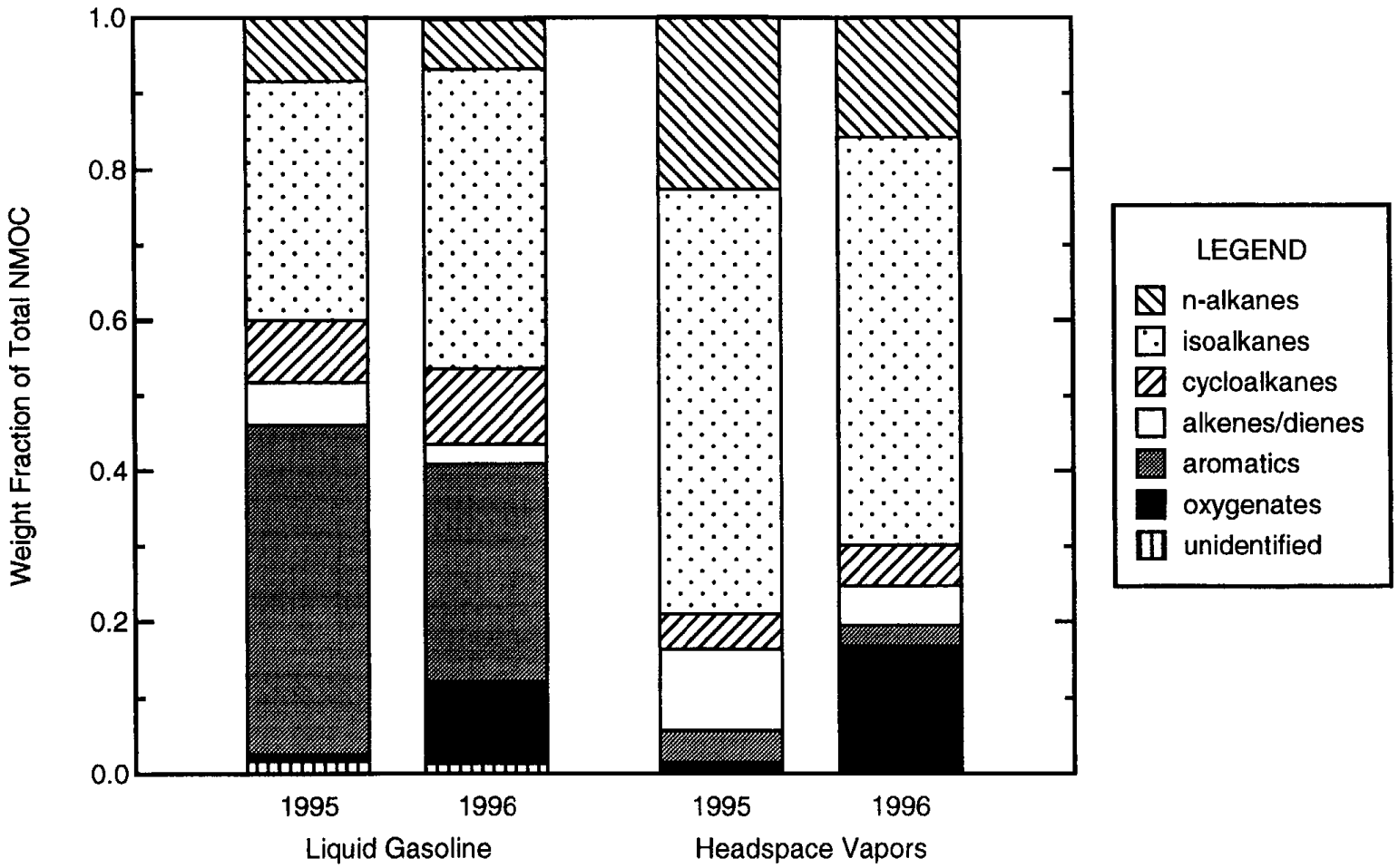


**Figure 3.1.** Composition of whole liquid gasoline and gasoline headspace vapors. Headspace vapor composition was predicted from measured liquid composition using eq 3.1.

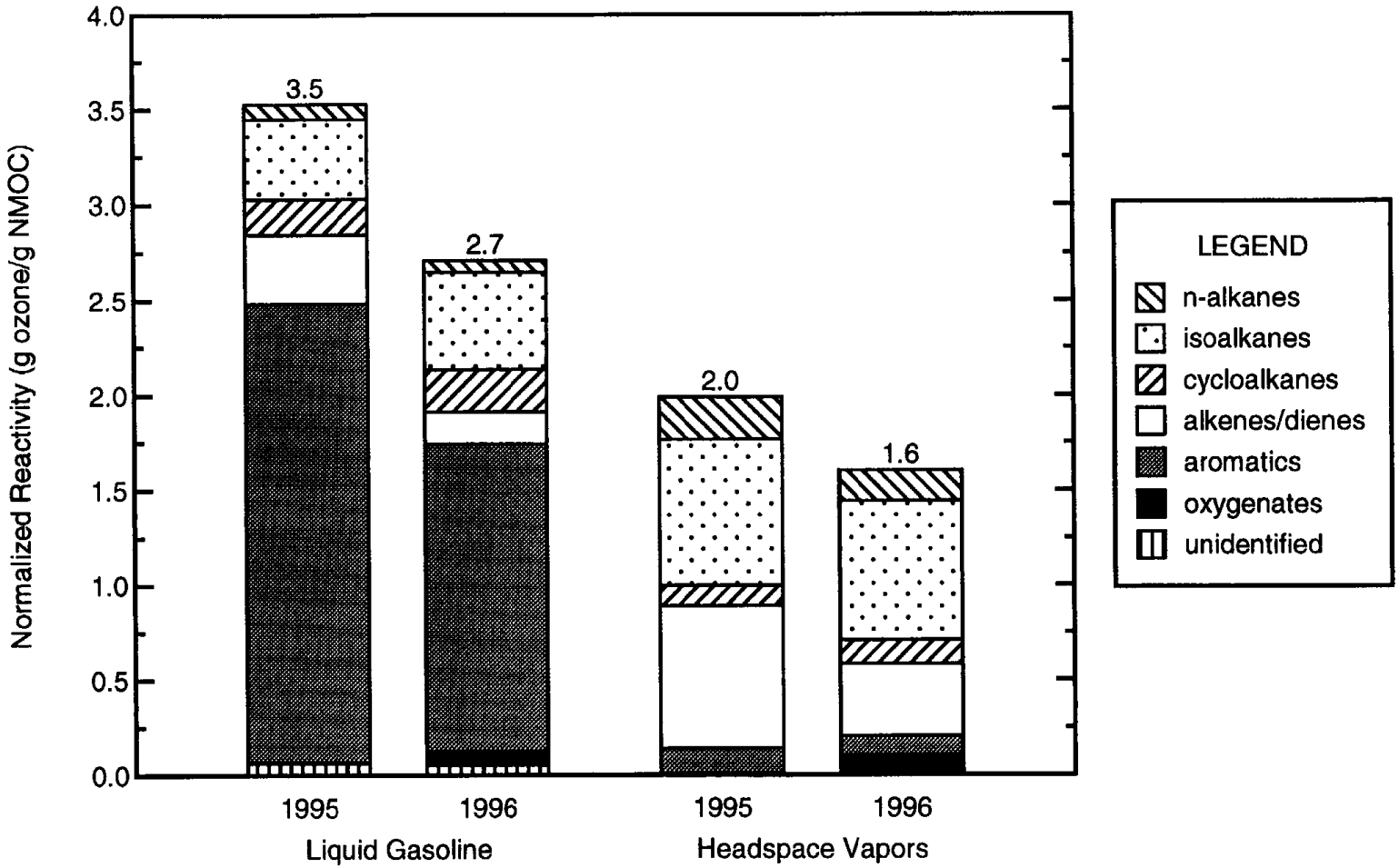


**Figure 3.2.** Contributions of organic compound groups to total normalized reactivity of whole liquid gasoline and gasoline headspace vapors. Calculated using eq 3.3 together with organic gas species profiles and MIR values presented in Appendix A and B.

### 3.3.2 Headspace Vapors

Headspace vapor composition profiles for 1995 and 1996 gasoline predicted using eq 3.1 are shown in Figure 3.1. The composition of headspace vapors is heavily weighted towards the lowest boiling components of gasoline. Low molecular weight alkanes are abundant; n-butane, n-pentane, and isopentane together accounted for about 50% of total headspace vapor mass for both 1995 and 1996 gasoline. Lighter aromatics, namely benzene and toluene, comprised more than 70% of the total aromatic hydrocarbon mass in headspace vapors. Consistent with changes in liquid gasoline composition between 1995 and 1996, the weight fractions of alkenes and aromatics in headspace vapors decreased, as shown in Figure 3.1. A large reduction of benzene in headspace vapors, from 1.2 to 0.4 wt%, contributed more than half of the reduction in aromatics. The weight fraction of MTBE in headspace vapors rose dramatically from 1.5 to 16.8%. Full headspace vapor speciation profiles are presented in Appendix B.

As indicated in Figure 3.2, the reactivity of gasoline headspace vapors in 1996 was 19% lower than that of 1995 gasoline. This decrease was mostly due to the reduction of $C_4$ and $C_5$ alkenes in gasoline. Overall, headspace vapors are less reactive than liquid gasoline (see Figure 3.2). Normal and isoalkanes, which dominate headspace vapor mass, have low reactivity. Also, compared to liquid gasoline, headspace vapors are depleted in the heaviest and most reactive aromatics, such as xylenes and trimethylbenzenes.

Predicted headspace vapor concentrations for the regular and premium grade gasoline samples were compared to those measured at 38 °C with a Reid vapor pressure bomb and a GC. GC analyses included determination of individual n-alkanes, isobutane, isopentane, 3-methylpentane, 3 cycloalkanes, 6 aromatic hydrocarbons, and MTBE. Other alkanes and aromatics, and all alkenes, were grouped by carbon number, e.g. total $C_5$ alkenes. As shown in Table 3.1, gasoline headspace vapor composition predicted using eq 3.1 agreed with measured values.

Whereas a fixed temperature of 38 °C was used to measure and predict headspace vapor composition, a range of temperatures are relevant when considering evaporative emissions to the atmosphere. However, since vapor pressures of all gasoline components increase with temperature, the relative abundance of individual VOC in headspace vapors varies much less with temperature than absolute gasoline vapor pressure. This was demonstrated by repeating the analysis (eqs 3.1 and 3.2) of headspace vapor composition using a lower temperature of 24 °C. While the total vapor pressure of gasoline decreased, predicted headspace vapor composition did not change significantly.

**Table 3.1.** Measured and predicted gasoline headspace vapor composition (wt% of total VOC) for regular and premium grade gasoline samples.

| | 1995 regular | | 1995 premium | | 1996 regular | | 1996 premium | |
|---|---|---|---|---|---|---|---|---|
| compound | meas[a] | pred[b] | meas | pred | meas | pred | meas | pred |
| n-butane | 9.1 | 9.3 | 10.8 | 11.3 | 6.2 | 6.4 | 6.0 | 6.0 |
| isobutane | 2.8 | 3.0 | 3.7 | 3.8 | 1.3 | 1.4 | 1.2 | 1.2 |
| n-pentane | 10.5 | 10.4 | 7.1 | 7.0 | 7.5 | 7.6 | 6.0 | 6.5 |
| isopentane | 38 | 37 | 40 | 38 | 38 | 34 | 39 | 37 |
| n-hexane | 2.2 | 2.1 | 1.4 | 1.4 | 1.7 | 1.7 | 0.6 | 0.8 |
| benzene | 1.5 | 1.3 | 1.3 | 1.1 | 0.5 | 0.4 | 0.4 | 0.3 |
| toluene | 2.1 | 1.8 | 2.6 | 2.2 | 1.2 | 1.6 | 1.9 | 1.6 |
| MTBE | 0.0 | 0.1 | 4.5 | 4.8 | 14.9 | 16.0 | 21.6 | 18.7 |
| total $C_4$ alkenes | 1.6 | 1.6 | 0.8 | 0.7 | 1.1 | 1.1 | 1.3 | 1.4 |
| total $C_5$ alkenes | 6.8 | 7.1 | 4.3 | 4.9 | 2.5 | 2.8 | 2.8 | 3.0 |
| total $C_6$ alkenes | 2.4 | 2.2 | 1.0 | 1.0 | 0.8 | 0.6 | 1.1 | 1.1 |

[a] Headspace vapor concentrations measured at 311 K with a Reid vapor pressure bomb and a GC.

[b] Equilibrium headspace vapor concentrations predicted using measured composition of liquid gasoline samples and eq 3.1 (see text).

### 3.3.3 On-Road Emissions

The composition of NMOC emissions measured in the Caldecott tunnel in summers 1994-1997 is summarized in Figure 3.3, and given in full detail in Appendix C. Changes to the composition of NMOC emissions between summers 1995 and 1996 were consistent with changes in gasoline composition that occurred over the same period. Weight fractions of total aromatics and benzene in tunnel NMOC emissions decreased from 33 to 26% and 5.4 to 3.3%, respectively, whereas MTBE increased from 0.7 to 5.5 wt%. Consistent with the addition of MTBE to gasoline, isobutene (included with alkenes in Figure 3.3) increased from 1.4 to 3.3 wt%, and formaldehyde (included with carbonyls) increased from 1.6 to 2.2 wt%. Other changes in on-road NMOC emissions between 1995 and 1996 included increases in the weight fractions of isoalkanes and cycloalkanes, and a decrease in the

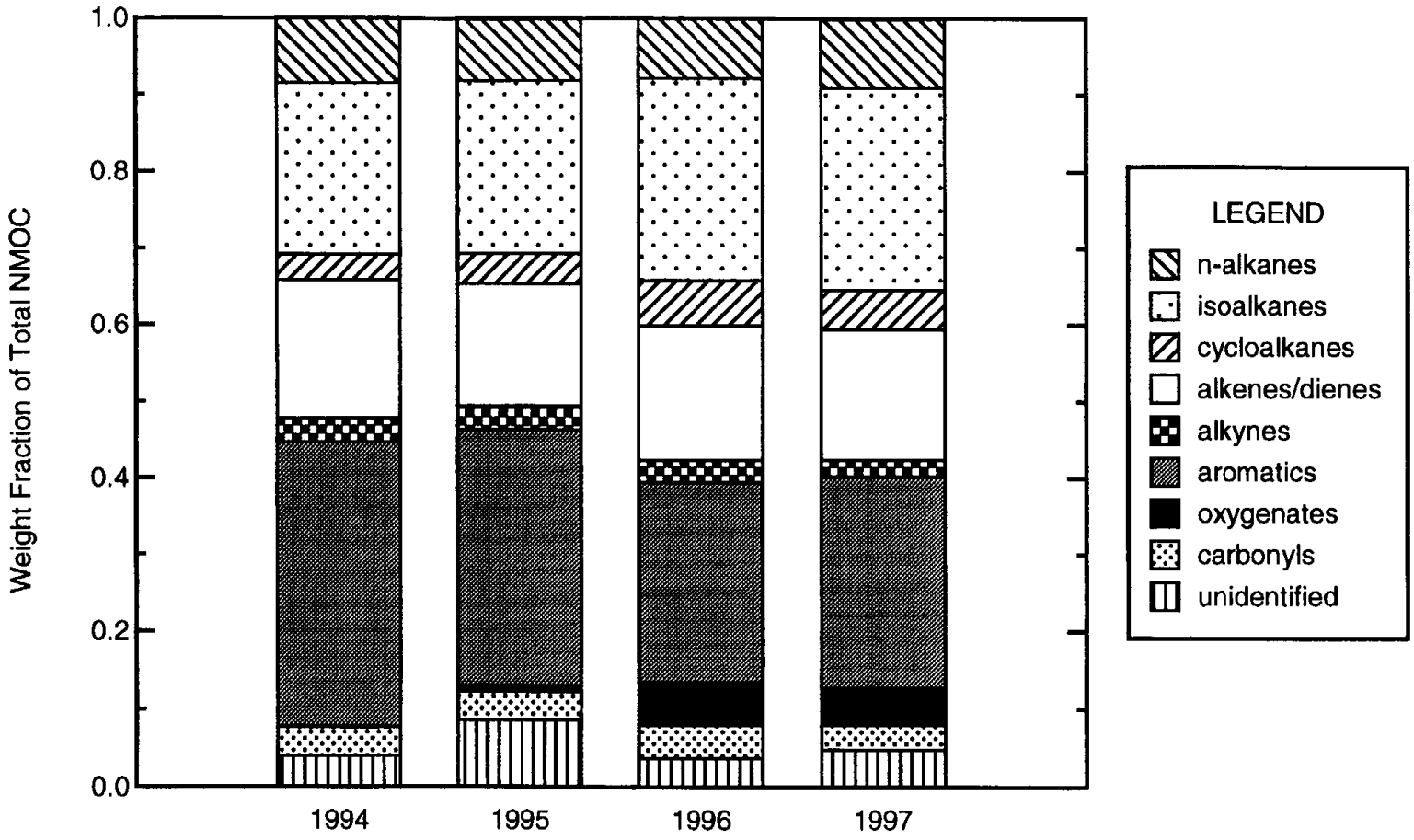


**Figure 3.3.** Composition of motor vehicle non-methane organic compound emissions measured in the Caldecott tunnel.

unidentified mass from 8.6 to 3.7 wt% of total NMOC. Increases in weight fractions of trimethylpentanes accounted for about half of the increase in total isoalkane content.

Changes in the composition of NMOC emissions between 1995 and 1996 resulted in an 8% decrease in reactivity, as shown in Figure 3.4. This reduction was less than the reductions found for liquid gasoline and headspace vapors because of increased weight fractions of combustion-derived isobutene and formaldehyde, which have high reactivity. While tailpipe exhaust is expected to contribute the majority of NMOC emissions in the tunnel, the 8% decrease in the reactivity of tunnel NMOC emissions may be due in part to changes in the reactivity of running evaporative emissions. Gertler et al. (1996) apportioned NMOC emissions in the Fort McHenry and Tuscarora Mountain tunnels and found that exhaust emissions comprised 85%, and evaporative emissions comprised 15% of total NMOC emissions in both tunnels.

The composition and reactivity of NMOC emissions was similar in summers 1994-1995 and in summers 1996-1997, as indicated in Figures 3.3 and 3.4. This was expected since the major changes to the properties of Bay Area gasoline occurred between summers 1995 and 1996. Gasoline MTBE content decreased from 11 to 8% between 1996 and 1997, and consistent with this decrease, weight fractions of MTBE, isobutene, and formaldehyde in on-road NMOC emissions also decreased.

Figure 3.5 compares the abundance of individual organic compounds in whole gasoline and tunnel NMOC. A distinctive feature is the linear relationship between the weight fractions of many individual compounds in tunnel NMOC and in whole gasoline. This relationship suggests that the origin of a significant fraction of NMOC in the tunnel is unburned gasoline. Combustion-derived species not present in gasoline, such as formaldehyde, ethene, propene, and isobutene, contribute significantly to NMOC mass and influence the overall reactivity of NMOC emissions. Taken together, $C_1$-$C_3$ organics plus isobutene contribute 20% of tunnel NMOC mass and 35% of tunnel NMOC reactivity. Compounds present in gasoline and found in tunnel NMOC at levels higher than expected due to emission of unburned gasoline alone, suggest a contribution from running loss evaporative emissions. As discussed above, n-butane, n-pentane, isopentane, benzene, and toluene are abundant in headspace vapors. Benzene emissions may also be higher than expected due to formation of benzene during combustion, and because benzene may escape oxidation to a greater degree than other gasoline constituents. The abundance of MTBE in tunnel NMOC is lower than expected based on its concentration in gasoline, indicating that MTBE may be preferentially oxidized compared to other fuel constituents. This is consistent with findings reported by Hoekman (1992).

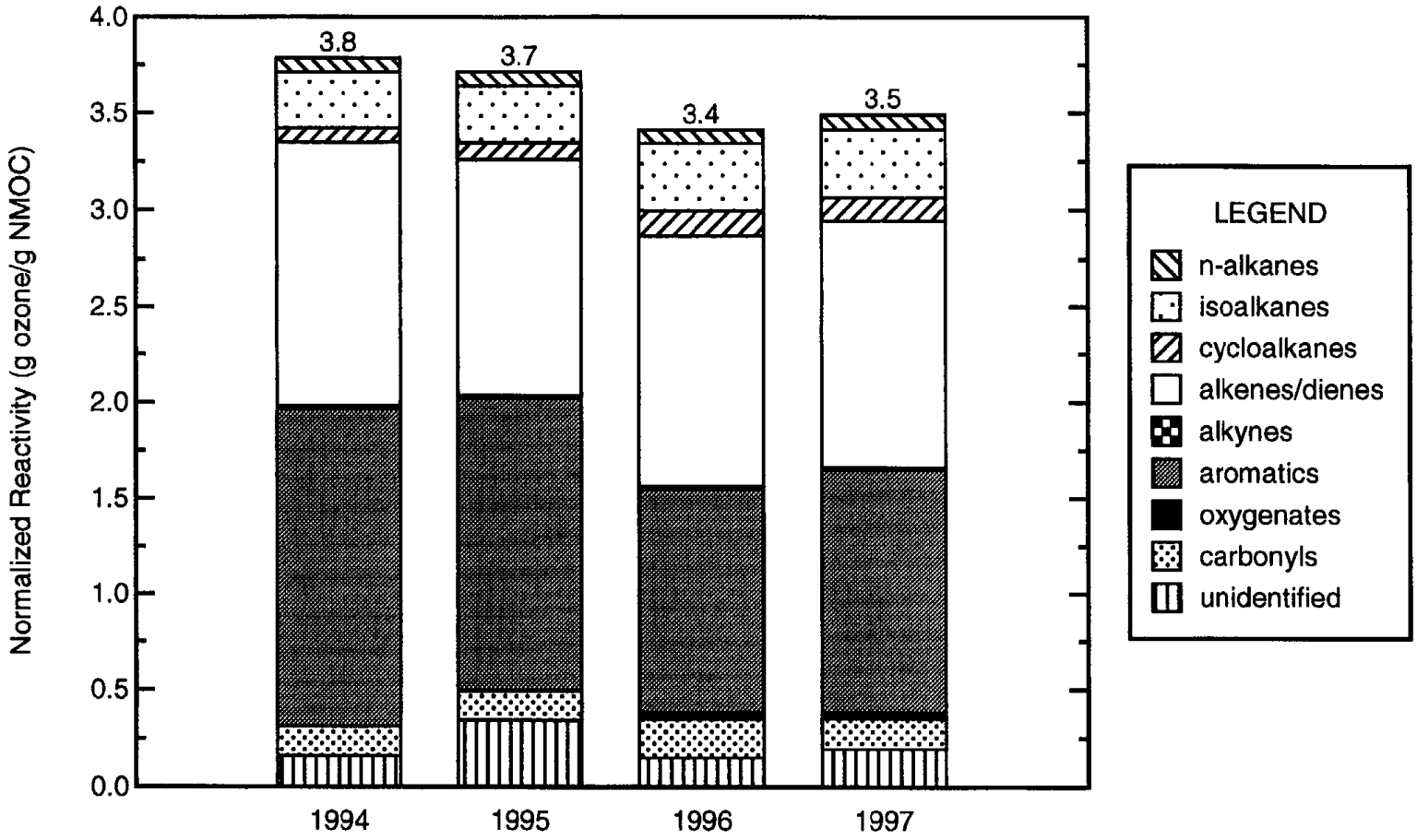


**Figure 3.4.** Contributions of organic compound groups to total normalized reactivity of vehicle emissions measured in the Caldecott tunnel. Calculated using eq 3.3 together with organic gas species profiles and MIR values presented in Appendix C.

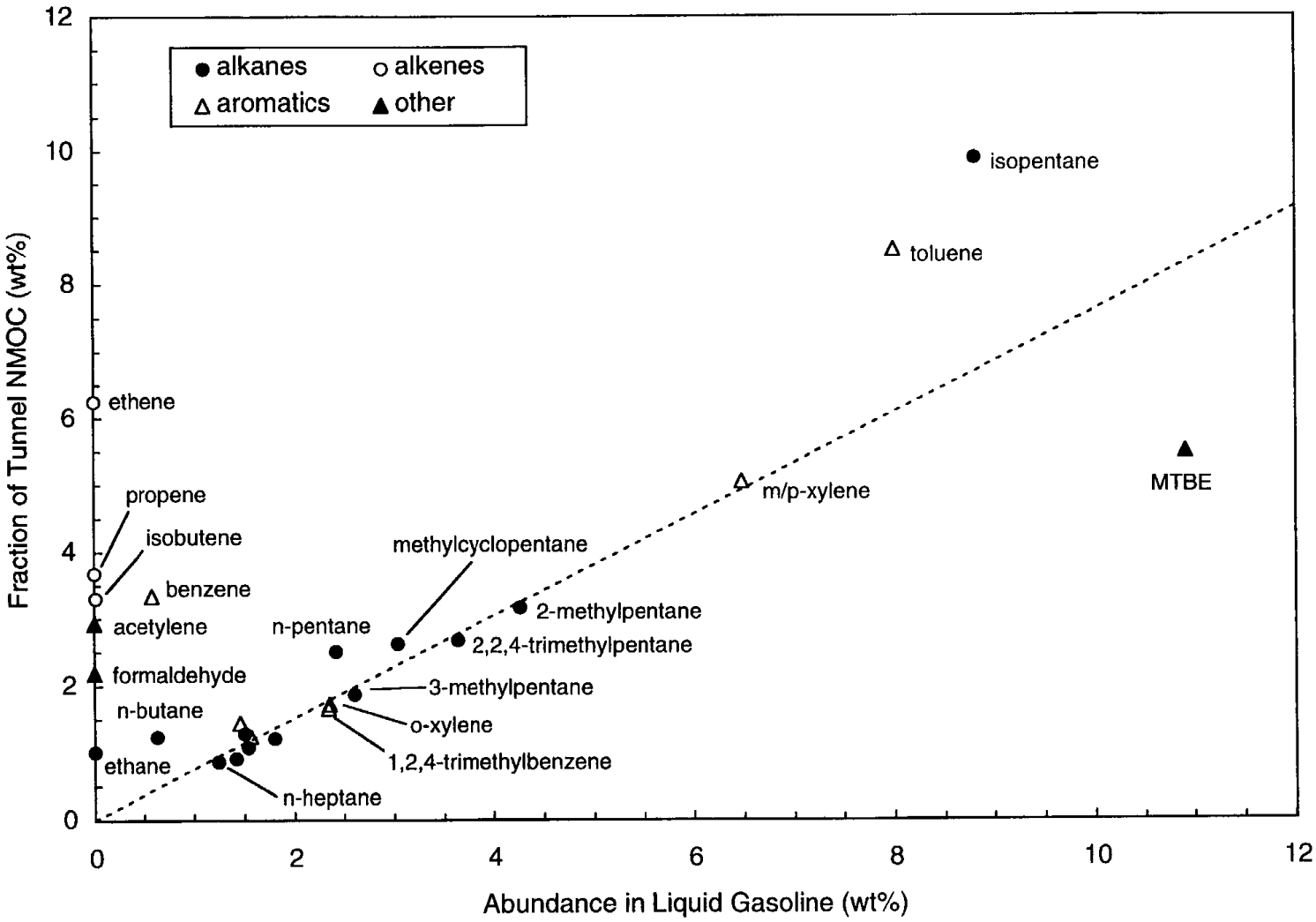


**Figure 3.5.** Comparison of concentrations of individual organic compounds in tunnel NMOC emissions with their abundance in liquid gasoline.

## 3.4 Discussion

### 3.4.1 Fleet Turnover

It was found during the 1994 field campaign (Kirchstetter et al., 1996), that the VOC speciation profile measured in the Caldecott tunnel for vehicles operating in a hot stabilized mode more closely resembled cold start exhaust than hot-stabilized emissions from well-maintained vehicles tested during the Auto/Oil program (Pollack et al., 1990; Hochhauser et al., 1991). In particular, Caldecott tunnel and cold-start NMOC emissions were abundant in ethene and acetylene, but depleted in methane. This suggested that on-road emissions were dominated by vehicles that lacked control of air/fuel ratio, and had reduced catalytic converter efficiency. As reported here, the composition of on-road NMOC emissions changed in response to changes in gasoline composition. However, over the course of this study, fleet turnover did not have a large impact on the speciation of NMOC emissions, as indicated by the similarity of tunnel NMOC emissions in summers 1994-1995 and summers 1996-1997 (see Figure 3.3 and Appendix C). The weight fraction of acetylene in tunnel NMOC was similar from 1994 to 1996, decreased from 2.9 to 2.2% between summers 1996 and 1997, and is still much higher than measured in new vehicle exhaust during the Auto/Oil study. The most recent VOC species profile measured in the tunnel in summer 1997 still closely resembles Auto/Oil cold start emission profiles.

### 3.4.2 Impact of Phase 2 RFG

Significant changes in the composition of gasoline occurred between 1995 and 1996 as a result of California's Phase 2 RFG program. As reported here for the San Francisco Bay Area, speciation profiles for exhaust and evaporative emissions changed significantly due to changes in gasoline composition. Liquid gasoline and headspace vapors now contain smaller amounts of compounds with high reactivity, such as alkenes and $C_8$+ aromatics. Emissions of headspace vapors that occur during refueling and emissions of whole gasoline that result from liquid leaks will therefore be less reactive. The reactivity of diurnal, hot-soak, and running loss evaporative emissions that have compositions lying between whole gasoline and gasoline headspace vapors also will be reduced. Therefore, part of the air quality benefit of Phase 2 RFG will be reductions on the order of 20% in the reactivity of evaporative emissions.

Inventory estimates for the Bay Area indicate that vehicle exhaust emissions comprised two-thirds, and evaporative emissions comprised one-third, of summertime reactive organic gas emissions from on-road motor vehicles before the introduction of RFG (ARB, 1995). Evaporative emissions that occur during gasoline distribution and refueling also contribute significantly to organic gas emissions (DeLuchi, 1993). Therefore, the

reactivity changes reported in this study for evaporative emissions do affect a significant fraction of organic gas emissions, but smaller reductions in reactivity are expected for exhaust, which is the larger contributor to total vehicle-related organic gas emissions.

The magnitude of the decrease in reactivity of tunnel NMOC emissions is uncertain because part of the decrease was due to reduced unidentified mass between 1995 and 1996, as shown in Figures 3.3 and 3.4. Not counting the change in reactivity due to the decrease in unidentified mass, the net effect of the other speciation changes in tunnel NMOC emissions was a 3% decrease in reactivity. This suggests the decrease in reactivity of on-road NMOC emissions due to RFG is likely between 3 and 8%. Alternatively, the effect of RFG on the reactivity of running emissions can be assessed by comparing NMOC composition measured in summers 1994 and 1996 since most gasoline properties were stable between summers 1994 and 1995, and the unidentified fraction of tunnel NMOC was the same in 1994 and 1996 (see Figure 3.3). Between 1994 and 1996, the reactivity of tunnel NMOC emissions decreased by 10%.

Reductions in gasoline vapor pressure due to use of RFG will reduce some types of evaporative emissions. For example, refueling and diurnal evaporative emissions will be reduced given reductions in gasoline vapor pressure. The ozone-forming potential of evaporative emissions therefore will be reduced both because of lower mass emission rates and because of reduced reactivity. Note however, that not all categories of evaporative emissions are sensitive to fuel vapor pressure. For example, evaporative emissions due to fuel spillage and leaks depend on the volume of liquid escaping, not the vapor pressure.

### 3.4.3 Implications for Ozone Control

The reactivity scale (MIR) used here is defined under conditions where VOC control is most effective in reducing ozone. Reactivity changes reported here are not applicable to conditions where ozone formation is $NO_x$-limited. Rather than focus on the absolute values of the calculated reactivities shown in Figures 3.2 and 3.4, it is more meaningful to consider the changes in reactivity relative to 1995 baseline values. Relative changes in reactivity are less sensitive than absolute values to environmental conditions, model assumptions, and $NO_x$ availability (Carter, 1994). To illustrate this point, reactivity calculations for gasoline headspace vapors were repeated using the maximum ozone incremental reactivity (MOIR) scale (Carter, 1994), under conditions where ozone formation is less sensitive to VOC emissions. Absolute reactivities were 1.01 and 0.87 g $O_3$ per g of NMOC in 1995 and 1996, respectively. While the calculated reactivities for headspace vapors using the MOIR scale are much lower than corresponding values based on the MIR scale (see Figure 3.2), the relative changes in reactivity between 1995 and 1996 are still similar: -19% based on MIR values, and -14% based on the MOIR scale. Thus,

changes to the speciation of evaporative emissions due to RFG use should lead to a less reactive mix of VOC emissions over a wide range of atmospheric conditions.

# 4 Fine Particles

## 4.1 Introduction

Engine dynamometer studies indicate that lowering fuel sulfur content reduces emissions of both sulfur dioxide and particulate sulfate (Wall et al., 1987). Increasing the cetane index, a measure of how readily diesel fuel autoignites, and lowering the aromatic content of diesel fuel have been shown to reduce $NO_x$ and PM emissions (Ullman et al., 1990; Nikanjam, 1993). Although carbon monoxide and hydrocarbon emissions from heavy-duty diesel trucks are of less concern, raising fuel cetane index also tends to reduce emissions of these pollutants (Ullman et al., 1990).

Prior to 1993, typical diesel fuel in California had an aromatic content of 31% by volume and a sulfur content (outside of the Los Angeles area) of 0.28% by mass (ARB, 1988). Effective nationwide in 1993, the composition of diesel fuel used for on-road applications was changed to reduce emissions. Diesel fuel was required to have either a cetane index of at least 40 or a maximum aromatic content of 35% by volume, and sulfur content was limited to 0.05% by mass. Additional requirements applicable to fuel sold in California limited diesel aromatic content to a maximum of 10% by volume (ARB, 1988). However, most refiners in California have chosen to develop alternative diesel fuel formulations having higher aromatic content that are less expensive to refine (e.g., Nikanjam, 1993). Alternative formulations are allowed if they provide equivalent emissions reductions. Use of California reformulated diesel fuel was expected to reduce oxides of nitrogen ($NO_x$), exhaust particulate matter (PM), and sulfur dioxide emissions from diesel vehicles by 7, 25, and 80%, respectively, in addition to reducing the carcinogenicity of diesel exhaust (ARB, 1988).

In recent years, diesel engine manufacturers have met increasingly stringent $NO_x$ and PM emission standards through advances in engine and control technology. Improvements to the fuel injection system including higher injection pressures, improved control of injection rate, and electronic control for precise timing of fuel injection have reduced particulate matter emissions. Improved combustion chamber design and increased

intake air swirl have also led to lower particulate emission levels (Sawyer and Johnson, 1995; Sawyer et al., 1998).

Whereas modern light-duty gasoline vehicles equipped with catalytic converters are generally not high emitters of PM, vehicles that burn oil or run very fuel-rich can have high PM emission rates. PM mass emission rates from light-duty vehicles that emit visible smoke (Cadle et al., 1997; Sagebiel et al., 1997), for example, are comparable to measured emission rates from heavy-duty diesel trucks (Hildemann et al., 1991; Lowenthal et al., 1994). Oxygenated gasolines (Kirchstetter et al., 1996; Chapters 2 and 3) now used in many areas of the country aim to reduce carbon monoxide and hydrocarbon emissions from vehicles that run fuel-rich through enleanment of the air/fuel mixture. Exhaust particulate emissions resulting from fuel-rich operation may also be reduced through the use of these gasolines.

In addition to emitting fine particles directly, motor vehicles emit precursor gases that react in the atmosphere to form secondary particulate matter. In California, secondary ammonium nitrate derived from direct emissions of $NO_x$ comprises a substantial fraction of fine particle mass during the fall and winter seasons, when ambient fine particle concentrations are typically highest (Solomon et al., 1989; Chow et al., 1992; Chow et al., 1993; Chow et al., 1994; Watson et al., 1994a; Chow et al., 1995). In the Los Angeles Area and the San Joaquin Valley, for example, ammonium nitrate constitutes from one-third to more than one-half of particulate mass on days with the highest 24 h average particle concentrations (Solomon et al., 1989; Chow et al., 1992; Watson et al., 1994a).

The recent adoption in the United States of a National Ambient Air Quality Standard for fine particles smaller than 2.5 μm in diameter ($PM_{2.5}$) requires a careful characterization of fine particle emissions from combustion sources such as motor vehicles. Given the introduction of reformulated gasoline in addition to the changes to diesel fuel and engine technology mentioned above, an updated assessment of on-road fine particle emissions is needed. The purpose of this research is (1) to measure on-road $PM_{2.5}$ and $NO_x$ emission factors for light- and heavy-duty vehicles, (2) to determine the chemical composition of $PM_{2.5}$ emissions, and (3) to assess the relative contributions of light- and heavy-duty vehicles to on-road fine particle and $NO_x$ emissions.

## 4.2 Methods

### 4.2.1 Field Sampling Site

Sampling was conducted in the two traffic bores of the Caldecott tunnel that carry traffic in the uphill direction: the southernmost bore (bore 1) which was used by both light- and heavy-duty vehicles, and the center bore (bore 2) which was reserved for light-duty

vehicles only. Measurements were made in bore 1 from 1230-1530 h when the percentage of heavy-duty trucks in the vehicle fleet was largest. Vehicle emissions were measured in bore 2 during the afternoon commuter traffic peak, from 1530-1830 h, when pollutant concentrations inside the tunnel were highest and traffic consisted almost entirely of light-duty vehicles. Field sampling took place during July and August of 1997, and included four days in bore 1 and four days in bore 2, as indicated in Table 4.1.

**Table 4.1.** Traffic volumes (vehicles $h^{-1}$) in the Caldecott tunnel, summer 1997.

| | axle class | | | |
|---|---|---|---|---|
| date | 3+ axles | 2-axle/6-tire | 2-axle/4-tire | % HD diesel |
| **Bore 1 (1230-1530 h)** | | | | |
| Jul 21 | 61 | 90 | 2040 | 4.8 |
| Jul 22 | 43 | 82 | 2208 | 3.7 |
| Jul 23 | 60 | 90 | 2149 | 4.6 |
| Jul 24 | 55 | 85 | 2377 | 3.9 |
| **Bore 2 (1530-1830 h)** | | | | |
| Jul 31 | 0 | 26 | 3871 | 0.33 |
| Aug 1 | 0 | 24 | 4115 | 0.29 |
| Aug 4 | 2 | 26 | 4163 | 0.36 |
| Aug 5 | 2 | 26 | 4188 | 0.36 |

### 4.2.2 Traffic Characterization

Vehicle attributes and driving conditions inside the tunnel were characterized each day of the study. Traffic volume, composition, age, and fuel type were determined through visual counts and license plate surveys. As shown in Table 4.1, traffic volumes in bore 1 from 1230-1530 h were typically 2200 vehicles per hour, and were about half as large as those in bore 2 from 1530-1830 h. Vehicles were counted in three categories according to number of axles and tires: 2-axle/4-tire; 2-axle/6-tire; and 3+ axles. The 1992 Truck Inventory and Use Survey (Bureau of Census, 1992), together with the results of license

plate surveys conducted at the tunnel, was used to determine the fraction of vehicles in each axle class that were heavy-duty diesel trucks. Analysis of truck census data for California suggested that almost all (>99%) vehicles with 3 or more axles are heavy-duty diesel trucks. License plate surveys conducted at the tunnel during this study (see below) and during previous summers indicate that <2% of 2-axle/4-tire vehicles are diesel-powered; most of those that are diesel-powered are light-duty passenger vehicles. The number of 2-axle/6-tire vehicles that were diesel-powered was less certain. Survey data indicated that 45-68% of these trucks were diesel-powered. The higher value resulted when pickups and vans as well as single-unit trucks were included in the analysis of survey data. For this study, we assumed that 50% of the 2-axle/6-tire vehicles were heavy-duty diesel trucks. Based on these classifications, traffic in bore 1 was estimated to include 4.2% heavy-duty diesel trucks on average. More than half (56%) of these were large trucks with three or more axles. By contrast, heavy-duty diesel trucks comprised only 0.3% of traffic in bore 2, and very few of these were large trucks with three or more axles, as indicated in Table 4.1. Traffic in bore 2 consisted of about two-thirds cars and one-third light-duty trucks (pickups, vans, and sport utility vehicles).

License plates were recorded as vehicles exited the tunnel and were later matched with vehicle registration data to determine vehicle model year. The average model year of 156 heavy-duty diesel trucks observed in bore 1 was 1988. The average model year of 788 randomly selected light-duty vehicles observed in bore 2 was 1991; fewer than 2% were pre-1975 model year and based on vehicle registration records only 1.8% were diesel-powered. Thus, greater than 95% of the light-duty vehicles in bore 2 were originally equipped with catalytic converters.

Two cars were used to measure the speed of vehicles traveling through the tunnel. One car was equipped with a computer to log vehicle speed at 1 s intervals, and the second car was used to measure average traffic speed based on manually recorded transit time through the tunnel. The average speed of traffic in bore 2 during rush hours (1530-1830 h) on all four sampling days was 59 ± 10 km $h^{-1}$ (n = 27). Average vehicle speeds inside bore 1 early in the afternoon (1230-1530 h) were faster because traffic volumes were smaller. Light-duty vehicles traveled through bore 1 at an average speed of 70 ± 9 km $h^{-1}$ (n = 17) on July 22-24, and 89 ± 11 km $h^{-1}$ (n = 8) on July 21. The average speed of heavy-duty diesel trucks in bore 1 was 65 ± 11 km $h^{-1}$ (n = 13). Traffic was generally smooth flowing; stop-and-go driving and heavy accelerations were rarely observed.

### 4.2.3 Gaseous Pollutant Measurements

Tunnel pollutant concentrations were measured in the traffic tube ~50 m before the tunnel exit. Background pollutant concentrations were measured at the fresh air intake ventilation

fans. Concentrations of carbon monoxide (CO), carbon dioxide ($CO_2$), and $NO_x$ were measured continuously. CO and $CO_2$ concentrations were quantified using gas filter correlation spectrometers (Thermo Environmental Instruments, Franklin, MA, models 48 and 41H, respectively), and $NO_x$ was measured with chemiluminescent analyzers (Thermo Environmental Instruments model 42). Analyzers used to measure pollutant concentrations inside the tunnel were located in the fan room above the tunnel exit. A ~50 m Teflon sample line was used to draw air samples directly from the traffic tube.

Using traceable gas standards, zero and span checks were performed several times a week on each analyzer. The Quality Assurance Section of the California Air Resources Board conducted a performance audit of the CO and $NO_x$ analyzers, as discussed in Chapter 2.

### 4.2.4 Continuous Particle Measurements

Particle concentrations in the tunnel were measured continuously and recorded as 15 s averages using a condensation nucleus counter (CNC), an optical particle counter (OPC), and an aethalometer. The CNC (model 3760, TSI Inc., St. Paul, MN) measured particle number concentrations for particles with diameters larger than 0.01 μm. The OPC (model LAS-X, Particle Measuring Systems, Boulder, CO) counted and optically sized particles with diameters between about 0.1 μm and 2 μm. The optical sizing by the OPC was calibrated with monodisperse fractions of tunnel aerosol selected using a differential mobility analyzer. The aethalometer (Magee Scientific, Berkeley, CA) measured a black carbon mass equivalence by optical attenuation of particles collected on a quartz filter.

The OPC and CNC sampled through 46 m of copper tubing with an inner diameter of 6.3 mm at a flow rate of 5.2 L $min^{-1}$. The transport flow was chosen to minimize particle losses due to turbulence ($Re < 1200$) or sedimentation. The pressure drop across this sampling line was 0.035 atm. All inlet tubes for the real-time instruments, including the sampling line for the gas-phase analyzers, were loosely tied together and inserted down into the vehicle bore through a ceiling vent, penetrating approximately 30 cm and facing the oncoming traffic to maximize aspiration efficiency. The aethalometer was placed inside the tunnel at the same ceiling vent.

A two-stage aerosol dilution chamber was constructed for use with the OPC and CNC to avoid the presence of multiple particles simultaneously passing the instrument's optical sensing region. In each stage, a major portion of the flow (60% for stage one, 99% for stage two) was siphoned off and filtered. The particle-free air was then recombined with the aerosol stream. The OPC siphoned off a small portion of the flow at 0.09 L $min^{-1}$ after the first stage with a dilution factor of 2.6. The CNC sampled at 1.5 L $min^{-1}$ after the second stage with a combined dilution factor of 380.

To simplify comparisons among data from different instruments, a single data acquisition system was used to collect data from the OPC, CNC, and gas analyzers on a common time basis (15 s averages). The difference in transport times between the real-time particle sampling line and the gas sampling line was measured to be ~1 s and was accounted for during the averaging of the gas analyzer signals. The aethalometer, which was stationed inside the tunnel, was offset by the sampling line transport time for the OPC and CNC.

Measured particle number concentrations might be biased low due to particle coagulation inside the 46 m sampling line and/or inside the tunnel. Coagulation is important within the vehicle exhaust system where primary particle concentrations are highest and dilution of the exhaust plume has not yet occurred. In the Caldecott tunnel, vehicle exhaust (which initially contains about 14% by volume $CO_2$) was diluted by a factor of at least 200:1 before it was sampled. To determine the significance of coagulation in the tunnel and in the sample line, the characteristic time for coagulation was calculated (Seinfeld and Pandis, 1998). To be conservative, the highest 3-h average particle number concentration measured in the tunnel, $4.0 \times 10^5$ $cm^{-3}$, and the smallest particle size measured, 0.01 μm, were used in the calculation. Using a typical value of the monodisperse coagulation coefficient, $1.8 \times 10^{-9}$ $cm^3$ $s^{-1}$, the characteristic time for a 50% decrease in particle number concentration was calculated to be 46 min. For polydisperse coagulation with a concentration of $1.4 \times 10^4$ $cm^{-3}$ of 0.2 μm particles, as indicated by the OPC, the coagulation coefficient is $5.4 \times 10^{-8}$ $cm^3$ $s^{-1}$ and the characteristic time is 15 min. These times are long compared to the residence time of air in the sample line (~15 s) and in the tunnel (~3 min). Sharp increases (spikes) in particle number concentration were observed in the tunnel over periods of 1-2 min, with the highest values and greatest variability in CNC counts observed in the diesel truck-influenced bore (bore 1). Coagulation rates would have been higher when these spikes in particle number concentration occurred.

### 4.2.5 Integrated Samples for Particle Chemistry

Filter samples for chemical characterization of $PM_{2.5}$ particles were collected inside and outside of the tunnel on each sampling day. Teflon filters were collected for determination of mass and inorganic ion concentrations, and were analyzed by the California Air Resources Board laboratory by gravimetry and ion chromatography. Quartz filters were collected for determination of organic and elemental carbon concentrations, and were analyzed by the thermal optical technique of Birch and Cary (1996; Sunset Laboratories, Beaverton, Oregon). AIHL cyclones (John and Reischl, 1980) operated at 24 L $min^{-1}$ were used to provide the 2.5 μm precut. All filters were 47 mm in diameter. The Teflon

and Teflon-coated glass fiber filters were collected at 24 L $min^{-1}$, with one filter per cyclone. Quartz filters were collected at 12 L $min^{-1}$ by splitting the flow from a single cyclone. The quartz filters were masked with annular stainless steel shims with an inner diameter of 24.7 mm to provide the same face velocity as for the Teflon filter samples. Tandem quartz filters were used on each sampler leg for analysis of carbon particles.

An experimental activated carbon denuder for scrubbing gas-phase organic compounds was used on one of the quartz filter sampling legs, as shown in Figure 4.1. The denuder was 10 cm long with approximately 1000 parallel channels. It was constructed from a block of activated carbon with a square cell structure (product discontinued, Graphite Sales Inc., Chagrin Falls, Ohio). The flow through each channel was laminar (Re~10). The Gormley-Kennedy equations (Fuchs, 1964) predict a removal efficiency of 99.8% for irreversibly depositing gas-phase species, and losses of 3% for particles with a diameter of 0.05 μm (decreasing to less than 1% for 0.1 μm particles). Shedding of carbon from the denuder was tested by drawing filtered air through the denuder at twice the sample flow rate, with the result that no visible darkening was found on a downstream filter. Inside the tunnel, tandem quartz filters were collected downstream

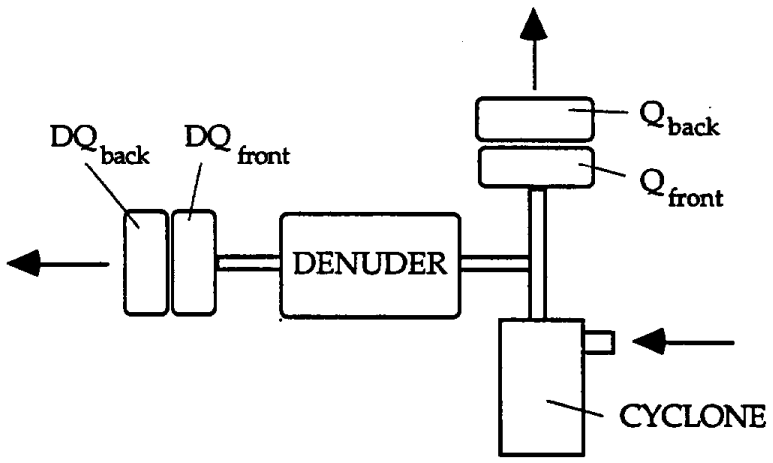


**Figure 4.1.** Schematic showing arrangement of quartz filters used to sample fine particulate carbon inside the tunnel. Q denotes quartz filter; DQ denotes denuded quartz filter located downstream of the activated carbon denuder.

of this denuder, in parallel to tandem, undenuded quartz filters. Outside the tunnel, quartz filters were collected with undenuded tandem quartz filters only, with a bypass line in place of the denuder-filter leg. Prior to use, the denuder was baked at 250 °C for 2 h. Quartz filters, which were baked before purchase, were again baked at 400-500 °C for 2 h prior to use at the tunnel.

### 4.2.6 Emission Factors

Fuel-based pollutant emission factors were computed by relating total carbon emissions in the tunnel (mainly in the form of $CO_2$) to the carbon content of fuel using the following equation:

$$E_P = 10^3 \left( \frac{\Delta[P]}{\Delta[CO_2] + \Delta[CO]} \right) w_c \qquad (4.1)$$

where $E_P$ is the emission factor (g emitted per kg of fuel burned) for pollutant P, $\Delta[P]$ is the increase in the concentration of pollutant P ($\mu g\ m^{-3}$) above background levels, $\Delta[CO_2]$ and $\Delta[CO]$ are the increases in the concentrations of $CO_2$ and CO ($\mu g$ of carbon $m^{-3}$) above background levels, and $w_c$ is the weight fraction of carbon in fuel. Carbon weight fractions of gasoline and diesel fuel used to calculate emission factors are reported in Table 4.2.

Light-duty vehicle emission factors were computed directly with eq 4.1 and pollutant concentrations measured in bore 2. Heavy-duty diesel truck emission factors could not be computed directly from bore 1 measurements because traffic in bore 1 comprised both light-duty vehicles and heavy-duty diesel trucks. Thus, it was necessary to apportion pollutant emissions in bore 1 to the two vehicle classes.

Prior roadway tunnel studies have shown that heavy-duty diesel trucks and light-duty gasoline-powered vehicles emit comparable amounts of CO per unit distance traveled (Pierson et al., 1996). Therefore, a small fraction of $\Delta[CO]$ in bore 1 was attributed to heavy-duty diesel truck emissions, equal to the fraction of heavy-duty diesel trucks in the traffic during each sample period. $CO_2$ emissions in bore 1 were apportioned using traffic counts and the fuel economies of light-duty gasoline vehicles and heavy-duty diesel trucks with the following equation:

$$\frac{\Delta[CO_2]_D}{\Delta[CO_2]} = \frac{f_D U_D \rho_D w_D}{(f_D U_D \rho_D w_D) + \left((1 - f_D) U_G \rho_G w_G\right)} \qquad (4.2)$$

where $\Delta[CO_2]_D$ is the component of $\Delta[CO_2]$ attributable to heavy-duty diesel emissions, $f_D$ is the fraction of traffic identified as heavy-duty diesel trucks, U is the fuel consumption rate (reciprocal of fuel economy), $\rho$ is fuel density, and w is the carbon weight fraction in fuel. The subscripts D and G denote diesel and gasoline, respectively. Fuel economies, fuel densities, and carbon weight fractions used to apportion $CO_2$ are given in Table 4.2.

For all other pollutants in bore 1, the portion of total emissions contributed by heavy-duty diesel trucks was determined by subtracting the contribution of light-duty vehicles. Light-duty vehicle emissions in bore 1 were determined using pollutant emission ratios measured in the light-duty vehicle bore (bore 2). The contribution from heavy-duty diesel trucks was expressed as:

$$\Delta[P]_D = \Delta[P] - \Delta[CO] \cdot (1 - f_D) \cdot \left( \frac{\Delta[P]_2}{\Delta[CO]_2} \right) \tag{4.3}$$

where $\Delta[P]_D$ is the component of $\Delta[P]$ in bore 1 attributable to heavy-duty vehicle emissions, and $\Delta[CO] \cdot (1\text{-}f_D)$ is the fraction of $\Delta[CO]$ in bore 1 attributed to light-duty vehicle emissions. The pollutant emission ratio for light-duty vehicles, $\Delta[P]_2/\Delta[CO]_2$, was measured in bore 2.

**Table 4.2.** Selected properties of diesel and gasoline fuels.

| parameter | diesel (heavy-duty) | gasoline (light-duty) |
|---|---|---|
| carbon weight fraction, $w_c$ | 0.87[a] | 0.85[b] |
| density, $\rho$ (g $L^{-1}$) | 840[c] | 740[b] |
| sulfur, (ppm by weight) | 135[c] | 12[b] |
| fuel consumption[d] (L/100 km) | 47 | 12 |
| fuel sales[e] (liters) | $8.0 \times 10^9$ | $5.1 \times 10^{10}$ |

[a] Typical properties for diesel fuel (Heywood, 1988).

[b] Average properties determined from 36 gasoline samples collected in the San Francisco Bay Area in summer 1997 (McGetrick, 1997).

[c] Average properties determined from diesel fuel samples collected from five Bay Area refineries (Lum, 1997).

[d] Measured fuel consumption for uphill traffic in the Fort McHenry tunnel (Pierson et al., 1996).

[e] On-road taxable fuel sales in California in 1995 (Board of Equalization, 1997).

## 4.3 Results and Discussion

### 4.3.1 OC Sampling Artifact

The measurement of particulate organic carbon concentrations with quartz filters is complicated by two sampling artifacts: the adsorption of gas-phase organic carbon onto the filter surface (positive artifact), and the evaporation of organic material from particles on the front filter (negative artifact). These artifacts have been investigated as they pertain to sampling in urban and remote environments (Turpin et al., 1994; Eatough et al., 1995; Eatough et al., 1996; Novakov et al., 1997).

To address this issue for the tunnel samples, parallel samples of denuded and undenuded pairs of quartz filters were collected, as shown in Figure 4.1. As reported in Table 4.3, the average OC mass collected on front filters downstream of the activated carbon denuder was 40% lower than the OC mass collected without the denuder. In contrast, the BC mass collected on front quartz filters downstream of the denuder ($DQ_{front}$) was 90%, on average, of the BC mass collected by the undenuded quartz filters ($Q_{front}$). The lower BC mass on denuded quartz filters is attributed to particle losses in the denuder.

Compared to filter samples collected without the denuder, vapor adsorption onto denuded filter samples was diminished. Evaporation of organic aerosol from the front denuded filter was likely enhanced due to the depletion of gaseous carbon constituents in the sample air stream. If the denuder was 100% efficient, then the OC found on the denuded backup filter would be entirely attributable to vaporized organic aerosol from the front filter. Thus, the OC on the denuded backup quartz filter, $DQ_{back}$, represents the upper limit for collection of evaporated organic particle mass by the backup filter. The upper limit of organic aerosol collected by denuded quartz filters is the sum of the front and back filters, or $DQ_{front}+DQ_{back}$. For this data set, the organic carbon collected on $DQ_{back}$ is small by comparison to that collected by the undenuded backup filter, $Q_{back}$. Organic carbon mass collected on backup filters below the denuded quartz filters, $DQ_{back}$, was 1/5 to 1/3 of that for the undenuded backup filters, $Q_{back}$. Since evaporation from the undenuded front filter must be less than from the denuded front filter, most of what is found on the undenuded backup filter, $Q_{back}$, must be due to adsorption of gas-phase organic compounds not adsorbed by the front filter, or the positive artifact. Thus for the undenuded leg, the particle-phase organic carbon concentration is most closely approximated by the difference between the front and backup filters, $Q_{front}-Q_{back}$. These two measures of organic carbon concentration (undenuded, $Q_{front}-Q_{back}$; and denuded $DQ_{front}+DQ_{back}$) are compared in Figure 4.2, with correction for the 10% loss of particles in the denuded leg indicated from the black carbon measurement. Also shown are

**Table 4.3.** Organic carbon (OC) and black carbon (BC) concentrations (μg of carbon $m^{-3}$) measured using quartz filters[a].

| | | tunnel | | | | background | |
|---|---|---|---|---|---|---|---|
| | | OC | | BC | | OC | BC |
| date | filter | w/o den[b] | denuded[c] | w/o den | denuded | w/o den | w/o den |
| **Bore 1[d] (1230-1530 h)** | | | | | | | |
| Jul 21 | front | 43.6 | 19.9 | 48.4 | 50.4 | 8.4 | 3.2 |
| | back | 3.2 | 1.4 | 0.1 | 0.1 | 1.2 | 0.0 |
| Jul 22 | front | 34.6 | 21.0 | 61.4 | 51.2 | 10.6[f] | 4.4 |
| | back | 8.4 | 3.4 | 0.0 | 0.4 | 3.5 | 0.5 |
| Jul 23 | front | 34.1 | 21.4 | 53.7 | 49.6 | 6.7 | 2.3 |
| | back | 7.2 | 2.4 | 0.0 | 0.0 | 3.8 | 0.1 |
| Jul 24 | front | 33.9 | 26.0 | 67.4 | 57.3 | 11.5 | 5.2 |
| | back | 5.6 | 1.4 | 0.0 | 0.1 | 3.6 | 0.0 |
| **Bore 2[e] (1530-1830 h)** | | | | | | | |
| Jul 31 | front | 23.5 | 15.8 | 15.5 | 14.1 | 6.2 | 1.7 |
| | back | 3.8 | 1.3 | 0.0 | 0.0 | 1.8 | 0.1 |
| Aug 01 | front | 22.6 | 15.4 | 12.3 | 11.0 | 4.9 | 1.7 |
| | back | 2.8 | 0.7 | 0.2 | 0.1 | 1.8 | 0.4 |
| Aug 04 | front | 26.8 | 15.3 | 16.2 | 13.5 | 7.5 | 2.6 |
| | back | 4.4 | 0.6 | 0.0 | 0.0 | 2.3 | 0.4 |
| Aug 05 | front | 25.0 | 13.8 | 16.8 | 14.2 | 7.7 | 1.7 |
| | back | 4.5 | 0.8 | 0.0 | 0.4 | 2.8 | 0.9 |

[a] The mass of carbon collected was determined using a thermal-optical analytical technique (Birch and Cary, 1996).

[b] These quartz filter samples (Q) were collected without the use of an activated carbon denuder.

[c] These quartz filter samples (DQ) were collected downstream of an activated carbon denuder used to scrub gas-phase organic compounds from the air stream (see text for further detail).

[d] Heavy-duty diesel trucks constituted about 4% of traffic in bore 1.

[e] Bore 2 was reserved for use by light-duty vehicles only.

[f] An anomalously high value of 53 μg $m^{-3}$ was measured; sample was probably contaminated. The value shown in the table was determined based on ambient OC/BC ratios and the measured background BC concentration on July 22.

1-standard deviation error limits from the analytical method. With the exception of one outlier, these two methods of estimating organic carbon are in reasonable agreement. The bore 1 results fall within the analytical uncertainty of the OC determination; the bore 2 results show a somewhat larger difference, but the two measures of OC agree to within 20%.

Based on these results, corrected particulate organic carbon concentrations inside the tunnel were calculated as the average of these two values, namely $0.5 \times [(Q_{front}-Q_{back}) + f(DQ_{front}+DQ_{back})]$ where f=1.1 accounts for particle losses in the denuder. We note that there may be additional organic carbon lost from the quartz filters by evaporation which is not collected by the backup quartz filters. However, for these experiments, sample times

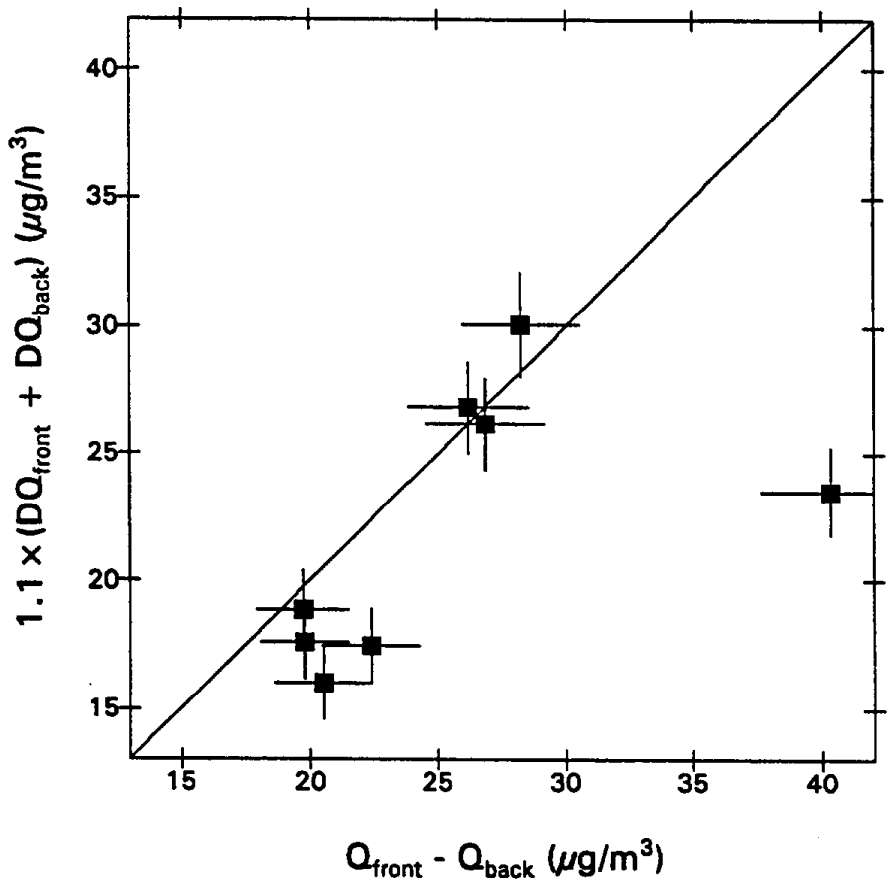


**Figure 4.2.** Plot of fine particulate organic carbon (OC) concentrations ($\mu gC\ m^{-3}$) estimated using denuded quartz (DQ) filters versus OC estimated using undenuded quartz (Q) filters. The factor of 1.1 applied to the denuded filters accounts for particle losses in the denuder (see text).

were short, filter samples were at the same temperature as the sampled air, and pressure drop across the filters was small (0.04 atm). These conditions will minimize evaporative losses as compared to that found for most ambient sampling conditions.

### 4.3.2 Pollutant Concentrations

Measured concentrations of CO, $CO_2$, $NO_x$, $PM_{2.5}$, BC, OC, $SO_4^{2-}$, and particle number are reported in Table 4.4. Concentrations of most pollutants were significantly higher inside the tunnel than in background air. For example, average CO, $NO_x$, and $PM_{2.5}$ concentrations measured in bore 1 were 17, 25, and 8 times higher than in background air. Particle number concentrations were not measured in background air. However, background levels were estimated from overnight measurements in the tunnel when concentrations of CO, $CO_2$, and $NO_x$ dropped to typical daytime background levels. Corresponding background particle number concentrations measured using the CNC and OPC were 5500 and 450 $cm^{-3}$, respectively.

CO and $CO_2$ concentrations (above background levels) in bore 1 were 60-70% of those measured in bore 2, consistent with the lower total traffic volumes observed earlier in the afternoon in bore 1. In contrast, bore 1 concentrations (again above background levels) of $NO_x$, $PM_{2.5}$, and BC were 1.1, 2.8, and 3.8 times the corresponding values measured in bore 2. This provides evidence that heavy-duty diesel trucks, which were present in bore 1 but largely absent from bore 2, are much higher emitters of these pollutants than light-duty vehicles.

### 4.3.3 Apportionment of Pollutant Emissions

Eq 4.3 was used to apportion emissions in bore 1 for cases where the influence of heavy-duty diesel trucks was evident (i.e., the emission ratio $\Delta[P]/\Delta[CO]$ was significantly higher in bore 1 than in bore 2). The apportionment was not attempted in cases where the influence of diesel trucks on pollutant concentrations measured in bore 1 was small. Emission factors were computed for the following pollutants: $NO_x$, $PM_{2.5}$, BC, OC, $SO_4^{2-}$, and fine particle number concentrations. For these pollutants, measured emission ratios were consistent from one day to the next. For example, the average $NO_x$ to CO ratio ($\pm$ 1 standard deviation) measured in bores 1 and 2 were 0.113 $\pm$ 0.003 and 0.071 $\pm$ 0.003, respectively. The apportionment indicated that heavy-duty diesels contributed approximately 40% of $NO_x$, 55% of OC, 70% of fine particles, 75% of $PM_{2.5}$ and $SO_4^{2-}$, and 85% of BC emissions in bore 1.

Accurate apportionment of emissions with eq 4.3 requires that light-duty vehicle emissions in bore 1 are well characterized by the emission ratio, $\Delta[P]_2/\Delta[CO]_2$, measured for light-duty vehicles in bore 2. Vehicle speeds were typically about 10 km $h^{-1}$ lower in bore 2 during the late afternoon sampling period (1530-1830 h) than in bore 1 during the

**Table 4.4.** Pollutant concentrations measured at the Caldecott tunnel in summer 1997.

| | tunnel concentrations | | | | | | | | |
|---|---|---|---|---|---|---|---|---|---|
| date | CO (ppm) | $CO_2$ (ppm) | $NO_x$ (ppm) | $PM_{2.5}$ ($\mu g\ m^{-3}$) | BC ($\mu g\ m^{-3}$) | OC[c] ($\mu g\ m^{-3}$) | $SO_4^{2-}$ ($\mu g\ m^{-3}$) | CNC[d] ($\#\ cm^{-3}$) | OPC[e] ($\#\ cm^{-3}$) |
| **Bore 1[a] (1230-1530 h)** | | | | | | | | | |
| Jul 21 | 19.0 | 720 | 2.09 | 139 | 48.3 | 44.7 | 4.5 | $4.0 \times 10^5$ | $1.4 \times 10^4$ |
| Jul 22 | 16.9 | 735 | 1.93 | 125 | 61.4 | 37.1 | 3.2 | $3.7 \times 10^5$ | $1.2 \times 10^4$ |
| Jul 23 | 19.4 | 747 | 2.07 | 130 | 53.7 | 37.1 | 5.2 | $3.3 \times 10^5$ | $1.2 \times 10^4$ |
| Jul 24 | 19.4 | 779 | 2.17 | 136 | 67.4 | 40.8 | 3.6 | $2.7 \times 10^5$ | $1.3 \times 10^4$ |
| **Bore 2[b] (1530-1830 h)** | | | | | | | | | |
| Jul 31 | 27.5 | 1008 | 1.92 | 56.1 | 15.5 | 27.0 | 3.0 | $2.1 \times 10^5$ | $5.7 \times 10^3$ |
| Aug 01 | 26.1 | 946 | 1.78 | 52.5 | 12.1 | 26.2 | 3.3 | $1.9 \times 10^5$ | $5.1 \times 10^3$ |
| Aug 04 | 27.5 | 1053 | 1.94 | 56.6 | 16.2 | 27.9 | 1.9 | $1.8 \times 10^5$ | $5.6 \times 10^3$ |
| Aug 05 | 27.6 | 1090 | 2.06 | 53.7 | 16.8 | 25.6 | 2.8 | $1.6 \times 10^5$ | $5.7 \times 10^3$ |

[a] Heavy-duty diesel trucks constituted about 4% of traffic in bore 1.

[b] Bore 2 was reserved for use by light-duty vehicles only.

[c] OC concentrations shown here were calculated from measurements presented in Table 4.3, correcting for sampling artifacts (see text), and multiplying by a factor of 1.4 to account for hydrogen and oxygen mass associated with organic carbon (Gray et al., 1986).

[d] The condensation nucleus counter measured particles > 0.01 μm.

[e] The optical particle counter measured particles in the size range 0.1-2 μm.

**Table 4.4.** continued.

| | background concentrations | | | | | | |
|---|---|---|---|---|---|---|---|
| date | CO (ppm) | $CO_2$ (ppm) | $NO_x$ (ppb) | $PM_{2.5}$ ($\mu g\ m^{-3}$) | BC ($\mu g\ m^{-3}$) | OC[c] ($\mu g\ m^{-3}$) | $SO_4^{2-}$ ($\mu g\ m^{-3}$) |
| **Bore 1[a] (1230-1530 h)** | | | | | | | |
| Jul 21 | 1.2 | 369 | 85 | 14.1 | 3.2 | 10.1 | 2.1 |
| Jul 22 | 0.9 | 370 | 65 | 19.2 | 3.9 | 10.0 | 1.5 |
| Jul 23 | 1.1 | 366 | 78 | 15.3 | 2.3 | 4.1 | 2.5 |
| Jul 24 | 1.3 | 384 | 103 | 18.8 | 5.2 | 11.0 | 1.7 |
| **Bore 2[b] (1530-1830 h)** | | | | | | | |
| Jul 31 | 0.8 | 365 | 48 | 13.4 | 1.6 | 6.2 | 2.4 |
| Aug 01 | 0.9 | 369 | 58 | 16.1 | 1.3 | 4.4 | 2.4 |
| Aug 04 | 1.3 | 387 | 82 | 11.8 | 2.3 | 7.3 | 1.1 |
| Aug 05 | 0.8 | 384 | 51 | 13.6 | 0.9 | 6.8 | 1.8 |

[a] Heavy-duty diesel trucks constituted about 4% of traffic in bore 1.

[b] Bore 2 was reserved for use by light-duty vehicles only.

[c] OC concentrations shown here were calculated from measurements presented in Table 4.3, correcting for sampling artifacts (see text), and multiplying by a factor of 1.4 to account for hydrogen and oxygen mass associated with organic carbon (Gray et al., 1986).

[d] The condensation nucleus counter measured particles > 0.01 μm.

[e] The optical particle counter measured particles in the size range 0.1-2 μm.

earlier afternoon sampling period (1230-1530 h). Given that vehicle speed may affect pollutant emission factors, it is necessary to consider how vehicle speed affects the pollutant emission ratio, $\Delta[P]/\Delta[CO]$. As reported in Chapter 2, CO emissions in bore 2 of the Caldecott tunnel increased more than $NO_x$ emissions as vehicle speeds increased, so the $\Delta[NO_x]/\Delta[CO]$ ratio for light-duty vehicle emissions was lower earlier in the afternoon, as shown in Figure 4.3. Thus, the $\Delta[NO_x]/\Delta[CO]$ ratio measured in bore 2 from 1530-1830 h may overstate the actual $\Delta[NO_x]/\Delta[CO]$ emission ratio for light-duty vehicles in bore 1 earlier in the afternoon.

The fraction of total $NO_x$ emissions (40%) attributed to heavy-duty diesels in bore 1 is therefore a lower bound value. Given the uncertainty in the $\Delta[NO_x]/\Delta[CO]$ ratio and $NO_x$ apportionment due to differences in vehicle speeds, it follows that heavy-duty diesels could be responsible for as much as 48% of total $NO_x$ emissions in bore 1. Thus, the heavy-duty diesel $NO_x$ emission factor may be as much as 20% higher than the value reported below.

Heavy-duty diesel truck emission factors for other pollutants (BC, OC, $SO_4^{2-}$, $PM_{2.5}$ mass, particle number concentrations) are less sensitive than the $NO_x$ emission factor to uncertainty in the apportionment using eq 4.3. This is because the diesel exhaust contribution to these other pollutants in bore 1 is larger than it is for $NO_x$. For example, light-duty vehicles in bore 1 were estimated to contribute only 15% of BC versus 60% of $NO_x$. Therefore, the same level of uncertainty in the light-duty emission ratio ($\Delta[P]_2/\Delta[CO]_2$) leads to a smaller error in the estimation of heavy-duty diesel emissions of BC relative to $NO_x$.

Carbon dioxide emissions were apportioned using eq 4.2 because the contribution of heavy-duty diesels to $CO_2$ in bore 1 was too small for eq 4.3 to produce reliable results (i.e., the $\Delta[CO_2]/\Delta[CO]$ ratio in bores 1 and 2 was about equal). Application of eq 4.2 using measured traffic counts and previously published fuel economies (see Table 4.2) indicated that heavy-duty diesel trucks were responsible for 17%, on average, of $CO_2$ emissions in bore 1. Based on traffic counts, 4.2% of CO emissions in bore 1 was attributed to heavy-duty diesel trucks.

There are two sources of uncertainty affecting the apportionment of $CO_2$ emissions in bore 1: use of measured fuel economies from the Fort McHenry tunnel (Pierson et al., 1996) to represent Caldecott tunnel vehicles, and the classification of 2-axle/6-tire trucks as gasoline or diesel-powered. Fuel economies shown in Table 4.2 were measured for uphill driving on a 3.3% grade, whereas the grade in the Caldecott tunnel is 4.2%. If the ratio of heavy-duty to light-duty fuel economy remains the same as grade changes from 3.3 to 4.2%, this difference will not affect the $CO_2$ apportionment. However, it is unknown how

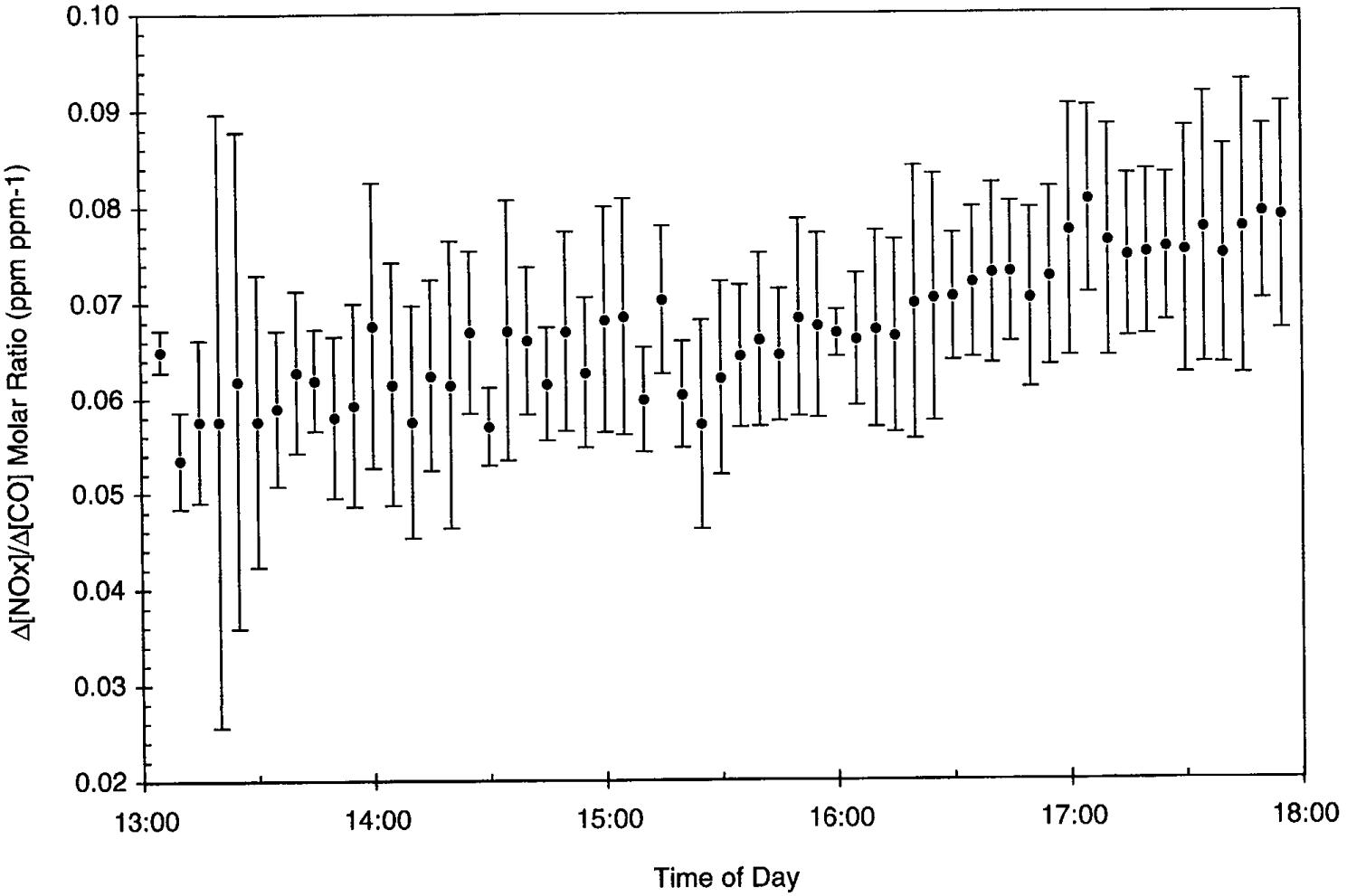


**Figure 4.3.** Average (±1 standard deviation) $NO_x$/CO emission ratio measured in bore 2 of the Caldecott tunnel.

well the vehicle weight distributions, and therefore fuel economies, match between the two tunnels. As discussed earlier, there are uncertainties about how many of the 2-axle/6-tire trucks were truly heavy-duty diesel. If 68% rather than 50% of these trucks are counted as heavy-duty diesel, then $\Delta[CO_2]_D$ calculated using eq 2 would increase, and emission factors shown in Table 4.5 for heavy-duty diesel trucks would decrease by ~10%.

### 4.3.4 Fine Particle Emission Rates

Vehicle emission factors, computed as mass of pollutant emitted per kg of fuel burned (eq 4.1), are reported in Table 4.5. Compared to light-duty vehicles, heavy-duty diesel trucks have higher emission factors for every pollutant listed in Table 4.5. The greatest differences are for $PM_{2.5}$, BC, and $SO_4^{2-}$, for which emission factors for heavy-duty diesel trucks were 24, 37, and 21 times higher than for light-duty vehicles. In addition to having higher fine particle mass emissions, heavy-duty diesel engines emit about 15-20 times the number of fine particles larger than 0.01 μm than do light-duty vehicles per unit mass of fuel burned. Note that if emission factors were expressed on a per vehicle km

**Table 4.5.** Light-duty vehicle and heavy-duty diesel truck emission factors[a] (± 1 standard deviation).

| species | units | HD diesel trucks | LD vehicles | ratio (HD/LD) |
|---|---|---|---|---|
| $NO_x$[b] | (g $kg^{-1}$) | 42 ± 5 | 9.0 ± 0.2 | 4.6 ± 0.6 |
| CNC counts[c] | (# $kg^{-1}$) | $(6.3 \pm 1.9) \times 10^{12}$ | $(4.6 \pm 0.7) \times 10^{10}$ | 14 ± 5 |
| OPC counts[d] | (# $kg^{-1}$) | $(2.5 \pm 0.4) \times 10^{11}$ | $(1.3 \pm 0.05) \times 10^{9}$ | 19 ± 3 |
| $PM_{2.5}$ | (g $kg^{-1}$) | 2.5 ± 0.2 | 0.11 ± 0.01 | 24 ± 3 |
| BC | (g $kg^{-1}$) | 1.3 ± 0.3 | 0.035 ± 0.003 | 37 ± 10 |
| OC[e] | (g $kg^{-1}$) | 0.50 ± 0.04 | 0.053 ± 0.008 | 9.4 ± 1.5 |
| $SO_4^{2-}$ | (mg $kg^{-1}$) | 45 ± 8 | 2.1 ± 0.4 | 21 ± 6 |

[a] Emission factors expressed per unit mass of fuel burned, computed using eq 4.1.
[b] $NO_x$ is reported as $NO_2$ (i.e., a molecular weight of 46 was used to convert measured $NO_x$ concentrations from ppm to μg $m^{-3}$).
[c] The condensation nucleus counter measured particles > 0.01 μm.
[d] The optical particle counter measured particles in the size range of ~0.1-2 μm.
[e] The mass emission rate of organic carbon was calculated from corrected organic carbon concentrations shown in Table 4.4.

traveled basis, the differences between heavy-duty and light-duty emission factors reported in Table 4.5 would be four times larger because heavy-duty vehicles burn about four times more fuel per km traveled (see Table 4.2).

In California, on-road diesel fuel sales are one-sixth the volume of gasoline sales (Table 4.2). Considering the relative magnitudes of light-duty vehicle and heavy-duty diesel truck emission factors measured in this study, it follows that exhaust emissions of $PM_{2.5}$ and BC from on-road sources are dominated by heavy-duty trucks, which emit about 80 and 90%, respectively, of the total mass. As noted above, however, visibly smoking light-duty vehicles can have fine particle emission rates comparable to heavy-duty diesel trucks. If smoking light-duty vehicles were underrepresented in the present study then light-duty vehicles would contribute a greater portion of fine particle emissions statewide. Furthermore, vehicles driving through the tunnel were operating in a fully warmed-up mode. The possibility of higher exhaust particle emission rates from both cars and trucks under cold-starting/wintertime conditions has not been considered here.

### 4.3.5 Chemical Composition of Fine Particles

Carbonaceous material comprised the majority of fine particle emissions. Diesel-derived particulate was more abundant in black carbon (51±11% of $PM_{2.5}$ mass) than light-duty vehicle particulate emissions, which showed a lower BC fraction (33±4%). Other studies also report black carbon to be more abundant in particle emissions from heavy-duty diesel trucks. Reported BC fractions range from 30 to 50% for heavy-duty diesel trucks (Hildemann et al., 1991; Lowenthal et al., 1994; Watson et al., 1994b), and from 14 to 23% for catalyst equipped light-duty vehicles (Hildemann et al., 1991; Watson et al., 1994b).

Organic carbon comprised 50±6% of $PM_{2.5}$ mass emissions from light-duty vehicles in the Caldecott tunnel, which agrees with values (30-50%) reported elsewhere (Hildemann et al., 1991; Watson et al., 1994b). Organic carbon constituted only 20±2% of $PM_{2.5}$ mass emissions from heavy-duty diesel trucks, whereas values ranging from 30 to 40% have been reported in the literature (Hildemann et al., 1991; Lowenthal et al., 1994; Watson et al., 1994b).

Sulfate was a small component of total fine particle emissions, comprising about 2% of total $PM_{2.5}$ mass emissions from both the light- and heavy-duty vehicle fleets. The sulfate emission factor measured for heavy-duty diesel trucks in the Caldecott tunnel (45 ± 8 mg per kg of diesel burned) is significantly lower than values reported in earlier studies. Measured heavy-duty diesel sulfate emission rates in the Tuscarora tunnel in 1977 were about 120 ± 15 mg per kg of diesel burned (Pierson and Brachaczek, 1983; Pierson et al., 1996). Sulfate emission rates measured for heavy-duty trucks in southern California in the late 1980s were approximately 350 ± 60 mg $kg^{-1}$ (Hildemann et al., 1991). Lower sulfate

emissions at the Caldecott tunnel were expected due to the reduction in sulfur content of diesel fuel since the time of the earlier studies.

### 4.3.6 Temporal Variability

Concentrations of CO, $NO_x$, black carbon mass, and particle number varied considerably during each 3-h sampling period. Much less variability was observed in the concentration of $CO_2$, which can be used as a measure of changes in traffic density and the tunnel air ventilation rate. The relative standard deviation in the measured concentration for each of these parameters is given in Table 4.6. These values reflect the variability in pollutant concentrations during a 3-h sampling period. All pollutant concentrations were measured with 15 s time resolution. Black carbon mass and particle number concentrations were generally more variable than gaseous pollutant concentrations. CNC counts and $NO_x$ concentrations showed greater time variability in bore 1 than in bore 2. The relative variation in OPC and aethalometer (black carbon) readings were similar for both bores.

Sample time series of continuously measured parameters are given in Figure 4.4 for bore 1, and Figure 4.5 for bore 2. Here the parameters are normalized to $\Delta[CO]+\Delta[CO_2]$, as used in eq 4.1. The sum $\Delta[CO]+\Delta[CO_2]$ is the increase of gas-phase carbon species due to fuel combustion in the tunnel, and is used here to correct for variations in the ventilation rate and traffic density inside the tunnel. The parameters shown are CO, $NO_x$, black carbon particle mass (AETH), and particle number concentrations in two size ranges. The line labeled CNC counts corresponds to particles above 0.01 μm; that labeled OPC corresponds to particles in the 0.1 to 2 μm size range.

**Table 4.6.** Temporal variability in pollutant concentrations within each sampling run.

| | coefficient of variation[a] | |
|---|---|---|
| pollutant | bore 1 | bore 2 |
| $CO_2$ | 11% | 7.5% |
| CO | 37% | 25% |
| $NO_x$ | 39% | 18% |
| CNC | 58% | 36% |
| OPC | 60% | 66% |
| BC | 102% | 97% |

[a] Average coefficient of variation ($\sigma/\mu$) for time-resolved pollutant concentrations measured inside the tunnel during each 3 h sampling run.

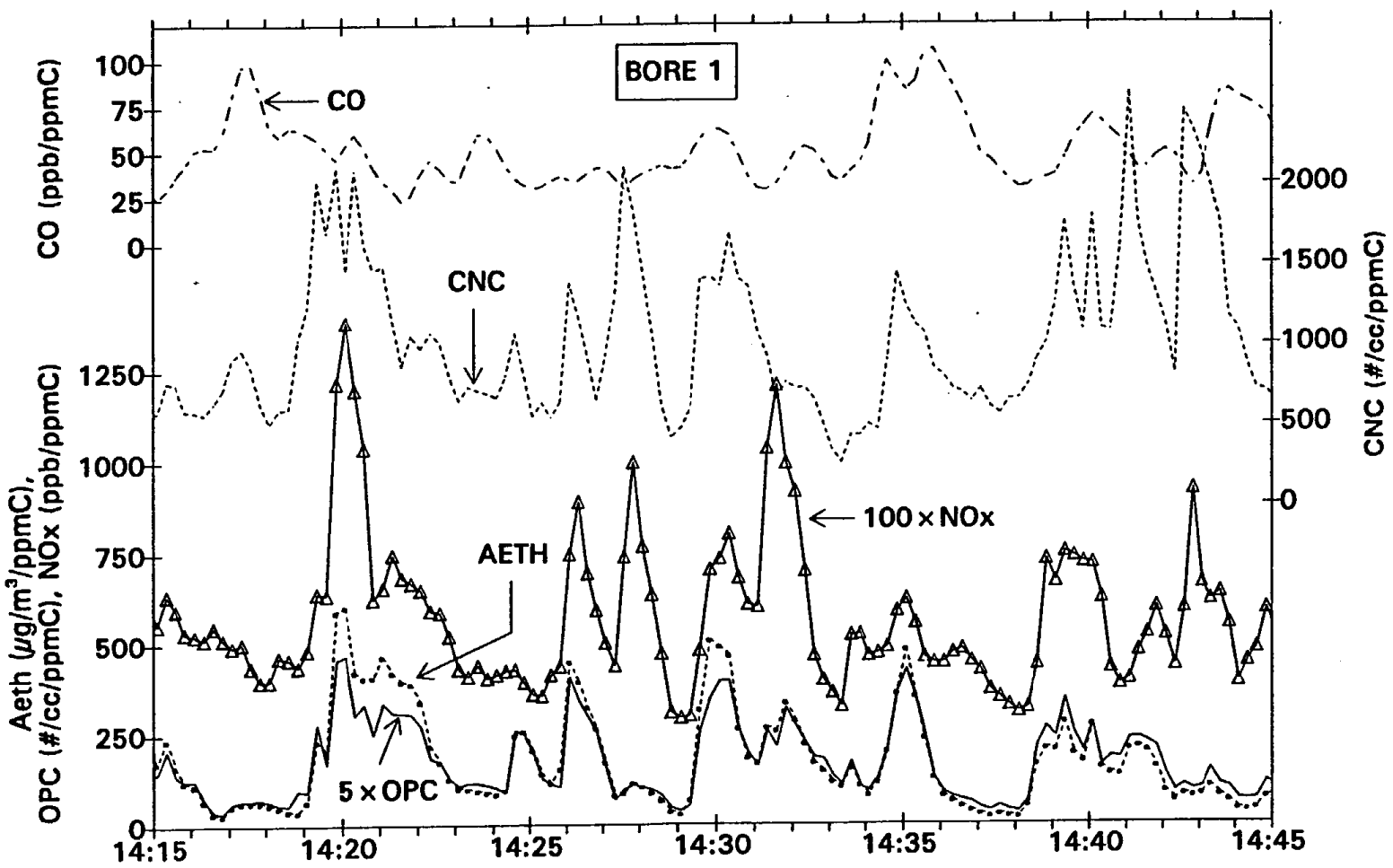


**Figure 4.4.** Time series plot from July 21, 1997 of pollutant concentrations in the diesel truck-influenced bore (bore 1) of the tunnel. All pollutant concentrations are normalized by $\Delta[CO]+\Delta[CO_2]$.

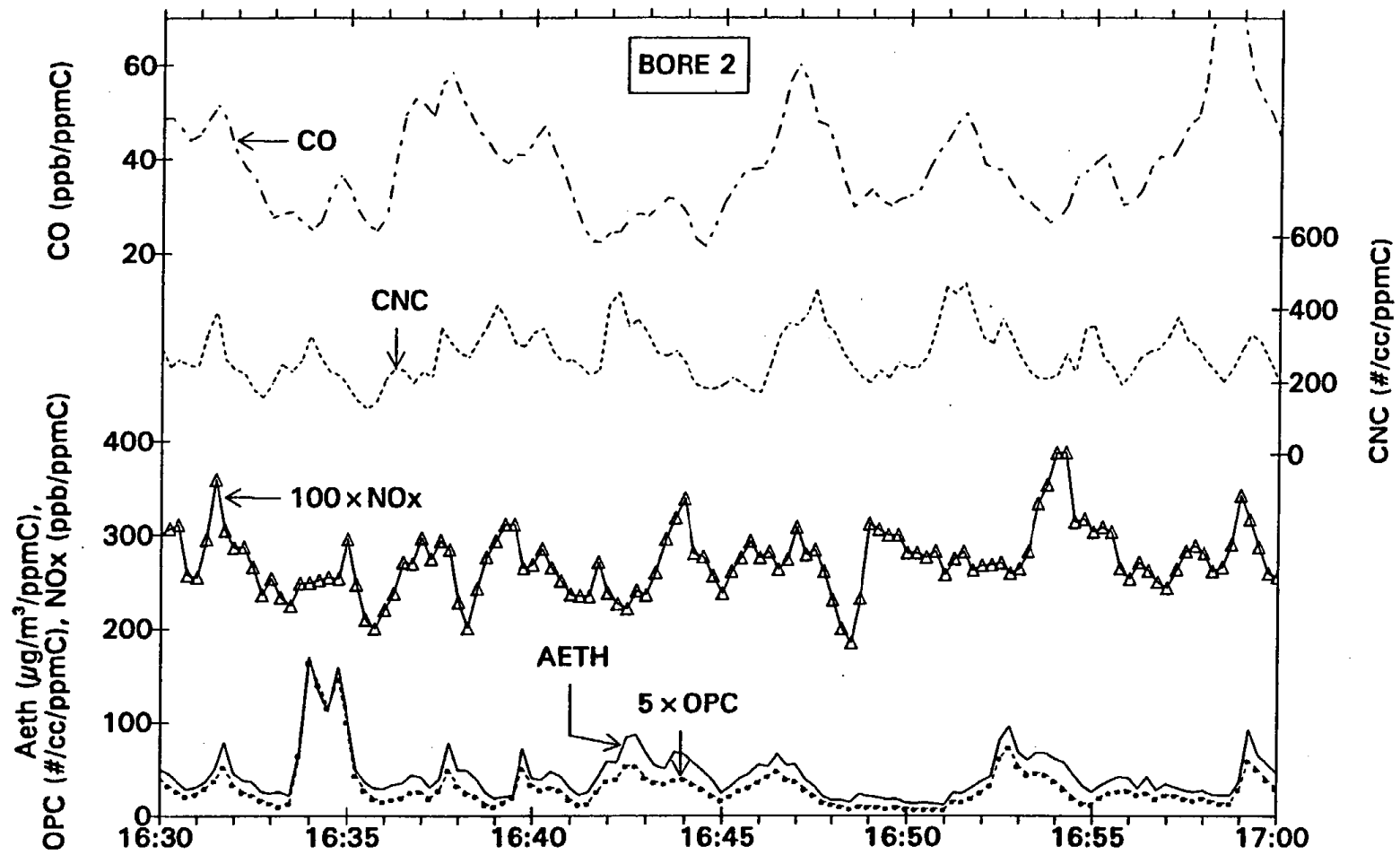


**Figure 4.5.** Time series plot from August 4, 1997 of pollutant concentrations in bore 2 of the tunnel (reserved for use by light-duty vehicles only). All pollutant concentrations are normalized by $\Delta[CO]+\Delta[CO_2]$.

The time correlation in these parameters was examined to determine whether high $NO_x$ or CO emitters might also be high particle emitters. As is evident from the time series plots, only the OPC counts and the BC measured by the aethalometer are strongly correlated ($r_{OPC,aeth}$=0.89 in bore 1, and 0.92 in bore 2). This finding is interesting given that the aethalometer measures black carbon, which is found predominantly in the ultrafine mode (below 0.12 μm, Venkataraman et al., 1994), whereas the OPC measures accumulation mode particles.

Other parameters measured in the tunnel are not as well correlated. In bore 1, local peaks in $NO_x$ sometimes correspond to a local peak in CNC counts, and at other times correspond to local peaks in OPC counts. The CNC and OPC both correlate better with $NO_x$ ($r_{NOx,CNC}$=0.55 and $r_{NOx,OPC}$=0.50, respectively) than with each other ($r_{CNC,OPC}$=0.32). These correlations are even weaker in bore 2.

### 4.3.7 $NO_x$ Emissions

On-road $NO_x$ emission factors for heavy-duty trucks measured during several roadway tunnel and remote sensing studies are reported in Table 4.7. As indicated, truck speeds and roadway grades varied across the different sampling sites. However, measured $NO_x$ emission factors, when expressed on a fuel consumed basis, were consistent from site to site, and did not exhibit a clear trend with roadway grade/speed. The stability of $NO_x$ emission factors when expressed on a fuel consumed basis supports their use in the development of fuel-based emission inventories (e.g., Dreher and Harley, 1998).

When combined with fuel density and on-road fuel sales for the state of California (see Table 4.2) the $NO_x$ emission factors shown in Table 4.5 suggest that heavy-duty diesel trucks are responsible for ~45% of total on-road $NO_x$ emissions. Thus, heavy-duty diesels are a significant source of $NO_x$, nearly equal in importance to light-duty vehicles. As a whole, on-road vehicles are the largest source (~60%) of $NO_x$ emissions in California (ARB, 1997). Therefore, the contribution of heavy-duty diesel truck emissions to secondary (ammonium nitrate) fine particle concentrations is expected to be significant.

**Table 4.7.** Measured on-road $NO_x$ emissions from heavy-duty vehicles.

| study | year | roadway grade | typical speeds (km $h^{-1}$) | $NO_x$ emissions[a] (g $kg^{-1}$) |
|---|---|---|---|---|
| **tunnel** | | | | |
| Caldecott (this study) Oakland, CA | 1997 | +4.2% | 65 ± 11 | 42 ± 5 |
| Tuscarora[b] Tuscarora, PA | 1992 | level | 87 ± 5 | 39 ± 3 |
| Fort McHenry[b] Baltimore, MD | 1992 | +3.3%<br>-1.8% | 70-80<br>80 | 37 ± 4<br>34 ± 2 |
| Cassiar[c] Vancouver, BC | 1995 | level | 90 | 48 ± 17 |
| **remote sensing** | | | | |
| Raleigh-Durham, NC[d] | 1997 | +2.1% | 90-110 | 45 ± 2 |
| Orange County, CA[e] | 1997 | +4.0% | 25[f] | 31 ± 0.2 |

[a] Emission factors are reported as mass of $NO_x$ emitted per kg of diesel fuel consumed. $NO_x$ is reported as $NO_2$ (i.e., a molecular weight of 46 was used to convert measured $NO_x$ concentrations from ppm to $\mu g\ m^{-3}$).

[b] Pierson et al. (1996)

[c] Rogak et al. (1998)

[d] Nelson et al. (1998)

[e] Countess et al. (1998)

[f] Trucks were accelerating on a freeway on-ramp after leaving a weigh station.

# 5 Polycyclic Aromatic Hydrocarbons

## 5.1 Introduction

Combustion-derived aerosol consists of solid carbonaceous particles (black carbon) that are associated with a complex mixture of organic compounds (Sawyer and Johnson, 1995). Black carbon contributes significantly to fine particle mass and is an important cause of atmospheric visibility impairment (Larson and Cass, 1989; Larson et al., 1989). Of the organic compounds associated with combustion-generated aerosols, polycyclic aromatic hydrocarbons (PAH) are of particular concern because they are potent mutagens and carcinogens (Nauss, 1995). Particulate PAH measured in urban air and in roadway tunnels has been found in the respirable size range (Miguel and Friedlander, 1978; Miguel and Rubenish, 1980; Miguel and Friedlander, 1984; Venkataraman and Friedlander, 1994; Venkataraman et al., 1994; Allen et al., 1996).

Characterization of aerosols in motor vehicle exhaust has indicated that PAH emission profiles are distinct for different vehicle classes. It has been suggested that selected PAH could be used as tracers for particulate emissions from motor vehicles (Daisey et al., 1986). Measurements in roadway tunnels carrying both light-duty gasoline and heavy-duty diesel vehicles indicate that diesel-derived aerosols are enriched in lower molecular weight PAH (e.g., alkylated phenanthrenes, chrysene), whereas higher molecular weight PAH are associated with gasoline engine-derived aerosol (Hering et al., 1984; Benner and Gordon, 1989; Venkataraman et al., 1994). Similarly, dynamometer measurements on catalyst-equipped and noncatalyst gasoline cars and diesel trucks show that PAH emissions from diesel trucks are weighted toward lower molecular weight PAH, whereas gasoline engine exhaust shows a greater abundance of higher molecular weight PAH (Rogge et al., 1993). The dynamometer tests also indicate that the total aerosol PAH emission rate per km driven for noncatalyst gasoline-powered cars was 25 times larger than for catalyst-equipped cars, and 7 times larger than for diesel trucks (Rogge et al., 1993).

PAH in motor vehicle exhaust has a number of possible sources, including unburned fuel, lubricating oil, and pyrosynthesis. PAH in unburned fuel has been shown to be the primary contributor to PAH in diesel engine exhaust (Abbass et al., 1989). In

radiotracer experiments, benzo[a]pyrene in the fuel was found to be the major source of benzo[a]pyrene in the exhaust of a diesel engine, whereas lubricating oil and pyrosynthesis combined were found to contribute no more than 20% to benzo[a]pyrene in exhaust emissions (Tancell et al., 1995). Similarly, unburned fuel was the predominant source of particle-phase exhaust PAH, from methylfluorenes to benzo[a]pyrene, for two direct-injection diesel engines (Williams et al., 1989). This investigation also concluded that the pyrosynthesis of lower molecular weight PAH may contribute to exhaust emissions of five-ring and larger PAH and that lubricating oil affects the behavior of PAH in the combustion process. Naphthalene surviving combustion has been identified as the source of 24% of naphthalene in diesel exhaust emissions, and the conversion of 2-methylnaphthalene to naphthalene in the combustion chamber has been confirmed, also by radiotracer experiments (Rhead and Pemberton, 1996). Less is known about the origin of PAH in gasoline engine exhaust, despite the fact that gasoline engines are more important than diesels as a source of some PAH (Benner et al., 1989; Li and Kamens, 1993; Rogge et al., 1993).

Numerous studies have quantified PAH in motor vehicle exhaust (Venkataraman et al., 1994; Benner et al., 1989; Rogge et al., 1993; Westerholm and Li, 1994; Khalili et al., 1995; Mi et al., 1996), but substantially fewer have examined PAH concentrations in fuels used by these vehicles. Naphthalene, fluorene, and phenanthrene were found to be the predominant PAH in French diesel fuel (Pointet et al., 1997). Analysis of eight diesel fuels in Sweden found phenanthrene, methylphenanthrene, and 2-methylanthracene to be the most abundant PAH in the fuels (Westerholm and Li, 1994). Another study involving two diesel fuels in England found that total PAH content of the fuels ranged from 1.7 to 4.5% and that one fuel had at least 20 times the benzo[a]pyrene content of the other (Abbass et al., 1989). Mi et al. (1996) found that PAH concentrations ranged up to 11.5 mg $L^{-1}$ in a sample of Taiwanese unleaded gasoline. In general, however, less is known about PAH in gasoline than in diesel fuel.

In the past, control strategies for motor vehicles emphasized improvements in engine and emission control technologies. More recently, fuels have been reformulated to reduce vehicle emissions. For example, oxygenated compounds such as methyl tert-butyl ether (MTBE) have been added to gasoline (Kirchstetter et al., 1996), and the sulfur and aromatic contents of diesel fuel have been reduced (Nikanjam, 1993). It is possible that some types of fuel reformulation might help to reduce PAH emissions from motor vehicles (Westerholm and Li, 1994). Improved understanding is therefore needed of the relationship between fuel composition and PAH emissions, for both gasoline and diesel engines.

The goal of this study was to characterize PAH emissions from a current on-road fleet of heavy-duty diesel and light-duty gasoline vehicles and to characterize PAH in the fuels used by these vehicles. Specific objectives were to: collect aerosol samples in a roadway tunnel carrying both light-duty gasoline vehicles and diesel trucks, develop PAH emission profiles for gasoline and diesel vehicles, determine the size distribution of PAH emissions, determine emission rates of PAH for light-duty gasoline and heavy-duty diesel vehicles, and quantify PAH concentrations in commercial gasoline and diesel fuel samples.

## 5.2 Methods

### 5.2.1 Field sampling site

Field sampling was conducted at the Caldecott tunnel on weekdays during the period from August 20 to 28, 1996 and from July 21 to August 5, 1997. Pollutant concentrations were measured in the traffic tubes ~50 m before the tunnel exit and in the background air injected into the tunnel by the ventilation fans. Sampling was conducted during uphill (eastbound) traffic events in bores 1 and 2 of the tunnel. Measurements in bore 2 (center bore) were made during afternoon rush hours, from 1600-1800 h, when the fleet was almost entirely light-duty vehicles. Measurements in bore 1, the truck-influenced bore, were made from 1300-1500 h when the fraction of heavy-duty trucks in the vehicle fleet was largest. In 1997, particle sampling times were modified slightly; the sample period was extended to three hours, 1230-1530 h in bore 1 and 1530-1830 in bore 2.

### 5.2.2 Pollutant sampling methods

Gas phase measurements included real-time determination of carbon monoxide (CO), carbon dioxide ($CO_2$), and oxides of nitrogen ($NO_x$) concentrations. Two-hour integrated air samples were collected in stainless steel canisters for subsequent analysis of hydrocarbon concentrations. Reported here are tunnel and background CO and $CO_2$ concentrations measured by gas-filter correlation spectrometry (Thermo Environmental Instruments, Models 48 and 41H, Franklin, MA).

Particle sampling included the collection of time-integrated filter and impactor samples for subsequent analysis of the chemical composition of the fine aerosol, and real-time measurement of particle number concentration and size distribution. Tunnel filter samples were collected for particles in two size fractions: below 1.3 μm ($PM_{1.3}$), and below 2.5 μm ($PM_{2.5}$) aerodynamic diameter. These samples were analyzed for carbon, mass, ions, and trace metals. Additional samples collected inside the tunnel ($PM_{1.3}$ in 1996 and $PM_{2.5}$ in 1997) were analyzed for speciated PAH and organics. Background $PM_{2.5}$ samples were collected and analyzed for PAH in 1997. $PM_{2.5}$ samples were collected at the clean air ventilation intake and analyzed for carbon, mass, ions, and trace

metals. $PM_{2.5}$ samples were collected using AIHL cyclones operated at 24 L $min^{-1}$ (John et al., 1988). $PM_{1.3}$ samples were collected using the same type of AIHL cyclone operated at 50 L $min^{-1}$ (John and Reischl, 1980). The 50 L $min^{-1}$ flow was split between two filter samples to maintain approximately equal face velocity across all filters.

Particle samples for determination of PAH were collected using 47 mm diameter Teflon-coated glass fiber filters (Pallflex T60A20, Putnam, CT). Size-segregated samples for PAH analysis were collected inside the tunnel using a low-pressure impactor with size cuts at 0.05 μm, 0.075 μm, 0.12 μm, 0.26 μm, 0.50 μm, 1.0 μm, 2.0 μm aerodynamic diameter (Hering et al., 1978; Hering et al., 1979). Impactor samples were collected onto glass disks coated with 1 μL of a 2% solution of Vaseline in cyclohexane to prevent particle bounce. The same impactor was used by Venkataraman et al. (1994) to measure vehicle-derived PAH. Impactor results are reported for a composite sample collected from 1530-1830 h on August 21-24, 1997 in bore 2 and from 1230-1530 on July 31, August 1, 4, and 5, 1997 in bore 1

All air flow standards were subjected to a quality assurance audit by the Monitoring and Lab Division of the California Air Resources Board before field sampling began. During sample collection, flow rates were monitored with rotameters and pressure gauges. Each rotameter was calibrated against the audited bubble flow meter for the complete range of operating pressures used in the tunnel measurements, and final sample volumes have been calculated accordingly. Impactor flow rates were measured at the beginning and end of each sampling period. Filter and impactor samples were placed in containers and put in a freezer within two hours from the conclusion of each sample period.

### 5.2.3 PAH extraction

In the laboratory, filter and impactor samples were handled under room light shielded with a yellow filter to avoid photooxidation of PAH. Each 47 mm sample filter was cut in half, placed in an amber vial and covered with 4 mL of HPLC-grade dichloromethane. PAH were extracted for 30 min in an ultrasonic bath. The bath water was replaced every 8 minutes to prevent overheating. Extracts were transferred into a disposable plastic syringe and filtered through a 5 μm Spartan-25 syringe filter into an amber vial. The syringe and filter were washed with dichloromethane and added to the extract. The extracts were reduced to ~0.5 mL under air at reduced pressure, and were evaporated to dryness under a gentle stream of helium at room temperature and pressure. Residues were dissolved with 0.25 and 1 mL of HPLC-grade acetonitrile for background and tunnel samples, respectively. Vials were sealed with a PTFE-lined cap. A second filter extraction was performed in the same way.

Similarly, each impactor disk was extracted for 24 min in a covered beaker with 5 mL of HPLC-grade dichloromethane. The extract was filtered into amber vials, the volume reduced, and the residue taken up with 250 μL of HPLC-grade dichloromethane. The extract was rotated over the vial walls and sonicated for 3 min. This step was repeated two additional times to ensure quantitative transfer. The extract was then transferred into a 250 μL glass insert, mounted with a spring and capped with a PTFE-lined screw cap septum.

### 5.2.4 PAH separation and quantification

Aerosol extracts were analyzed for the last ten PAH listed in Table 5.1. Measurements of vehicle exhaust in prior roadway tunnel experiments show that PAH with molecular weights ≥ 228 (e.g., benzo[a]anthracene, chrysene, and larger PAH) are entirely in the particle phase; PAH less volatile than fluoranthene and pyrene have not been found in the gas phase (Benner and Gordon, 1989). The distribution of fluoranthene and pyrene between the gas and particle phases is affected by ambient temperature. Concentrations of lower molecular weight PAH such as naphthalene, phenanthrene, and anthracene were not quantified in the tunnel air samples, although they were quantified in the gasoline and diesel fuel samples.

PAH were separated using a Supelcosil LC-PAH, 15 cm, 5 μm column that was adapted with a Supelcosil guard-column (Supelco, Bellefonte, PA). A mobile phase solvent gradient of acetonitrile and water (40-100% acetonitrile over 20 min, held at 100% acetonitrile for 7.5 min) was maintained at a flow rate of 0.9 mL $min^{-1}$ using a Waters (Milford, MA) 626 pump and associated 600S controller. PAH were quantified using a McPherson (Acton, MA) FL-Spectrophotometer (150 W Xe-lamp) in the following configurations: excitation wavelength = 265 nm; emission wavelength = 0.001 (zero order); excitation and emission slits of 2 and 4, respectively; a CF-300 filter in the emission side (no filter in the excitation side); sensitivity ranges (R) of 0.03, 0.1, 0.3 and 1.0; time constant = 0.5 sec; photomultiplier gain = 904; 10 mV output signal into the Waters SAT/IN module.

The system was calibrated using a Radian (Austin, TX) 16 Priority PAH standard (no. ERS-010, 10 μg $mL^{-1}$ in acetonitrile) that was diluted with HPLC-grade acetonitrile to produce individual standards of 5, 10, 20 and 50 pg $\mu L^{-1}$. Under optimized chromatographic and instrumental conditions, the detection limits (in picograms) for a 20 μL standard injection were: FLT, 25; PYR, 26; BAA, 13; CRY, 9; BBF, 9; BKF, 7; BAP, 6; BGP, 35; IND, 35; DBA, 67. Each extract was injected at least twice, and sometimes more when a peak was lost due to saturation in the fluorescence system. Final filter PAH concentrations were calculated taking into consideration secondary extraction yields, which averaged ~6% of the mass found in the primary extractions. Analysis precision for the

standard was ~2%; for the samples it ranged from 2-16%. All reported PAH concentrations were blank-corrected.

**Table 5.1.** Sixteen PAH measured in this study.

| species name | abbreviation | molecular weight | number of rings |
|---|---|---|---|
| naphthalene | NAP | 128 | 2 |
| acenaphthylene | ACY | 152 | 3 |
| acenaphthene | ACE | 154 | 3 |
| fluorene | FLU | 166 | 3 |
| anthracene | ANT | 178 | 3 |
| phenanthrene | PHE | 178 | 3 |
| fluoranthene | FLT | 202 | 4 |
| pyrene | PYR | 202 | 4 |
| benz[a]anthracene | BAA | 228 | 4 |
| chrysene | CRY | 228 | 4 |
| benzo[b]fluoranthene | BBF | 252 | 5 |
| benzo[k]fluoranthene | BKF | 252 | 5 |
| benzo[a]pyrene | BAP | 252 | 5 |
| benzo[ghi]perylene | BGP | 276 | 6 |
| indeno[1,2,3-cd]pyrene | IND | 276 | 6 |
| dibenz[a,h]anthracene | DBA | 278 | 5 |

### 5.2.5 Traffic characterization

Several methods were used to characterize the vehicles traveling through the tunnel. In 1996, visual traffic counts indicated average traffic volumes of 2100 vehicles per hour in bore 1 from 1300-1500 h, and 4300 vehicles per hour in bore 2 from 1600-1800 h. The vehicle fleet in bore 2 comprised 66% cars; 34% pick-ups, small trucks, and vans; and < 0.3% heavy-duty trucks. In bore 1, the traffic composition was 62% cars; 32% pickups, small trucks, and vans; and 6% heavy-duty trucks. A license plate survey of traffic in bore

2 indicated that 1.5% of the light-duty vehicles were diesel fueled. The mean vehicle model year was 1990, and < 1% of the vehicles were pre-1975 model year.

The 1992 Truck Inventory and Use Survey (Bureau of Census, 1992) was used to determine the fraction of heavy-duty trucks in each axle class that were diesel-powered. Census data for California indicate that a negligible fraction of 2-axle, 4-tire trucks meet the definition of a heavy-duty diesel truck; ~50% of 2-axle, 6-tire trucks are heavy-duty diesel; and > 90% of trucks with 3 or more axles are heavy-duty diesel. Using these classifications and the traffic counts mentioned above, heavy-duty diesel trucks accounted for 4.7% of total traffic in bore 1 from 1300-1500 h in 1996, whereas the percentage in bore 2 from 1600-1800 h was < 0.2%. Approximately 70% of the heavy-duty diesels in bore 1 were large trucks with three or more axles. Traffic counts were similar in 1997.

Driving conditions inside the tunnel were determined using an instrumented vehicle equipped to log speed at 1 sec intervals. The average speed of traffic in bore 2 during the 1600-1800 h sample period was 66 ± 8 km $h^{-1}$ (n = 31). Light-duty vehicles in bore 1 during the 1300-1500 h sample period traveled faster, 79 ± 6 km $h^{-1}$ (n = 4), because there was less traffic congestion in the early afternoon. Heavy-duty trucks in bore 1 traveled at an average speed of 68 ± 11 km $h^{-1}$ (n = 16). Average speed measured inside the tunnel in 60 independent drivethroughs confirmed the instrumented vehicle data. Due to merging traffic and large numbers of vehicles using the tunnel during the 1600-1800 h periods, traffic was often backed up before entering bore 2. There was less traffic congestion ahead of the entrance to bore 1 during the 1300-1500 h sample periods because traffic flow was lighter earlier in the afternoon. During all sample periods, traffic inside the tunnel flowed smoothly, lacking heavy accelerations and stop-and-go driving.

### 5.2.6 Fuel sampling

Gasoline and diesel fuel samples were collected in August 1997 using standard sampling procedures developed by the California Air Resources Board. Gasoline samples were collected from service stations in Berkeley and Oakland, representing the five major brands of gasoline sold in the Bay Area. Regular and premium grades were collected at four of the service stations, and mid-grade and premium gasoline were sampled at one station. Approximately 750 mL of each gasoline sample was dispensed from service station pumps into 1 L steel canisters, and these samples were stored in a refrigerator at 4 °C. The Compliance Division of the Air Resources Board collected five diesel fuel samples from four oil refineries in the San Francisco Bay Area. These were also stored in 1 L steel canisters at 4 °C.

### 5.2.7 Fuel analysis

Gasoline samples were diluted 10 to 2000 times in *n*-heptane and were analyzed on a Hewlett-Packard 5890 gas chromatograph connected to a Hewlett-Packard 5872 mass spectrometer (GC/MS). The autoinjector was programmed to make 1 μL splitless injections of all samples and standards onto a 30 m, 25 μm inner diameter, 86% dimethyl, 14% cyanopropyl column (J&W Scientific DB-1701, #05 600 367). The oven temperature was increased from 40 to 280 °C at a rate of 7 °C $min^{-1}$ and then held at 280 °C for 30 min for a total run time of 64 min. The mass spectrometer was programmed in single ion mode to detect two m/z ions for each PAH. PAH were identified by comparing retention times and ion ratios to those of a reference standard.

The same 16 PAH standard used for HPLC analysis was also used to develop calibration curves for the GC/MS analysis. In addition to the ten PAH listed in Table 5.1, it also contained naphthalene (NAP), acenaphthylene (ACY), acenaphthene (ACE), fluorene (FLU), anthracene (ANT), and phenanthrene (PHE). The limit of detection for PAH analysis by GC/MS was ~5 μg $L^{-1}$, with slightly lower limits for the low molecular weight PAH and slightly higher limits for the high molecular weight PAH. The coefficient of variation for repeat injections of a standard was less than 5% for all sixteen PAH.

Because PAH peaks in diesel fuel samples were difficult to distinguish from other fuel components, a solid phase extraction technique was used to separate PAH from other diesel fuel components. The method for PAH separation in the fuel samples was modified slightly from a published method (Bundt et al., 1991). PAH in diesel fuel samples were separated by using silica gel cleanup. First, Sep-Pak silica cartridges (Waters WAT051900, Franklin, MA) were conditioned with 5 mL *n*-heptane. A 100 μL aliquot of fuel was added to the top of the column. Fuel components were then eluted in ~2.5 mL fractions using increasing concentrations (0%, 20%, and 50%) of dichloromethane in heptane, and fractions were blown down to 2 mL under a gentle stream of nitrogen. This step may have promoted the loss of more volatile, lower molecular weight PAH. The extent of the losses are unknown, but this step was required to carry out the analysis. The PAH eluted mainly with 20% dichloromethane in heptane, although fuels with large amounts of naphthalene showed this PAH in all fractions. Precision for the solid phase extraction and subsequent analysis was approximately 25%, and recovery tests of this extraction method on standards gave mean recoveries ranging from 60 to 115%, depending on the PAH. Solid phase extraction of gasoline samples followed by GC/MS analysis compared to analysis without solid phase extraction showed that some of the higher molecular weight PAH (five rings and more) were lost in the extraction procedure when their concentration in the fuel was less than ~0.5 mg $L^{-1}$.

## 5.3 Results and Discussion

### 5.3.1 Pollutant concentrations

Concentrations of PAH, CO, and $CO_2$ measured in the truck-influenced bore (bore 1) and the light-duty vehicle bore (bore 2) of Caldecott tunnel are presented, together with traffic count data, in Table 5.2. As indicated in Table 5.2, the PAH concentration profile was quite different in the two bores. Even though light-duty traffic volumes were higher during sampling in bore 2, concentrations of lower molecular weight PAH (FLT, PYR, and BAA) were much higher in the truck-influenced bore (bore 1) than in the light-duty vehicle bore (bore 2). This suggests that heavy-duty diesel trucks emit much more of these lower molecular weight PAH than do light-duty vehicles. Conversely, concentrations of higher molecular weight PAH (BGP, IND, and DBA) were higher in bore 2 compared to bore 1. Concentrations of CRY, BBF, and BKF were similar in both bores in 1996.

Compared to 1996 observations in the light-duty bore, PAH concentrations were slightly higher in 1997 for the first seven PAH and BGP. The concentration of IND was slightly lower, and DBA was significantly lower in 1997. Increases in PAH concentrations were expected given the higher cutpoint (2.5 μm) used in collecting particle samples in 1997 versus the 1.3 μm cutpoint used in 1996. In bore 1, concentrations of the first seven PAH also were higher in 1997, as expected. Concentrations of the three heaviest PAH, especially DBA, were lower in 1997.

Average PAH concentrations measured in bore 2 were compared to a PAH profile measured previously for gasoline engine exhaust (Li and Kamens, 1993). The profiles were highly correlated ($r = 0.93$), indicating that gasoline engines were the dominant contributor to PAH emissions in bore 2. This is not surprising because light-duty gasoline vehicles comprised ~98% of traffic in bore 2, and most of the remaining vehicles in bore 2 were light-duty diesel.

**Table 5.2.** Measured pollutant concentrations and vehicle counts at the Caldecott tunnel.

| | 1996 measurements | | | | |
|---|---|---|---|---|---|
| | bore 2 (1600-1800 h) | | bore 1 (1300-1500 h) | | |
| species | Aug 20 | Aug 21 | Aug 22 | Aug 23 | Aug 28 |
| tunnel PAH[a] (ng $m^{-3}$) | | | | | |
| FLT | 3.1 | 3.3 | 17 | 25 | 17 |
| PYR | 3.2 | 4.0 | 22 | 37 | 25 |
| BAA | 1.8 | 2.0 | 5.8 | 8.1 | 5.2 |
| CRY | 2.9 | 2.8 | 4.0 | 5.3 | 3.5 |
| BBF | 3.1 | 3.0 | 2.7 | 3.8 | 2.3 |
| BKF | 1.1 | 0.86 | 0.75 | 0.85 | 0.5 |
| BAP | 2.9 | 2.3 | 1.0 | NA[b] | 1.1 |
| BGP | 7.2 | 7.3 | 1.7 | 2.6 | 1.2 |
| IND | 3.9 | 3.3 | 0.6 | 1.3 | 0.8 |
| DBA | 5.9 | 7.1 | 2.2 | 2.5 | 1.6 |
| tunnel CO (ppm) | 28.0 | 26.9 | 19.6 | 21.2 | 20.7 |
| background CO (ppm) | 0.8 | 0.6 | 1.7 | 2.4 | 3.2 |
| tunnel $CO_2$ (ppm) | 1017 | 1011 | 719 | 763 | 735 |
| background $CO_2$ (ppm) | 347 | 346 | 364 | 383 | 410 |
| traffic count (vehicles $h^{-1}$) | 4400 | 4300 | 2100 | 2200 | 2100 |
| % HD diesel[c] | 0.07 | 0.2 | 4.6 | 4.6 | 4.8 |

[a] Pollutant concentrations determined from $PM_{1.3}$ samples collected in the tunnel bores.

[b] Not available. The concentration of BAP was not determined for this filter sample because an instability in the spectrophotometer resulted in signal saturation during analysis of this peak.

[c] Percentage of heavy-duty diesel trucks in the tunnel vehicle fleet.

[d] Pollutant concentrations determined from $PM_{2.5}$ samples collected in the tunnel bores.

[e] Filters from two days of sampling were extracted and combined prior to quantification of PAH.

**Table 5.2.** continued.

| species | 1997 measurements | | | |
|---|---|---|---|---|
| | bore 2 (1530-1830 h) | | bore 1 (1230-1530 h) | |
| | Jul 31<br>Aug 1[e] | Aug 4<br>Aug 5 | Jul 21<br>Jul 22 | Jul 23<br>Jul 24 |
| tunnel PAH[d] (ng $m^{-3}$) | | | | |
| FLT | 4.7 | 4.9 | 32 | 31 |
| PYR | 6.2 | 6.8 | 41 | 41 |
| BAA | 3.3 | 3.9 | 8.9 | 10 |
| CRY | 3.2 | 3.8 | 7.8 | 9.0 |
| BBF | 3.5 | 3.1 | 5.7 | 6.8 |
| BKF | 1.2 | 1.1 | 3.0 | 3.6 |
| BAP | 3.3 | 3.2 | 7.6 | 8.4 |
| BGP | 8.5 | 8.0 | 1.0 | 2.3 |
| IND | 3.1 | 2.8 | 0.32 | 0.73 |
| DBA | 0.59 | 0.49 | 0.57 | 0.41 |
| tunnel CO (ppm) | 26.8 | 27.6 | 18.0 | 19.4 |
| background CO (ppm) | 0.9 | 1.1 | 1.1 | 1.2 |
| tunnel $CO_2$ (ppm) | 977 | 1072 | 728 | 764 |
| background $CO_2$ (ppm) | 367 | 386 | 370 | 375 |
| traffic count (vehicles $h^{-1}$) | 4000 | 4200 | 2300 | 2400 |
| % HD diesel[c] | 0.3 | 0.4 | 4.2 | 4.3 |

[a] Pollutant concentrations determined from $PM_{1.3}$ samples collected in the tunnel bores.

[b] Not available. The concentration of BAP was not determined for this filter sample because an instability in the spectrophotometer resulted in signal saturation during analysis of this peak.

[c] Percentage of heavy-duty diesel trucks in the tunnel vehicle fleet.

[d] Pollutant concentrations determined from $PM_{2.5}$ samples collected in the tunnel bores.

[e] Filters from two days of sampling were extracted and combined prior to quantification of PAH.

**Table 5.3.** Selected properties of gasoline and diesel engines and fuels.

| parameter | gasoline (light-duty) | diesel (heavy-duty) |
|---|---|---|
| carbon weight fraction, $w_c$ | 0.85[a] | 0.87[b] |
| density, $\rho$ (g $L^{-1}$) | 743[a] | 830[b] |
| fuel consumption (L/100 km) | 47[c] | 12[c] |

[a] Average properties determined from 36 gasoline samples collected in the San Francisco Bay Area in summer 1996 (McGetrick, 1997).

[b] Typical properties for diesel fuel (Heywood, 1988).

[c] Measured fuel consumption for uphill traffic in the Fort McHenry tunnel (Pierson et al., 1996).

### 5.3.2 Emission factors

Fuel-based emission factors for individual PAH were calculated from measured pollutant concentrations in bores 1 and 2 of the tunnel using eq 4.1. In order to facilitate comparison between 1996 and 1997 emission factors, they were not corrected for background concentrations, which were measured in 1997 only. Ambient PAH concentrations amounted to an average of 6% of tunnel PAH concentrations on bore 2 sampling days and were higher on bore 1 sampling days but showed evidence of contamination by tunnel exhaust. Pollutant emissions in bore 1 were apportioned between light-duty vehicles and heavy-duty diesel trucks using eqs 4.2 and 4.3 as outlined in Chapter 4. Properties of gasoline and diesel fuels and engines used to calculate PAH emission factors are shown in Table 5.3.

Heavy-duty diesel trucks were estimated to have contributed 80-90% of the FLT, PYR, and BAA in bore 1, whereas all of the DBA, BGP, and IND in bore 1 could be attributed to light-duty vehicles in 1996.

Emission factors for particle phase PAH calculated using eq 4.1 are reported in Table 5.4. Emission factors are reported as mass of pollutant emitted per unit mass of fuel burned. When comparing emission factors, it is important to note that by weight, ~6 times more gasoline than diesel fuel is sold for use by on-road vehicles in California. Therefore, in cases where the emission factors shown in Table 5.4 are comparable, light-duty vehicles are the dominant source. Heavy-duty diesel trucks are the dominant on-road source of black carbon and lighter PAH such as FLT, PYR, and BAA; light-duty vehicles are the major source of heavier PAH including BGP, IND, and DBA.

Some changes in emission factors were evident between 1996 and 1997. For light-duty vehicles, PAH emission factors were higher by no more than a factor of two in 1997 than in 1996 for all species except IND, which had a slightly lower emission factor in

1997, and DBA, which had a significantly lower emission factor in 1997. Higher particle-phase PAH emission factors were expected because of the higher cutpoint diameter (2.5 versus 1.3 μm) used in 1997 particle sampling. For heavy-duty vehicles, emission factors were significantly higher in 1997 for CRY, BBF, BKF, and BAP. Note, however, that as discussed in Chapter 4, there are larger uncertainties associated with the heavy-duty diesel emission factors because of the need to apportion pollutant concentrations in bore 1 between light- and heavy-duty vehicles.

**Table 5.4.** Fine particulate PAH mass emitted per kg of fuel burned for light-duty vehicles and for heavy-duty diesel trucks in the Caldecott tunnel.

| | light-duty vehicles ($\mu g\ kg^{-1}$) | | heavy-duty diesel ($\mu g\ kg^{-1}$) | |
|---|---|---|---|---|
| species | 1996[a] | 1997[b] | 1996[a] | 1997[b] |
| FLT | 8.0 ± 0.3 | 12.3 ± 0.6 | 480 ± 100 | 785 ± 79 |
| PYR | 9.0 ± 1.5 | 16.6 ± 0.2 | 690 ± 170 | 1009 ± 74 |
| BAA | 4.8 ± 0.4 | 9.1 ± 0.3 | 140 ± 30 | 203 ± 13 |
| CRY | 7.0 ± 0.1 | 9.0 ± 0.5 | 66 ± 20 | 170 ± 8 |
| BBF | 7.6 ± 0.3 | 8.4 ± 1.4 | 25 ± 17 | 115 ± 12 |
| BKF | 2.5 ± 0.4 | 3.1 ± 0.4 | 2.8 ± 2.5 | 71 ± 6 |
| BAP | 6.4 ± 1.1 | 8.5 ± 0.9 | NS[c] | 162 ± 1 |
| BGP | 18.0 ± 0.3 | 21.3 ± 2.7 | NS | NS |
| IND | 9.0 ± 1.1 | 7.7 ± 1.1 | NS | NS |
| DBA | 16.2 ± 2.1 | 1.4 ± 0.3 | NS | 4.1 ± 3.9 |

[a] PAH associated with particles < 1.3 μm aerodynamic diameter ($PM_{1.3}$).
[b] PAH associated with particles < 2.5 μm aerodynamic diameter ($PM_{2.5}$). Higher values are expected because of the higher cutpoint diameter used in summer 1997 particle sampling.
[c] Not a significant source. Use of eq 4.3 to apportion individual PAH in bore 1 indicated that gasoline vehicles could account for 100% of these PAH emissions.

### 5.3.3 PAH size distributions

PAH size distributions measured in bores 1 and 2 in 1997 are shown in Figures 5.1 and 5.2, respectively. PAH were found mainly in two modes centered at 0.1 and 1 μm. More PAH was found in the ultrafine mode relative to the accumulation mode in bore 2. In this bore, as PAH molecular weight increased, in general more of the PAH was found in the ultrafine mode (<0.26 μm) and less in the accumulation mode (0.26-4 μm). The average ratio of ultrafine mode particle-phase PAH concentration (0.05 to 0.26 μm) to accumulation mode concentration (0.26 to 4 μm) for FLT through CRY was 1.2, while for BBF through BGP it was 6.5. This ratio was 1.3 for IND and DBA, but the tunnel concentrations of these PAH were not significantly above background. In bore 1, there was not a clear relationship between the molecular weight of the PAH and the size distributions. The average ratio of accumulation mode to ultrafine mode concentration was 1.9 for all PAH in this bore.

The total mass concentrations measured by low-pressure impactor (Figures 5.1 and 5.2) versus filter (Table 5.2) were similar for most PAH. In the light-duty bore, impactor-derived concentrations of DBA were significantly higher than filter-derived concentrations. In the truck-influenced bore, impactor-derived concentrations of FLT, PYR, BBF, BKF, and BAP were higher than filter-derived concentrations, and the reverse was true for BGP. The reasons for these differences are unclear.

PAH size distributions shown in Figures 5.1 and 5.2 explain some of the increase in emission factors in 1997. The expected increase in the mass of PAH collected in changing from a 1.3 to 2.5 μm cutpoint diameter can be estimated by calculating the percent increase in mass associated with particles less than 1 μm compared to mass associated with particles less than 2 μm. In bore 2, this factor accounts for 2-48% increase in PAH collected, and the increase in bore 2 emission factors in 1997 are generally consistent with this range except for IND and DBA. In bore 1, the comparison of mass distribution to changes in emission factors is complicated by the need to apportion pollutants between light- and heavy-duty vehicles, but for the four ring and smaller PAH whose emissions are dominated by heavy-duty diesel trucks, the change in cutpoint diameter should account for a 12-28% increase in PAH collected. This alone does not explain the observed increases in heavy-duty diesel PAH emission factors; uncertainties in the apportionment of pollutants are likely to account for the remaining differences.

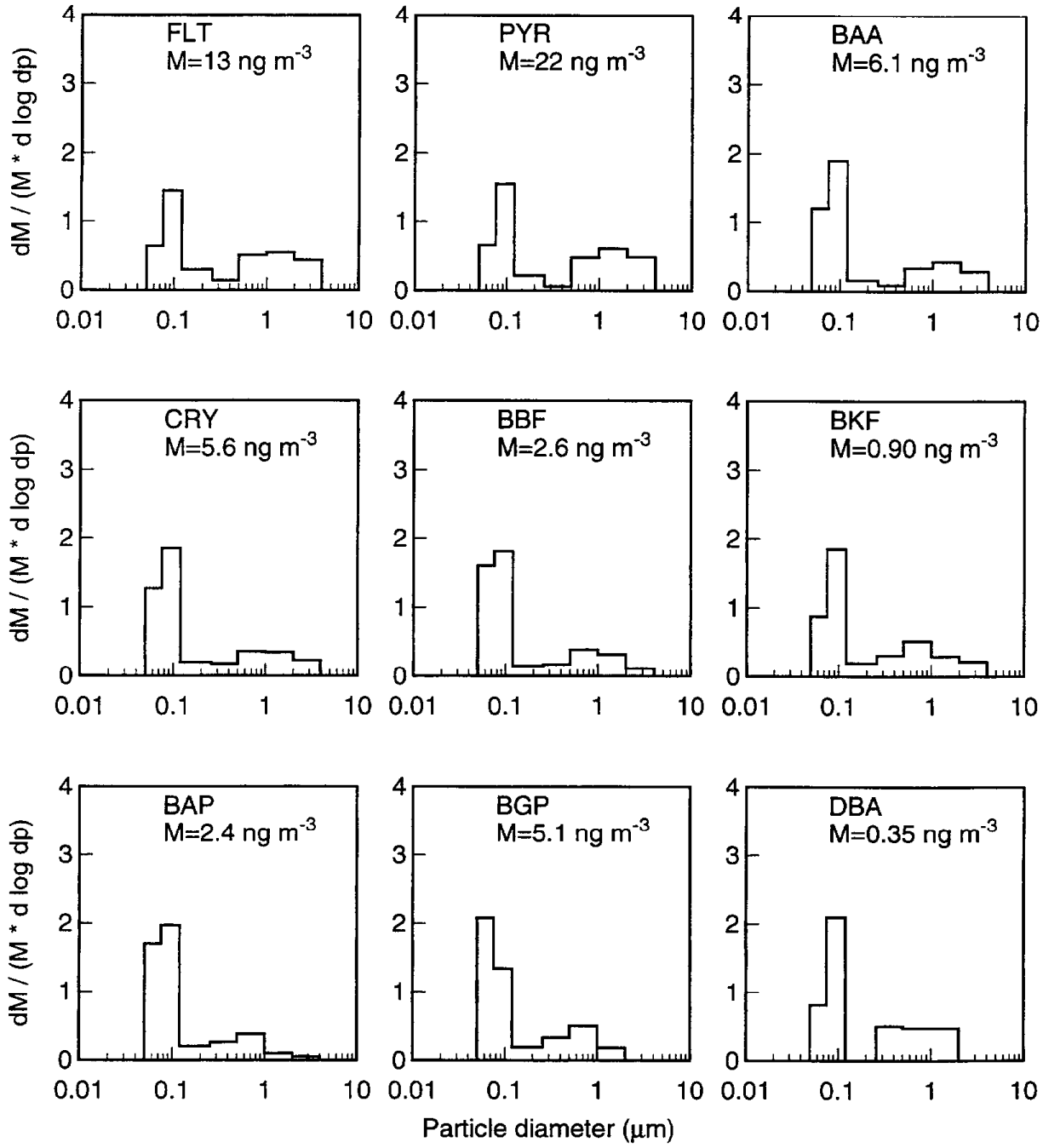


**Figure 5.1.** Size distribution and total mass concentration (M) of PAH measured in summer 1997 with a low-pressure impactor in the truck-influenced bore (bore 1) of the Caldecott tunnel.

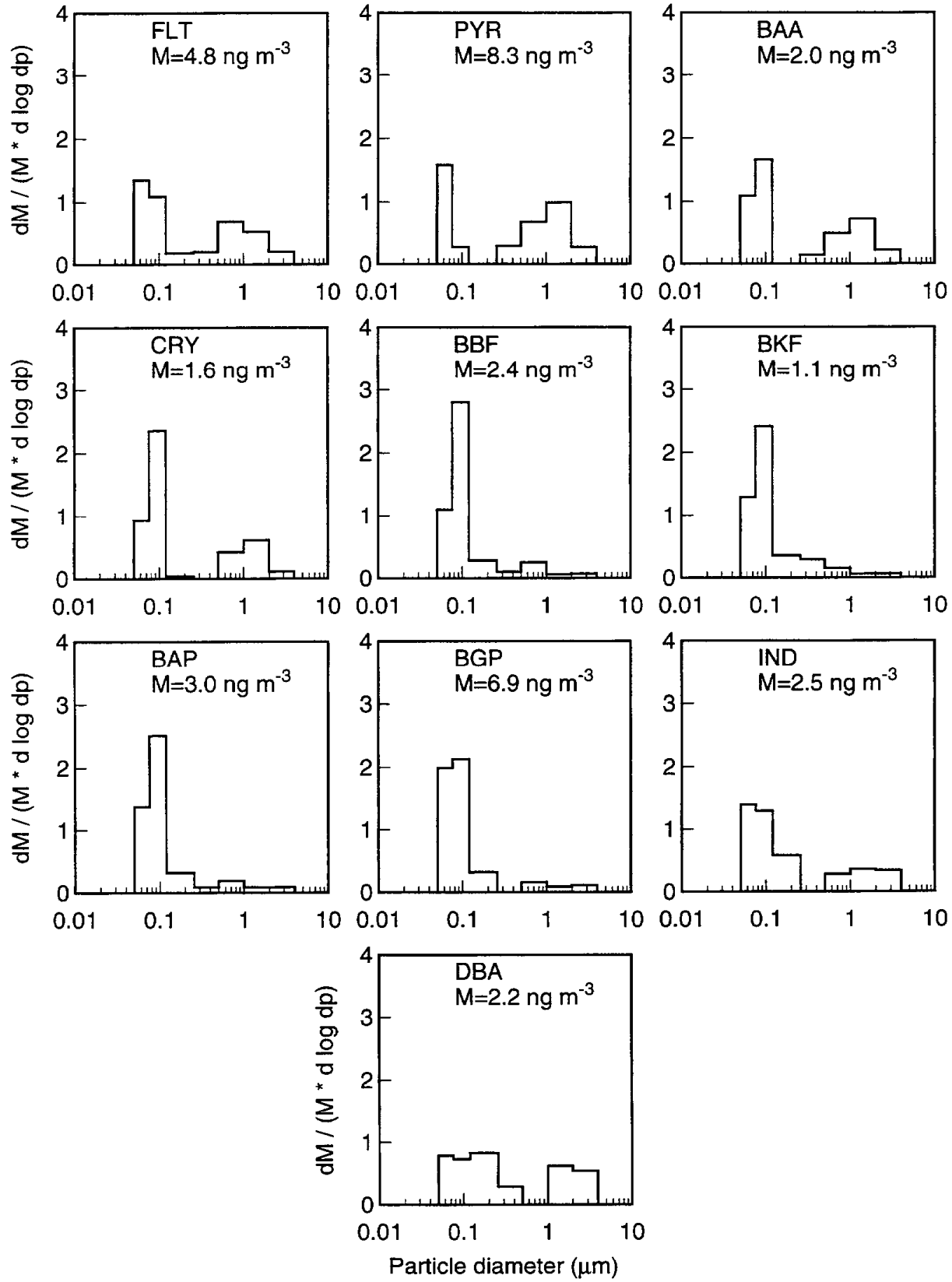


**Figure 5.2.** Size distribution and total mass concentration (M) of PAH measured in summer 1997 with a low-pressure impactor in the light-duty vehicle bore (bore 2) of the Caldecott tunnel.

### 5.3.4 Fuel PAH concentrations

Measured PAH concentrations in each gasoline sample are shown in Table 5.5. On average, NAP contributes 97±1% of the total concentration of the 16 PAH measured. Variation of PAH concentrations among different brands of gasoline is greater than variation between regular and premium grades of the same brand. Within a single brand, premium gasoline tends to have higher PAH concentrations than regular grade, and typically, PAH concentrations are no more than 50% higher or lower in one grade than another. One brand of gasoline (E) has markedly lower PAH concentrations than the other four brands. Concentrations of PAH other than ACY are 5 to 500 times lower in brand E gasoline relative to other brands. Differences in crude oil properties and/or in refinery operations may explain the much lower PAH content of brand E gasoline.

Measured PAH concentrations in each diesel sample are shown in Table 5.6. The fraction of NAP in the diesel fuels is not as consistent as in gasoline; in diesel fuel, NAP contributions range from 4% in brand 5 to 95% in brand 4 of the total PAH measured. Some of this variability may be due to loss of lower molecular weight PAH during blow down of the diesel fuel samples. Like gasoline, the diesel samples show large variations in PAH concentrations among different brands. Samples 2 and 5 have lower PAH concentrations than the other brands. Note that the gasoline samples do not correspond in brand to the diesel fuel samples collected in this study.

**Table 5.5.** PAH concentrations in Bay Area gasoline samples, summer 1997

| species | A | | B | | C | | D | | E | |
|---|---|---|---|---|---|---|---|---|---|---|
| (mg $L^{-1}$) | reg[a] | prem[b] | mid[c] | prem | reg | prem | reg | prem | reg | prem |
| NAP | 800 | 2100 | 1800 | 2400 | 790 | 900 | 1900 | 2600 | 120 | 69 |
| ACY | 0.21 | 0.29 | 0.27 | 0.27 | 0.28 | 0.21 | 0.27 | 0.32 | 0.12 | 0.10 |
| ACE | 3.3 | 6.3 | 6.8 | 7.2 | 3.6 | 4.8 | 7.4 | 6.2 | 0.25 | 0.19 |
| FLU | 5.1 | 7.8 | 7.2 | 7.9 | 4.4 | 7.4 | 7.8 | 6.0 | 0.76 | 0.62 |
| ANT | 7.2 | 14 | 14 | 16 | 8.0 | 9.8 | 14 | 15 | 0.51 | 0.52 |
| PHE | 13 | 20 | 23 | 25 | 14 | 19 | 10 | 18 | 0.23 | 0.47 |
| FLT | 0.90 | 2.6 | 2.4 | 3.3 | 1.0 | 1.7 | 2.6 | 3.5 | 0.022 | 0.061 |
| PYR | 1.1 | 3.1 | 3.4 | 3.9 | 1.2 | 1.9 | 4.8 | 4.1 | 0.030 | 0.072 |
| BAA | 0.40 | 1.4 | 1.6 | 2.0 | 0.44 | 0.42 | 1.1 | 2.0 | < lod | 0.025 |
| CHR | 0.19 | 0.82 | 0.83 | 1.3 | 0.20 | 0.33 | 0.91 | 1.5 | < lod | 0.016 |
| BBF | 0.092 | 0.28 | 0.34 | 0.34 | 0.11 | 0.22 | 0.29 | 0.44 | < lod | 0.0080 |
| BKF | 0.026 | 0.16 | 0.24 | 0.21 | 0.050 | 0.10 | 0.20 | 0.27 | < lod | 0.0068 |
| BAP | 0.18 | 0.50 | 0.95 | 0.84 | 0.29 | 0.50 | 0.47 | 0.71 | < lod | 0.031 |
| BGP | 0.14 | 0.55 | 0.68 | 0.74 | 0.18 | 0.36 | 0.76 | 0.85 | < lod | 0.022 |
| IND | 0.040 | 0.074 | 0.10 | 0.16 | 0.051 | 0.14 | 0.096 | 0.17 | < lod | 0.0055 |
| DBA | < lod[d] | < lod | < lod | < lod | < lod | < lod | < lod | < lod | < lod | < lod |

[a]Regular grade gasoline. [b]Premium grade gasoline. [c]Mid-grade gasoline. [d]Less than limit of detection, ~0.005 mg $L^{-1}$.

**Table 5.6.** PAH concentrations in Bay Area diesel fuel samples, summer 1997

| species ($mg\ L^{-1}$) | 1 | 2 | 3 | 4 | 5 |
|---|---|---|---|---|---|
| NAP | 1600 | 30 | 280 | 570 | 6.6 |
| ACY | 1.4 | 0.28 | 1.7 | 0.53 | 3.7 |
| ACE | 59 | 14 | 33 | 5.1 | 28 |
| FLU | 150 | 30 | 110 | 11 | < lod |
| ANT | 240 | 15 | 93 | 8.6 | 36 |
| PHE | < lod[a] | < lod | < lod | < lod | < lod |
| FLT | 3.5 | 0.071 | 0.90 | 0.089 | < lod |
| PYR | 39 | 6.7 | 15 | 4.9 | 86 |
| BAA | < lod | < lod | < lod | < lod | < lod |
| CRY | < lod | < lod | 2.5 | < lod | < lod |
| BBF | < lod | < lod | < lod | < lod | < lod |
| BKF | < lod | < lod | < lod | < lod | < lod |
| BAP | < lod | < lod | < lod | < lod | < lod |
| BGP | 2.5 | < lod | < lod | < lod | 0.93 |
| IND | < lod | < lod | < lod | < lod | < lod |
| DBA | < lod | < lod | < lod | < lod | < lod |

[a]Less than limit of detection, ~0.1 $mg\ L^{-1}$.

Figure 5.3 summarizes the average concentrations of the sixteen PAH in gasoline and diesel fuel samples. In calculating the mean PAH concentrations, brands were weighted equally, and for gasoline, different grades within each brand were weighted according to the market share of each grade: 58% regular, 20% mid, and 22% premium (Gilson, 1995). The market share of mid-grade was divided equally between regular and premium, resulting in weightings of 68% for regular and 32% for premium. For one brand of gasoline (B) for which no regular grade sample was available, a mid-grade sample was analyzed instead. Values below the limit of detection were treated as zeroes.

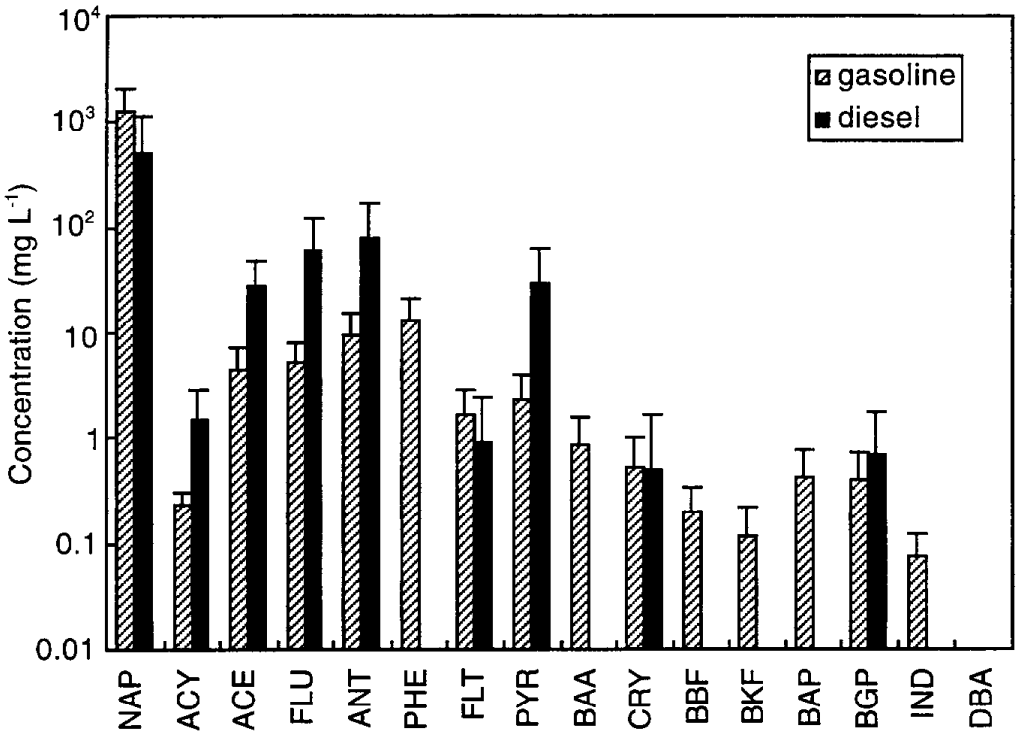


**Figure 5.3.** Average PAH concentration (±1 standard deviation) in ten gasoline samples and five diesel fuel samples.

PAH concentrations in the fuels ranged from undetectable for several of the higher molecular weight PAH in diesel fuel to ~1000 mg $L^{-1}$ for NAP in both gasoline and diesel fuel. While fifteen of the PAH, all but DBA, were detected in gasoline, only nine were detected in diesel fuel. Notably absent from diesel fuel were five of the six highest molecular weight PAH; a similar trend was observed in exhaust emissions in the tunnel. Diesel fuel contained five to ten times more of all the three ring PAH except PHE, which was difficult to quantify. In contrast, gasoline contained higher concentrations of all the four and five ring PAH except PYR.

### 5.3.5 Relationship between fuel and exhaust PAH

For gasoline-powered vehicles, PAH emission factors were correlated with fuel PAH concentrations ($R^2 = 0.79$, excluding BGP). Figure 5.4 shows the emission factor for ten PAH plotted versus PAH concentration in the fuel. Fuel PAH concentrations have been converted from mg $L^{-1}$ to mg $kg^{-1}$ by dividing by the gasoline density. In general, those

PAH with higher concentrations in gasoline also had higher emission factors. BGP, a five ring PAH, had an unusually high emission factor relative to its fuel concentration.

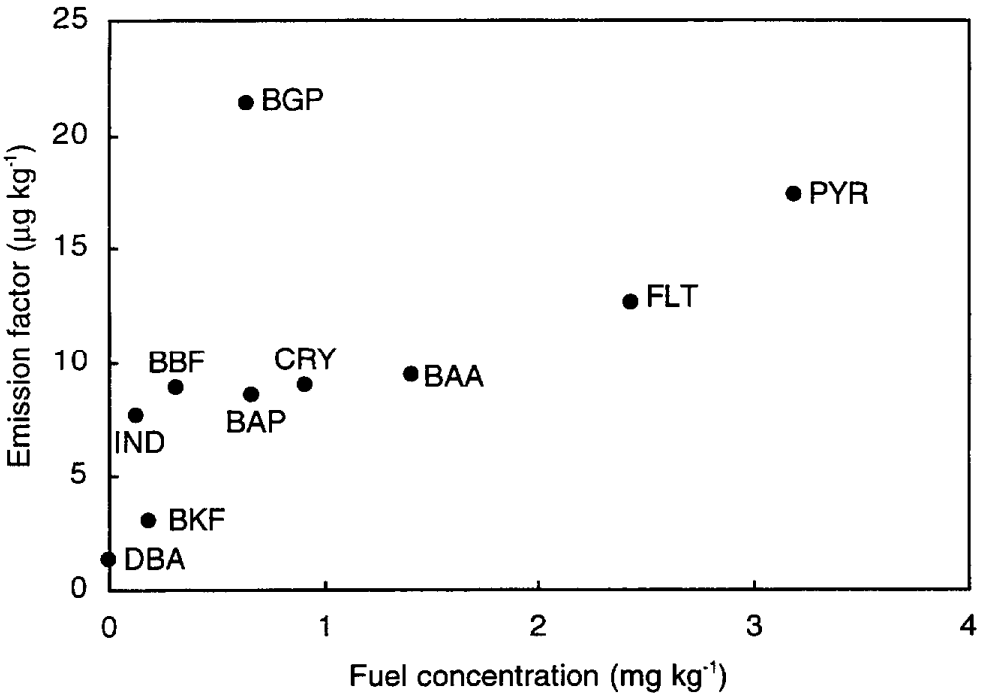


**Figure 5.4.** Light-duty PAH emission factor versus PAH concentration in gasoline.

PAH in motor vehicle exhaust can have several sources: PAH in fuel that escapes combustion, PAH in lubricating oil, and pyrosynthesis. If the relative concentrations of PAH in fuel escaping combustion remained the same as in the original fuel and if this were the only source of PAH in the exhaust, then a linear relationship between emission factor and fuel concentration would be expected. In Figure 5.4, most of the PAH fall near a line of slope 6 µg $mg^{-1}$, i.e. 6 µg of PAH emitted per mg of PAH in gasoline. For comparison, 0.48% (4.8 µg $mg^{-1}$) of naphthalene in diesel fuel was found to survive combustion in radiotracer experiments involving a diesel engine (Rhead and Pemberton, 1996). BGP has a much higher emission factor relative to its fuel concentration than other PAH in Figure 5.4, which suggests that other sources such as lubricating oil and/or pyrosynthesis are significant.

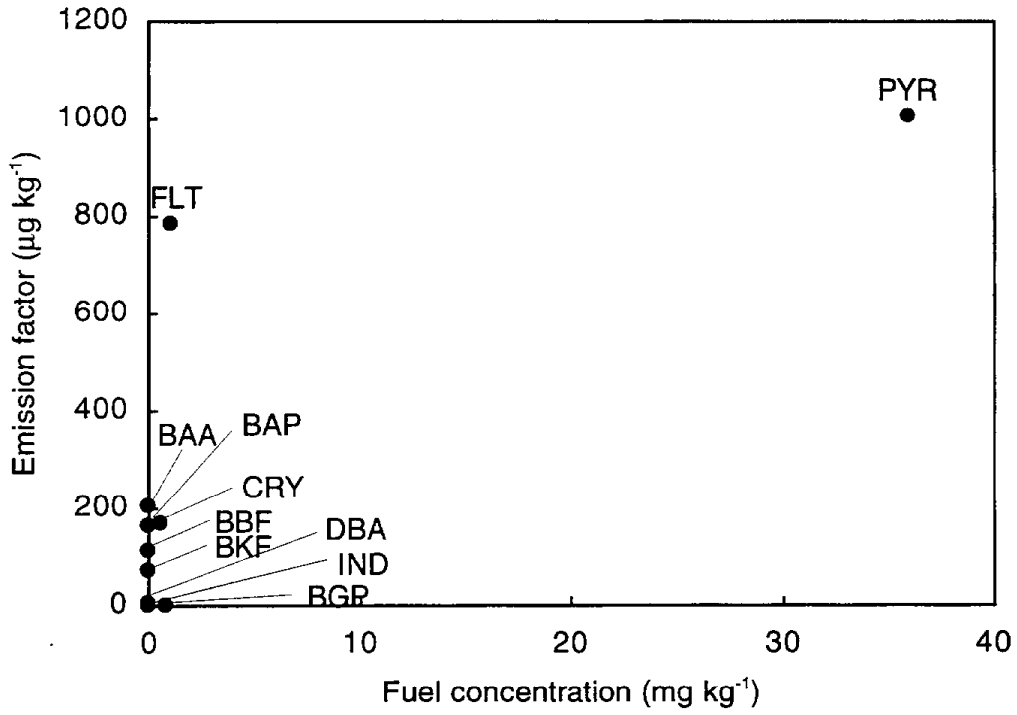


**Figure 5.5.** Heavy-duty diesel PAH emission factor versus PAH concentration in diesel fuel.

Comparison of emission factors and fuel concentrations for diesel, shown in Figure 5.5, was less informative. First, only four of the ten PAH measured in the tunnel were detected in diesel fuel: FLT, PYR, CRY, and BGP. Four PAH (BAA, BBF, BKF, and BAP) were not detected in the fuel but did have measurable emission factors. It is possible they were present in diesel fuel at levels below the limit of detection or that they have sources other than unburned fuel. BGP was found in the fuel but not in the exhaust, while DBA was found in the exhaust but not the fuel. IND was not detected in either diesel fuel or diesel exhaust. For the three PAH for which matched diesel fuel and tunnel data are available, the ratios of emission factors to PAH concentrations in diesel fuel are 720, 28, and 290 µg $mg^{-1}$ for FLT, PYR, and CRY, respectively. Some of the lower molecular weight PAH in diesel exhaust may originate from unburned diesel fuel, but the presence of higher molecular weight PAH in diesel exhaust which are not found in the fuel suggests that these PAH originate from other sources such as lubricating oil or pyrosynthesis.

# 6 Summary and Conclusions

The impacts of reformulated gasoline use on light-duty motor vehicle emissions have been assessed through measurements of pollutant concentrations in the Caldecott tunnel and the analysis of gasoline samples collected in the San Francisco Bay Area. Changes in vehicle emission rates of gas-phase pollutants including: carbon monoxide (CO), oxides of nitrogen ($NO_x$), non-methane organic compounds (NMOC), benzene, formaldehyde, acetaldehyde, 1,3-butadiene, and other $C_1$-$C_{10}$ organic compounds have been assessed. New chemical speciation profiles for NMOC and particulate matter emissions representative of vehicles using reformulated gasoline and low-sulfur, low-aromatic diesel fuel were developed. Heavy-duty diesel truck and light-duty vehicle exhaust emissions of fine particulate matter and oxides of nitrogen were measured, and the relative contributions of both vehicle types to air pollution were evaluated.

## 6.1 Reformulated Gasoline

The introduction of California Phase 2 reformulated gasoline (RFG) in the San Francisco Bay Area resulted in large changes to gasoline composition including: an increase in oxygen content from 0.2 to 2.0 wt%; and decreases in alkene, aromatic, benzene, and sulfur contents. Gasoline density and $T_{50}$ and $T_{90}$ distillation temperatures also decreased. Most of these changes occurred between summers 1995 and 1996. Light-duty vehicle emission rates measured in the Caldecott tunnel during summers 1994-1997 were used to evaluate the exhaust emission impacts of RFG use. Vehicle speeds and driving conditions inside the tunnel were similar each year. The average model year of the vehicle fleet was about one year newer each successive summer. Large reductions in pollutant emissions were measured in the tunnel over the course of this study, due to a combination of RFG and fleet turnover effects. Between summers 1994 and 1997, emissions of CO decreased by $31 \pm 5\%$, non-methane organic compounds decreased by $43 \pm 8\%$, and $NO_x$ decreased by $18 \pm 4\%$. It was difficult to separate clearly the fleet turnover and RFG contributions to these changes. Nevertheless, it was clear that the effect of RFG was greater for NMOC than for $NO_x$. The RFG effect on vehicle emissions of benzene was estimated to be a 30-40% reduction. Use of RFG increased formaldehyde emissions by about 10%, while acetaldehyde emissions did not change significantly.

The switch to reformulated gasoline also affected evaporative emissions. The combined effect of Phases 1 and 2 of California's RFG program was a 20% reduction in gasoline vapor pressure, about one fifth of which occurred following the introduction of Phase 2 RFG. A model was developed to predict equilibrium gasoline headspace vapor composition from measured liquid gasoline composition. Addition of MTBE and reduction of alkenes and aromatics in gasoline between summers 1995 and 1996 led to corresponding changes in the composition of gasoline headspace vapors. Normalized reactivity of liquid gasoline and headspace vapors decreased by 23 and 19%, respectively. Reduced mass emissions due to lower gasoline vapor pressure, together with reduced normalized reactivity of gasoline and its vapors, both decrease the ozone formed due to gasoline evaporation. The reactivity of on-road emissions measured in the tunnel decreased by ~5% or less. The reduction in reactivity of on-road emissions was less than that of evaporative emissions because of increased weight fractions of highly-reactive isobutene and formaldehyde in vehicle exhaust, which resulted from the increased use of MTBE in gasoline.

## 6.2 Fine Particles

An updated assessment of fine particle emissions from light- and heavy-duty vehicles was needed due to recent changes to the composition of gasoline and diesel fuel, more stringent emission standards applying to new vehicles sold in the 1990s, and the adoption of a new ambient air quality standard for fine particulate matter ($PM_{2.5}$) in the United States. In the summers of 1996 and 1997, separate measurements were made of uphill traffic in two bores of the Caldecott tunnel: one bore carried both light-duty vehicles and heavy-duty diesel trucks, and the second bore was reserved for light-duty vehicles.

Compared to gasoline-fueled light-duty vehicles, heavy-duty diesel trucks were found to emit 24, 38, and 21 times more fine particle, black carbon, and sulfate mass per unit mass of fuel burned, respectively. In addition, heavy-duty diesel trucks emitted 15-20 times the number of fine particles per unit mass of fuel burned compared to light-duty vehicles. Fine particle emissions from both vehicle classes are composed mostly of carbon; diesel-derived particulate matter contains more black carbon (51±11% of $PM_{2.5}$ mass) than does light-duty fine particle emissions (33±4%). Sulfate comprises only 2% of total fine particle emissions for both vehicle classes. Sulfate emissions measured in this study for heavy-duty diesel vehicles are significantly lower than values reported in earlier studies conducted before the introduction of low-sulfur diesel fuel. Diesel trucks were the major source of lighter PAH, whereas light-duty gasoline vehicles were a significant source of higher molecular weight PAH. Size-resolved measurements of particulate PAH showed significant fractions of diesel-derived PAH to be present in both the ultrafine size mode

(<0.12 μm) and the accumulation mode (0.12–2 μm). In contrast, the ultrafine mode was more prominent for gasoline engine-derived PAH emissions. Light-duty vehicle exhaust emission factors for PAH were correlated with PAH concentrations in gasoline.

Combination of measured emission factors and fuel consumption data indicates that diesel vehicles in California are responsible for nearly half of $NO_x$ emissions and greater than three quarters of exhaust fine particle emissions from on-road motor vehicles.

# 7 Recommendations

## 7.1 Continued On-Road Surveillance

The introduction of new gasoline formulations throughout the state of California provided unique opportunities to assess the impacts of changes in gasoline composition on motor vehicle emissions. The measurement of vehicle emissions in a heavily used roadway tunnel facilitated the characterization of a wide range of gas- and particle phase pollutants from thousands of vehicles driven under real-world conditions. The trends in vehicle emissions recorded during this multi-year research project illustrate the effects of changes in gasoline composition and an evolving vehicle fleet. Continued surveillance of on-road emissions is highly recommended to provide a clear picture of the emission impacts of fleet turnover. A better understanding of the effects of fleet turnover will be needed to track the changing contribution of motor vehicles to air pollution problems in the future.

As a result of increasingly stringent emission standards and increasingly robust emission control equipment, the on-road vehicle population will include growing numbers of very clean vehicles. Emission rates of CO, VOC, and $NO_x$ will likely decline, but emission rates of other pollutants may increase. Fraser and Cass (1998) reported increased on-road emissions of ammonia since the introduction of the 3-way catalytic converter. Others (Dasch, 1992; Berges et al., 1993) have reported increased emissions of nitrous oxide from catalyst-equipped vehicles. On-road monitoring will be helpful for tracking emission trends for these pollutants over time.

While no further changes to fuel composition are currently required in California, continued efforts to reduce vehicle emissions may lead to rethinking of fuel reformulation requirements. Concerns about ground and surface water contamination may lead to the elimination or reduction of MTBE in gasoline (Nakamura, 1998). Diesel engine manufacturers have expressed interest in reformulated diesel fuel to help in the attainment of emission standards for heavy-duty trucks (Slodowske, 1993). Changes to diesel fuel may include further reduction of sulfur and aromatic contents, a cetane number increase, modified distillation properties, and use of oxygenated compounds. The emission impacts

of any future changes in fuel properties should be assessed through continued study of on-road emissions.

For this reason, permanent installation of continuous CO, $CO_2$, $NO_x$, and hydrocarbon analyzers in climate-controlled rooms at both ends of the Caldecott tunnel is recommended.

## 7.2 Air Quality Modeling

While this research identified many of the emission impacts of reformulated gasoline, the impacts on ozone air quality were not evaluated in this study. It is difficult to assess changes in air quality from direct measurements of ambient pollutant concentrations because of meteorological variability. For example, meteorological effects such as changes in temperature, cloud cover, and atmospheric dispersion can mask changes in ozone formation that are due to changes in gasoline composition. Alternatively, Eulerian photochemical air quality models could be employed to estimate the ambient air quality effects of reformulated gasoline.

Photochemical air quality models have been developed to study the complex couplings between atmospheric chemistry, meteorology, pollutant emissions, and formation of ozone and other air pollutants. Harley et al. (1997) used the CIT airshed model to assess various motor vehicle emission inventory scenarios for California's South Coast Air Basin. The air quality impacts of changes in motor vehicle emissions that resulted from use of reformulated gasoline in the San Francisco Bay Area can be investigated in much the same manner.

## 7.3 Heavy-Duty Truck Emissions

This research indicated that heavy-duty diesel trucks contribute significantly to on-road $NO_x$ emissions and dominate on-road emissions of fine particles. Emissions from off-road diesel engines also contribute to air pollution problems. For instance, $NO_x$ emissions from mobile sources are roughly divided equally among heavy-duty on-road, heavy-duty off-road, and light-duty vehicles (Sawyer et al., 1998). Improved characterization of emissions from off-road diesel engines is needed.

Whereas light-duty vehicle emissions have been studied extensively and controlled stringently over the past 20 years, much less has been done to address emissions from heavy-duty vehicles. Further study is needed of the contribution of heavy-duty diesel engine emissions to air pollution. The distribution of emissions across the heavy-duty fleet deserves special attention. For light-duty vehicles, small numbers of gross-polluting vehicles contribute disproportionately to total emissions. An early assessment of the

heavy-duty vehicle fleet suggests that while high-emitters are found for CO and hydrocarbons, $NO_x$ emissions are normally distributed (Countess et al., 1998). Similar information on the distribution and overall contributions of light-duty and heavy-duty vehicles to fine particle emissions is needed to determine appropriate emission control strategies.

## 7.4 Polycyclic Aromatic Hydrocarbons

While the presence of PAH in diesel exhaust was confirmed in this study, it is not the case that diesel exhaust is the only significant on-road source of all PAH. This study suggests that light-duty vehicles are an important source of some of the heavier particle-phase PAH. Further consideration is needed of the relative importance of light-duty (gasoline) versus heavy-duty diesel engine emissions as sources of PAH.

This study found a correlation between PAH concentrations in gasoline and PAH emission factors from light-duty vehicles. Significant brand-to-brand variability in PAH concentrations was found among gasoline samples collected at Bay Area service stations. This suggests that it may be possible to reformulate gasoline to reduce its PAH content, and thus to reduce particle-phase exhaust PAH emissions. Relationships between PAH emissions and fuel composition should be studied further for both gasoline and diesel-powered vehicles.

# References


Abbass M.K., Andrews G.E. and Williams P.T. (1989). The influence of diesel fuel composition on particulate PAH emissions. *SAE technical paper*, no. 892079.

Allen J.O., Dookeran N.M., Smith K.A., Sarofim A.F., Taghizadeh K. and Lafleur A.L. (1996). Measurement of polycyclic aromatic hydrocarbons associated with size-segregated atmospheric aerosols in Massachusetts. *Environmental Science & Technology* **30**, 1023-1031.

ARB (1988). Proposed adoption of regulations limiting the sulfur content and the aromatic hydrocarbon content of motor vehicle diesel fuel. Stationary Source Division, California Air Resources Board, Sacramento, CA.

ARB (1990) Reformulated gasoline: proposed phase 1 specifications. California Air Resources Board, Sacramento, CA.

ARB (1991). Proposed regulations for California phase 2 reformulated gasoline. California Air Resources Board, Sacramento, CA.

ARB (1993a). California exhaust emission standards and test procedures for 1988 and subsequent model passenger cars, light-duty trucks, and medium-duty vehicles. California Air Resources Board, Sacramento, CA.

ARB (1993b). Predicted California on-road motor vehicle emissions (BURDEN7F). Mobile Source Emission Inventory Branch, California Air Resources Board, Sacramento, CA.

ARB (1994). Proposed amendments to the California phase 2 reformulated gasoline regulations, including amendments providing for the use of a predictive model. California Air Resources Board, Sacramento, CA.

ARB (1995). Emission Inventory—1993. Technical Support Division, California Air Resources Board, Sacramento, CA.

ARB (1996a). Predicted California on-road motor vehicle emissions, Volume I: EMFAC7G. Mobile Source Emission Inventory Branch, California Air Resources Board, Sacramento, CA.

ARB (1996b). CaRFG performance and compatibility test program. California Air Resources Board, Sacramento, CA.

ARB (1997). Emission Inventory—1995. Emission Inventory Branch, Technical Support Division, California Air Resources Board, Sacramento, CA.

Arnts R.R. and Tejada S.B. (1989). 2,4-Dinitrophenylhydrazine-coated silica gel cartridge method for determination of formaldehyde in air: identification of an ozone interference. *Environmental Science & Technology* **23**, 1428-1430.

ASTM (1987). American Society for Testing and Materials, Method D2622, Standard test method for sulfur in petroleum products by x-ray spectrometry.

ASTM (1993). American Society for Testing and Materials, Method D4815, Standard test method for determination of MTBE, ETBE, TAME, DIPE, and tertiary-amyl alcohol.

Auto/Oil (1992). Auto/Oil Air Quality Improvement Research Program, SP-920. Society of Automotive Engineers, Inc., Warrendale, PA.

Auto/Oil (1993). Auto/Oil Air Quality Improvement Research Program, Volume II, SP-1000. Society of Automotive Engineers, Inc., Warrendale, PA.

Auto/Oil (1995). Auto/Oil Air Quality Improvement Research Program, Volume III, SP-1117. Society of Automotive Engineers, Inc., Warrendale, PA.

BAAQMD (1998). Toxic air contaminant control program, 1996 annual report. Bay Area Air Quality Management District, San Francisco, CA.

Benner B.A. and Gordon G.E. (1989). Mobile sources of atmospheric polycyclic aromatic hydrocarbons: a roadway tunnel study. *Environmental Science & Technology* **23**, 1269-1278.

Bennett A., Lamm S., Orbey H. and Sandler S.I. (1993). Vapor-liquid equilibria of hydrocarbons and fuel oxygenates. 2. *Journal of Chemical and Engineering Data* **38**, 263-269.

Benson J.D., Burns V.R., Gorse R.A., Hochhauser A.M., Koehl W.J., Painter L.J. and Reuter R.M. (1991). Effects of gasoline sulfur level on mass exhaust emissions. *SAE technical paper series*, no. 912323.

Berges M.G.M., Hofmann R.M., Scharffe D., Crutzen P.J. (1993). Nitrous oxide emissions from motor vehicles in tunnels and their global extrapolation. *Journal of Geophysical Research-Atmospheres* **98**, 18527-18531.

Birch M.E. and Cary R.A. (1996). Elemental carbon-based method for monitoring occupational exposures to particulate diesel exhaust. *Aerosol Science and Technology* **25**, 221-241.

Bishop G.A. and Stedman D.H. (1990). On-road carbon monoxide emission measurement comparisons for the 1988-1989 Colorado oxy-fuels program. *Environmental Science & Technology* **24**, 843-847.

Black D.R., Singer B.C., Harley R.A., Martien P.T. and Fanai A.K. (1997). A fuel-based motor vehicle emission inventory for the San Francisco Bay Area. Paper no. 97-RP143.03 presented at the Air and Waste Management Association's 90th Annual Meeting and Exhibition, Toronto, Canada.

Black F.M. (1991). Control of vehicle emissions—the U.S. experience. *Critical Reviews in Environmental Control* **21**, 373-410.

Board of Equalization (1997). 1996-1997 Annual report. California State Board of Equalization, Sacramento, CA.

Brooks D.J., Peltier R.J., Baldus S.L., Reuter R.M., Bandy W.J. and Sprik T.L. (1995). Real world hot soak evaporative emissions—a pilot study. *SAE technical paper series*, no. 951007.

Bundt J., Herbel W., Steinhart H., Franke S. and Franke W. (1991). Structure-type separation of diesel fuels by solid phase extraction and identification of the two- and three-ring aromatics by capillary GC-mass spectrometry. *Journal of High Resolution Chromatography* **14**, 91-98.

Bureau of Census (1992). Truck inventory and use survey. United States Bureau of Census, Washington D.C.

Burns V.R., Benson J.D., Hochhauser A.M., Koehl W.J., Kreucher W.M. and Reuter R.M. (1991). Description of Auto/Oil Air Quality Improvement Research Program. *SAE technical paper series*, no. 912320.

Burns V.R., Reuter R.M., Benson J.D., Gorse R.A., Hochhauser A.M., Koehl W.J. and Painter L.J. (1992). Effects of gasoline composition on evaporative and running loss emissions. *SAE technical paper series*, no. 920323.

Cadle S.H., Mulawa P.A., Ball J., Donase C., Weibel A., Sagebiel J.C., Knapp K.T. and Snow R. (1997). Particulate emission rates from in-use high-emitting vehicles recruited in Orange County, California. *Environmental Science & Technology* **31**, 3405-3412.

Calvert J.G., Heywood J.B., Sawyer R.F. and Seinfeld J.H. (1993). Achieving acceptable air quality: some reflections on controlling vehicle emissions. *Science* **261**, 37-45.

Carter W.P.L. (1994). Development of ozone reactivity scales for volatile organic compounds. *Journal of the Air & Waste Management Association* **44**, 881-899.

Cass G. R. and Gray H. A. (1995). Regional emissions and atmospheric concentrations of diesel engine particulate matter: Los Angeles as a case study. In *Diesel Exhaust: a critical analysis of emissions, exposure, and health effects*, pp. 125-137. Health Effects Institute, Cambridge, MA.

Chow J.C., Watson J.G., Lowenthal D.H., Solomon P.A., Magliano K.L., Ziman S.D. and Richards L.W. (1992). $PM_{10}$ source apportionment in California's San Joaquin valley. *Atmospheric Environment* **26A**, 3335-3354.

Chow J.C., Watson J.G., Lowenthal D.H., Solomon P.A., Magliano K.L., Ziman S.D. and Richards L.W. (1993). $PM_{10}$ and $PM_{2.5}$ compositions in California's San Joaquin Valley. *Aerosol Science and Technology* **18**, 105-128.

Chow J.C., Watson J.G., Fujita E.M., Lu Z., Lawson D.R. and Ashbaugh L.L. (1994). Temporal and spatial variations of $PM_{2.5}$ and $PM_{10}$ aerosol in the southern California air quality study. *Atmospheric Environment* **28**, 2061-2080.

Chow J.C., Fairley D., Watson J.G., DeMandel R., Fujita E.M., Lowenthal D.H., Lu Z., Frazier C.A., Long G. and Cordova J. (1995). Source apportionment of wintertime $PM_{10}$ at San Jose, Calif. *Journal of Environmental Engineering* **121**, 378-387.

Countess R.J., Cohen L.H., Countess S.J., Bishop G.A. and Stedman D.H. (1998). Remote sensing of heavy-duty diesel truck exhaust. Eighth CRC on-road vehicle emissions workshop, San Diego, CA, April 20-22. Coordinating Research Council, Atlanta, GA.

Daisey J.M., Cheney J.L. and Lioy P.J. (1986). Profiles of organic particulate emissions from air pollution sources: status and needs for receptor source apportionment modeling. *Journal of the Air Pollution Control Association* **36**, 17-33.

Dasch J.M. (1992). Nitrous oxide emissions from vehicles. *Journal of the Air & Waste Management Association* **42**, 63-67.

DeLuchi M.A. (1993). Emissions from the production, storage, and transport of crude oil and gasoline. *Journal of the Air & Waste Management Association* **43**, 1486-1495.

Dolislager, L.J. (1997). The effect of California's wintertime oxygenated fuels program on ambient carbon monoxide concentrations. *Journal of the Air & Waste Management Association* **47**, 775-783.

Dreher D.B. and Harley R.A. (1998). A fuel-based inventory for heavy-duty diesel truck emissions. *Journal of the Air & Waste Management Association* **48**, 352-358.

Eatough D.J., Tang H., Cui W. and Machir J. (1995). Determination of the size distribution and chemical composition of fine particulate semivolatile organic material in urban environments using diffusion denuder technology. *Inhalation Toxicology* **7**, 691-710.

Eatough D.J., Eatough D.A., Lewis L. and Lewis E.A. (1996). Fine particulate chemical composition and light extinction at Canyonlands National Park using organic particulate material concentrations obtained with a multisystem, multichannel diffusion denuder sampler. *Journal of Geophysical Research* **101**, 19515-19531.

EPA (1996). National air pollutant emission trends, 1990 - 1995. United States Environmental Protection Agency Office of Air Quality Planning and Standards, Research Triangle Park, NC.

EPA (1997). National air quality and emissions trends report, 1996. United States Environmental Protection Agency Office of Air Quality Planning and Standards, Research Triangle Park, NC.

Fraser M.P. and Cass G.R. (1998). Detection of excess ammonia emissions from in-use vehicles and the implications for fine particle control. *Environmental Science & Technology* **32**, 1053-1057.

Fuchs N.A. (1964). *The mechanics of aerosols*, p. 204. Pergamon Press Ltd., Oxford, England.

Gertler A.W., Fujita E.M., Pierson W.R. and Wittorff D.N. (1996). Apportionment of NMHC tailpipe vs non-tailpipe emissions in the Fort McHenry and Tuscarora mountain tunnels. *Atmospheric Environment* **30**, 2297-2305.

Gertler A.W., Sagebiel J.C., Dippel W.A., Gillies J.A., Gofa F. and O'Connor C.M. (1997). Comparison of 1995 and 1996 emissions at the Los Angeles Sepulveda tunnel including the impact of California phase 2 RFG. Desert Research Institute, Reno, NV. Report to the Coordinating Research Council, Project No. E-27.

Gilson D. (1995). Chevron Products Co., San Francisco, CA. Personal communication.

Gorse R.A., Benson J.D., Hochhauser A.M., Koehl W.J., Painter L.J. and Reuter R.M. (1991). Toxic air pollutant vehicle exhaust emissions with reformulated gasoline. *SAE technical paper series*, no. 912324.

Gray H.A., Cass G.R., Huntzicker J.J., Heyerdahl E.K., Rau J.A. (1986). Characteristics of atmospheric organic and elemental carbon particle concentrations in Los Angeles. *Environmental Science & Technology* **20**, 580-589.

Harley R.A., Sawyer R.F. and Milford J.B. (1997). Updated photochemical modeling for California's South Coast Air Basin: comparison of chemical mechanisms and motor vehicle emission inventories. *Environmental Science & Technology* **31**, 2829-2839.

Hering S.V., Flagan R.C. and Friedlander S.K. (1978). Design and evaluation of a new low pressure impactor. *Environmental Science & Technology* **12**, 667-673.

Hering S.V., Friedlander S.K., Collins J.J. and Richards L.W. (1979). Design and evaluation of a new low pressure impactor II. *Environmental Science & Technology* **13**, 184-188.

Hering S.V., Miguel A.H. and Dod R.L. (1984). Tunnel measurements of the PAH, carbon thermogram and elemental source signature for vehicular exhaust. *The Science of the Total Environment* **36**, 39-45.

Heywood J.B. (1988). *Internal Combustion Engine Fundamentals*, p. 915. McGraw-Hill Publishing Company, New York, NY.

Hildemann L.M., Markowski G.R. and Cass G.R. (1991). Chemical composition of emissions from urban sources of fine organic aerosol. *Environmental Science & Technology* **25**, 744-759.

Hochhauser A.M., Benson J.D., Burns V., Gorse R.A., Koehl W.J., Painter L.J., Rippon B.H., Reuter R.M. and Rutherford J.A. (1991). The effect of aromatics, MTBE, olefins and $T_{90}$ on mass exhaust emissions from current and older vehicles. *SAE technical paper series*, no. 912322.

Hochhauser A.M., Benson J.D., Burns V., Gorse R.A., Koehl W.J., Painter L.J., Rippon B.H., Reuter R.M. and Rutherford J.A. (1993). Fuel composition effects on automotive fuel economy. *SAE technical paper series*, no. 930138.

Hoekman S.K. (1992). Speciated measurements and calculated reactivities of vehicle exhaust emissions from conventional and reformulated gasolines. *Environmental Science & Technology* **26**, 1206-1216.

Howard C.J., Russell A.G., Atkinson R. and Calvert J.G. (1997). Air quality effects of the winter oxyfuel program. In *Interagency assessment of oxygenated fuels*, pp. 1-57. Office of Science and Technology Policy, Washington, DC.

John W. and Reischl G. (1980). A cyclone for size-selective sampling of ambient air. *Journal of the Air Pollution Control Association* **30**, 872-876.

John W., Wall S.M. and Ondo J.L. (1988). A new method for nitric acid and nitrate aerosol measurement using the dichotomous sampler. *Atmospheric Environment* **22**, 1627-1635.

Khalili N.R., Scheff P.A. and Holsen T.M. (1995). PAH source fingerprints for coke ovens, diesel and gasoline engines, highway tunnels, and wood combustion emissions. *Atmospheric Environment* **29**, 533-542.

Kirchstetter T.W., Singer B.C., Harley R.A, Kendall G.R. and Chan W. (1996). Impact of oxygenated gasoline use on California light-duty vehicle emissions. *Environmental Science & Technology* **30**, 661-670.

Knepper J.C., Koehl W.J., Benson J.D., Burns V.R., Gorse R.A., Hochhauser A.M., Leppard W.R., Rapp L.A. and Reuter R.M. (1993). Fuel Effects in Auto/Oil High Emitting Vehicles. *SAE technical paper series*, no. 912322.

Koehl W.J., Benson J.D., Burns V.R., Gorse R.A., Hochhauser A.M., Knepper J.C., Leppard W.R., Painter L.J., Rapp L.A., Reuter R.M. and Rutherford J.A. (1993). Effects of gasoline sulfur level on exhaust mass and speciated emissions: the question of linearity. *SAE technical paper series*, no. 932727.

Kohler D.A. (1997). Chevron Research and Technology Co., Richmond, CA. Personal communication.

Larson S.M. and Cass G.R. (1989). Characteristics of summer midday low-visibility events in the Los Angeles area. *Environmental Science & Technology* **23**, 281-289.

Larson S.M., Cass G.R. and Gray H.A. (1989). Atmospheric carbon particles and the Los Angeles visibility problem. *Aerosol Science & Technology* **10**, 118-130.

Leppard W.R., Rapp L.A., Burns V.R., Gorse R.A., Knepper J.C. and Koehl W.J. (1992). Effects of gasoline composition on vehicle engine-out and tailpipe hydrocarbon emissions. *SAE technical paper series*, no. 920329.

Li C.K. and Kamens R.M. (1993). The use of polycyclic aromatic hydrocarbons as source signatures in receptor modeling. *Atmospheric Environment* **27A**, 523-532.

Lowenthal D.H., Zielinska B., Chow J.C., Watson J.G., Gautam M., Ferguson D.H., Neuroth G.R. and Stevens K.D. (1994). Characterization of heavy-duty diesel vehicle emissions. *Atmospheric Environment* **28**, 731-743.

Lum D. (1997). Compliance Division, California Air Resources Board, Sacramento, CA. Personal communication.

Lyons C.E. and Fox R.J. (1993). Quantifying the air pollution emissions reduction effectiveness and costs of oxygenated fuels. *SAE technical paper series*, no. 930374.

Mi H.-H., Lee W.-J., Wu T.-L., Lin T.-C., Wang L.-C. and Chao H.-R. (1996). PAH emission from a gasoline-powered engine. *Journal of Environmental Science and Health* **A31**, 1981-2003.

Miguel A.H. and Friedlander S.K. (1978). Distribution of benzo(a)pyrene and coronene with respect to particle size in Pasadena aerosols in the submicron range. *Atmospheric Environment* **12**, 2407-2413.

Miguel A.H. and Rubenish L.M. (1980). Submicron size distributions of particulate polycyclic aromatic hydrocarbons in combustion emissions. In *Polynuclear Aromatic Hydrocarbons: Chemistry and Biological Effects*, pp. 1077-1083. Battelle Press, Cleveland, OH.

Miguel A.H. and Friedlander S.K. (1984). Size distribution of elemental carbon in atmospheric aerosols. In *Aerosols*, pp. 407-410. Elsevier Science, New York, NY.

McGetrick J. (1996). ARCO Products Co., Los Angeles, CA. Personal communication.

McGetrick J. (1997). ARCO Products Co., Los Angeles, CA. Personal communication.

Nakamura D.M. (1998). The end of MTBE? *Hydrocarbon Processing* **77**, 15-15.

Nauss K.M. (1995). Critical issues in assessing the carcinogenicity of diesel exhaust: a synthesis of current knowledge. In *Diesel Exhaust: a critical analysis of emissions, exposure, and health effects*, pp. 11-61. Health Effects Institute, Cambridge, MA.

Nelson D.D., Zahniser M.S., McManus J.B., Kolb C.E., Jimenez J.L. and McRae G.J. (1998). Remote sensing of heavy duty diesel truck $NO_x$ emissions using tunable diode lasers. Eighth CRC on-road vehicle emissions workshop, San Diego, CA, April 20-22. Coordinating Research Council, Atlanta, GA.

Nikanjam M. (1993). Development of the first CARB certified California alternative diesel fuel. *SAE technical paper series*, no. 930728.

Novakov T., Corrigan C.E., Penner J.E., Chuang C.C., Rosario O. and Mayol Bracero O.L. (1997). Organic aerosols in the Caribbean trade winds: a natural source? *Journal of Geophysical Research* **102**, 21307-21313.

Pahl R.H. and McNally M.J. (1990). Fuel blending and analysis for the Auto/Oil Air Quality Improvement Research Program. *SAE technical paper series*, no. 902098.

Pierson W.R. and Brachaczek W.W. (1983). Particulate matter associated with vehicles on the road. II. *Aerosol Science and Technology* **2**, 1-40.

Pierson W.R. (1995). Automotive CO emission trends derived from measurements in highway tunnels. *Journal of the Air & Waste Management Association* **45**, 831-832.

Pierson W.R., Gertler A.W., Robinson N.F., Sagebiel J.C., Zielinska B., Bishop G.A., Stedman D.H., Zweidinger R.B. and Ray W.D. (1996). Real-world automotive emissions–summary of studies in the Fort McHenry and Tuscarora Mountain tunnels. *Atmospheric Environment* **30**, 2233-2256.

Pointet K., Renou-Gonnord M.-F., Milliet A. and Jaudon P. (1997). Quantification of polycyclic aromatic hydrocarbons (PAHs) in diesel engine combustion by GC/MS. *Bulletin de la Societe Chimique de France* **134**, 133-140.

Pollack A.K., Cohen J.P. and Noda A.M. (1990). Auto/Oil Air Quality improvement research program: description of working data set, Systems Applications International, San Rafael, CA.

Reid R.C., Prausnitz J.M. and Poling B.E. (1987). *The properties of gases and liquids*, pp. 212-215. McGraw-Hill Book Company, New York, NY.

Reuter R.M., Benson J.D., Brooks D.J., Dunker A.M., Gorse R.A. and Koehl W.J. (1994). Sources of vehicles emissions in three day diurnal SHED tests. *SAE technical paper series*, no. 941965.

Reuter R.M., Benson J.D., Burns V.R., Gorse R.A., Hochhauser A.M., Koehl W.J., Painter L.J., Rippon B.H. and Rutherford J.A. (1992). Effects of oxygenated fuels and RVP on automotive emissions. *SAE technical paper series*, no. 920326.

Rhead, M.M. and Pemberton, R.D. (1996). Sources of naphthalene in diesel exhaust emissions. *Energy and Fuels* **10**, 837-843.

Rogak S.N., Green S.I. and Pott U. (1998a). Use of a tracer gas for direct calibration of emission-factor measurements in a traffic tunnel. *Journal of the Air & Waste Management Association* **48**, 545-552.

Rogak S.N., Pott U., Dann T. and Wang D. (1998b). Gaseous emissions from vehicles in a traffic tunnel in Vancouver, BC. *Journal of the Air & Waste Management Association* **48**, 604-615.

Rogge W.F., Hildemann L.M., Mazurek M.A. and Cass G.R. (1993). Sources of fine organic aerosol. 2. Noncatalyst and catalyst-equipped automobiles and heavy-duty diesel trucks. *Environmental Science & Technology* **27**, 636-651.

Sagebiel J.C., Zielinska B., Walsh P.A., Chow J.C., Cadle S.H., Mulawa P.A., Knapp K.T., Zweidinger R.B. and Snow R. (1997). PM-10 exhaust samples collected during IM-240 dynamometer tests of in-service vehicles in Nevada. *Environmental Science & Technology* **31**, 75-83.

Sawyer R.F. and Johnson J.H. (1995). Diesel emissions and control technology. In *Diesel Exhaust: a critical analysis of emissions, exposure, and health effects*, pp. 65-81. Health Effects Institute, Cambridge, MA.

Sawyer R.F., Harley R.A., Cadle S.H., Norbeck J.M., Slott R. and Bravo H.A. (1998). Mobile sources critical review, 1998 NARSTO assessment. Report to Coordinating Research Council.

Seinfeld J.H. and Pandis S.N. (1998). *Atmospheric chemistry and physics: from air pollution to climate change*, p. 662. Wiley, New York, NY.

Siegl W.O., Richert J.F.O., Jensen T.E., Schuetzle D., Swarin S.J., Loo J.F., Prostak A., Nagy D. and Schlenker A.M. (1993). Improved speciation methodology for Phase II of the Auto/Oil Air Quality Improvement Research Program—hydrocarbons and oxygenates. *SAE technical paper series*, no. 930142.

Singer B.C. and Harley R.A. (1996). A fuel-based motor vehicle emission inventory. *Journal of the Air & Waste Management Association* **46**, 581-593.

Singer B.C., Kirchstetter T.W., Harley R.A., Kendall G.R. and Hesson J.M. (1998). A fuel-based approach to estimating motor vehicle cold start emissions. *Journal of Air & Waste Management Association* **49**, 125-135.

Slodowske, W.J. (1993). An engine manufacturer's perspective on diesel fuels and the environment. Society of Automotive Engineers Panel presentation at SAE Fuels and Lubricants Meeting.

Solomon P.A., Fall T., Salmon L., Cass G.R., Gray H.A. and Davidson A. (1989). Chemical characteristics of $PM_{10}$ aerosols collected in the Los Angeles area. *Journal of the Air Pollution Control Association* **39**, 154-163.

Stedman D.H., Bishop G.A., Beaton S.P., Peterson J.E., Guenther P.L., McVey I.F. and Zhang Y. (1994). On-road remote sensing of CO and HC emissions in California. University of Denver, Denver, CO. Final Report to the California Air Resources Board under contract A032-093.

Stump F.D., Knapp K.T., Ray W.D., Siudak P.D. and Snow R.F. (1994). Influence of oxygenated fuels on the emissions from three pre-1985 light-duty passenger vehicles. *Journal of the Air & Waste Management Association* **44**, 781-786.

Tancell P.J., Rhead M.M., Trier C.J., Bell M.A. and Fussey D.E. (1995). The sources of benzo[a]pyrene in diesel exhaust emissions. *The Science of the Total Environment* **162**, 179-186.

Thorson P. (1997). Lawrence Berkeley National Laboratory, Berkeley, CA. Personal communication.

Turpin B.J., Huntzicker J.J. and Hering S.V. (1994). Investigation of organic aerosol sampling artifacts in the Los Angeles basin. *Atmospheric Environment* **28**, 3061-3071.

Ullman T.L., Mason R.L. and Montalvo D.A. (1990). Effects of fuel aromatics, cetane number, and cetane improver on emissions from a 1991 prototype heavy-duty diesel engine. *SAE technical paper series*, no. 902171.

Vanderwal R.L., Jensen K.A. and Choi M.Y. (1997). Simultaneous laser-induced emission of soot and polycyclic aromatic hydrocarbons within a gas-diffusion jet flame. *Combustion and Flame* **109**, 399-414.

Venkataraman C., Lyons J.M. and Friedlander S.K. (1994). Size distributions of polycyclic aromatic hydrocarbons and elemental carbon. 1. Sampling, measurement methods, and source characterization. *Environmental Science & Technology* **28**, 555-562.

Wall J.C., Shimpi S.A. and Yu M.L. (1987). Fuel sulfur reduction for control of diesel particulate emissions. *SAE technical paper series*, no. 872139.

Watson J.G., Chow J.C., Lu Z., Fujita E.M., Lowenthal D.H., Lawson D.R. and Ashbaugh L.L. (1994a). Chemical mass balance source apportionment of $PM_{10}$ during the southern California air quality study. *Aerosol Science and Technology* **21**, 1-36.

Watson J.G., Chow J.C., Lowenthal D.H., Pritchett L.C., Frazier C.A., Neuroth G.R. and Robbins R. (1994b). Differences in the carbon composition of source profiles for diesel- and gasoline-powered vehicles. *Atmospheric Environment* **28**, 2493-2505.

Westerholm R. and Li H. (1994). A multivariate statistical analysis of fuel-related polycyclic aromatic hydrocarbon emissions from heavy-duty diesel vehicles. *Environmental Science & Technology* **28**, 965-972.

Williams P.T., Abbass M.K., Andrews G.E. and Bartle K.D. (1989). Diesel particulate emissions: the role of unburned fuel. *Combustion and Flame* **75**, 1-24.

Zhang Y., Stedman D.H., Bishop G.A., Guenther P. and Beaton S.P. (1995). Worldwide on-road vehicle exhaust emissions study by remote sensing. *Environmental Science & Technology* **29**, 2286-2294.

Zhang Y., Stedman D.H., Bishop G.A., Beaton S.P., Guenther P.L. and McVey I.F. (1996). Enhancement of remote sensing for mobile source nitric oxide. *Journal of the Air & Waste Management Association* **46**, 25-29.

Zielinska B. and Fung K. (1992). Composition and concentrations of semivolatile hydrocarbons. Desert Research Institute, Reno, NV. Report to the California Air Resources Board under contract A032-130.

# List of Publications

The list of publications that resulted from this research is provided below.


Kirchstetter, T.W.; Harley, R.A.; Kendall, G.R.; Hesson, J.M. (1997). Impact of California Phase 2 reformulated gasoline on atmospheric reactivity of exhaust and evaporative emissions. Paper 97-RP139.01 presented at the 92nd annual meeting of the Air & Waste Management Association, Toronto, Canada, June 1997.

Miguel, A.H.; Kirchstetter, T.W.; Harley, R.A.; Hering, S.V. (1998). On-road emissions of particulate polycyclic aromatic hydrocarbons and black carbon from gasoline and diesel vehicles. *Environmental Science & Technology*, **32**, 450-455.

Kirchstetter, T.W.; Singer, B.C.; Harley, R.A.; Kendall, G.R.; Traverse, M. (1999a). Impact of California reformulated gasoline on motor vehicle emissions: 1. Mass emission rates. *Environmental Science & Technology,* **33**, 318-328.

Kirchstetter, T.W.; Singer, B.C.; Harley, R.A.; Kendall, G.R.; Hesson, J.M. (1999b). Impact of California reformulated gasoline on motor vehicle emissions: 2. Volatile organic compound speciation and reactivity. *Environmental Science & Technology*, **33**, 329-336.

Kirchstetter, T.W.; Harley, R.A.; Kreisberg, N.M.; Stolzenburg, M.R.; Hering, S.V. (1999c). On-road measurement of fine particle and nitrogen oxide emissions from light- and heavy-duty motor vehicles. *Atmospheric Environment,* **33**, in press.

Marr, L.C.; Kirchstetter, T.W.; Harley, R.A.; Miguel, A.H.; Hering, S.V.; Hammond, S.K. (1999). Characterization of polycylic aromatic hydrocarbons in motor vehicle fuels and exhaust emissions. Submitted to *Environmental Science & Technology*.

# Appendix A

# Composition of Whole Liquid Gasoline

**Appendix A**

| compound | $\Delta h_c$[a] kJ $g^{-1}$ | MIR $gO_3/gOC_i$ | weight % of total: 1995 gasoline grade regular | 1995 premium | 1995 composite[b] | 1996 gasoline grade regular | 1996 premium | 1996 composite |
|---|---|---|---|---|---|---|---|---|
| **n-alkanes** | | | | | | | | |
| propane | -46.4 | 0.48 | 0.01 | 0.06 | 0.03 | 0.01 | 0.01 | 0.01 |
| n-butane | -45.7 | 1.02 | 0.97 | 1.10 | 1.01 | 0.65 | 0.59 | 0.63 |
| n-pentane | -45.4 | 1.04 | 3.57 | 2.27 | 3.15 | 2.56 | 2.13 | 2.42 |
| n-hexane | -45.1 | 0.98 | 2.27 | 1.42 | 2.00 | 1.80 | 0.87 | 1.50 |
| n-heptane | -44.9 | 0.81 | 1.54 | 1.04 | 1.38 | 1.35 | 1.03 | 1.24 |
| n-octane | -44.8 | 0.61 | 0.45 | 0.50 | 0.47 | 0.58 | 0.37 | 0.52 |
| n-nonane | -44.7 | 0.54 | 0.17 | 0.17 | 0.17 | 0.23 | 0.13 | 0.20 |
| n-decane | -44.6 | 0.47 | 0.06 | 0.04 | 0.06 | 0.06 | | 0.04 |
| n-undecane | -44.5 | 0.42 | 0.05 | 0.03 | 0.04 | 0.03 | 0.03 | 0.03 |
| n-dodecane | -44.5 | 0.38 | 0.03 | 0.00 | 0.02 | 0.01 | 0.01 | 0.01 |
| n-tridecane | -44.4 | 0.35 | 0.01 | 0.01 | 0.01 | 0.00 | 0.01 | 0.00 |
| n-tetradecane | -44.4 | 0.32 | 0.00 | 0.00 | 0.00 | | | |
| n-pentadecane | -44.3 | 0.29 | 0.01 | 0.01 | 0.01 | 0.00 | 0.00 | 0.00 |
| total n-alkanes | | | 9.14 | 6.66 | 8.34 | 7.29 | 5.17 | 6.61 |
| **isoalkanes** | | | | | | | | |
| 2-methylpropane | -45.6 | 1.21 | 0.22 | 0.27 | 0.24 | 0.10 | 0.08 | 0.09 |
| 2-methylbutane | -45.2 | 1.38 | 9.55 | 9.32 | 9.48 | 8.63 | 9.18 | 8.81 |
| 2-methylpentane | -45.0 | 1.53 | 4.85 | 3.64 | 4.46 | 4.75 | 3.22 | 4.26 |
| 3-methylpentane | -45.0 | 1.52 | 3.03 | 2.41 | 2.83 | 2.91 | 1.96 | 2.60 |
| 2,2-dimethylbutane | -44.9 | 0.82 | 0.73 | 1.45 | 0.96 | 0.88 | 0.69 | 0.82 |

**Appendix A** (continued)

| compound | $\Delta h_c$[a] kJ $g^{-1}$ | MIR $gO_3/gOC_i$ | weight % of total: 1995 gasoline grade regular | 1995 gasoline grade premium | 1995 gasoline grade composite[b] | 1996 gasoline grade regular | 1996 gasoline grade premium | 1996 gasoline grade composite |
|---|---|---|---|---|---|---|---|---|
| 2,3-dimethylbutane | -45.0 | 1.07 | 1.03 | 1.21 | 1.09 | 1.33 | 1.43 | 1.36 |
| 2-methylhexane | -44.8 | 1.08 | 2.14 | 1.16 | 1.83 | 1.75 | 1.08 | 1.54 |
| 3-methylhexane | -44.9 | 1.40 | 2.28 | 1.44 | 2.01 | 1.96 | 1.46 | 1.80 |
| 2,3-dimethylpentane | -44.8 | 1.51 | 1.02 | 0.94 | 0.99 | 1.20 | 1.88 | 1.42 |
| 2,4-dimethylpentane | -44.8 | 1.78 | 0.48 | 0.58 | 0.51 | 0.66 | 1.11 | 0.80 |
| 2,2-dimethylpentane | -44.7 | 1.40 | 0.15 | 0.14 | 0.15 | 0.10 | 0.08 | 0.09 |
| 3-ethylpentane | -44.9 | 1.40 | 0.19 | 0.13 | 0.17 | 0.16 | | 0.11 |
| 2-methylheptane | -44.7 | 0.96 | 0.63 | 0.64 | 0.63 | 0.88 | 0.56 | 0.78 |
| 3-methylheptane | -44.7 | 0.99 | 0.77 | 0.83 | 0.79 | 0.94 | 0.64 | 0.84 |
| 4-methylheptane | -44.8 | 1.20 | 0.31 | 0.34 | 0.32 | 0.42 | 0.32 | 0.39 |
| 224-trime-pentane | -44.6 | 0.93 | 0.38 | 2.08 | 0.92 | 2.45 | 6.16 | 3.64 |
| 233-trime-pentane | -44.7 | 1.20 | 0.20 | 1.10 | 0.49 | 1.06 | 2.98 | 1.67 |
| 234-trime-pentane | -44.7 | 1.60 | 0.19 | 0.95 | 0.43 | 1.11 | 2.80 | 1.65 |
| 223-trime-pentane | -44.7 | 1.20 | 0.03 | 0.15 | 0.07 | 0.13 | 0.35 | 0.20 |
| 2-me-3-et-pentane | -44.8 | 1.20 | 0.12 | 0.38 | 0.21 | 0.43 | 0.76 | 0.53 |
| 2,2-dimethylhexane | -44.6 | 1.20 | 0.06 | 0.07 | 0.06 | 0.05 | 0.05 | 0.05 |
| 2,3-dimethylhexane | -44.7 | 1.32 | 0.15 | 0.03 | 0.11 | 0.06 | 0.04 | 0.05 |
| 2,4-dimethylhexane | -44.7 | 1.50 | 0.28 | 0.46 | 0.34 | 0.52 | 0.77 | 0.60 |
| 2,5-dimethylhexane | -44.7 | 1.63 | 0.21 | 0.41 | 0.28 | 0.47 | 0.81 | 0.58 |
| 3,3-dimethylhexane | -44.7 | 1.20 | 0.06 | 0.08 | 0.07 | 0.05 | 0.05 | 0.05 |
| 225-trimethylhexane | -44.5 | 0.97 | 0.19 | 0.41 | 0.26 | 0.74 | 1.92 | 1.11 |

**Appendix A** (continued)

| compound | $\Delta h_c$[a] kJ $g^{-1}$ | MIR $gO_3/gOC_i$ | weight % of total: 1995 gasoline grade regular | 1995 premium | 1995 composite[b] | 1996 gasoline grade regular | 1996 premium | 1996 composite |
|---|---|---|---|---|---|---|---|---|
| 2,2-dimethylpropane | -45.1 | 1.38 | 0.01 | 0.02 | 0.01 | 0.01 | 0.01 | 0.01 |
| 2,2-dimethylheptane | -44.5 | 1.14 | 0.02 | 0.02 | 0.02 | 0.02 | 0.02 | 0.02 |
| 2,3-dimethylheptane | *-44.5* | 1.14 | 0.07 | 0.07 | 0.07 | 0.11 | 0.13 | 0.12 |
| 2,4-dimethylheptane | *-44.5* | 1.34 | 0.07 | | 0.04 | 0.33 | 0.04 | 0.24 |
| 2,5-dimethylheptane | *-44.5* | 1.14 | 0.01 | 0.01 | 0.01 | 0.01 | 0.02 | 0.01 |
| 2,6-dimethylheptane | *-44.5* | 1.14 | 0.07 | 0.07 | 0.07 | 0.21 | 0.11 | 0.18 |
| 3,3-dimethylheptane | *-44.5* | 1.14 | 0.03 | 0.01 | 0.03 | 0.06 | 0.01 | 0.04 |
| 3,4-dimethylheptane | *-44.5* | 1.14 | 0.04 | 0.03 | 0.04 | 0.08 | 0.05 | 0.07 |
| 3,5-dimethylheptane | *-44.5* | 1.14 | 0.22 | 0.21 | 0.21 | 0.40 | 0.25 | 0.36 |
| 4,4-dimethylheptane | *-44.5* | 1.14 | | 0.01 | 0.00 | 0.04 | 0.02 | 0.03 |
| 3-ethylheptane | -44.7 | 1.14 | 0.06 | 0.05 | 0.06 | 0.11 | 0.04 | 0.09 |
| 4-ethylheptane | -44.7 | 1.14 | 0.04 | 0.04 | 0.04 | 0.05 | 0.03 | 0.05 |
| 223-trimethylhexane | *-44.5* | 1.14 | 0.03 | | 0.02 | | 0.02 | 0.01 |
| 2235-tetmethylhexane | *-44.5* | 1.01 | 0.01 | | 0.01 | | | |
| 235-trimethylhexane | *-44.5* | 1.14 | 0.06 | 0.09 | 0.07 | 0.13 | 0.37 | 0.20 |
| 244-trimethylhexane | *-44.5* | 1.14 | 0.12 | 0.04 | 0.10 | 0.08 | 0.09 | 0.09 |
| 2-methyloctane | -44.7 | 1.14 | 0.21 | 0.17 | 0.20 | 0.34 | 0.16 | 0.28 |
| 3-methyloctane | -44.7 | 1.14 | | | | 0.44 | | 0.30 |
| 4-methyloctan | -44.7 | 1.14 | 0.17 | 0.16 | 0.16 | 0.28 | 0.13 | 0.23 |
| 3-me-4-et-hexane | *-44.6* | 1.14 | 0.02 | 0.02 | 0.02 | | 0.03 | 0.01 |
| 2,2-dimethyloctane | *-44.5* | 1.01 | 0.03 | 0.03 | 0.03 | 0.06 | 0.03 | 0.05 |

**Appendix A** (continued)

| compound | $\Delta h_c$[a] kJ $g^{-1}$ | MIR $gO_3/gOC_i$ | weight % of total: 1995 gasoline grade regular | 1995 gasoline grade premium | 1995 gasoline grade composite[b] | 1996 gasoline grade regular | 1996 gasoline grade premium | 1996 gasoline grade composite |
|---|---|---|---|---|---|---|---|---|
| 2,3-dimethyloctane | *-44.5* | 1.01 | 0.02 | 0.02 | 0.02 | 0.03 | 0.02 | 0.02 |
| 2,6-dimethyloctane | *-44.5* | 1.01 | | | | 0.03 | | 0.02 |
| 4,4-dimethyloctane | *-44.5* | 1.01 | 0.02 | 0.01 | 0.01 | 0.02 | 0.01 | 0.02 |
| 223-trimethylheptane | *-44.5* | 1.01 | 0.04 | 0.03 | 0.04 | 0.07 | 0.04 | 0.06 |
| 224-trimethylheptane | *-44.5* | 1.01 | 0.01 | 0.02 | 0.01 | 0.02 | 0.05 | 0.03 |
| 225-trimethylheptane | *-44.5* | 1.01 | 0.03 | 0.01 | 0.02 | 0.06 | 0.02 | 0.05 |
| 236-trimethylheptane | *-44.5* | 1.01 | 0.02 | 0.02 | 0.02 | 0.04 | 0.07 | 0.05 |
| 244-trimethylheptane | *-44.5* | 1.01 | | | | 0.24 | | 0.16 |
| 245-trimethylheptane | *-44.5* | 1.01 | 0.02 | 0.01 | 0.02 | 0.02 | 0.02 | 0.02 |
| 246-trimethylheptane | *-44.5* | 1.01 | 0.02 | 0.01 | 0.02 | 0.02 | 0.02 | 0.02 |
| 255-trimethylheptane | *-44.5* | 1.01 | 0.03 | 0.03 | 0.03 | 0.06 | 0.11 | 0.08 |
| 335-trimethylheptane | -44.5 | 1.01 | 0.00 | 0.00 | 0.00 | | | |
| 2-me-3-et-heptane | *-44.5* | 1.01 | 0.04 | | | 0.06 | 0.03 | 0.05 |
| 4-ethyloctane | *-44.5* | 1.01 | 0.04 | 0.02 | 0.03 | 0.05 | 0.03 | 0.05 |
| 2-methylnonane | -44.6 | 1.01 | 0.09 | 0.05 | 0.08 | 0.10 | 0.05 | 0.09 |
| 3-methylnonane | -44.6 | 1.01 | 0.08 | 0.06 | 0.08 | 0.09 | 0.05 | 0.07 |
| 4-methylnonane | -44.6 | 1.01 | 0.08 | 0.13 | 0.10 | 0.19 | 0.31 | 0.23 |
| C-10 isoalkane | *-44.5* | 1.01 | | 0.01 | 0.00 | 0.02 | 0.02 | 0.02 |
| 2,6-dimethylnonane | *-44.4* | 1.17 | 0.02 | 0.01 | 0.02 | 0.01 | 0.01 | 0.01 |
| 2-methyldecane | *-44.4* | 1.17 | | 0.03 | 0.01 | 0.05 | 0.11 | 0.07 |
| 3-methyldecane | *-44.4* | 1.17 | 0.04 | 0.02 | 0.03 | 0.02 | 0.01 | 0.02 |

**Appendix A** (continued)

| compound | $\Delta h_c$[a] kJ $g^{-1}$ | MIR $gO_3/gOC_i$ | weight % of total: 1995 gasoline grade regular | 1995 premium | 1995 composite[b] | 1996 gasoline grade regular | 1996 premium | 1996 composite |
|---|---|---|---|---|---|---|---|---|
| C-11isoalkane | *-44.4* | 1.17 | 0.07 | 0.09 | 0.08 | 0.17 | 0.31 | 0.22 |
| 2,6,10-trime-dodecane | *-44.1* | 0.70 | 0.02 | 0.02 | 0.02 | 0.00 | 0.00 | 0.00 |
| 2,6-dime-hendecane | *-44.2* | 0.96 | 0.02 | 0.02 | 0.02 | 0.00 | 0.01 | 0.01 |
| 2,6,10-trim-hendecane | *-44.2* | 0.76 | 0.01 | 0.00 | 0.01 | 0.00 | 0.01 | 0.01 |
| C-12 isoalkane | *-44.3* | 1.23 | 0.02 | 0.02 | 0.02 | 0.01 | 0.05 | 0.02 |
| total isoalkanes | | | 31.29 | 32.32 | 31.59 | 37.88 | 43.26 | 39.60 |
| **cycloalkanes** | | | | | | | | |
| cyclopentane | -44.2 | 2.38 | 0.56 | 0.55 | 0.56 | 0.57 | 0.41 | 0.51 |
| methylcyclopentane | -44.0 | 2.82 | 3.04 | 1.59 | 2.57 | 3.63 | 1.80 | 3.04 |
| cyclohexane | -43.8 | 1.28 | 1.17 | 0.82 | 1.05 | 1.84 | 0.85 | 1.53 |
| methylcyclohexane | -43.7 | 1.85 | 1.37 | 0.40 | 1.06 | 1.54 | 0.55 | 1.22 |
| ethylcyclopentane | -44.0 | 2.31 | 0.22 | 0.08 | 0.18 | 0.33 | 0.13 | 0.27 |
| 1-c-2-dimecyclohexane | -43.8 | 1.94 | 0.05 | 0.01 | 0.04 | 0.09 | 0.02 | 0.07 |
| 1,1-dimecyclopentane | -43.9 | 1.85 | 0.02 | 0.00 | 0.01 | 0.00 | 0.00 | 0.00 |
| 1-c-3-dimecyclopentane | *-43.9* | 2.55 | 0.75 | 0.15 | 0.56 | 0.63 | 0.27 | 0.52 |
| 1-t-2-dimecyclopentane | -43.9 | 1.85 | 0.59 | 0.14 | 0.44 | 0.48 | 0.24 | 0.41 |
| 1-t-3-dimecyclopentane | *-43.9* | 2.55 | 0.62 | 0.13 | 0.47 | 0.52 | 0.23 | 0.43 |
| 112-trimecypentane | -43.9 | 1.94 | 0.02 | 0.01 | 0.02 | 0.01 | 0.00 | 0.01 |
| 113-trimecypentane | -43.9 | 1.94 | 0.09 | 0.04 | 0.07 | 0.13 | 0.05 | 0.10 |
| 1-c-2-c-3-trimecypentane | -43.9 | 1.94 | 0.01 | 0.00 | 0.01 | 0.00 | 0.00 | 0.00 |
| 1-c-2-c-4-trimecypentane | -43.9 | 1.94 | 0.02 | 0.00 | 0.01 | 0.00 | 0.00 | 0.00 |

**Appendix A** (continued)

| | | | weight % of total | | | | | |
|---|---|---|---|---|---|---|---|---|
| | $\Delta h_c$[a] | MIR | 1995 gasoline grade | | | 1996 gasoline grade | | |
| compound | kJ $g^{-1}$ | $gO_3/gOC_i$ | regular | premium | composite[b] | regular | premium | composite |
| 1-c-2-t-3-trimecypentane | -43.9 | 1.94 | 0.02 | 0.01 | 0.02 | 0.01 | 0.01 | 0.01 |
| 1-t-2-c-3-trimecypentane | -43.9 | 1.94 | 0.06 | 0.03 | 0.05 | 0.14 | 0.04 | 0.11 |
| 1-t-2-c-4-trimecypentane | -43.9 | 1.94 | 0.12 | 0.06 | 0.10 | 0.25 | 0.08 | 0.20 |
| 1me-1-etcyclopentane | -43.9 | 1.94 | 0.05 | 0.03 | 0.04 | 0.13 | | 0.09 |
| 1me-c-2-etcyclopentane | -43.9 | 1.94 | 0.04 | 0.01 | 0.03 | 0.07 | 0.02 | 0.05 |
| 1me-c-3-etcyclopentane | -43.9 | 1.94 | 0.09 | 0.04 | 0.07 | 0.21 | 0.06 | 0.16 |
| propylcyclopentane | -44.0 | 2.06 | 0.01 | 0.01 | 0.01 | 0.03 | 0.01 | 0.02 |
| 113-T4-tetramecypent | -43.9 | 2.30 | 0.06 | 0.03 | 0.05 | 0.13 | 0.04 | 0.10 |
| C-9 cyclopentane | -43.9 | 2.30 | 0.09 | 0.03 | 0.07 | 0.02 | 0.04 | 0.03 |
| 1,1-dimecyclohexane | -43.7 | 1.94 | 0.02 | 0.02 | 0.02 | 0.04 | 0.01 | 0.03 |
| 1-c-3-dimecyclohexane | -43.6 | 2.08 | 0.10 | 0.09 | 0.10 | 0.37 | 0.08 | 0.28 |
| 1-c-4-dimecyclohexane | -43.7 | 1.94 | 0.05 | 0.02 | 0.04 | | 0.03 | 0.01 |
| 1-t-2-dimecyclohexane | -43.7 | 1.94 | 0.05 | 0.04 | 0.05 | 0.16 | 0.06 | 0.13 |
| 1-t-3-dimecyclohexane | -43.7 | 2.08 | 0.11 | 0.05 | 0.09 | 0.30 | 0.07 | 0.23 |
| ethylcyclohexane | -43.8 | 1.94 | 0.06 | 0.11 | 0.08 | 0.11 | 0.09 | 0.10 |
| 1-m-t-2-propcyhexane | *-43.7* | 1.78 | 0.03 | 0.03 | 0.03 | 0.04 | 0.07 | 0.05 |
| 113-trimecyclohexane | *-43.7* | 2.30 | 0.03 | 0.02 | 0.03 | 0.06 | 0.03 | 0.05 |
| 1-c-2-c-3-trimecyhexane | *-43.7* | 2.30 | 0.01 | | 0.01 | | | |
| 1-c-2-t-3-trimecyhexane | *-43.7* | 2.30 | 0.06 | 0.01 | 0.05 | 0.04 | 0.02 | 0.03 |
| 1-c-3-t-5-trimecyhexane | *-43.7* | 2.30 | 0.06 | 0.03 | 0.05 | 0.20 | 0.09 | 0.17 |
| 1me-c-3etcyclohexane | *-43.7* | 2.30 | 0.07 | 0.06 | 0.07 | | 0.14 | 0.05 |

**Appendix A** (continued)

| | | | weight % of total | | | | | |
|---|---|---|---|---|---|---|---|---|
| | $\Delta h_c$[a] | MIR | 1995 gasoline grade | | | 1996 gasoline grade | | |
| compound | kJ $g^{-1}$ | $gO_3/gOC_i$ | regular | premium | composite[b] | regular | premium | composite |
| 1me-c-4etcyclohexane | *-43.7* | 2.30 | 0.03 | 0.01 | 0.02 | 0.01 | 0.01 | 0.01 |
| 1me-t-4etcyclohexane | *-43.7* | 2.30 | 0.02 | 0.01 | 0.02 | 0.04 | 0.01 | 0.03 |
| propylcyclohexane | -43.8 | 2.30 | 0.03 | 0.01 | 0.02 | 0.06 | 0.02 | 0.05 |
| iso-bu-cyclohexane | *-43.8* | 1.70 | 0.01 | | 0.01 | 0.00 | 0.00 | 0.00 |
| sec-bu-cyclohexane | *-43.8* | 1.70 | 0.01 | 0.01 | 0.01 | 0.01 | 0.01 | 0.01 |
| C-9 cyclohexane | *-43.7* | 2.30 | 0.01 | | 0.01 | 0.02 | 0.01 | 0.01 |
| C-10 cyclohexane | *-43.7* | 1.70 | 0.02 | | 0.01 | 0.02 | | 0.02 |
| C-9 naphthenes | -43.9 | 2.30 | | | | | 0.01 | 0.00 |
| cis-hydrindane | *-43.7* | 2.30 | 0.01 | 0.01 | 0.01 | 0.02 | 0.01 | 0.01 |
| total cycloalkanes | | | 9.86 | 4.68 | 8.20 | 12.27 | 5.63 | 10.14 |
| **alkenes** | | | | | | | | |
| propene | -45.8 | 9.40 | 0.01 | 0.00 | 0.01 | | | |
| 1-butene | -45.3 | 8.91 | 0.02 | 0.01 | 0.02 | 0.01 | 0.01 | 0.01 |
| cis-2-butene | -45.2 | 9.94 | 0.06 | 0.03 | 0.05 | 0.04 | 0.04 | 0.04 |
| trans-2-butene | -45.1 | 9.94 | 0.05 | 0.02 | 0.04 | 0.05 | 0.08 | 0.06 |
| 2-methylpropene | -45.0 | 5.31 | 0.03 | 0.01 | 0.02 | 0.01 | 0.01 | 0.01 |
| 1-pentene | -45.0 | 6.22 | 0.25 | 0.19 | 0.23 | 0.06 | 0.05 | 0.06 |
| cis-2-pentene | -44.9 | 8.80 | 0.30 | 0.17 | 0.26 | 0.10 | 0.10 | 0.10 |
| trans-2-pentene | -44.8 | 8.80 | 0.53 | 0.32 | 0.46 | 0.23 | 0.27 | 0.25 |
| 2-methyl-1-butene | -44.8 | 4.90 | 0.38 | 0.21 | 0.33 | 0.12 | 0.11 | 0.12 |
| 3-methyl-1-butene | -44.9 | 6.22 | 0.06 | 0.09 | 0.07 | 0.02 | 0.01 | 0.02 |

**Appendix A** (continued)

| | | | weight % of total | | | | | |
|---|---|---|---|---|---|---|---|---|
| | $\Delta h_c$[a] | MIR | 1995 gasoline grade | | | 1996 gasoline grade | | |
| compound | kJ $g^{-1}$ | $gO_3/gOC_i$ | regular | premium | composite[b] | regular | premium | composite |
| 2-methyl-2-butene | -44.7 | 6.41 | 0.73 | 0.44 | 0.64 | 0.35 | 0.41 | 0.37 |
| cyclopentene | -43.6 | 7.66 | 0.14 | 0.07 | 0.12 | 0.04 | 0.03 | 0.04 |
| 1-hexene | -44.8 | 4.42 | 0.14 | 0.03 | 0.11 | 0.03 | 0.02 | 0.02 |
| trans-2-hexene | -44.7 | 6.69 | 0.27 | 0.11 | 0.22 | 0.07 | 0.14 | 0.09 |
| cis-2-hexene | -44.7 | 6.69 | 0.14 | 0.05 | 0.11 | 0.04 | 0.05 | 0.04 |
| cis-3-hexene | -44.7 | 6.69 | 0.18 | 0.07 | 0.14 | 0.04 | 0.06 | 0.05 |
| 2-methyl-2-pentene | -44.5 | 6.69 | 0.33 | 0.22 | 0.29 | 0.09 | 0.37 | 0.18 |
| c-3me-2-pentene | -44.6 | 6.69 | 0.15 | 0.04 | 0.11 | 0.05 | 0.03 | 0.04 |
| t-3me-2-pentene | -44.5 | 6.69 | 0.24 | 0.06 | 0.18 | 0.07 | 0.05 | 0.06 |
| c-4me-2-pentene | -44.6 | 6.69 | 0.04 | 0.03 | 0.03 | 0.01 | 0.03 | 0.01 |
| t-4me-2-pentene | -44.6 | 6.69 | 0.14 | 0.13 | 0.14 | 0.04 | 0.15 | 0.07 |
| 2-me-1-pentene | *-44.6* | 4.42 | 0.17 | 0.07 | 0.14 | 0.05 | 0.07 | 0.06 |
| 4-methyl-1-pentene | *-44.6* | 4.42 | 0.10 | 0.04 | 0.08 | 0.03 | 0.02 | 0.02 |
| 2-et-1-butene | *-44.6* | 4.42 | 0.06 | 0.01 | 0.04 | 0.02 | 0.01 | 0.02 |
| 2,3dimethyl-1-butene | *-44.6* | 4.42 | 0.06 | 0.02 | 0.04 | | | |
| 2,3dimethyl-2-butene | -44.5 | 6.69 | 0.06 | 0.03 | 0.05 | 0.02 | 0.05 | 0.03 |
| 3,3-dimethylbutene | -44.6 | 4.42 | 0.01 | 0.00 | 0.01 | 0.00 | | |
| 1-heptene | -44.7 | 3.48 | 0.04 | 0.01 | 0.03 | 0.02 | | |
| 2-me-1-hexene | *-44.4* | 3.48 | 0.05 | 0.01 | 0.04 | 0.02 | 0.01 | 0.02 |
| 2-me-2-hexene | *-44.4* | 5.53 | 0.10 | 0.03 | 0.07 | 0.03 | 0.02 | 0.03 |
| 2-me-t-3-hexene | *-44.4* | 5.53 | 0.06 | 0.02 | 0.05 | 0.02 | 0.01 | 0.02 |

**Appendix A** (continued)

| compound | $\Delta h_c$[a] kJ $g^{-1}$ | MIR $gO_3/gOC_i$ | weight % of total: 1995 gasoline grade regular | 1995 premium | 1995 composite[b] | 1996 gasoline grade regular | 1996 premium | 1996 composite |
|---|---|---|---|---|---|---|---|---|
| 3-me-1-hexene | *-44.4* | 3.48 | 0.01 | 0.00 | 0.01 | 0.00 | 0.00 | 0.00 |
| 3-me-c-3-hexene | *-44.4* | 5.53 | 0.07 | 0.02 | 0.05 | 0.02 | 0.02 | 0.02 |
| 3-me-t-3-hexene | *-44.4* | 5.53 | 0.04 | 0.01 | 0.03 | 0.02 | 0.01 | 0.01 |
| 5-me-1-hexene | *-44.4* | 3.48 | 0.03 | 0.01 | 0.02 | 0.01 | 0.01 | 0.01 |
| 23-dime-1-pentene | *-44.4* | 3.48 | 0.03 | 0.01 | 0.02 | 0.01 | 0.01 | 0.01 |
| 23-dime-2-pentene | *-44.4* | 5.53 | 0.09 | 0.03 | 0.07 | 0.03 | 0.02 | 0.03 |
| 23-dimethyl-2-pentene | *-44.4* | 5.53 | 0.00 | | 0.00 | | | |
| 24-dime-1-pentene | *-44.4* | 3.48 | 0.02 | 0.01 | 0.02 | 0.01 | 0.00 | 0.01 |
| 24-dimethyl-2-pentene | *-44.4* | 5.53 | 0.01 | | 0.00 | | | |
| 33-dime-1-pentene | *-44.4* | 3.48 | 0.01 | 0.00 | 0.00 | | | |
| 34-dime-c-2-pentene | *-44.4* | 5.53 | 0.04 | 0.01 | 0.03 | 0.01 | 0.02 | 0.01 |
| 44-dime-1-pentene | *-44.4* | 3.48 | 0.04 | 0.01 | 0.03 | 0.01 | | 0.01 |
| 44-dime-c-2-pentene | *-44.4* | 5.53 | 0.01 | 0.00 | 0.01 | 0.00 | 0.00 | 0.00 |
| 3-et-2-pentene | *-44.4* | 5.53 | 0.20 | 0.05 | 0.15 | 0.07 | 0.04 | 0.06 |
| cis-2-heptene | *-44.4* | 5.53 | 0.00 | | 0.00 | | | 0.00 |
| t-3-heptene | *-44.4* | 5.53 | 0.09 | 0.02 | 0.07 | 0.02 | 0.02 | 0.02 |
| Trans-2-heptene | *-44.4* | 5.53 | | | | 0.01 | 0.02 | 0.01 |
| C-7 olefin | *-44.4* | 3.48 | 0.03 | 0.00 | 0.02 | 0.01 | 0.00 | 0.01 |
| 4-m-1-heptene | *-44.2* | 2.69 | 0.04 | 0.02 | 0.04 | 0.05 | 0.02 | 0.04 |
| c-2-m-3-heptene | *-44.2* | 5.29 | 0.07 | 0.05 | 0.06 | 0.20 | 0.04 | 0.15 |
| c-6-m-2-heptene | *-44.2* | 5.29 | 0.01 | 0.00 | 0.01 | 0.00 | | 0.00 |

**Appendix A** (continued)

| compound | $\Delta h_c$[a] kJ $g^{-1}$ | MIR $gO_3/gOC_i$ | weight % of total: 1995 gasoline grade regular | 1995 gasoline grade premium | 1995 gasoline grade composite[b] | 1996 gasoline grade regular | 1996 gasoline grade premium | 1996 gasoline grade composite |
|---|---|---|---|---|---|---|---|---|
| t-4-m-2-heptene | *-44.2* | 5.29 | 0.02 | | 0.02 | | | |
| 1-octene | -44.6 | 2.69 | 0.02 | 0.00 | 0.01 | | | |
| octene B-I | *-44.2* | 5.29 | 0.11 | 0.03 | 0.09 | 0.04 | 0.03 | 0.03 |
| C2-octene | *-44.2* | 5.29 | 0.04 | 0.01 | 0.03 | 0.01 | 0.02 | 0.01 |
| C4-octene | *-44.2* | 5.29 | 0.08 | 0.01 | 0.06 | 0.07 | | 0.05 |
| C-8 olefin | *-44.2* | 5.29 | 0.08 | 0.03 | 0.06 | 0.05 | 0.03 | 0.04 |
| 2-methyl-2-heptene | *-44.2* | 4.58 | 0.04 | 0.01 | 0.03 | 0.05 | 0.02 | 0.04 |
| nonenes | *-44.1* | 4.58 | 0.01 | 0.00 | 0.01 | | 0.01 | 0.00 |
| 1-me-cyclopentene | *-44.6* | 6.85 | 0.34 | 0.08 | 0.26 | 0.09 | 0.06 | 0.08 |
| 3-me-cyclopentene | *-44.6* | 6.85 | 0.10 | 0.02 | 0.07 | 0.02 | 0.01 | 0.02 |
| c-7 cyclopentene | *-44.4* | 5.64 | 0.18 | 0.04 | 0.14 | 0.06 | 0.04 | 0.05 |
| 1,7-octadiene | *-44.4* | 5.38 | 0.00 | | 0.00 | | | |
| 1-me-cyclopentadiene | *-44.4* | 6.85 | 0.03 | 0.03 | 0.03 | 0.03 | | 0.02 |
| 2-me-1,3-butadiene | -44.2 | 9.08 | 0.01 | 0.01 | 0.01 | 0.01 | 0.00 | 0.00 |
| c-1,3-pentadiene | *-44.2* | 8.00 | 0.01 | 0.00 | 0.01 | 0.00 | 0.00 | 0.00 |
| cyclopentadiene | *-44.4* | 9.34 | 0.01 | 0.01 | 0.01 | 0.01 | 0.01 | 0.01 |
| octadiene A | *-44.4* | 5.38 | 0.07 | 0.02 | 0.06 | 0.03 | 0.02 | 0.02 |
| t-1,3-pentadiene | -44.2 | 8.00 | 0.02 | 0.01 | 0.01 | 0.01 | 0.00 | 0.01 |
| t-1me-1,3-pentadiene | *-44.4* | 6.85 | 0.00 | | 0.00 | | | |
| t-2-t-4-hexadiene | *-44.5* | 6.85 | 0.01 | 0.00 | 0.01 | 0.00 | 0.00 | 0.00 |
| 1,4-pentadiene | -44.6 | 8.00 | | 0.00 | 0.00 | | | |

**Appendix A** (continued)

| compound | $\Delta h_c$[a] kJ $g^{-1}$ | MIR $gO_3/gOC_i$ | weight % of total: 1995 gasoline grade regular | 1995 premium | 1995 composite[b] | 1996 gasoline grade regular | 1996 premium | 1996 composite |
|---|---|---|---|---|---|---|---|---|
| total alkenes | | | 6.91 | 3.13 | 5.70 | 2.63 | 2.70 | 2.64 |
| **aromatics** | | | | | | | | |
| benzene | -40.6 | 0.42 | 2.12 | 1.67 | 1.98 | 0.64 | 0.46 | 0.58 |
| toluene | -40.9 | 2.73 | 9.36 | 10.65 | 9.77 | 7.94 | 8.11 | 8.00 |
| ethylbenzene | -41.3 | 2.70 | 1.94 | 2.48 | 2.11 | 1.59 | 1.50 | 1.56 |
| o-xylene | -41.2 | 6.46 | 3.01 | 3.74 | 3.24 | 2.24 | 2.61 | 2.36 |
| m-xylene | -41.2 | 8.16 | 6.20 | 8.08 | 6.80 | 4.95 | 5.20 | 5.03 |
| p-xylene | -41.2 | 6.60 | 1.50 | 1.79 | 1.59 | 1.42 | 1.48 | 1.44 |
| 1-me-2-et-benzene | -41.5 | 7.20 | 0.70 | 0.88 | 0.76 | 0.48 | 0.51 | 0.49 |
| 1-me-3-et-benzene | -41.5 | 7.20 | 2.08 | 2.69 | 2.28 | 1.41 | 1.55 | 1.46 |
| 1-me-4-et-benzene | -41.5 | 7.20 | 0.90 | 1.17 | 0.99 | 0.62 | 0.69 | 0.65 |
| 123-trime-benzene | -41.5 | 8.85 | 0.63 | 0.77 | 0.67 | 0.42 | 0.53 | 0.46 |
| 124-trime-benzene | -41.4 | 8.83 | 3.18 | 4.08 | 3.47 | 2.21 | 2.64 | 2.35 |
| 135-trime-benzene | -41.4 | 10.12 | 1.05 | 1.36 | 1.15 | 0.71 | 0.84 | 0.75 |
| propylbenzene | -41.6 | 2.12 | 0.62 | 0.75 | 0.66 | 0.46 | 0.41 | 0.45 |
| naphthalene | -39.4 | 1.18 | 0.44 | 0.57 | 0.48 | 0.13 | 0.14 | 0.13 |
| 1,2-diethylbenzene | *-41.8* | 6.45 | 0.54 | 0.70 | 0.59 | 0.24 | 0.28 | 0.26 |
| 1,3-diethylbenzene | *-41.8* | 6.45 | 0.19 | 0.24 | 0.21 | 0.08 | 0.08 | 0.08 |
| 1-me-2-pr-benzene | *-41.7* | 6.45 | 0.15 | 0.19 | 0.16 | 0.06 | 0.07 | 0.07 |
| 1-me-3-pr-benzene | -41.7 | 6.45 | 0.49 | 0.63 | 0.54 | 0.19 | 0.20 | 0.19 |
| 1-me-4-pr-benzene | *-41.7* | 6.45 | 0.28 | 0.38 | 0.31 | 0.11 | 0.12 | 0.12 |

**Appendix A** (continued)

| compound | $\Delta h_c$[a] kJ $g^{-1}$ | MIR $gO_3/gOC_i$ | weight % of total: 1995 gasoline grade regular | 1995 gasoline grade premium | 1995 gasoline grade composite[b] | 1996 gasoline grade regular | 1996 gasoline grade premium | 1996 gasoline grade composite |
|---|---|---|---|---|---|---|---|---|
| 12-dime3et-benzene | *-41.7* | 8.21 | 0.15 | 0.17 | 0.16 | 0.06 | 0.07 | 0.06 |
| 12-dime4et-benzene | *-41.7* | 8.21 | 0.50 | 0.64 | 0.54 | 0.22 | 0.25 | 0.23 |
| 13-dime2et-benzene | *-41.7* | 8.21 | 0.03 | 0.04 | 0.04 | 0.02 | 0.03 | 0.02 |
| 13-dime4et-benzene | *-41.7* | 8.21 | 0.30 | 0.37 | 0.32 | 0.14 | 0.16 | 0.15 |
| 14-dime2et-benzene | *-41.7* | 8.21 | 0.39 | 0.42 | 0.40 | 0.17 | 0.18 | 0.17 |
| 1234-tetme-benzene | *-41.6* | 9.07 | 0.12 | 0.13 | 0.12 | 0.06 | 0.08 | 0.06 |
| 1235-tetme-benzene | -41.6 | 9.07 | 0.37 | 0.45 | 0.40 | 0.18 | 0.22 | 0.19 |
| 1245-tetme-benzene | -41.6 | 9.07 | 0.29 | 0.35 | 0.31 | 0.14 | 0.16 | 0.15 |
| butylbenzene | -41.8 | 1.87 | 0.12 | 0.17 | 0.14 | 0.06 | 0.05 | 0.05 |
| isobutylbenzene | -41.8 | 1.87 | 0.08 | 0.10 | 0.09 | 0.05 | 0.08 | 0.06 |
| sec-butylbenzene | -41.8 | 1.89 | 0.07 | 0.09 | 0.07 | 0.03 | 0.03 | 0.03 |
| 1-me-3bu-benzene | *-41.9* | 5.84 | 0.08 | | 0.05 | 0.04 | 0.04 | 0.04 |
| 1-me35diet-benzene | *-41.9* | 8.21 | 0.07 | 0.07 | 0.07 | 0.02 | 0.01 | 0.02 |
| 12-dime-3pr-benzene | *-41.9* | 8.21 | 0.10 | 0.10 | 0.10 | 0.03 | 0.03 | 0.03 |
| 12-dime-4pr-benzene | *-41.9* | 8.21 | 0.05 | 0.02 | 0.04 | 0.03 | 0.07 | 0.05 |
| 123-trime-5etbenzene | *-41.9* | 8.21 | 0.06 | 0.05 | 0.05 | 0.01 | 0.01 | 0.01 |
| 123-trime4et-benzene | *-41.9* | 8.21 | 0.03 | | 0.02 | 0.01 | 0.01 | 0.01 |
| 124-trime-3etbenzene | *-41.9* | 8.21 | 0.01 | | 0.01 | | 0.00 | 0.00 |
| 124-trime-5etbenzene | *-41.9* | 8.21 | 0.05 | 0.05 | 0.05 | 0.02 | 0.02 | 0.02 |
| 125-trime-3etbenzene | *-41.9* | 8.21 | 0.07 | 0.08 | 0.07 | 0.02 | 0.03 | 0.02 |
| 135-trime-2etbenzene | *-41.9* | 8.21 | 0.02 | 0.02 | 0.02 | 0.01 | 0.03 | 0.02 |

**Appendix A** (continued)

| compound | $\Delta h_c$[a] kJ $g^{-1}$ | MIR $gO_3/gOC_i$ | weight % of total: 1995 gasoline grade regular | 1995 gasoline grade premium | 1995 gasoline grade composite[b] | 1996 gasoline grade regular | 1996 gasoline grade premium | 1996 gasoline grade composite |
|---|---|---|---|---|---|---|---|---|
| pentamethylbenzene | -41.9 | 8.21 | 0.03 | 0.03 | 0.03 | 0.01 | 0.01 | 0.01 |
| C-10 alkenylbenzenes | *-41.7* | 9.07 | 0.01 | 0.04 | 0.02 | | | |
| 1-ethylnaphthalene | *-39.8* | 2.98 | 0.01 | 0.02 | 0.02 | 0.00 | 0.00 | 0.00 |
| 1-methylnaphthalene | -39.8 | 3.27 | 0.13 | 0.20 | 0.15 | 0.03 | 0.03 | 0.03 |
| 1-phenyl-2me butane | *-41.9* | 1.70 | 0.05 | 0.06 | 0.05 | 0.02 | 0.03 | 0.02 |
| 1-phenyl-3me butane | *-41.9* | 1.70 | 0.01 | 0.01 | 0.01 | 0.01 | 0.02 | 0.01 |
| 12-dime-naphthalene | *-39.8* | 5.13 | 0.01 | 0.01 | 0.01 | | 0.00 | 0.00 |
| 13-dime-naphthalene | *-39.8* | 5.13 | 0.03 | 0.06 | 0.04 | 0.01 | 0.01 | 0.01 |
| 16-dime-naphthalene | *-39.8* | 5.13 | 0.02 | 0.03 | 0.02 | 0.00 | 0.01 | 0.00 |
| 2-methylnaphthalene | -39.8 | 3.27 | 0.29 | 0.41 | 0.33 | 0.07 | 0.07 | 0.07 |
| 23-dime-naphthalene | *-39.8* | 5.13 | 0.02 | 0.02 | 0.02 | 0.00 | 0.00 | 0.00 |
| indan | *-41.5* | 1.06 | 0.39 | 0.46 | 0.42 | 0.20 | 0.20 | 0.20 |
| indene | *-41.5* | 1.06 | 0.01 | 0.00 | 0.01 | | | |
| cumene | -41.6 | 2.24 | 0.11 | 0.16 | 0.13 | 0.09 | 0.09 | 0.09 |
| m-cymene | -41.7 | 6.45 | 0.08 | 0.11 | 0.09 | 0.04 | 0.05 | 0.04 |
| o-cymene | *-41.7* | 6.45 | 0.03 | 0.04 | 0.03 | 0.03 | 0.03 | 0.03 |
| p-cymene | *-41.7* | 6.45 | 0.02 | 0.03 | 0.02 | 0.01 | 0.01 | 0.01 |
| methylindane | *-41.7* | 0.86 | 0.60 | 0.62 | 0.61 | 0.19 | 0.19 | 0.19 |
| tetralin | -40.8 | 0.95 | 0.04 | 0.09 | 0.06 | | | |
| dimethylindane | *-41.9* | 0.86 | 0.35 | 0.17 | 0.29 | 0.09 | 0.10 | 0.09 |
| C-11 aromatic | *-41.9* | 5.48 | 0.15 | 0.15 | 0.15 | 0.06 | 0.06 | 0.06 |

**Appendix A** (continued)

| compound | $\Delta h_c$[a] kJ $g^{-1}$ | MIR $gO_3/gOC_i$ | weight % of total: 1995 gasoline grade regular | 1995 gasoline grade premium | 1995 gasoline grade composite[b] | 1996 gasoline grade regular | 1996 gasoline grade premium | 1996 gasoline grade composite |
|---|---|---|---|---|---|---|---|---|
| C-11 indane H | *-42.1* | 0.86 | 0.04 | 0.03 | 0.04 | 0.01 | 0.01 | 0.01 |
| C-12 aromatic | *-42.1* | 5.34 | 0.02 | 0.01 | 0.02 | 0.00 | 0.00 | 0.00 |
| heavy aromatics | *-39.8* | 4.00 | 0.11 | 0.19 | 0.13 | 0.03 | 0.05 | 0.03 |
| total aromatics | | | 40.91 | 49.07 | 43.52 | 28.16 | 29.95 | 28.73 |
| **oxygenates** | | | | | | | | |
| MTBE | -35.5 | 0.62 | 0.05 | 3.01 | 0.99 | 10.43 | 11.93 | 10.91 |
| TAME | -36.7 | 0.62 | | 0.12 | 0.04 | 0.02 | 0.01 | 0.02 |
| total oxygenates | | | 0.05 | 3.13 | 1.03 | 10.44 | 11.95 | 10.92 |
| **unidentified** C8 to C15 | *-43.9* | 4.00 | 1.85 | 1.02 | 1.59 | 1.34 | 1.34 | 1.34 |
| total NMOC | | | 100.0 | 100.0 | 100.0 | 100.0 | 100.0 | 100.0 |
| total normalized reactivity ($gO_3$/gNMOC) | | | 3.48 | 3.64 | 3.53 | 2.68 | 2.76 | 2.71 |
| total enthalpy of combustion (kJ $g^{-1}$) | | | -43.3 | -42.8 | -43.1 | -42.8 | -42.6 | -42.7 |

[a] Enthalpy of combustion. Calculated from tabulated enthalpies of formation given in Appendix A of Reid et al. (1987) assuming complete combustion to carbon dioxide and water vapor. Italicized values are estimated based on combustion enthalpies of similar compounds.

[b] Regular and premium grade gasoline samples were collected from high-volume service stations. Composite samples for each gasoline grade were prepared by mixing measured amounts of individual samples. The resulting regular and premium grade composites were sales-weighted mixtures of the individual brand samples (Gilson, 1995). Analytical results for these two composite gasoline samples were combined in proportions of 68% by volume regular and 32% premium to estimate the composition of the overall gasoline pool (Gilson, 1995).

# Appendix B

# Composition of Gasoline Headspace Vapors

**Appendix B**

| | | | weight % of total | | | | | |
|---|---|---|---|---|---|---|---|---|
| | MOIR | MIR | 1995 headspace vapor | | | 1996 headspace vapor | | |
| compound | $gO_3/gOC_i$ | | regular | premium | composite | regular | premium | composite |
| **n-alkanes** | | | | | | | | |
| n-propane | 0.31 | 0.48 | 0.49 | 2.20 | 1.04 | 0.24 | 0.39 | 0.28 |
| n-butane | 0.66 | 1.02 | 9.35 | 11.27 | 9.96 | 6.45 | 5.95 | 6.29 |
| n-pentane | 0.68 | 1.04 | 10.39 | 6.98 | 9.30 | 7.64 | 6.50 | 7.28 |
| n-hexane | 0.65 | 0.98 | 2.10 | 1.39 | 1.88 | 1.71 | 0.84 | 1.44 |
| n-heptane | 0.53 | 0.81 | 0.46 | 0.33 | 0.42 | 0.42 | 0.33 | 0.39 |
| n-octane | 0.41 | 0.61 | 0.05 | 0.05 | 0.05 | 0.06 | 0.04 | 0.05 |
| n-nonane | 0.36 | 0.54 | 0.01 | 0.01 | 0.01 | 0.01 | 0.00 | 0.01 |
| other n-alkanes | 0.28 | 0.43 | 0.00 | 0.00 | 0.00 | 0.00 | 0.00 | 0.00 |
| total n-alkanes | | | 22.85 | 22.24 | 22.65 | 16.53 | 14.05 | 15.74 |
| **isoalkanes** | | | | | | | | |
| 2-me-propane | 0.73 | 1.21 | 3.04 | 3.81 | 3.28 | 1.36 | 1.18 | 1.30 |
| 2-me-butane | 0.87 | 1.38 | 36.59 | 37.82 | 36.99 | 33.93 | 36.90 | 34.88 |
| 2-me-pentane | 0.90 | 1.53 | 6.14 | 4.89 | 5.74 | 6.18 | 4.28 | 5.57 |
| 3-me-pentane | 0.94 | 1.52 | 3.45 | 2.91 | 3.28 | 3.40 | 2.34 | 3.06 |
| 2,2-dm-butane | 0.51 | 0.82 | 1.34 | 2.84 | 1.82 | 1.66 | 1.33 | 1.55 |
| 2,3-dm-butane | 0.67 | 1.07 | 1.44 | 1.78 | 1.55 | 1.89 | 2.09 | 1.95 |
| 2-me-hexane | 0.68 | 1.08 | 0.91 | 0.52 | 0.79 | 0.76 | 0.48 | 0.67 |
| 3-me-hexane | 0.83 | 1.40 | 0.90 | 0.60 | 0.81 | 0.80 | 0.61 | 0.74 |
| 2,3-dm-pentane | 0.90 | 1.51 | 0.45 | 0.44 | 0.45 | 0.54 | 0.87 | 0.65 |
| 2,4-dm-pentane | 0.99 | 1.78 | 0.30 | 0.38 | 0.32 | 0.42 | 0.72 | 0.51 |

**Appendix B** (continued)

| | | | weight % of total | | | | | |
|---|---|---|---|---|---|---|---|---|
| | MOIR | MIR | 1995 headspace vapor | | | 1996 headspace vapor | | |
| compound | $gO_3/gOC_i$ | | regular | premium | composite | regular | premium | composite |
| 2,2-dm-pentane | 0.83 | 1.40 | 0.10 | 0.10 | 0.10 | 0.07 | 0.06 | 0.06 |
| 3-et-pentane | 0.83 | 1.40 | 0.07 | 0.05 | 0.07 | 0.06 | 0.00 | 0.04 |
| 2-me-heptane | 0.60 | 0.96 | 0.09 | 0.10 | 0.09 | 0.13 | 0.08 | 0.12 |
| 3-me-heptane | 0.62 | 0.99 | 0.10 | 0.12 | 0.11 | 0.13 | 0.09 | 0.12 |
| 4-me-heptane | 0.70 | 1.20 | 0.04 | 0.05 | 0.05 | 0.06 | 0.05 | 0.06 |
| 2,2,4-tm-pentane | 0.54 | 0.93 | 0.12 | 0.71 | 0.31 | 0.81 | 2.07 | 1.21 |
| 2,3,3-tm-pentane | 0.70 | 1.20 | 0.04 | 0.21 | 0.09 | 0.20 | 0.57 | 0.31 |
| 2,3,4-tm-pentane | 0.92 | 1.60 | 0.03 | 0.18 | 0.08 | 0.21 | 0.54 | 0.31 |
| 2,2,3-tm-pentane | 0.70 | 1.20 | 0.01 | 0.03 | 0.02 | 0.03 | 0.08 | 0.04 |
| 2-me-3-ethylpentane | 0.70 | 1.20 | 0.02 | 0.07 | 0.03 | 0.07 | 0.13 | 0.09 |
| 2,2-dm-hexane | 0.70 | 1.20 | 0.01 | 0.02 | 0.01 | 0.01 | 0.01 | 0.01 |
| 2,3-dm-hexane | 0.78 | 1.32 | 0.02 | 0.01 | 0.02 | 0.01 | 0.01 | 0.01 |
| 2,4-dm-hexane | 0.86 | 1.50 | 0.06 | 0.10 | 0.07 | 0.11 | 0.17 | 0.13 |
| 2,5-dm-hexane | 0.93 | 1.63 | 0.04 | 0.09 | 0.06 | 0.10 | 0.18 | 0.12 |
| 3,3-dm-hexane | 0.46 | 1.20 | 0.01 | 0.02 | 0.01 | 0.01 | 0.01 | 0.01 |
| 2,2,5-tm-hexane | 0.58 | 0.97 | 0.02 | 0.05 | 0.03 | 0.09 | 0.24 | 0.14 |
| other isoalkanes | 0.66 | 1.12 | 0.23 | 0.20 | 0.22 | 0.48 | 0.33 | 0.43 |
| total isoalkanes | | | 55.58 | 58.09 | 56.39 | 53.51 | 55.39 | 54.11 |
| **cycloalkanes** | | | | | | | | |
| cyclopentane | 1.41 | 2.38 | 1.04 | 1.08 | 1.06 | 1.07 | 0.79 | 0.98 |
| me-cyclopentane | 1.55 | 2.82 | 2.55 | 1.42 | 2.19 | 3.13 | 1.58 | 2.64 |

**Appendix B** (continued)

| | | | weight % of total | | | | | |
|---|---|---|---|---|---|---|---|---|
| | MOIR | MIR | 1995 headspace vapor | | | 1996 headspace vapor | | |
| compound | $gO_3/gOC_i$ | | regular | premium | composite | regular | premium | composite |
| cyclohexane | 0.74 | 1.28 | 0.71 | 0.53 | 0.66 | 1.16 | 0.55 | 0.96 |
| me-cyclohexane | 1.00 | 1.85 | 0.41 | 0.13 | 0.32 | 0.48 | 0.18 | 0.38 |
| et-cyclopentane | 1.30 | 2.31 | 0.06 | 0.02 | 0.05 | 0.09 | 0.04 | 0.07 |
| 1-c-2-dm-cyclohexane | 1.02 | 1.94 | 0.00 | 0.00 | 0.00 | 0.01 | 0.00 | 0.01 |
| other cycloalkanes | 1.22 | 2.18 | 0.37 | 0.13 | 0.30 | 0.46 | 0.20 | 0.38 |
| total cycloalkanes | | | 5.15 | 3.32 | 4.57 | 6.40 | 3.34 | 5.42 |
| **alkenes** | | | | | | | | |
| propene | 3.77 | 9.40 | 0.59 | 0.15 | 0.45 | 0.00 | 0.00 | 0.00 |
| 1-butene | 3.51 | 8.91 | 0.29 | 0.11 | 0.23 | 0.12 | 0.13 | 0.12 |
| c-2-butene | 3.76 | 9.94 | 0.47 | 0.25 | 0.40 | 0.32 | 0.38 | 0.34 |
| t-2-butene | 3.76 | 9.94 | 0.48 | 0.22 | 0.40 | 0.51 | 0.75 | 0.59 |
| 2-me-propene | 1.93 | 5.31 | 0.32 | 0.14 | 0.26 | 0.15 | 0.18 | 0.16 |
| 1-pentene | 2.46 | 6.22 | 0.88 | 0.72 | 0.83 | 0.23 | 0.18 | 0.22 |
| c-2-pentene | 3.30 | 8.80 | 0.84 | 0.52 | 0.74 | 0.30 | 0.30 | 0.30 |
| t-2-pentene | 3.30 | 8.80 | 1.52 | 0.97 | 1.35 | 0.69 | 0.83 | 0.73 |
| 2-me-1-butene | 1.90 | 4.90 | 1.32 | 0.78 | 1.15 | 0.43 | 0.39 | 0.41 |
| 3-me-1-butene | 2.46 | 6.22 | 0.29 | 0.47 | 0.35 | 0.09 | 0.07 | 0.08 |
| 2-me-2-butene | 2.30 | 6.41 | 1.97 | 1.26 | 1.74 | 0.96 | 1.16 | 1.02 |
| cyclopentene | 2.78 | 7.66 | 0.31 | 0.15 | 0.26 | 0.10 | 0.07 | 0.09 |
| 1-hexene | 1.74 | 4.42 | 0.16 | 0.04 | 0.12 | 0.03 | 0.03 | 0.03 |
| t-2-hexene | 2.50 | 6.69 | 0.26 | 0.12 | 0.21 | 0.07 | 0.14 | 0.09 |

**Appendix B** (continued)

| | | | weight % of total | | | | | |
|---|---|---|---|---|---|---|---|---|
| | MOIR | MIR | 1995 headspace vapor | | | 1996 headspace vapor | | |
| compound | $gO_3/gOC_i$ | | regular | premium | composite | regular | premium | composite |
| c-2-hexene | 2.50 | 6.69 | 0.13 | 0.05 | 0.10 | 0.03 | 0.05 | 0.04 |
| c-3-hexene | 2.50 | 6.69 | 0.18 | 0.07 | 0.14 | 0.05 | 0.07 | 0.05 |
| 2-me-2-pentene | 2.50 | 6.69 | 0.32 | 0.23 | 0.29 | 0.09 | 0.38 | 0.18 |
| c-3-me-2-pentene | 2.50 | 6.69 | 0.14 | 0.04 | 0.11 | 0.05 | 0.03 | 0.04 |
| t-3-me-2-pentene | 2.50 | 6.69 | 0.20 | 0.05 | 0.16 | 0.06 | 0.04 | 0.06 |
| c-4-me-2-pentene | 2.50 | 6.69 | 0.05 | 0.04 | 0.05 | 0.01 | 0.04 | 0.02 |
| t-4-me-2-pentene | 2.50 | 6.69 | 0.19 | 0.19 | 0.19 | 0.05 | 0.21 | 0.10 |
| 2-me-1-pentene | 1.74 | 4.42 | 0.19 | 0.08 | 0.16 | 0.05 | 0.08 | 0.06 |
| 4-me-1-pentene | 1.74 | 4.42 | 0.12 | 0.04 | 0.09 | 0.03 | 0.03 | 0.03 |
| 2-et-1-butene | 1.74 | 4.42 | 0.09 | 0.02 | 0.07 | 0.03 | 0.02 | 0.02 |
| 2,3-dm-1-butene | 1.74 | 4.42 | 0.09 | 0.03 | 0.07 | 0.00 | 0.00 | 0.00 |
| 2,3-dm-2-butene | 2.50 | 6.69 | 0.05 | 0.03 | 0.04 | 0.02 | 0.04 | 0.03 |
| 3,3-dm-1-butene | 1.74 | 4.42 | 0.01 | 0.01 | 0.01 | 0.00 | 0.00 | 0.00 |
| 1-heptene | 1.38 | 3.48 | 0.02 | 0.00 | 0.01 | 0.01 | 0.00 | 0.00 |
| other olefins | 2.11 | 5.53 | 0.83 | 0.25 | 0.64 | 0.38 | 0.20 | 0.32 |
| total alkenes | | | 12.31 | 7.02 | 10.62 | 4.86 | 5.78 | 5.15 |
| **aromatics** | | | | | | | | |
| benzene | 0.14 | 0.42 | 1.28 | 1.07 | 1.21 | 0.40 | 0.29 | 0.36 |
| toluene | 0.63 | 2.73 | 1.80 | 2.17 | 1.92 | 1.57 | 1.64 | 1.59 |
| ethylbenzene | 0.63 | 2.70 | 0.13 | 0.18 | 0.15 | 0.11 | 0.11 | 0.11 |
| o-xylene | 1.95 | 6.46 | 0.15 | 0.20 | 0.16 | 0.11 | 0.14 | 0.12 |

**Appendix B** (continued)

| | | | weight % of total | | | | | |
|---|---|---|---|---|---|---|---|---|
| | MOIR | MIR | 1995 headspace vapor | | | 1996 headspace vapor | | |
| compound | $gO_3/gOC_i$ | | regular | premium | composite | regular | premium | composite |
| m-xylene | 2.45 | 8.16 | 0.38 | 0.52 | 0.42 | 0.31 | 0.33 | 0.32 |
| p-xylene | 1.99 | 6.60 | 0.10 | 0.12 | 0.10 | 0.09 | 0.10 | 0.10 |
| o-ethyltoluene | 2.16 | 7.20 | 0.01 | 0.02 | 0.02 | 0.01 | 0.01 | 0.01 |
| m-ethyltoluene | 2.16 | 7.20 | 0.05 | 0.07 | 0.06 | 0.03 | 0.04 | 0.04 |
| p-ethyltoluene | 2.16 | 7.20 | 0.02 | 0.03 | 0.02 | 0.02 | 0.02 | 0.02 |
| 1,2,3-tm-benzene | 2.67 | 8.85 | 0.01 | 0.01 | 0.01 | 0.01 | 0.01 | 0.01 |
| 1,2,4-tm-benzene | 2.67 | 8.83 | 0.05 | 0.07 | 0.06 | 0.04 | 0.05 | 0.04 |
| 1,3,5-tm-benzene | 3.05 | 10.12 | 0.02 | 0.03 | 0.02 | 0.02 | 0.02 | 0.02 |
| propylbenzene | 0.49 | 2.12 | 0.02 | 0.02 | 0.02 | 0.01 | 0.01 | 0.01 |
| naphthalene | 0.09 | 1.18 | 0.00 | 0.00 | 0.00 | 0.00 | 0.00 | 0.00 |
| other aromatics | 1.57 | 5.75 | 0.00 | 0.00 | 0.00 | 0.00 | 0.00 | 0.00 |
| total aromatics | | | 4.03 | 4.52 | 4.19 | 2.73 | 2.76 | 2.74 |
| **oxygenates** | | | | | | | | |
| MTBE | 0.41 | 0.62 | 0.07 | 4.75 | 1.57 | 15.96 | 18.68 | 16.83 |
| TAME | 0.41 | 0.62 | 0.00 | 0.05 | 0.02 | 0.01 | 0.01 | 0.01 |
| total oxygenates | | | 0.07 | 4.80 | 1.58 | 15.97 | 18.69 | 16.84 |
| **unidentified** C8-C15 | 1.89 | 4.00 | 0.00 | 0.00 | 0.00 | 0.00 | 0.00 | 0.00 |
| total NMOC | | | 100.0 | 100.0 | 100.0 | 100.0 | 100.0 | 100.0 |
| total normalized MIR reactivity ($gO_3$/gNMOC) | | | 2.10 | 1.75 | 1.99 | 1.60 | 1.62 | 1.60 |
| total normalized MOIR reactivity ($gO_3$/gNMOC) | | | 1.05 | 0.92 | 1.01 | 0.87 | 0.87 | 0.87 |

# Appendix C

# Composition of Tunnel NMOC

## Appendix C

| compound | MIR $gO_3/gOC_i$ | tunnel NMOC, weight % ± 1 standard deviation summer 1994 | summer 1995 | summer 1996 | summer 1997 |
|---|---|---|---|---|---|
| **n-alkanes** | | | | | |
| ethane | 0.25 | 1.46 ± 0.16 | 0.54 ± 0.25 | 1.01 ± 0.32 | 1.16 ± 0.12 |
| propane | 0.48 | 0.28 ± 0.03 | 0.22 ± 0.04 | 0.14 ± 0.05 | 0.10 ± 0.07 |
| n-butane | 1.02 | 2.06 ± 0.18 | 2.13 ± 0.31 | 1.23 ± 0.14 | 2.12 ± 0.26 |
| n-pentane | 1.04 | 2.38 ± 0.17 | 2.51 ± 0.31 | 2.51 ± 0.20 | 2.55 ± 0.28 |
| n-hexane | 0.98 | 1.35 ± 0.53 | 1.44 ± 0.20 | 1.28 ± 0.11 | 1.34 ± 0.14 |
| n-heptane | 0.81 | 0.66 ± 0.09 | 0.81 ± 0.13 | 0.87 ± 0.09 | 0.84 ± 0.08 |
| n-octane | 0.61 | 0.16 ± 0.08 | 0.19 ± 0.26 | 0.37 ± 0.15 | 0.84 ± 0.10 |
| n-nonane | 0.54 | 0.04 ± 0.06 | 0.12 ± 0.06 | 0.21 ± 0.09 | 0.11 ± 0.04 |
| n-undecane | 0.42 | 0.19 ± 0.14 | 0.30 ± 0.18 | 0.11 ± 0.05 | 0.05 ± 0.05 |
| n-dodecane | 0.38 | 0.03 ± 0.07 | 0.00 ± 0.00 | 0.07 ± 0.05 | 0.01 ± 0.02 |
| total n-alkanes | | 8.61 | 8.26 | 7.81 | 9.15 |
| **isoalkanes** | | | | | |
| 2-me-propane (isobutane) | 1.21 | 0.54 ± 0.06 | 0.54 ± 0.12 | 0.31 ± 0.04 | 0.25 ± 0.03 |
| 2-me-butane (isopentane) | 1.38 | 8.90 ± 0.65 | 8.79 ± 1.19 | 9.88 ± 0.89 | 9.98 ± 1.02 |
| C5 paraffin | 1.38 | 0.00 ± 0.00 | 0.00 ± 0.00 | 0.00 ± 0.00 | 0.56 ± 0.11 |
| 2,2-dm-butane | 0.82 | 0.67 ± 0.23 | 0.87 ± 0.16 | 0.86 ± 0.07 | 0.99 ± 0.11 |
| 2-me-pentane | 1.53 | 2.76 ± 0.48 | 2.51 ± 0.35 | 3.17 ± 0.41 | 3.30 ± 0.27 |
| 3-me-pentane | 1.52 | 1.47 ± 0.27 | 1.54 ± 0.17 | 1.87 ± 0.14 | 2.00 ± 0.20 |
| C6 paraffin | 1.53 | 0.46 ± 0.16 | 0.55 ± 0.17 | 0.19 ± 0.07 | 0.18 ± 0.10 |
| 2,4-dm-pentane | 1.78 | 0.00 ± 0.00 | 0.02 ± 0.07 | 0.00 ± 0.00 | 0.01 ± 0.03 |

**Appendix C** (continued)

| compound | MIR $gO_3/gOC_i$ | tunnel NMOC, weight % ± 1 standard deviation summer 1994 | summer 1995 | summer 1996 | summer 1997 |
|---|---|---|---|---|---|
| 2,3-dm-pentane | 1.51 | 0.46 ± 0.13 | 0.44 ± 0.16 | 0.91 ± 0.07 | 0.85 ± 0.45 |
| 2-me-hexane | 1.08 | 1.17 ± 0.19 | 1.35 ± 0.20 | 1.08 ± 0.10 | 0.49 ± 0.16 |
| 3-me-hexane | 1.40 | 1.05 ± 0.18 | 1.07 ± 0.19 | 1.22 ± 0.09 | 0.75 ± 0.18 |
| 2,2,4-tm-pentane | 0.93 | 1.32 ± 0.14 | 1.28 ± 0.17 | 2.67 ± 0.20 | 2.58 ± 0.18 |
| 2,5-dm-hexane | 1.63 | 0.05 ± 0.03 | 0.04 ± 0.07 | 0.14 ± 0.01 | 0.12 ± 0.03 |
| 2,3,4-tm-pentane | 1.60 | 0.38 ± 0.05 | 0.41 ± 0.13 | 0.89 ± 0.10 | 1.14 ± 0.08 |
| 2,3-dm-hexane | 1.32 | 0.26 ± 0.25 | 0.55 ± 0.21 | 0.72 ± 0.31 | 0.14 ± 0.06 |
| 2-me-heptane | 0.96 | 0.33 ± 0.09 | 0.12 ± 0.13 | 0.72 ± 0.12 | 0.45 ± 0.23 |
| 3-me-heptane | 0.99 | 0.21 ± 0.11 | 0.18 ± 0.13 | 0.00 ± 0.00 | 0.72 ± 0.26 |
| 3-et-hexane | 1.20 | 0.00 ± 0.00 | 0.09 ± 0.12 | 0.08 ± 0.07 | 0.35 ± 0.45 |
| C8 paraffin | 1.20 | 0.30 ± 0.19 | 0.00 ± 0.00 | 0.00 ± 0.00 | 0.00 ± 0.00 |
| 2,6-dm-heptane | 1.14 | 0.00 ± 0.00 | 0.15 ± 0.12 | 0.25 ± 0.08 | 0.08 ± 0.02 |
| 2,4-dm-heptane | 1.34 | 0.14 ± 0.07 | 0.17 ± 0.08 | 0.22 ± 0.05 | 0.11 ± 0.06 |
| 3,5-dm-heptane | 1.14 | 0.07 ± 0.05 | 0.21 ± 0.28 | 0.15 ± 0.05 | 0.12 ± 0.06 |
| 4,4-dimethylheptane | 1.14 | 0.00 ± 0.00 | 0.00 ± 0.00 | 0.00 ± 0.00 | 0.09 ± 0.05 |
| 2,5-dimethylheptane | 1.14 | 0.00 ± 0.00 | 0.00 ± 0.00 | 0.00 ± 0.00 | 0.19 ± 0.23 |
| 3-me-octane | 1.14 | 0.03 ± 0.02 | 0.04 ± 0.03 | 0.22 ± 0.13 | 0.18 ± 0.06 |
| 2,3,5-tm-hexane | 1.14 | 0.06 ± 0.03 | 0.00 ± 0.00 | 0.00 ± 0.00 | 0.00 ± 0.00 |
| 2,6-dm-octane | 1.01 | 0.00 ± 0.00 | 0.09 ± 0.09 | 0.00 ± 0.00 | 0.00 ± 0.00 |
| 2,4-dm-octane | 1.01 | 0.26 ± 0.09 | 0.20 ± 0.06 | 0.13 ± 0.02 | 0.17 ± 0.06 |
| 2,2-dm-octane | 1.01 | 0.10 ± 0.12 | 0.00 ± 0.00 | 0.07 ± 0.03 | 0.13 ± 0.03 |

**Appendix C** (continued)

| | | tunnel NMOC, weight % ± 1 standard deviation | | | |
|---|---|---|---|---|---|
| | MIR | summer | summer | summer | summer |
| compound | $gO_3/gOC_i$ | 1994 | 1995 | 1996 | 1997 |
| C10 paraffin | 1.01 | 0.00 ± 0.00 | 0.00 ± 0.00 | 0.00 ± 0.00 | 0.03 ± 0.06 |
| C10+ paraffin | 1.00 | 1.33 ± 0.31 | 1.27 ± 0.35 | 0.53 ± 0.16 | 0.31 ± 0.22 |
| total isoalkanes | | 22.31 | 22.48 | 26.27 | 26.26 |
| **cycloalkanes** | | | | | |
| me-cyclopentane | 2.82 | 1.71 ± 0.44 | 1.95 ± 0.15 | 2.62 ± 0.15 | 3.16 ± 0.29 |
| cyclohexane | 1.28 | 0.00 ± 0.00 | 0.00 ± 0.00 | 0.92 ± 0.07 | 0.35 ± 0.09 |
| cycpentane & 2,3-dm-butane | 1.44 | 1.15 ± 0.23 | 1.07 ± 0.13 | 1.11 ± 0.42 | 1.24 ± 0.32 |
| c/t-1,3-dm-cyclopentane | 2.55 | 0.00 ± 0.00 | 0.00 ± 0.00 | 0.41 ± 0.10 | 0.00 ± 0.00 |
| me-cyclohexane | 1.85 | 0.40 ± 0.08 | 0.91 ± 0.55 | 0.86 ± 0.36 | 0.47 ± 0.18 |
| total cycloalkanes | | 3.26 | 3.94 | 5.92 | 5.22 |
| **alkenes/dienes** | | | | | |
| ethene | 7.29 | 8.69 ± 0.84 | 6.20 ± 1.13 | 6.25 ± 1.15 | 7.15 ± 0.76 |
| propene | 9.40 | 3.90 ± 0.35 | 3.36 ± 0.30 | 3.68 ± 0.47 | 3.65 ± 0.52 |
| 1,3-butadiene | 10.89 | n/a[a] | 0.63 ± 0.16 | 0.49 ± 0.12 | 0.73 ± 0.09 |
| 2-me-propene (isobutene) | 5.31 | 1.66 ± 0.22 | 1.38 ± 0.09 | 3.31 ± 0.35 | 2.47 ± 0.23 |
| 1-butene | 8.91 | 0.53 ± 0.06 | 0.47 ± 0.03 | 0.48 ± 0.05 | 0.40 ± 0.03 |
| t-2-butene | 9.94 | 0.32 ± 0.16 | 0.39 ± 0.05 | 0.43 ± 0.10 | 0.28 ± 0.04 |
| c-2-butene | 9.94 | 0.18 ± 0.08 | 0.26 ± 0.11 | 0.28 ± 0.09 | 0.17 ± 0.04 |
| isoprene (2-me-1,3-butadiene) | 9.08 | 0.01 ± 0.03 | 0.10 ± 0.08 | 0.03 ± 0.05 | 0.00 ± 0.00 |
| cyclopentene | 7.66 | 0.20 ± 0.14 | 0.20 ± 0.02 | 0.14 ± 0.01 | 0.08 ± 0.05 |
| 3-me-1-butene | 6.22 | 0.05 ± 0.05 | 0.06 ± 0.04 | 0.23 ± 0.23 | 0.12 ± 0.03 |

**Appendix C** (continued)

| compound | MIR $gO_3/gOC_i$ | tunnel NMOC, weight % ± 1 standard deviation summer 1994 | summer 1995 | summer 1996 | summer 1997 |
|---|---|---|---|---|---|
| 1-pentene | 6.22 | 0.20 ± 0.09 | 0.24 ± 0.03 | 0.14 ± 0.04 | 0.16 ± 0.08 |
| 2-me-1-butene | 4.90 | 0.26 ± 0.15 | 0.39 ± 0.05 | 0.27 ± 0.03 | 0.06 ± 0.03 |
| t-2-pentene | 8.80 | 0.26 ± 0.14 | 0.41 ± 0.05 | 0.31 ± 0.05 | 0.23 ± 0.03 |
| c-2-pentene | 8.80 | 0.12 ± 0.04 | 0.20 ± 0.03 | 0.11 ± 0.02 | 0.10 ± 0.01 |
| 2-me-2-butene | 6.41 | 0.50 ± 0.08 | 0.59 ± 0.08 | 0.47 ± 0.09 | 0.01 ± 0.02 |
| other C5 olefin | 8.80 | 0.00 ± 0.00 | 0.00 ± 0.00 | 0.00 ± 0.00 | 0.24 ± 0.15 |
| 4-me-1-pentene | 4.42 | 0.01 ± 0.03 | 0.01 ± 0.01 | 0.01 ± 0.02 | 0.12 ± 0.06 |
| 4-me-2-pentene | 6.69 | 0.00 ± 0.00 | 0.04 ± 0.09 | 0.00 ± 0.00 | 0.00 ± 0.01 |
| 2-me-1-pentene | 4.42 | 0.03 ± 0.06 | 0.00 ± 0.00 | 0.02 ± 0.03 | 0.00 ± 0.00 |
| 1-hexene | 4.42 | 0.13 ± 0.07 | 0.19 ± 0.07 | 0.08 ± 0.02 | 0.12 ± 0.02 |
| other C6 olefin | 6.69 | 0.00 ± 0.00 | 0.00 ± 0.00 | 0.00 ± 0.00 | 0.34 ± 0.60 |
| 1-me-cyclohexene | 5.64 | 0.06 ± 0.07 | 0.00 ± 0.00 | 0.03 ± 0.05 | 0.00 ± 0.00 |
| c/t-1,3-dm-cycpentene | 5.64 | 0.00 ± 0.00 | 0.42 ± 0.07 | 0.00 ± 0.00 | 0.00 ± 0.00 |
| 2-me-2-hexene | 5.53 | 0.05 ± 0.05 | 0.15 ± 0.17 | 0.02 ± 0.02 | 0.02 ± 0.03 |
| c/t-2-heptene | 5.53 | 0.00 ± 0.01 | 0.00 ± 0.00 | 0.00 ± 0.00 | 0.00 ± 0.00 |
| 1-heptene | 3.48 | 0.39 ± 0.08 | 0.00 ± 0.00 | 0.00 ± 0.00 | 0.22 ± 0.03 |
| 1,2,4-tm-cycpentene | 5.38 | 0.00 ± 0.00 | 0.09 ± 0.04 | 0.48 ± 0.23 | 0.09 ± 0.01 |
| 2,2,4-tri-me-pentene | 2.69 | 0.07 ± 0.02 | 0.00 ± 0.00 | 0.22 ± 0.05 | 0.09 ± 0.06 |
| 1-octene | 2.69 | 0.05 ± 0.05 | 0.15 ± 0.10 | 0.17 ± 0.05 | 0.13 ± 0.06 |
| total alkenes/dienes | | 18.07 | 15.95 | 17.64 | 16.99 |

**Appendix C** (continued)

| compound | MIR $gO_3/gOC_i$ | tunnel NMOC, weight % ± 1 standard deviation summer 1994 | summer 1995 | summer 1996 | summer 1997 |
|---|---|---|---|---|---|
| **aromatics** | | | | | |
| benzene | 0.42 | 6.21 ± 0.78 | 5.36 ± 0.37 | 3.34 ± 0.29 | 3.64 ± 0.26 |
| toluene | 2.73 | 9.78 ± 0.71 | 8.64 ± 0.75 | 8.50 ± 0.34 | 8.26 ± 0.73 |
| styrene | 2.22 | 0.43 ± 0.09 | 0.41 ± 0.05 | 0.31 ± 0.04 | 0.16 ± 0.03 |
| ethylbenzene | 2.70 | 1.54 ± 0.08 | 1.36 ± 0.11 | 1.24 ± 0.06 | 1.15 ± 0.09 |
| m/p-xylene | 7.38 | 6.35 ± 0.29 | 5.62 ± 0.49 | 5.04 ± 0.27 | 5.09 ± 0.32 |
| o-xylene | 6.46 | 2.62 ± 0.11 | 2.05 ± 0.26 | 1.72 ± 0.08 | 1.54 ± 0.23 |
| i-pr-benzene (cumene) | 2.24 | 0.06 ± 0.06 | 0.09 ± 0.06 | 0.13 ± 0.04 | 0.09 ± 0.06 |
| n-pr-benzene | 2.12 | 0.27 ± 0.06 | 0.27 ± 0.05 | 0.22 ± 0.01 | 0.20 ± 0.04 |
| m-et-toluene | 7.20 | 1.90 ± 0.27 | 1.66 ± 0.24 | 1.45 ± 0.07 | 0.69 ± 0.08 |
| 1,3,5-tm-benzene | 10.12 | 0.18 ± 0.28 | 0.24 ± 0.24 | 0.00 ± 0.00 | 0.11 ± 0.02 |
| p-et-toluene | 7.20 | 0.85 ± 0.20 | 0.72 ± 0.16 | 0.60 ± 0.03 | 0.56 ± 0.07 |
| o-et-toluene | 7.20 | 0.60 ± 0.14 | 0.45 ± 0.07 | 0.36 ± 0.04 | 0.33 ± 0.12 |
| n-decane/1,2,4-tm-benz | 7.93 | 2.63 ± 0.11 | 2.36 ± 0.22 | 1.66 ± 0.13 | 2.32 ± 0.22 |
| 1,2,3-tm-benzene | 8.85 | 0.43 ± 0.06 | 0.39 ± 0.04 | 0.24 ± 0.02 | 0.36 ± 0.11 |
| sec-butylbenzene | 1.89 | 0.17 ± 0.09 | 0.04 ± 0.02 | 0.05 ± 0.07 | 0.12 ± 0.08 |
| 1,2-de-benzene | 6.45 | 0.31 ± 0.08 | 0.35 ± 0.20 | 0.10 ± 0.03 | 1.27 ± 2.85 |
| 1,3-de-benzene | 6.45 | 0.15 ± 0.10 | 0.21 ± 0.03 | 0.08 ± 0.04 | 0.18 ± 0.16 |
| 1,4-de-benzene | 6.45 | 0.49 ± 0.05 | 0.50 ± 0.05 | 0.24 ± 0.07 | 0.44 ± 0.16 |
| n-butylbenzene | 1.87 | 0.76 ± 0.14 | 0.68 ± 0.06 | 0.31 ± 0.02 | 0.39 ± 0.09 |
| tetra-me-benzene | 9.07 | 0.27 ± 0.15 | 0.46 ± 0.08 | 0.13 ± 0.06 | 0.10 ± 0.08 |

**Appendix C** (continued)

| compound | MIR $gO_3/gOC_i$ | tunnel NMOC, weight % ± 1 standard deviation summer 1994 | summer 1995 | summer 1996 | summer 1997 |
|---|---|---|---|---|---|
| other C10+ aromatic | 5.84 | 0.99 ± 0.44 | 1.56 ± 0.44 | 0.29 ± 0.19 | 0.51 ± 0.51 |
| total aromatics | | 36.97 | 33.42 | 26.02 | 27.52 |
| **oxygenates** | | | | | |
| MTBE | 0.62 | not measured | 0.70 ± 0.14 | 5.47 ± 0.74 | 4.72 ± 0.67 |
| **carbonyls** | | | | | |
| formaldehyde | 7.15 | 1.57 ± 0.16 | 1.60 ± 0.16 | 2.19 ± 0.34 | 1.54 ± 0.25 |
| acetaldehyde | 5.52 | 0.37 ± 0.04 | 0.33 ± 0.03 | 0.36 ± 0.04 | 0.34 ± 0.06 |
| acetone | 0.56 | 0.14 ± 0.03 | 0.15 ± 0.12 | 0.22 ± 0.06 | 0.15 ± 0.09 |
| acrolein (propenal) | 6.77 | 0.09 ± 0.01 | 0.06 ± 0.01 | 0.08 ± 0.03 | 0.00 ± 0.00 |
| propionaldehyde | 6.53 | 0.04 ± 0.01 | 0.03 ± 0.01 | 0.05 ± 0.01 | 0.06 ± 0.03 |
| crotonaldehyde (butenal) | 5.42 | 0.04 ± 0.01 | 0.03 ± 0.01 | 0.04 ± 0.01 | 0.23 ± 0.03 |
| methyl ethyl ketone (MEK) | 1.18 | 0.04 ± 0.01 | 0.05 ± 0.04 | 0.06 ± 0.03 | 0.09 ± 0.04 |
| methacrolein | 5.26 | 0.07 ± 0.01 | 0.05 ± 0.01 | 0.09 ± 0.03 | 0.00 ± 0.00 |
| butyraldehyde | 5.26 | 0.17 ± 0.02 | 0.18 ± 0.02 | 0.17 ± 0.02 | 0.02 ± 0.02 |
| benzaldehyde | -0.55 | 0.43 ± 0.05 | 0.37 ± 0.04 | 0.30 ± 0.06 | 0.23 ± 0.03 |
| Isopentanal | 4.41 | 0.00 ± 0.00 | 0.03 ± 0.01 | 0.05 ± 0.02 | 0.00 ± 0.00 |
| pentanaldehyde | 4.41 | 0.00 ± 0.00 | 0.01 ± 0.01 | 0.00 ± 0.00 | 0.16 ± 0.03 |
| tolualdehyde | -0.55 | 0.64 ± 0.07 | 0.44 ± 0.05 | 0.39 ± 0.06 | 0.01 ± 0.01 |
| hexanal | 3.79 | 0.00 ± 0.00 | 0.01 ± 0.00 | 0.00 ± 0.00 | 0.01 ± 0.02 |
| di-me-benzaldehyde | -0.55 | 0.00 ± 0.00 | 0.29 ± 0.04 | 0.22 ± 0.04 | 0.00 ± 0.00 |
| 2-pentanone | 0.99 | 0.00 ± 0.00 | 0.00 ± 0.00 | 0.00 ± 0.00 | 0.07 ± 0.03 |

**Appendix C** (continued)

| compound | MIR $gO_3/gOC_i$ | tunnel NMOC, weight % ± 1 standard deviation summer 1994 | summer 1995 | summer 1996 | summer 1997 |
|---|---|---|---|---|---|
| 3-pentanone | 0.99 | 0.00 ± 0.00 | 0.00 ± 0.00 | 0.00 ± 0.00 | 0.00 ± 0.00 |
| 2-me-3-pentanone | 0.85 | 0.00 ± 0.00 | 0.00 ± 0.00 | 0.00 ± 0.00 | 0.01 ± 0.02 |
| MIBK (4-me-2-pentanone) | 0.85 | 0.00 ± 0.00 | 0.00 ± 0.00 | 0.00 ± 0.00 | 0.13 ± 0.05 |
| 2-heptanone | 0.75 | 0.00 ± 0.00 | 0.00 ± 0.00 | 0.00 ± 0.00 | 0.04 ± 0.04 |
| total carbonyls | | 3.59 | 3.63 | 4.22 | 3.09 |
| **alkynes** | | | | | |
| acetylene | 0.50 | 3.08 ± 0.27 | 3.07 ± 0.33 | 2.92 ± 0.28 | 2.18 ± 0.50 |
| **unidentified** | | | | | |
| unidentified hydrocarbon | 4.00 | 3.67 ± 4.69 | 8.43 ± 5.81 | 3.71 ± 2.26 | 4.88 ± 1.30 |
| unidentified carbonyl | 3.00 | 0.44 ± 0.05 | 0.12 ± 0.03 | 0.01 ± 0.02 | 0.00 ± 0.00 |
| total unidentified | | 4.11 | 8.56 | 3.72 | 4.88 |
| total NMOC | | 100.0 | 100.0 | 100.0 | 100.0 |
| total normalized reactivity ($gO_3$/gNMOC) | | 3.79 | 3.71 | 3.41 | 3.49 |
| NMOC emission factor, ± 95% C.I. (g/L) | | 4.04 ± 0.26 | 3.67 ± 0.26 | 2.78 ± 0.13 | 2.25 ± 0.22 |
| TOG[b] emission factor, ± 95% C.I. (g/L) | | 4.48 ± 0.31 | 4.01 ± 0.28 | 3.07 ± 0.13 | 2.55 ± 0.25 |
| methane (wt% TOG) | | 9.79 ± 2.24 | 8.38 ± 1.06 | 9.12 ± 1.26 | 11.52 ± 3.50 |

[a] Not available. Butadiene was found to be unstable in the stainless steel sampling canisters in summer 1994; see text.

[a] Total organic gases, TOG = NMOC + methane.

# Appendix D

# Prediction of Organic Compound Vapor Pressures

## Appendix D

| compound[a] | # C | MW g mol$^{-1}$ | $P^o$ atm | $T_c$ K | $P_c$ atm | constants used to predict vapor pressure a | b | c | d |
|---|---|---|---|---|---|---|---|---|---|
| **alkanes** | | | | | | | | | |
| n-propane | 3 | 44 | 12.88 | 369.8 | 41.9 | -6.72219 | 1.33236 | -2.13868 | -1.38551 |
| n-butane | 4 | 58 | 3.53 | 425.2 | 37.5 | -6.88709 | 1.15157 | -1.99873 | -3.13003 |
| n-pentane | 5 | 72 | 1.06 | 469.7 | 33.3 | -7.28936 | 1.53679 | -3.08367 | -1.02456 |
| n-hexane | 6 | 86 | 0.34 | 507.5 | 29.7 | -7.46765 | 1.44211 | -3.28222 | -2.50941 |
| n-heptane | 7 | 100 | 0.110 | 540.3 | 27.0 | -7.67468 | 1.37068 | -3.5362 | -3.20243 |
| n-octane | 8 | 114 | 0.037 | 568.8 | 24.6 | -7.91211 | 1.38007 | -3.80435 | -4.50132 |
| n-nonane | 9 | 128 | 0.012 | 594.6 | 22.6 | -8.2448 | 1.57885 | -4.38155 | -4.04412 |
| other n-alkanes | 10 | 142 | 0.004 | 617.7 | 20.9 | -8.56523 | 1.97756 | -5.81971 | -0.29982 |
| **isoalkanes** | | | | | | | | | |
| 2-me-propane | 4 | 58 | 4.92 | 408.2 | 36.0 | -6.95579 | 1.5009 | -2.52717 | -1.49776 |
| 2-me-butane | 5 | 72 | 1.40 | 460.4 | 33.5 | -7.12727 | 1.38996 | -2.54302 | -2.45657 |
| 2-me-pentane | 6 | 86 | 0.46 | 497.5 | 29.7 | -7.31728 | 1.3394 | -3.06807 | -1.99255 |
| 3-me-pentane | 6 | 86 | 0.41 | 504.5 | 30.8 | -7.27084 | 1.26113 | -2.81741 | -2.17642 |
| 2,2-dm-butane | 6 | 86 | 0.672 | 488.8 | 30.4 | -7.24296 | 1.66876 | -3.23718 | -0.53171 |
| 2,3-dm-butane | 6 | 86 | 0.506 | 500.0 | 30.9 | -7.2787 | 1.56349 | -3.05387 | -1.57752 |
| 2-me-hexane | 7 | 100 | 0.155 | 530.4 | 26.9 | -7.62477 | 1.47806 | -3.53616 | -2.70794 |
| 3-me-hexane | 7 | 100 | 0.145 | 535.5 | 27.7 | -7.58592 | 1.47394 | -3.52511 | -2.35419 |
| 2,3-dm-pentane | 7 | 100 | 0.161 | 537.4 | 28.7 | -7.46078 | 1.47778 | -3.37079 | -1.88997 |
| 2,4-dm-pentane | 7 | 100 | 0.225 | 519.8 | 27.0 | -7.46358 | 1.43203 | -3.42422 | -2.20238 |
| 2,2-dm-pentane | 7 | 100 | 0.238 | 520.5 | 27.3 | -7.45564 | 1.56232 | -3.4462 | -1.80802 |

**Appendix D** (continued)

| compound[a] | # C | MW g mol$^{-1}$ | $P^o$ atm | $T_c$ K | $P_c$ atm | constants used to predict vapor pressure a | b | c | d |
|---|---|---|---|---|---|---|---|---|---|
| 3-et-pentane | 7 | 100 | 0.137 | 540.6 | 28.5 | -7.58305 | 1.58587 | -3.56732 | -2.42625 |
| 2-me-heptane | 8 | 114 | 0.052 | 559.6 | 24.5 | -7.80701 | 1.38191 | -3.78286 | -3.50395 |
| 3-me-heptane | 8 | 114 | 0.050 | 563.7 | 25.2 | -7.82876 | 1.50656 | -3.86146 | -3.52377 |
| 4-me-heptane | 8 | 114 | 0.052 | 561.7 | 25.1 | -7.78757 | 1.40709 | -3.76234 | -3.50643 |
| 2,2,4-tm-pentane | 8 | 114 | 0.117 | 544.0 | 25.4 | -7.3889 | 1.25294 | -3.16606 | -2.22001 |
| 2,3,3-tm-pentane | 8 | 114 | 0.066 | 573.6 | 27.8 | -7.41747 | 1.42778 | -3.19166 | -1.81367 |
| 2,3,4-tm-pentane | 8 | 114 | 0.067 | 566.4 | 26.9 | -7.62 | 1.60334 | -3.57834 | -2.04401 |
| 2,2,3-tm-pentane | 8 | 114 | 0.078 | 563.5 | 26.9 | -7.48839 | 1.52208 | -3.44481 | -2.12538 |
| 2-me-3-ethylpentane | 8 | 114 | 0.060 | 567.1 | 26.6 | -7.65393 | 1.54032 | -3.64686 | -2.5238 |
| 2,2-dm-hexane | 8 | 114 | 0.083 | 549.9 | 25.0 | -7.69898 | 1.56083 | -3.75189 | -3.01869 |
| 2,3-dm-hexane | 8 | 114 | 0.059 | 563.5 | 26.0 | -7.7518 | 1.58578 | -3.80794 | -2.58547 |
| 2,4-dm-hexane | 8 | 114 | 0.075 | 553.5 | 25.3 | -7.65152 | 1.41393 | -3.62789 | -3.06548 |
| 2,5-dm-hexane | 8 | 114 | 0.075 | 550.1 | 24.6 | -7.76508 | 1.51236 | -3.78809 | -3.07843 |
| 3,3-dm-hexane | 8 | 114 | 0.070 | 562.0 | 26.2 | -7.59847 | 1.50336 | -3.49912 | -2.38236 |
| 2,2,5-tm-hexane | 9 | 128 | 0.043 | 568.0 | 23.0 | -7.80573 | 1.68023 | -4.50859 | -0.78808 |
| other isoalkanes | 9 | 128 | 0.043 | | | | | | |
| **cycloalkanes** | | | | | | | | | |
| cyclopentane | 5 | 70 | 0.675 | 511.7 | 44.5 | -6.51809 | 0.38442 | -1.11706 | -4.50275 |
| me-cyclopentane | 6 | 84 | 0.307 | 532.7 | 37.3 | -7.15937 | 1.48017 | -2.92482 | -1.98377 |
| cyclohexane | 6 | 84 | 0.223 | 553.5 | 40.2 | -6.96009 | 1.31328 | -2.75683 | -2.45491 |
| me-cyclohexane | 7 | 98 | 0.110 | 572.2 | 34.2 | -7.01915 | 1.09615 | -2.37009 | -3.37562 |

**Appendix D** (continued)

| compound[a] | # C | MW g mol$^{-1}$ | $P^o$ atm | $T_c$ K | $P_c$ atm | constants used to predict vapor pressure a | b | c | d |
|---|---|---|---|---|---|---|---|---|---|
| et-cyclopentane | 7 | 98 | 0.096 | 569.5 | 33.6 | -7.68089 | 2.28014 | -4.40365 | 0.54338 |
| 1-c-2-dm-cyclohexane | 8 | 112 | 0.037 | 606.0 | 29.2 | -7.01944 | 1.3186 | -3.96577 | 0.08142 |
| other cycloalkanes | 8 | 112 | 0.037 | | | | | | |
| **alkenes** | | | | | | | | | |
| propene | 3 | 42 | 15.466 | 364.9 | 45.4 | -6.64231 | 1.21857 | -1.81005 | -2.48212 |
| 1-butene | 4 | 56 | 4.260 | 419.6 | 39.7 | -6.88204 | 1.27051 | -2.26284 | -2.61632 |
| c-2-butene | 4 | 56 | 3.125 | 435.6 | 41.5 | -6.88706 | 1.15941 | -2.19304 | -3.12758 |
| t-2-butene[b] | 4 | 56 | 3.422 | 428.6 | 39.4 | 43.517 | 4174.56 | -5.041 | 1995 |
| 2-me-propene | 4 | 56 | 4.328 | 417.9 | 39.5 | -6.95542 | 1.35673 | -2.45222 | -1.4611 |
| 1-pentene | 5 | 70 | 1.301 | 464.8 | 34.8 | -7.04875 | 1.17813 | -2.45105 | -2.21727 |
| c-2-pentene | 5 | 70 | 1.032 | 476.0 | 36.0 | -6.8016 | 0.544458 | -1.55279 | -5.68029 |
| t-2-pentene | 5 | 70 | 1.053 | 475.0 | 36.1 | -6.99461 | 1.00724 | -2.42146 | -2.51692 |
| 2-me-1-butene | 5 | 70 | 1.257 | 465.0 | 34.1 | -6.8299 | 0.7266 | -2.15363 | -3.62225 |
| 3-me-1-butene | 5 | 70 | 1.798 | 450.0 | 34.6 | -7.1887 | 1.42502 | -2.27292 | -2.04323 |
| 2-me-2-butene | 5 | 70 | 0.977 | 470.0 | 34.1 | -7.71438 | 1.95946 | -3.1571 | -2.22515 |
| cyclopentene[c] | 5 | 68 | 0.804 | 506.0 | | 9.3154 | 2583.07 | -39.7 | |
| 1-hexene | 6 | 84 | 0.410 | 504.0 | 31.3 | -7.76467 | 2.29843 | -4.44302 | 0.89947 |
| t-2-hexene[b] | 6 | 84 | 0.352 | 516.0 | 32.3 | 53.818 | 5734.51 | -6.348 | 3548 |
| c-2-hexene[c] | 6 | 84 | 0.335 | 518.0 | 32.4 | 9.5855 | 2897.97 | -39.3 | |
| c-3-hexene[c] | 6 | 84 | 0.367 | 517.0 | 32.4 | 9.2182 | 2680.52 | -48.4 | |
| 2-me-2-pentene[c] | 6 | 84 | 0.353 | 518.0 | 32.4 | 9.3221 | 2725.89 | -47.64 | |

**Appendix D** (continued)

| compound[a] | # C | MW g mol$^{-1}$ | $P^o$ atm | $T_c$ K | $P_c$ atm | constants used to predict vapor pressure a | b | c | d |
|---|---|---|---|---|---|---|---|---|---|
| c-3-me-2-pentene[c] | 6 | 84 | 0.351 | 518.0 | 32.4 | 9.2922 | 2731.79 | -46.47 | |
| t-3-me-2-pentene[c] | 6 | 84 | 0.315 | 521.0 | 32.5 | 9.3282 | 2750.5 | -48.33 | |
| c-4-me-2-pentene[c] | 6 | 84 | 0.528 | 490.0 | 30.0 | 9.1325 | 2580.52 | -46.56 | |
| t-4-me-2-pentene[c] | 6 | 84 | 0.486 | 493.0 | 30.0 | 9.2223 | 2631.57 | -46 | |
| 2-me-1-pentene[d] | 6 | 84 | 0.406 | | | | | | |
| 4-me-1-pentene[d] | 6 | 84 | 0.406 | | | | | | |
| 2-et-1-butene[e] | 6 | 84 | 0.573 | | | | | | |
| 2,3-dm-1-butene[c] | 6 | 84 | 0.544 | 501.0 | 32.0 | 9.181 | 2612.69 | -43.78 | |
| 2,3-dm-2-butene | 6 | 84 | 0.284 | 524.0 | 33.2 | -7.15852 | 1.36868 | -4.1289 | 1.53046 |
| 3,3-dm-1-butene | 6 | 84 | 0.892 | 490.0 | 32.1 | -6.54633 | 1.50412 | -4.54855 | 2.96466 |
| 1-heptene | 7 | 98 | 0.133 | 537.3 | 27.9 | -8.26875 | 3.02688 | -6.18709 | 4.33049 |
| other olefins | 7 | 98 | 0.133 | | | | | | |
| **aromatics** | | | | | | | | | |
| benzene | 6 | 78 | 0.220 | 562.2 | 48.3 | -6.98273 | 1.33213 | -2.62863 | -3.33399 |
| toluene | 7 | 92 | 0.070 | 591.8 | 40.5 | -7.28607 | 1.38091 | -2.83433 | -2.79168 |
| ethylbenzene | 8 | 106 | 0.025 | 617.2 | 35.5 | -7.48645 | 1.45488 | -3.37538 | -2.23048 |
| o-xylene | 8 | 106 | 0.018 | 630.3 | 36.8 | -7.53357 | 1.40968 | -3.10985 | -2.85992 |
| m-xylene | 8 | 106 | 0.022 | 617.1 | 34.9 | -7.59222 | 1.39441 | -3.22746 | -2.40376 |
| p-xylene | 8 | 106 | 0.023 | 616.2 | 34.6 | -7.63495 | 1.50724 | -3.19678 | -2.7871 |
| o-ethyltoluene | 9 | 120 | 0.008 | 651.0 | 30.0 | -7.58007 | 2.20412 | -6.68027 | 6.06587 |
| m-ethyltoluene | 9 | 120 | 0.009 | 637.0 | 28.0 | -7.86301 | 2.47961 | -6.98644 | 6.35609 |

**Appendix D** (continued)

| compound[a] | # C | MW g mol$^{-1}$ | $P^o$ atm | $T_c$ K | $P_c$ atm | constants used to predict vapor pressure a | b | c | d |
|---|---|---|---|---|---|---|---|---|---|
| p-ethyltoluene | 9 | 120 | 0.009 | 640.0 | 29.0 | -7.68892 | 1.92605 | -5.51788 | 2.76399 |
| 1,2,3-tm-benzene | 9 | 120 | 0.005 | 664.5 | 34.1 | -8.44191 | 2.92198 | -5.66712 | 2.28086 |
| 1,2,4-tm-benzene | 9 | 120 | 0.006 | 649.2 | 31.9 | -8.50002 | 2.98227 | -6.02665 | 3.51307 |
| 1,3,5-tm-benzene | 9 | 120 | 0.008 | 637.3 | 30.9 | -8.33715 | 2.4116 | -5.30321 | 2.67635 |
| propylbenzene | 10 | 134 | 0.010 | 638.2 | 31.6 | -7.92198 | 1.97403 | -4.27504 | -1.28568 |
| naphthalene | 10 | 134 | 0.001 | 748.4 | 40.0 | -7.85178 | 2.17172 | -3.70504 | -4.81238 |
| other aromatics | 10+ | | 0.000 | | | | | | |
| **oxygenates** | | | | | | | | | |
| MTBE | 5 | 88 | 0.544 | 496.4 | 33.3 | -7.82516 | 2.95493 | -6.94079 | 12.17416 |
| TAME[f] | 6 | 102 | 0.135 | 531.0 | 30.0 | -8.30292 | 2.02889 | -3.26245 | -6.32274 |

[a] Compound vapor pressures were predicted for T = 311 K using the Wagner equation (eq 4.2) unless otherwise noted. Values of $T_c$, $P_c$, a, b, c, and d are taken from Appendix A of Reid et al. (1987).

[b] Vapor pressure calculated using Frost-Kalkwarf-Thodos eqn (see eq 7-6.1 of Reid et al. (1987)).

[c] Vapor pressure calculated using Antoine's modification of Clasius-Clapeyron equation (see eq 7-3.1 of Reid et al. (1987)).

[d] 2-me-1-pentene and 4-me-1-pentene have been assigned a vapor pressure equal to the average vapor pressure of the other methyl-substituted pentenes.

[e] 2-et-1-butene has been assigned a vapor pressure equal to the average of the other C6 alkyl substituted butenes.

[f] TAME was assigned a vapor pressure equal to that of ethyl tert-butyl ether (ETBE).

# Appendix E

# Time Series Plots of Pollutant Concentrations

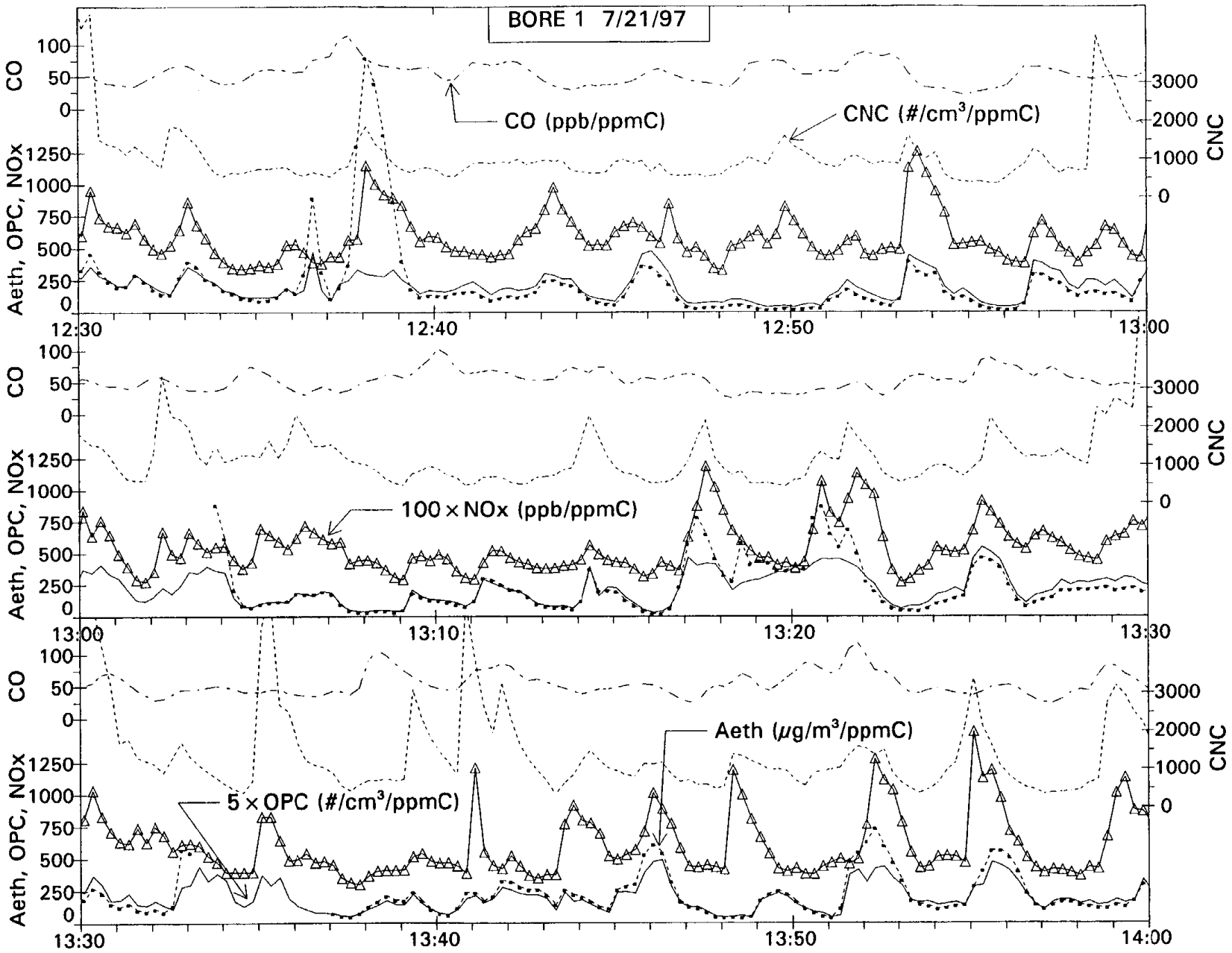
BORE 1 7/21/97
CO
Aeth, OPC, NOx
CNC
CO (ppb/ppmC)
CNC (#/cm³/ppmC)
100 × NOx (ppb/ppmC)
5 × OPC (#/cm³/ppmC)
Aeth (μg/m³/ppmC)
12:30
12:40
12:50
13:00
13:10
13:20
13:30
13:40
13:50
14:00

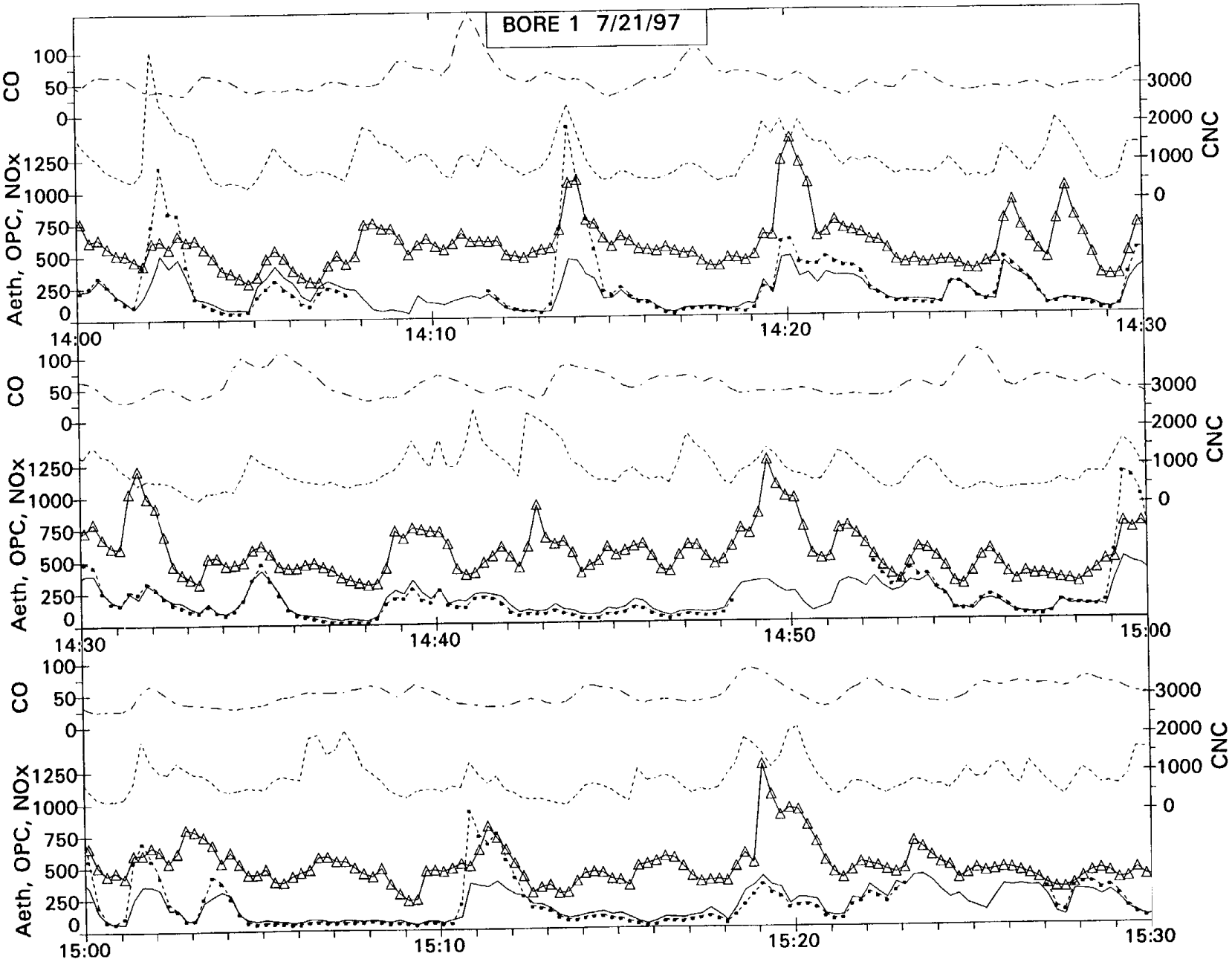
BORE 1 7/21/97
CO
Aeth, OPC, NOx
CNC
100
50
0
1250
1000
750
500
250
0
3000
2000
1000
0
14:00
14:10
14:20
14:30
14:40
14:50
15:00
15:10
15:20
15:30

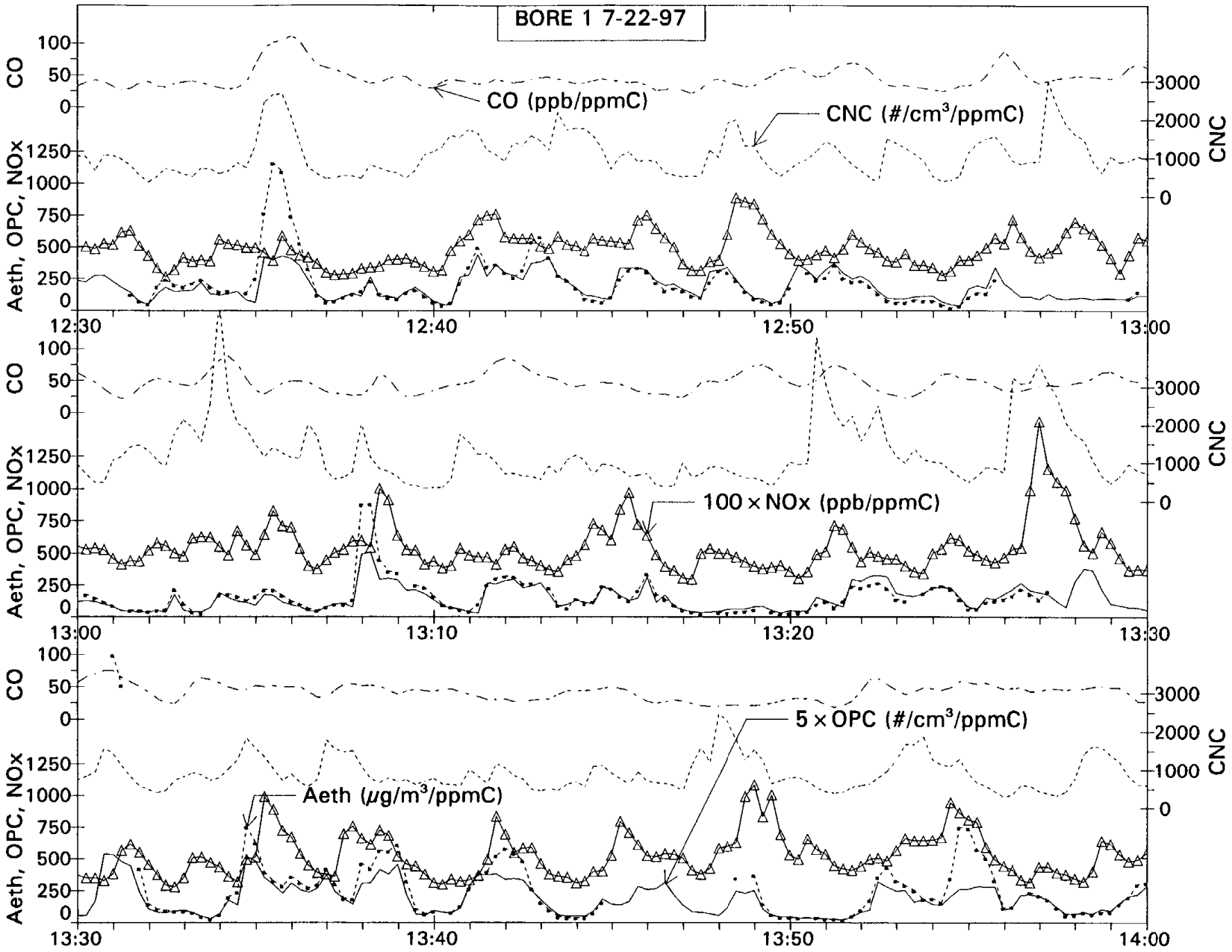
BORE 1 7-22-97
CO
Aeth, OPC, NOx
CNC
CO (ppb/ppmC)
CNC (#/cm³/ppmC)
100 × NOx (ppb/ppmC)
5 × OPC (#/cm³/ppmC)
Aeth (μg/m³/ppmC)
12:30
12:40
12:50
13:00
13:10
13:20
13:30
13:40
13:50
14:00

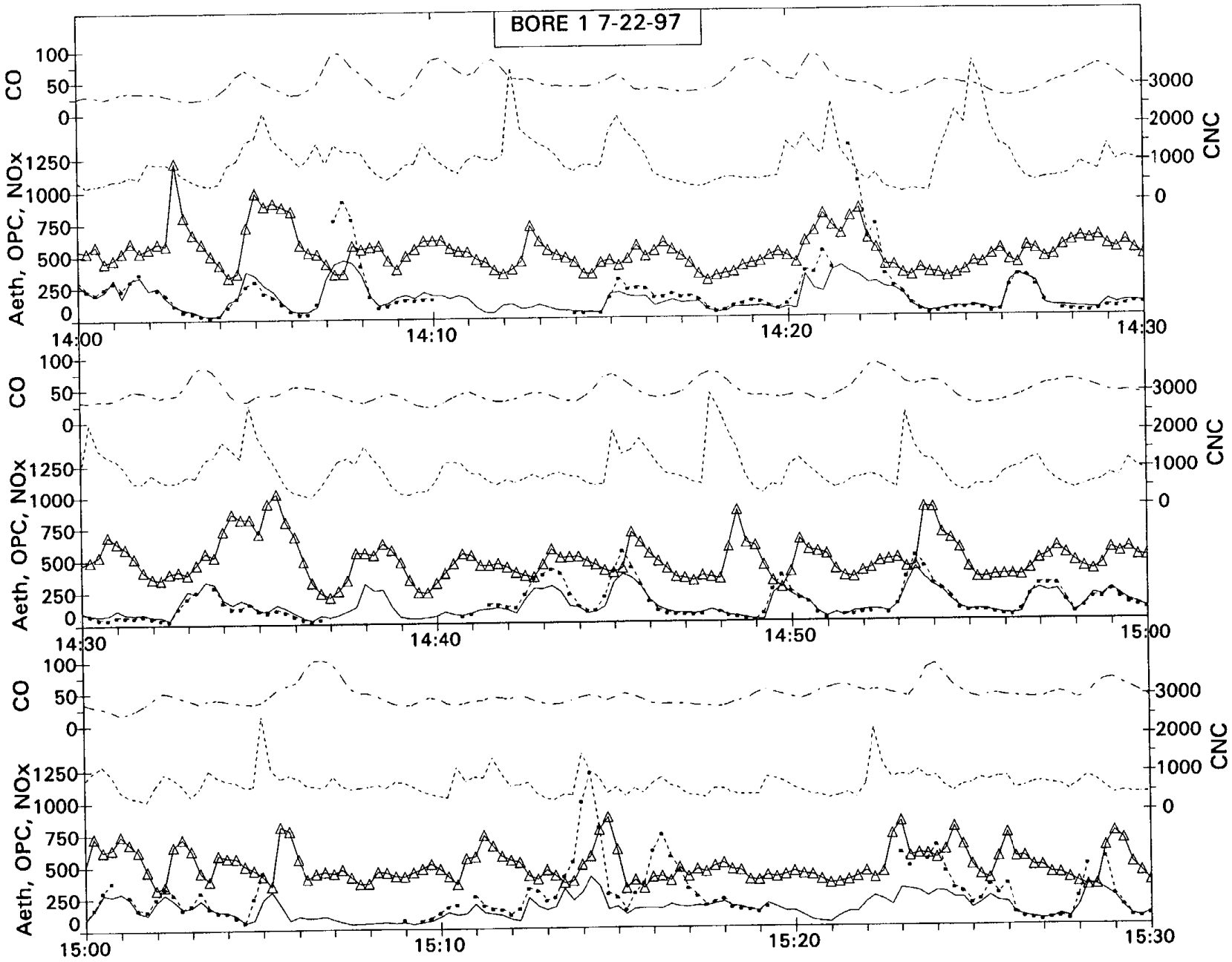
BORE 1 7-22-97
CO
Aeth, OPC, NOx
CNC
100
50
0
1250
1000
750
500
250
0
3000
2000
1000
0
14:00
14:10
14:20
14:30
14:40
14:50
15:00
15:10
15:20
15:30

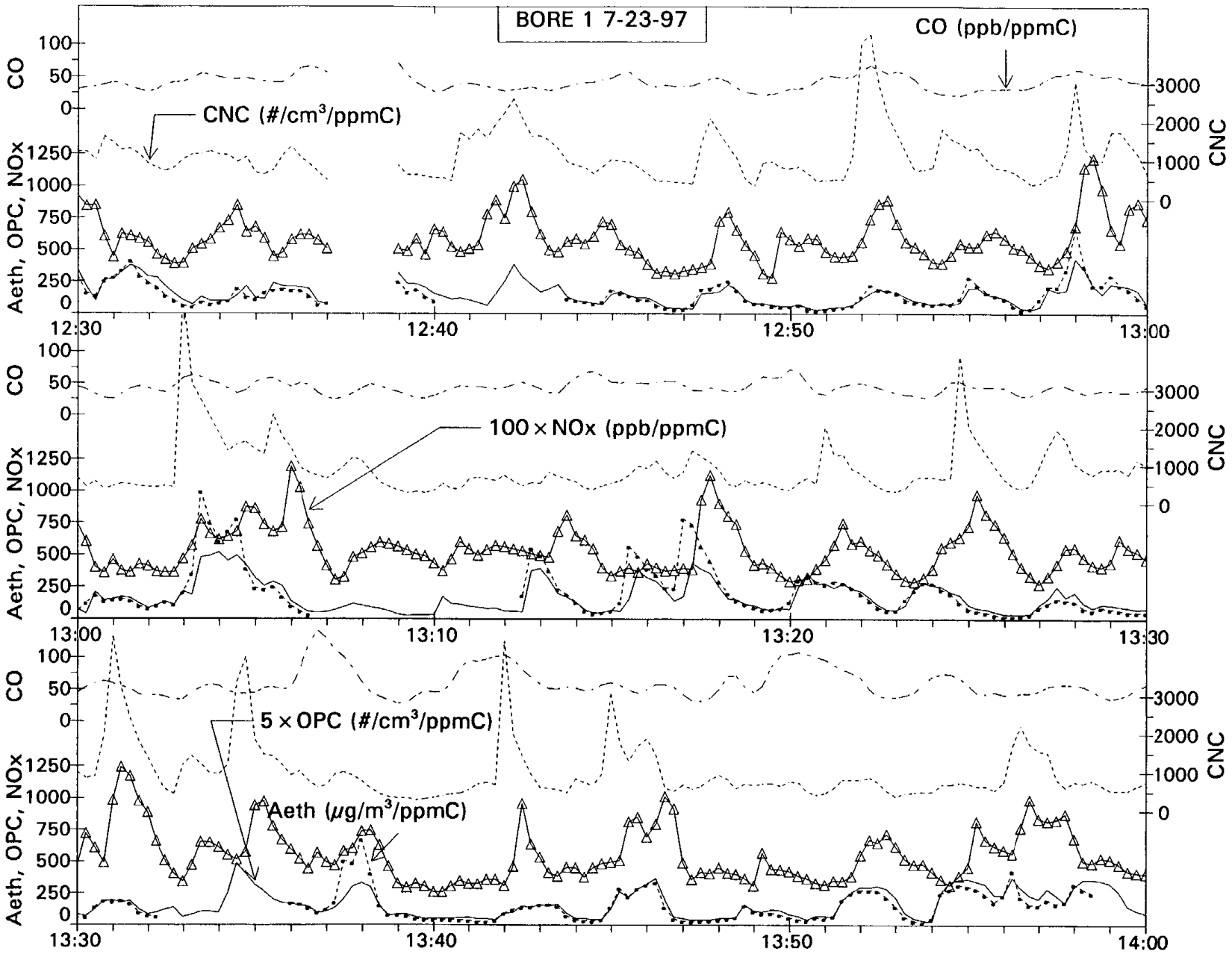
BORE 1 7-23-97
CO (ppb/ppmC)
CNC (#/cm³/ppmC)
100 × NOx (ppb/ppmC)
5 × OPC (#/cm³/ppmC)
Aeth (μg/m³/ppmC)
CO
Aeth, OPC, NOx
CNC
12:30
12:40
12:50
13:00
13:10
13:20
13:30
13:40
13:50
14:00

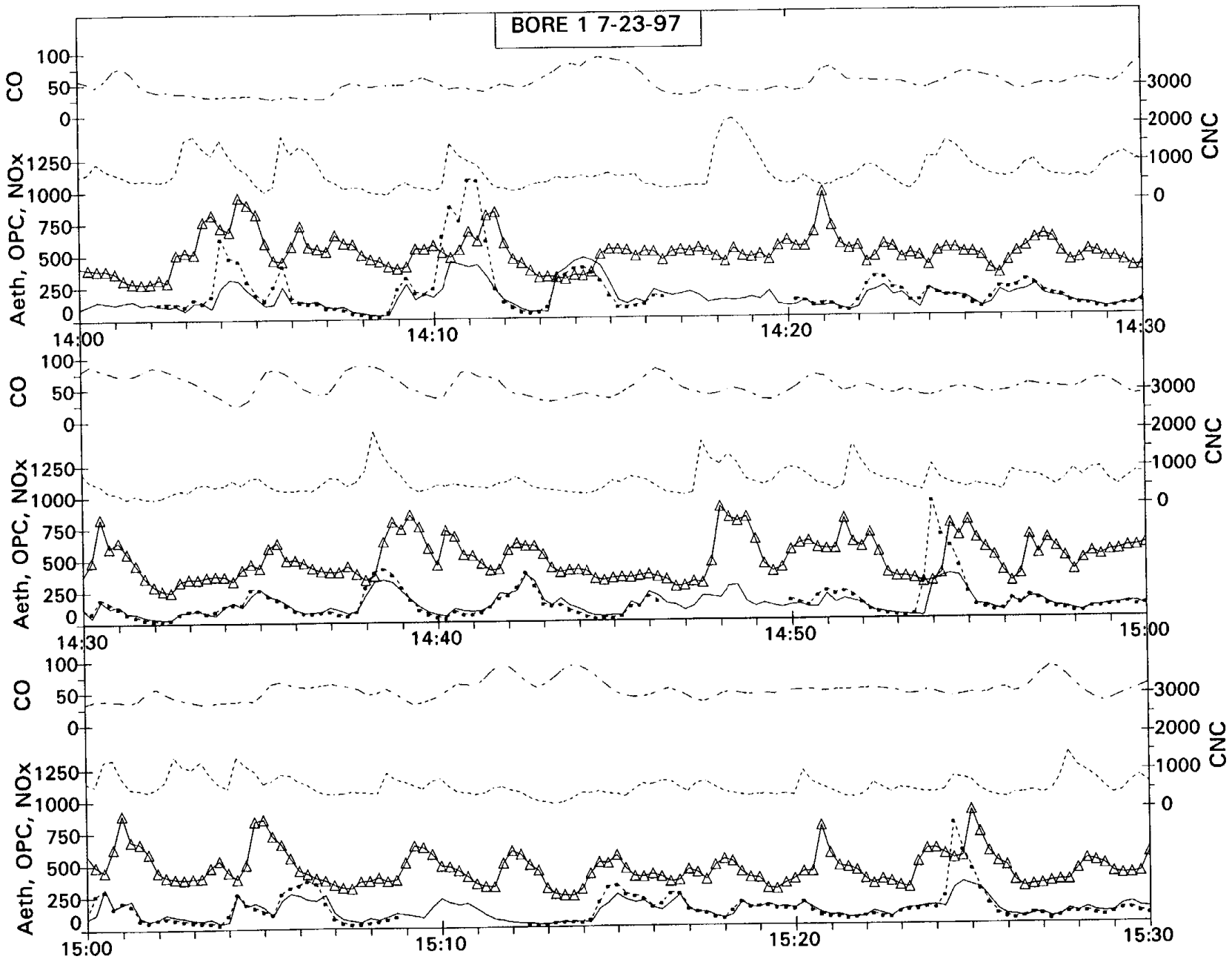
BORE 1 7-23-97
CO
Aeth, OPC, NOx
CNC
100
50
0
1250
1000
750
500
250
0
3000
2000
1000
0
14:00
14:10
14:20
14:30
14:40
14:50
15:00
15:10
15:20
15:30

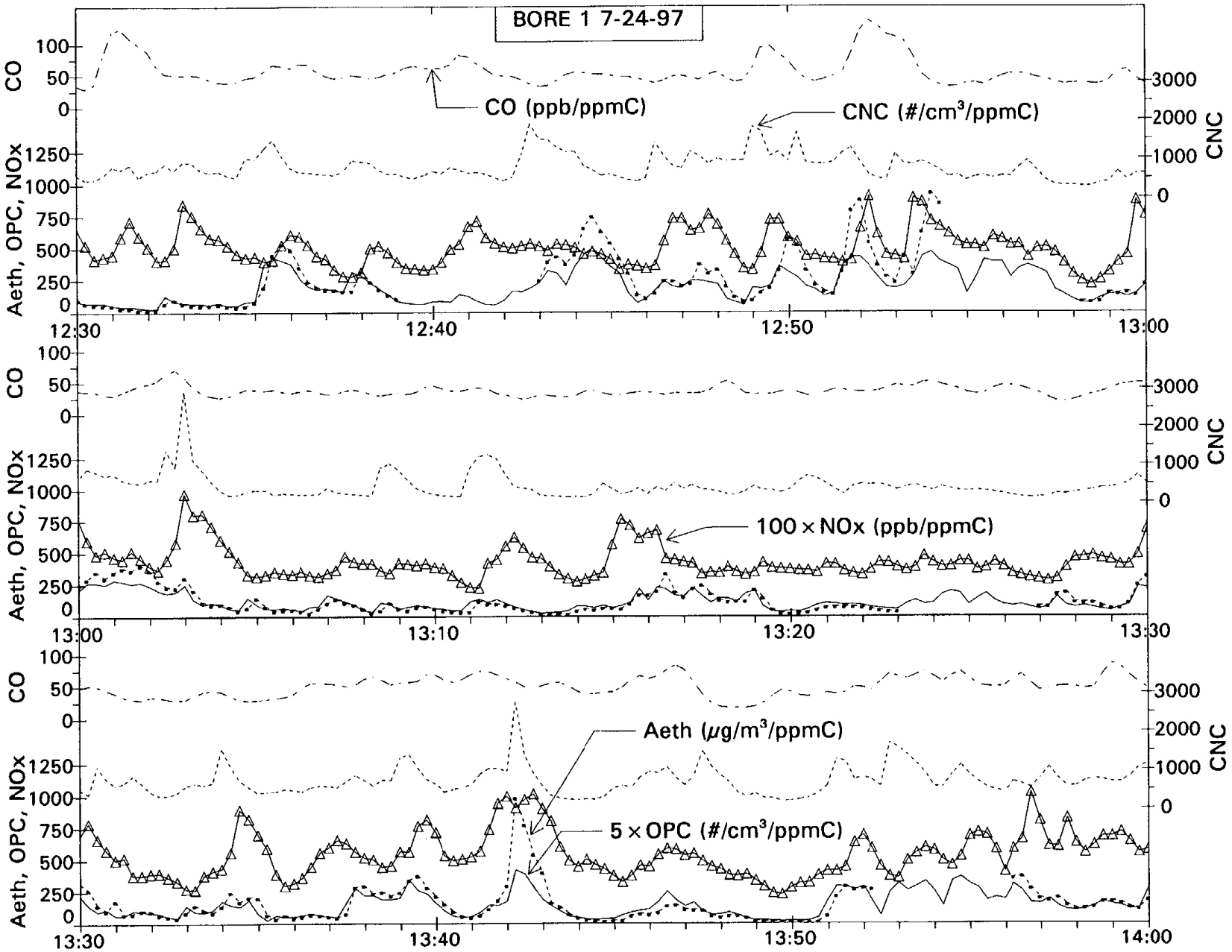
BORE 1 7-24-97
CO
Aeth, OPC, NOx
CNC
CO (ppb/ppmC)
CNC (#/cm³/ppmC)
100 × NOx (ppb/ppmC)
Aeth (μg/m³/ppmC)
5 × OPC (#/cm³/ppmC)
12:30
12:40
12:50
13:00
13:10
13:20
13:30
13:40
13:50
14:00

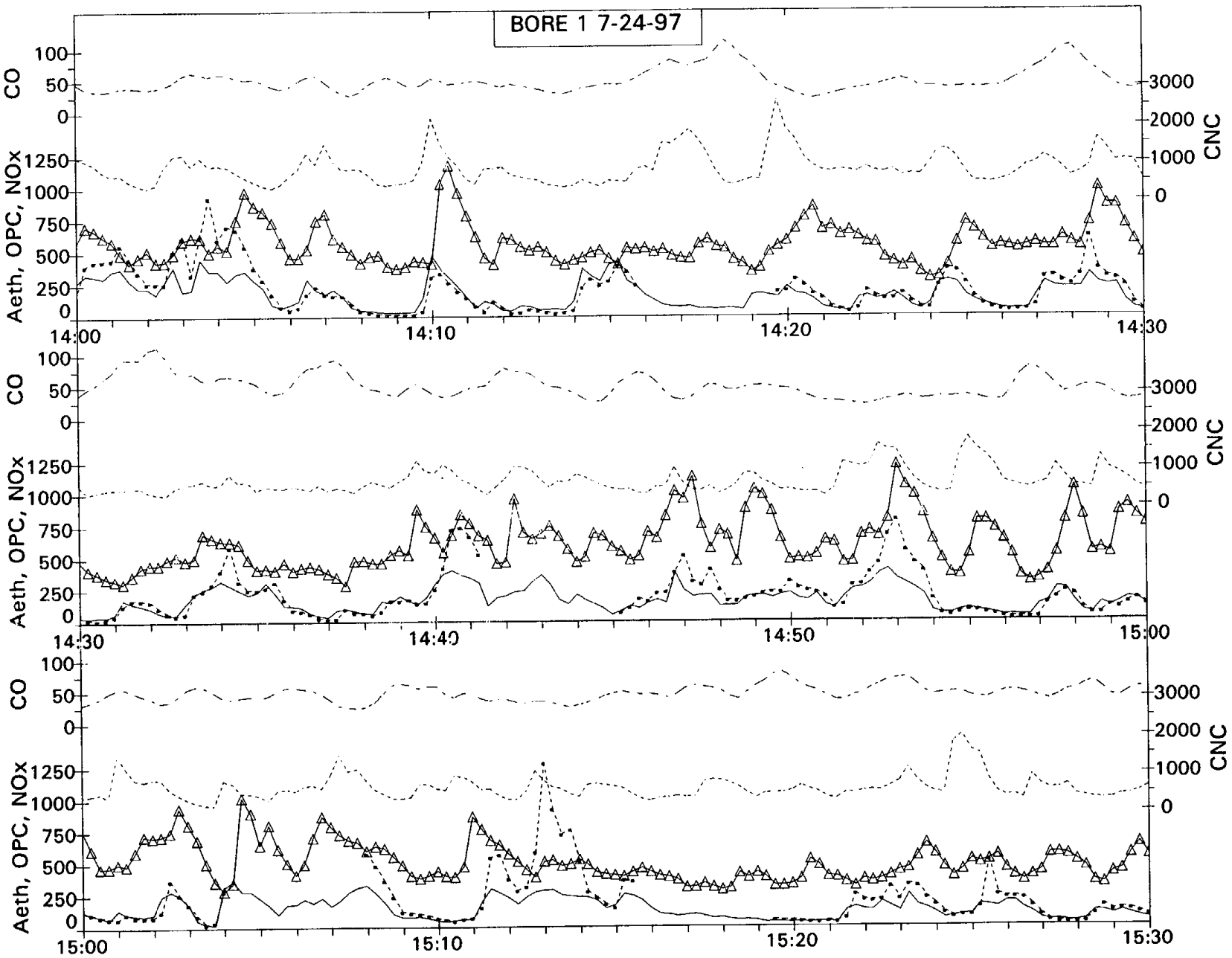
BORE 1 7-24-97
CO
Aeth, OPC, NOx
CNC
100
50
0
1250
1000
750
500
250
0
3000
2000
1000
0
14:00
14:10
14:20
14:30
14:40
14:50
15:00
15:10
15:20
15:30

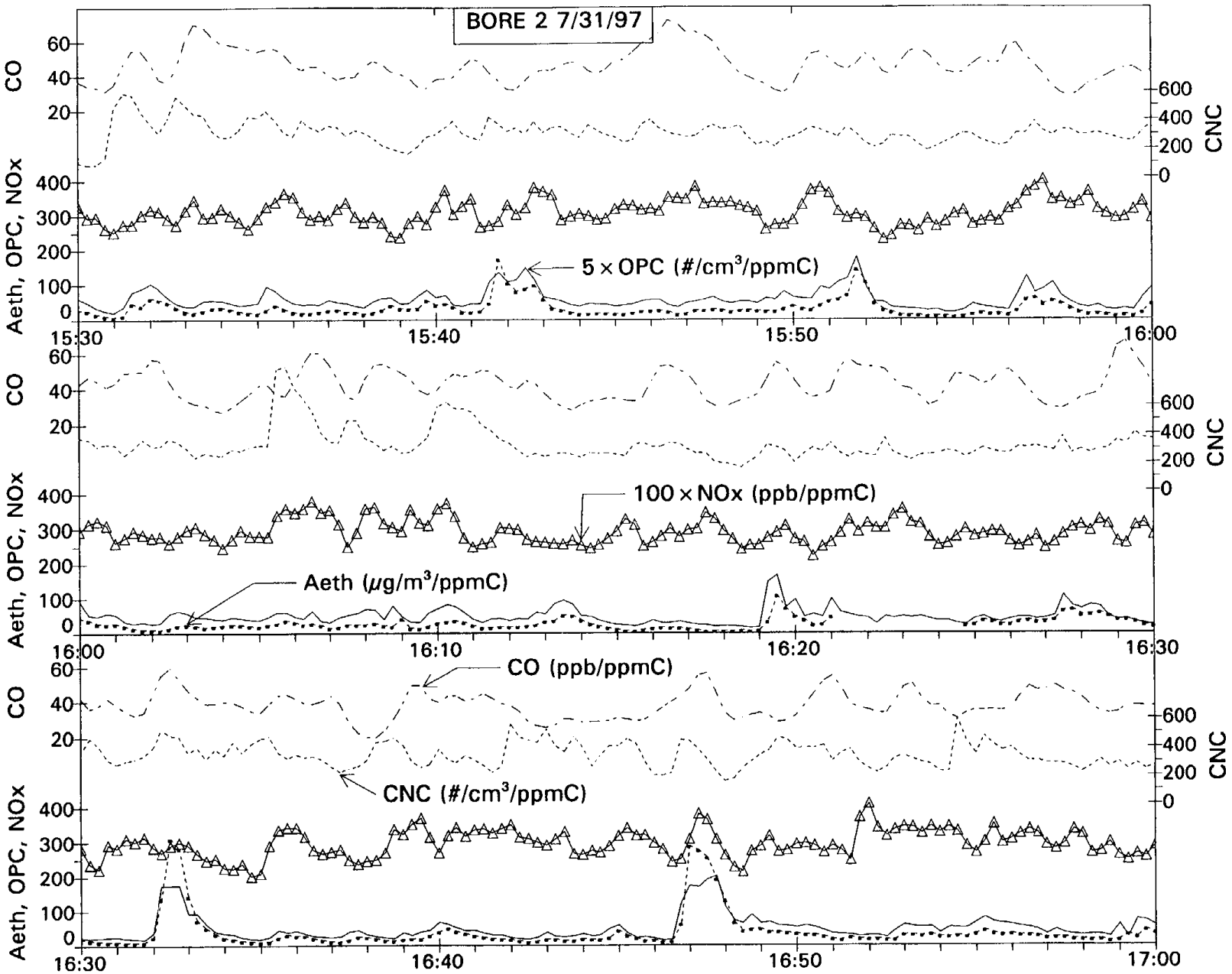
BORE 2 7/31/97
CO
Aeth, OPC, NOx
CNC
5 × OPC (#/cm³/ppmC)
100 × NOx (ppb/ppmC)
Aeth (μg/m³/ppmC)
CO (ppb/ppmC)
CNC (#/cm³/ppmC)
15:30
15:40
15:50
16:00
16:10
16:20
16:30
16:40
16:50
17:00

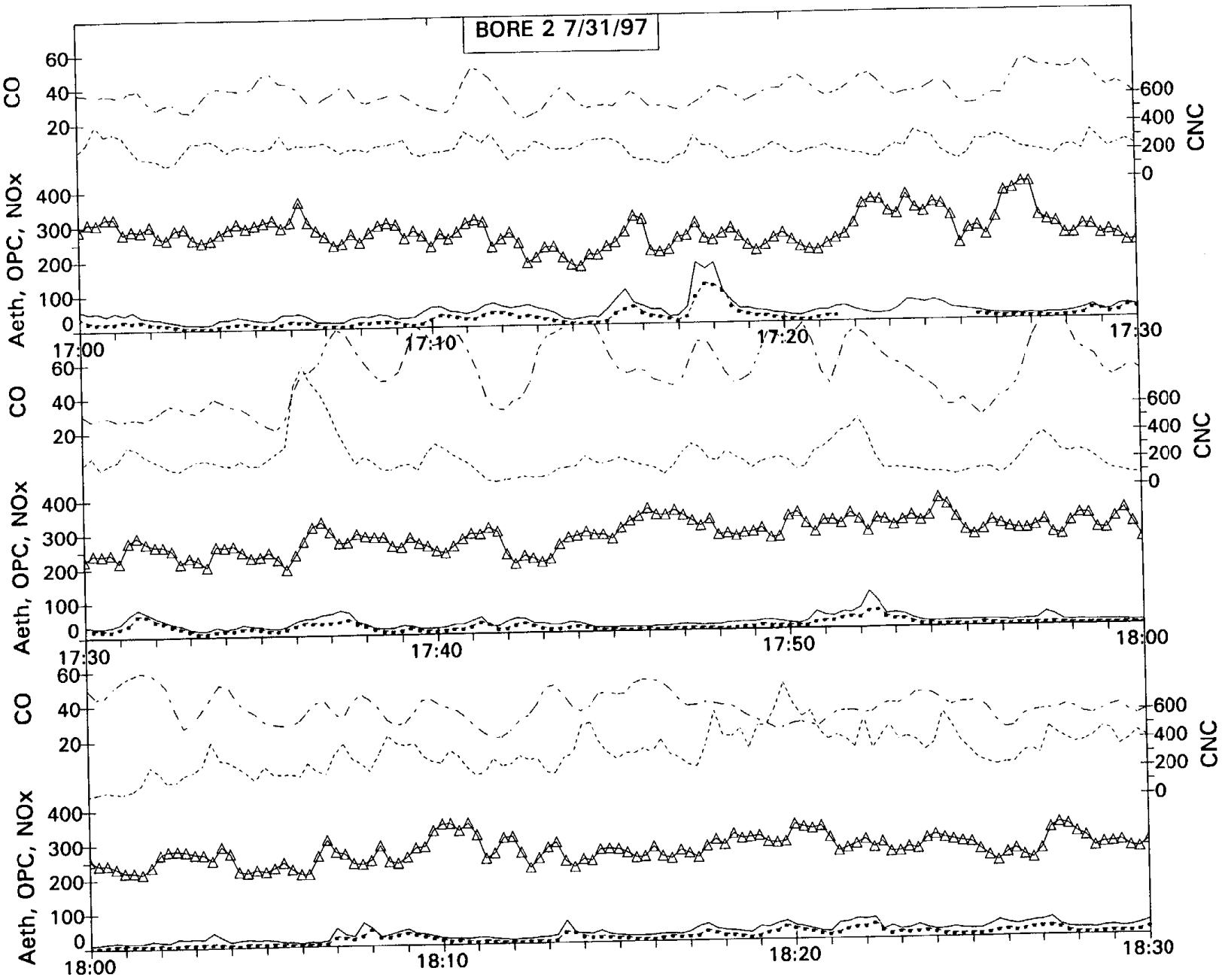
BORE 2 7/31/97
CO
Aeth, OPC, NOx
CNC
60
40
20
400
300
200
100
0
600
400
200
0
17:00
17:10
17:20
17:30
17:40
17:50
18:00
18:10
18:20
18:30

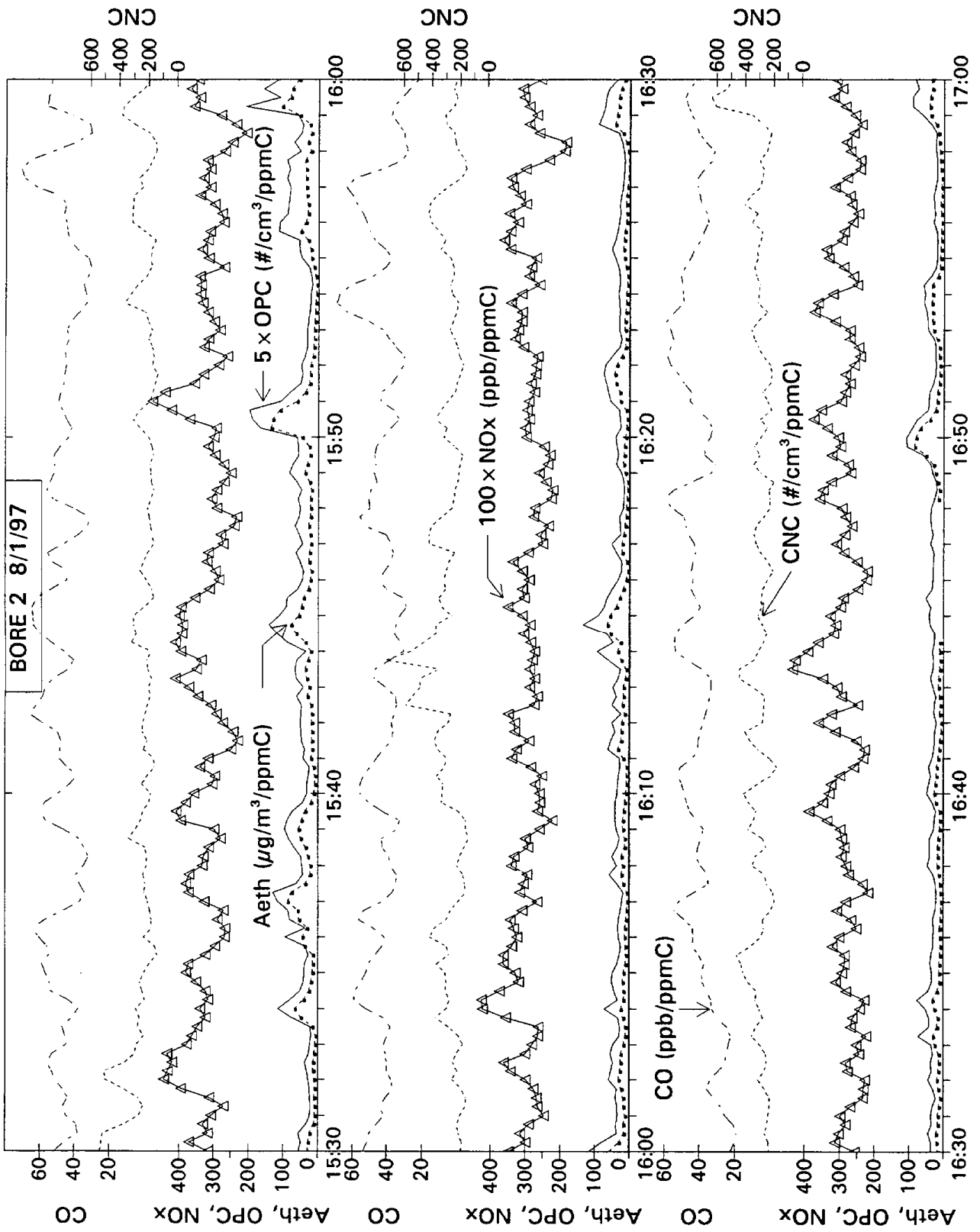
BORE 2 8/1/97
Aeth (μg/m³/ppmC)
5 × OPC (#/cm³/ppmC)
100 × NOx (ppb/ppmC)
CO (ppb/ppmC)
CNC (#/cm³/ppmC)
Aeth, OPC, NOx
CO
CNC
15:30
15:40
15:50
16:00
16:10
16:20
16:30
16:40
16:50
17:00

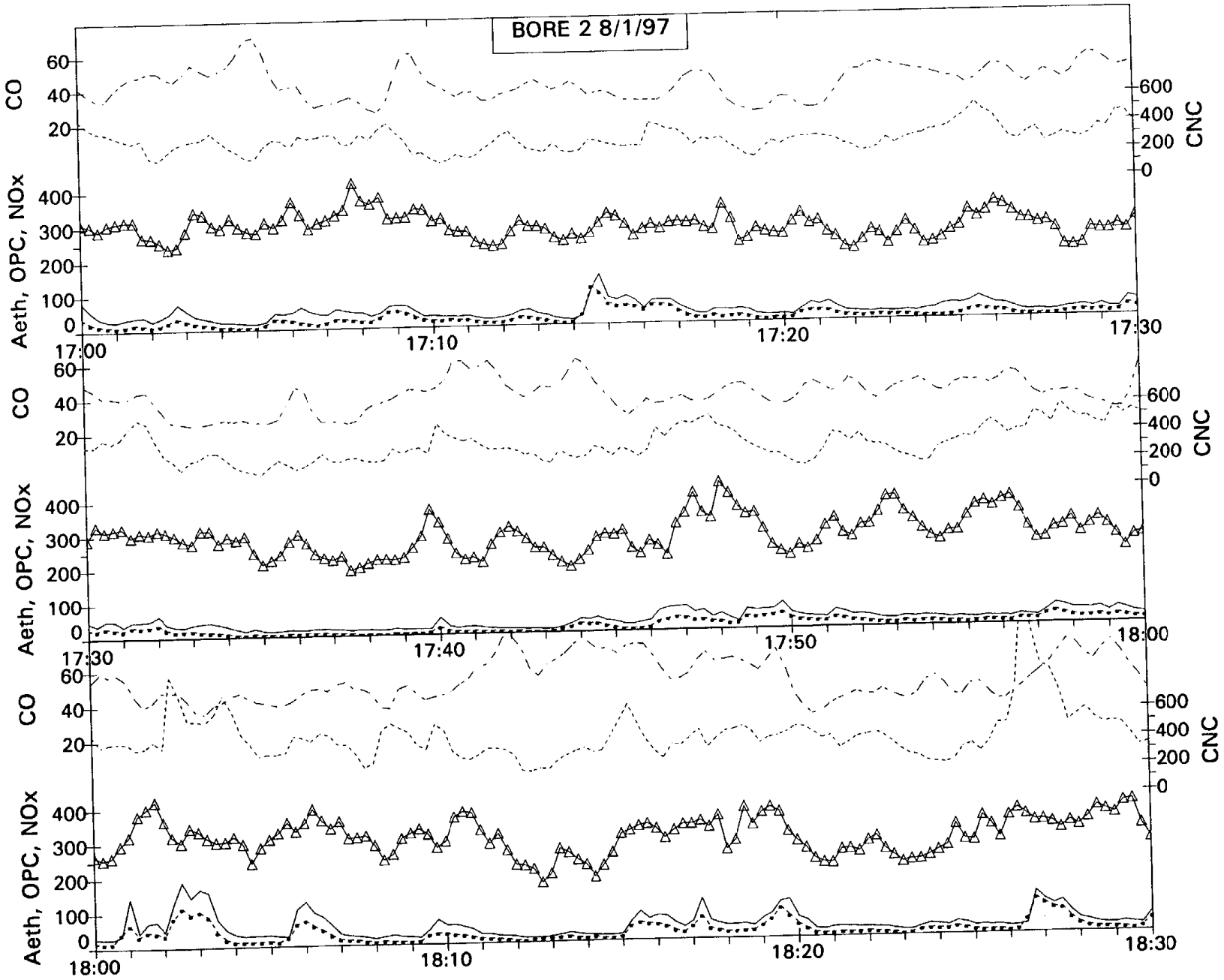
BORE 2 8/1/97
CO
Aeth, OPC, NOx
CNC
60
40
20
400
300
200
100
0
600
400
200
0
17:00
17:10
17:20
17:30
17:40
17:50
18:00
18:10
18:20
18:30

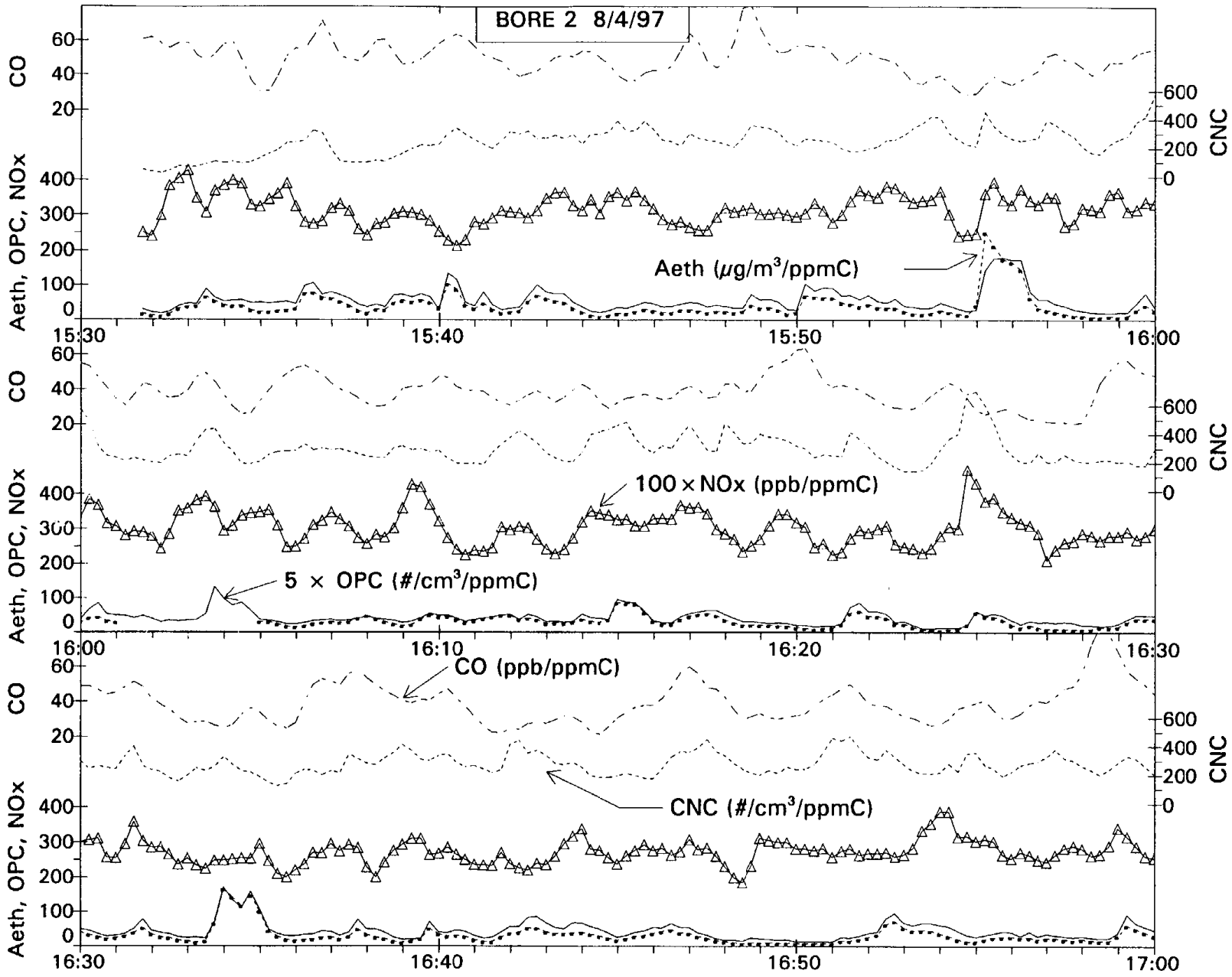
BORE 2 8/4/97
CO
Aeth, OPC, NOx
CNC
Aeth (μg/m³/ppmC)
100 × NOx (ppb/ppmC)
5 × OPC (#/cm³/ppmC)
CO (ppb/ppmC)
CNC (#/cm³/ppmC)
15:30
15:40
15:50
16:00
16:10
16:20
16:30
16:40
16:50
17:00

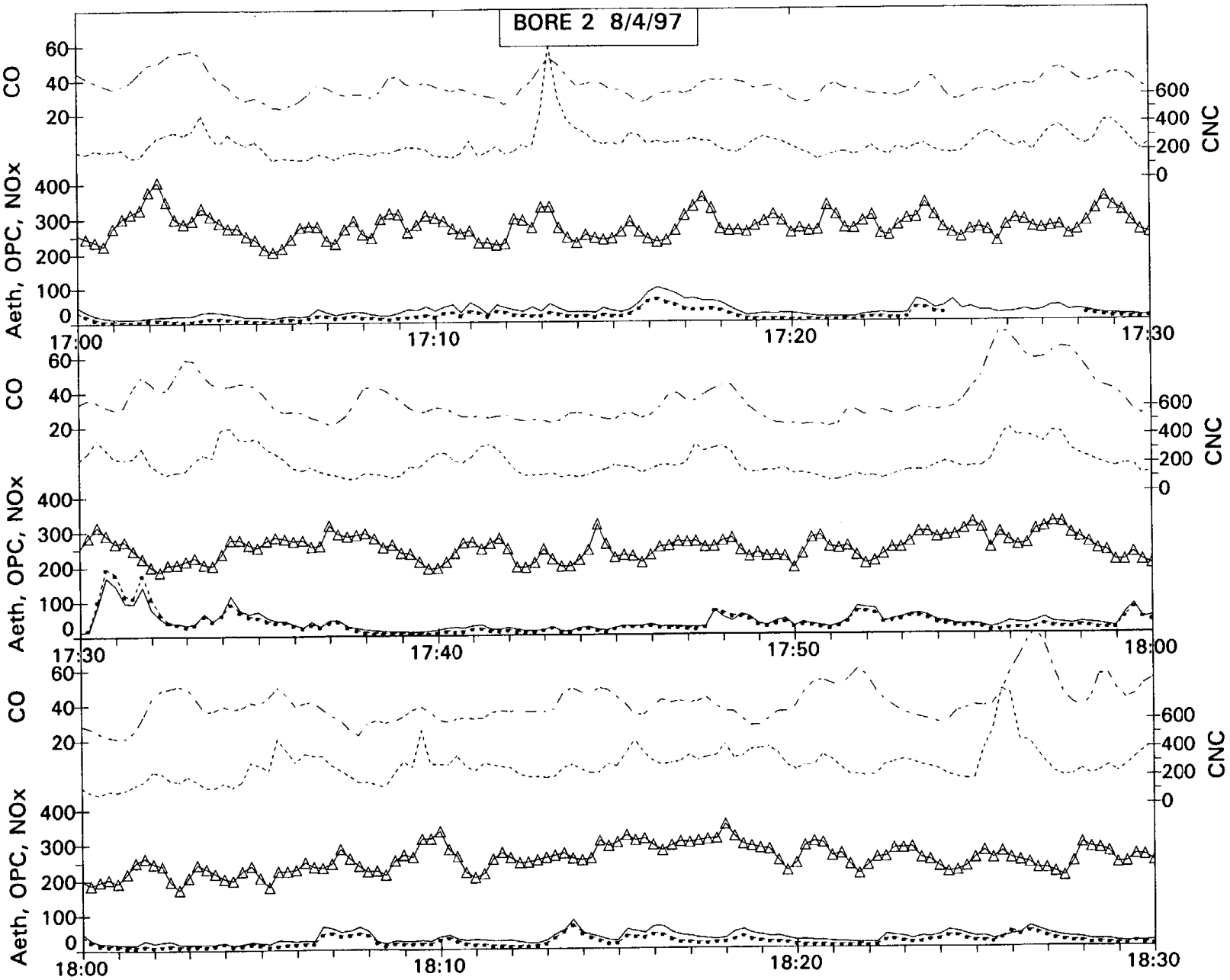
BORE 2 8/4/97
CO
Aeth, OPC, NOx
CNC
60
40
20
400
300
200
100
0
600
400
200
0
17:00
17:10
17:20
17:30
17:40
17:50
18:00
18:10
18:20
18:30

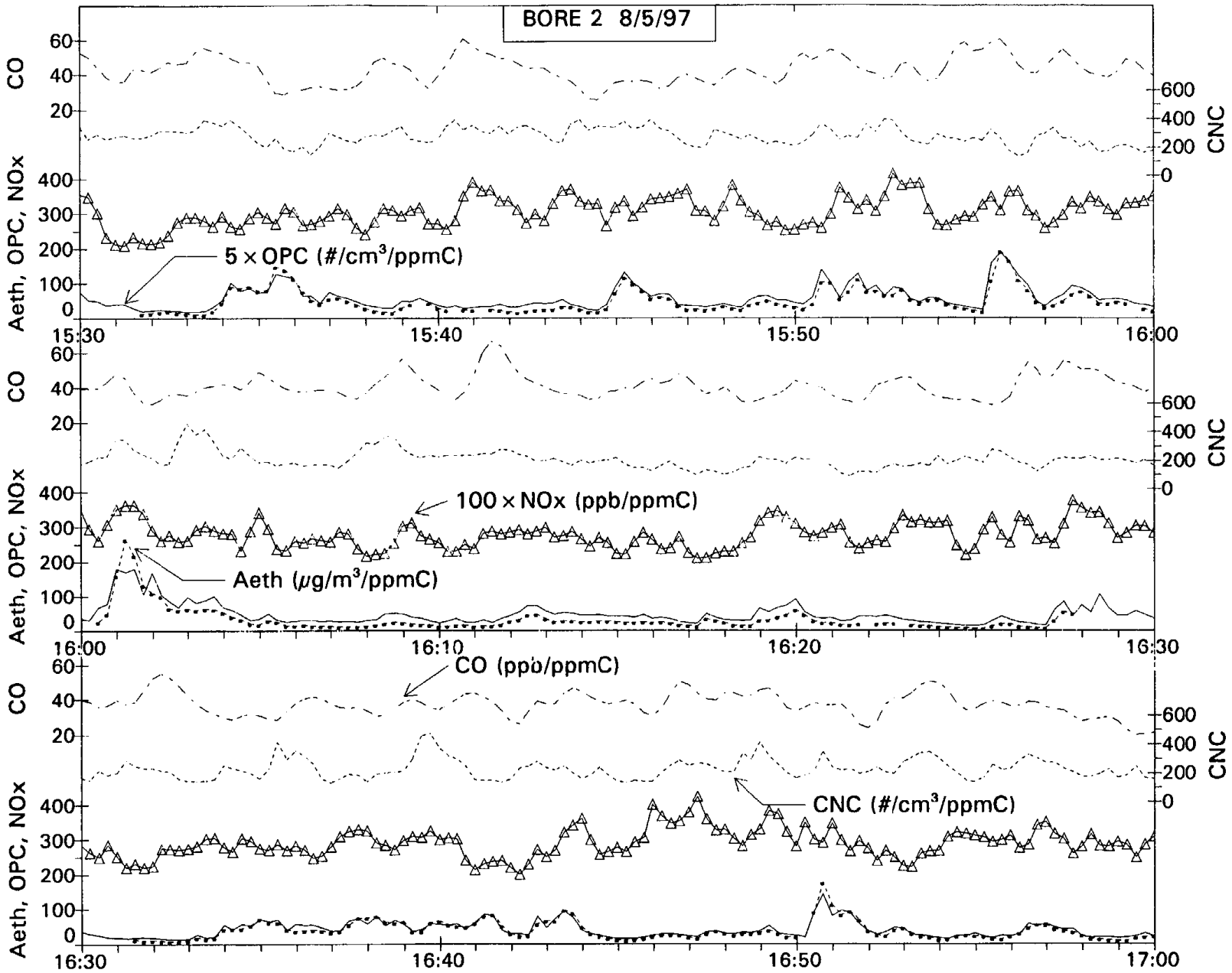
BORE 2 8/5/97
CO
Aeth, OPC, NOx
CNC
5 × OPC (#/cm³/ppmC)
100 × NOx (ppb/ppmC)
Aeth (μg/m³/ppmC)
CO (ppb/ppmC)
CNC (#/cm³/ppmC)
15:30
15:40
15:50
16:00
16:10
16:20
16:30
16:40
16:50
17:00

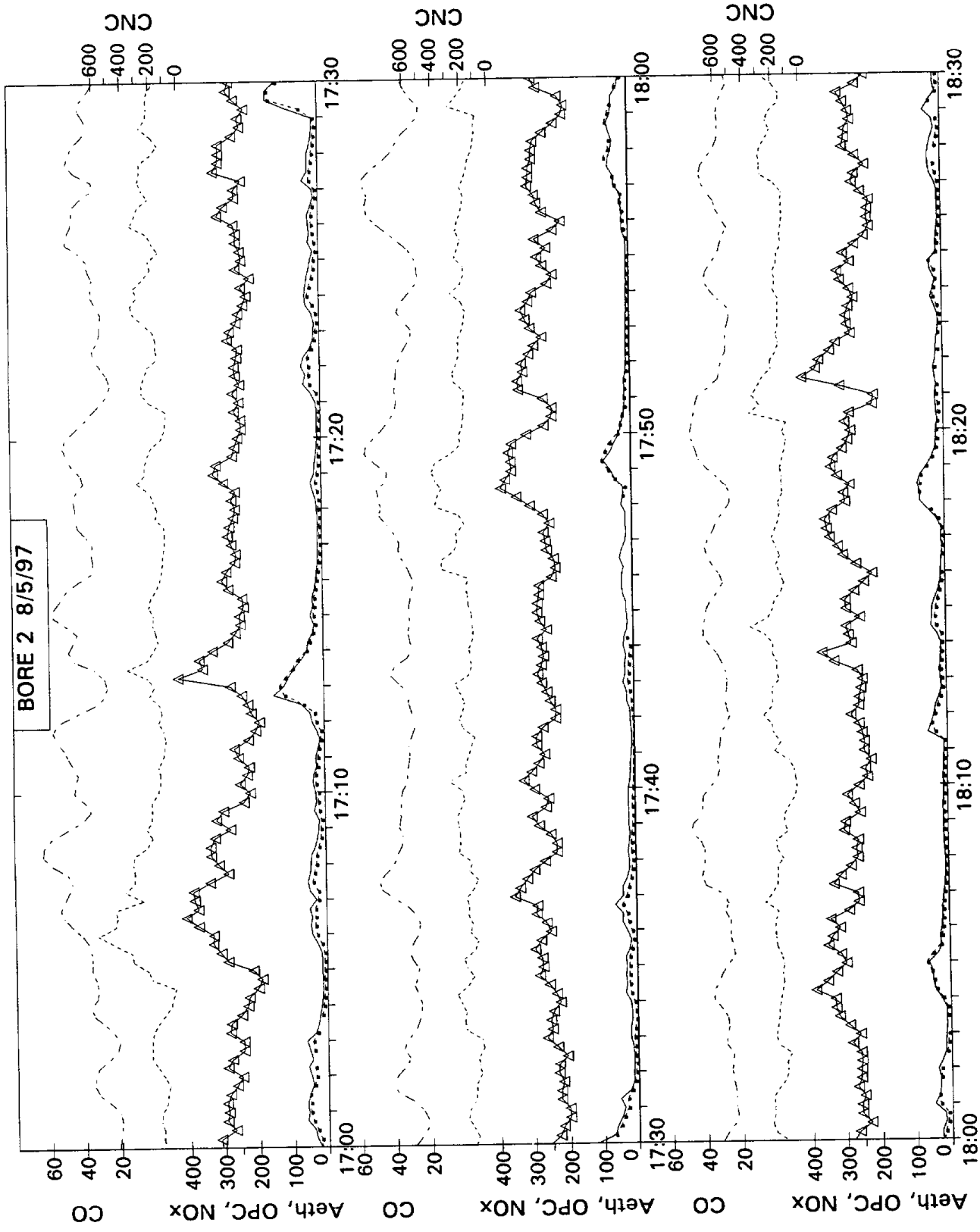
BORE 2 8/5/97
CNC
CO
Aeth, OPC, NOx
17:00
17:10
17:20
17:30
17:40
17:50
18:00
18:10
18:20
18:30